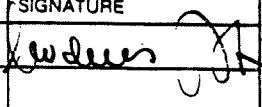
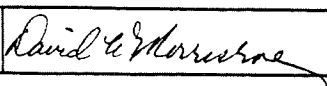
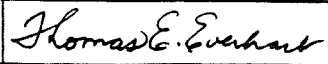


COVER SHEET FOR PROPOSALS TO THE NATIONAL SCIENCE FOUNDATION

FOR CONSIDERATION BY NSF ORGANIZATIONAL UNIT <small>(indicate the most specific unit known, i. e. program, division, etc.)</small>		PROGRAM ANNOUNCEMENT/SOLICITATION NO./CLOSING DATE	
Gravitational Physics/Division of Physics			
SUBMITTING INSTITUTION CODE <small>(if known)</small>	FOR RENEWAL <input checked="" type="checkbox"/> CONTINUING AWARD <input type="checkbox"/> ACCOMPLISHMENT BASED RENEWAL <input type="checkbox"/> REQUEST. LIST PREVIOUS AWARD NO.:	IS THIS PROPOSAL BEING SUBMITTED TO ANOTHER FEDERAL AGENCY? Yes ___ No <u>X</u> IF YES, LIST ACRONYM(S)	
		PHY-8803557	
NAME OF SUBMITTING ORGANIZATION TO WHICH AWARD SHOULD BE MADE (INCLUDE BRANCH/CAMPUS/OTHER COMPONENTS)			
California Institute of Technology			
ADDRESS OF ORGANIZATION (INCLUDE ZIP CODE)			
Pasadena, CA 91125			
IS SUBMITTING ORGANIZATION: <input type="checkbox"/> For-Profit Organization: <input type="checkbox"/> Small Business: <input type="checkbox"/> Minority Business: <input type="checkbox"/> Woman-Owned Business			
TITLE OF PROPOSED PROJECT			
The Construction, Operation, and Supporting Research and Development of a Laser Interferometer Gravitational-Wave Observatory			
REQUESTED AMOUNT	PROPOSED DURATION	DESIRED STARTING DATE	
\$193,918,509 (1989 dollars)	Four (4) Years	December 1, 1990	
CHECK APPROPRIATE BOX(ES) IF THIS PROPOSAL INCLUDES ANY OF THE ITEMS LISTED BELOW:			
<input type="checkbox"/> Animal Welfare	<input type="checkbox"/> National Environmental Policy Act	<input type="checkbox"/> International Cooperative Activity	
<input type="checkbox"/> Endangered Species	<input type="checkbox"/> Research Involving Recombinant DNA Molecules	<input type="checkbox"/> Research Opportunity Award	
<input type="checkbox"/> Human Subjects	<input type="checkbox"/> Historical Sites	<input type="checkbox"/> Facilitation Award for Handicapped	
<input type="checkbox"/> Marine Mammal Protection	<input type="checkbox"/> Interdisciplinary	<input type="checkbox"/> Proprietary and Privileged Information	
<input type="checkbox"/> Pollution Control			
PI/PD DEPARTMENT	PI/PD ORGANIZATION	PI/PD PHONE NO. & ELECTRONIC MAIL	
Division of Physics, Mathematics & Astronomy	California Institute of Technology	818/356-3800 vogt@caltech.edu	
PI/PD NAME/TITLE	SOCIAL SECURITY NO.*	HIGHEST DEGREE & YEAR	SIGNATURE
Rochus E. Vogt Director, LIGO; Prof. of Physics	345-30-2172	Ph.D. - 1961	
ADDITIONAL PI/PD (TYPED)			
ADDITIONAL PI/PD (TYPED)			
ADDITIONAL PI/PD (TYPED)			
ADDITIONAL PI/PD (TYPED)			
For NSF Use:			
TO BE COMPLETED BY THE AUTHORIZED ORGANIZATIONAL REPRESENTATIVE. By signing and submitting this proposal, the prospective grantee is providing the certifications set forth in (1) Grants for Research and Education in Science and Engineering, NSF 83-57 (rev. 11/87), and (2) Appendix C, 45CFR 620, Subpart F (Requirements for a Drug-Free Workplace).			
(If answering yes to either, please provide explanation.)			YES NO
Is the organization delinquent on any Federal Debt?			YES NO
Is the organization presently debarred, suspended, proposed for debarment, declared ineligible, or voluntarily excluded from covered transactions by any Federal department or agency?			YES NO
AUTHORIZED ORGANIZATIONAL REP.	SIGNATURE	DATE	TELEPHONE NO.
NAME/TITLE (TYPED)	NAME/TITLE (TYPED)	DATE	TELEPHONE NO.
David W. Morrisroe, V. P. For Business & Finance & Treas.		12/1/89	(818) 356-6218
OTHER ENDORSEMENT (optional)			
NAME/TITLE (TYPED)	NAME/TITLE (TYPED)	DATE	TELEPHONE NO.
Thomas E. Everhart, President		12/1/89	(818) 356-6301

*Submission of social security numbers is voluntary and will not affect the organization's eligibility for an award. However, they are an integral part of the NSF information system and assist in processing the proposal. SSN solicited under NSF Act of 1950, as amended.

Proposal to the National Science Foundation

**THE CONSTRUCTION, OPERATION, AND
SUPPORTING RESEARCH AND DEVELOPMENT
OF A**

**LASER INTERFEROMETER
GRAVITATIONAL-WAVE
OBSERVATORY**

Submitted by the
CALIFORNIA INSTITUTE OF TECHNOLOGY
Copyright © 1989

Rochus E. Vogt
Principal Investigator and Project Director
California Institute of Technology

Ronald W. P. Drever
Co-Investigator
California Institute of Technology

Kip S. Thorne
Co-Investigator
California Institute of Technology

Frederick J. Raab
Co-Investigator
California Institute of Technology

Rainer Weiss
Co-Investigator
Massachusetts Institute of Technology

Table of Contents: Volume 1

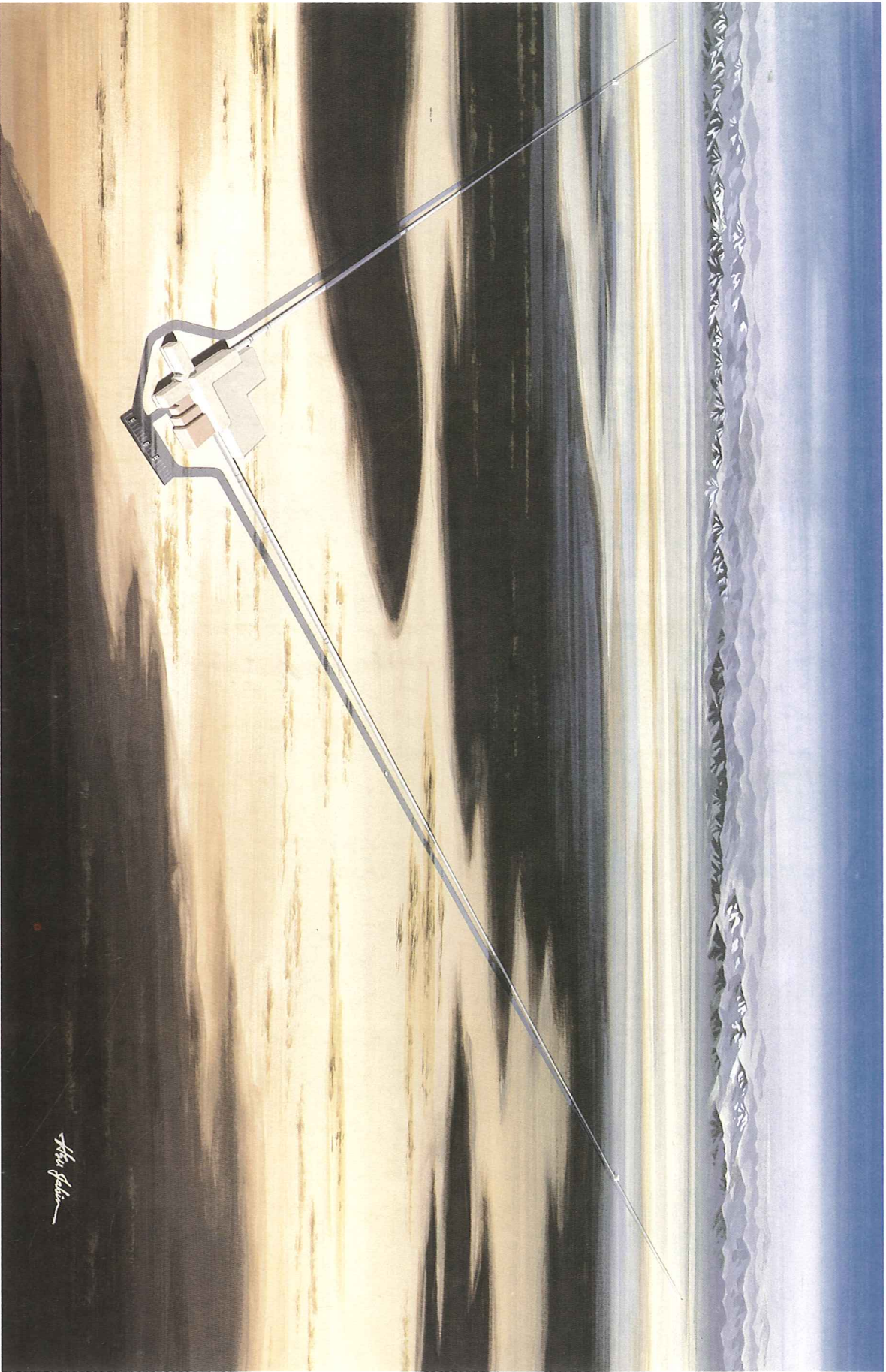
PREFACE	i
SUMMARY.....	1
I. INTRODUCTION	3
II. PHYSICS OF GRAVITATIONAL WAVES, SOURCES, AND DETECTORS	5
III. LASER INTERFEROMETERS.....	13
A. General Characteristics and Noise Effects	13
B. 40-meter Prototype Interferometer	22
IV. LIGO CONCEPT	31
A. Requirements	31
B. Implementation	35
V. DESIGN AND SITING OF INTERFEROMETERS.....	43
A. Conceptual Design of the Initial LIGO Interferometers	43
B. Evolution of LIGO Interferometers	52
C. LIGO Sites: Scientific Aspects	58
VI. LIGO OPERATIONS.....	61
VII. STRATEGY FOR IDENTIFICATION OF GRAVITATIONAL WAVES	67
VIII. CAMPUS RESEARCH AND DEVELOPMENT IN SUPPORT OF LIGO	76
A. Results from Prior NSF Support	76
B. Future Activities	82
IX. ORGANIZATION AND MANAGEMENT	90
X. INTERNATIONAL AND DOMESTIC COLLABORATION	92
XI. REFERENCES.....	94
XII. SCHEDULE AND BUDGET	96
RESPONSE TO NSF NOTICE NO. 107.....	98
KEY PERSONNEL: VITAE	
KEY PERSONNEL: PUBLICATIONS	

APPENDICES:

- A. The Physics of Gravitational Waves, and
 Comparison of Source Strengths with Detector Sensitivities
- B. Interferometer Concepts and Noise
- C. Concepts for Advanced Interferometers
- D. Calculation of Vibration Isolation
- E. Power Spectral Density and Detector Sensitivity
- F. Scattering and Optical Properties of the Beam Tubes
- G. LIGO Project Gravitational-Wave Searches
- H. Report on Recent Progress
- J. History of the Project
- K. Memoranda of Understanding

Outline of Contents: Volume 2

- I. Introduction
 - II. Design Requirements, Specifications, and Goals
 - III. Phased Implementation
 - IV. Design Description
 - A. Overview
 - B. Initial Interferometer Design Description
 - C. Vacuum System: Mechanical Design
 - D. Vacuum System: Vacuum Design
 - E. Enclosure Design
 - F. Instrumentation, Control, and Data System
 - G. Electrical Power
 - V. Sites
 - VI. Implementation Plan
 - A. Work-Breakdown Structure
 - B. Organization and Responsibilities
 - C. Design and Construction Schedule
 - D. Subcontracting Plan
 - E. Interferometer Design and Fabrication
 - VII. Cost Summary
 - (Including: Proposal Budget in NSF Format,
Current and Pending Support, and Residual Funds Statement)
- Appendices:
- A. Expansion to Phase-B and Phase-C Configurations
 - B. Post-Construction Operations Cost
 - C. Design and Construction Cost Detail
 - D. Measured Outgassing Properties of Stainless Steel



John G. Miller

*“There is nothing more difficult to take in hand,
more perilous to conduct,
or more uncertain in its success,
than to take the lead
in the introduction of a new order of things.”*
—MACHIAVELLI, *The Prince* (1513)

PREFACE

This proposal requests support for the design and construction of a novel scientific facility—a gravitational-wave observatory—that will open a new observational window on the universe.

The scale of this endeavor is indicated by the frontispiece illustration, which shows a perspective of one of the two proposed detector installations. Each installation includes two arms, and each arm is 4 km in length.

In view of the magnitude of the proposed project, and because reviewers will have varying degrees of familiarity with the subject matter, we have provided a substantial amount of tutorial material and scientific justification. While this should provide a comprehensive basis for forming a reasoned judgment, it also challenges the readers’ fortitude and endurance in absorbing the material.

A reader who wishes to come quickly to the heart of the proposal may want to scan Section I, then read Section II, which introduces the characteristics and sources of gravitational waves and the principles of their detection, and then proceed to Section IV, which outlines our basic concept of a gravitational-wave observatory. The remaining sections of Volume 1 may be studied as the spirit—and the Table of Contents—moves the reader. Volume 2 presents the plans for construction and implementation of the concepts introduced in Volume 1.

SUMMARY

This proposal requests support for a 4-year program to build and operate a Laser Interferometer Gravitational-Wave Observatory (LIGO) and to continue research and development of interferometric detectors of ever higher sensitivities. The proposed LIGO includes interferometer installations of 4-km arm length and support facilities; these installations would be located at two widely separated sites in the continental United States and operate in coincidence for the detection of gravitational waves. The LIGO project is a joint effort of scientists at the California Institute of Technology and the Massachusetts Institute of Technology and includes collaborative programs with scientists at other institutions. The observatory will be open for use by the national community, and will become part of a planned worldwide network of gravitational-wave observatories. The proposed LIGO is based on almost two decades of science research and development. The ultimate objectives of the LIGO program include (1) tests of Einstein's General Theory of Relativity—in particular, measurement of the graviton's rest mass and spin and studies of the domain of highly nonlinear, dynamic gravity, and (2) the opening of an observational window on the universe that differs fundamentally from that provided by electromagnetic or particle astronomy.

I. INTRODUCTION

Gravitational waves are traveling perturbations in the curvature of spacetime. They are predicted by Einstein's theory of general relativity and all other relativistic theories of gravity [I-1]. Gravitational waves should be emitted by coherent bulk motions of matter (e.g., collapsing stellar cores) and by coherent, nonlinear vibrations of spacetime curvature (e.g., colliding black holes).

Gravitational waves have not been directly detected as yet. Their observation will open a new window on the universe and may materially change our view of a cosmos based primarily upon the study of electromagnetic waves.

Research and development by members of the Laser Interferometer Gravitational-Wave Observatory (LIGO) Project team and others over almost two decades, largely supported by the National Science Foundation, have created technology and techniques that are likely to make possible the detection of gravitational waves and the successful pursuit of gravitational-wave astronomy. In particular, experience with prototype laser-interferometer gravitational-wave detectors has made it possible to design full-scale instruments with sensitivities in the range of anticipated astrophysical signals.

This proposal requests support for the construction of the LIGO and for its initial operations. The proposed 4-year program will be conducted by members of the LIGO Project, a joint undertaking of the California Institute of Technology (Caltech) and the Massachusetts Institute of Technology (MIT).¹

The LIGO will consist of two observatory facilities located far apart, but within the continental United States. These facilities will incorporate L-shaped vacuum systems with arms of 4-km length that house the laser interferometer detectors for gravitational waves. Comparison of data from interferometers at the two sites will give convincing identification of gravitational waves and will extract a significant portion of the information they carry. The LIGO concept incorporates capabilities for concurrent observation and detector development. LIGO facilities will support an extensive program of gravitational-wave astronomy open to participation by the broader scientific community. The LIGO will become part of a planned worldwide network of gravitational-wave detectors coordinated to extract the full information carried by gravitational waves.

This proposal consists of two volumes. Volume 1, **LIGO Science and Concepts**, presents the scientific justification, with Section II introducing the characteristics and sources of gravitational waves and the principles of their detection. Section IV outlines our basic concept of a gravitational-wave observatory. For greater depth, Section III.A provides a tutorial on the principles and capabilities of laser interferometer detectors, and Section III.B describes our working prototype interferometer. Sections V.A and V.B discuss the concept of the initial LIGO detectors and their

¹ For details on the history of the LIGO project, see Appendix J.

evolution. Section VI describes plans for initial observatory operations, and Section VII explains how we plan to produce credible results. Section V.C addresses how interferometer facilities need to be located in order to optimize astrophysical observations. Section VIII summarizes the key developments of the enabling research leading to the present proposal and outlines future research and development tasks. Sections IX and XII present a management, schedule, and budget overview.

Appendices provide in-depth discussion of scientific or technical issues or historical perspective. In particular, Appendix A presents a more comprehensive discussion of astrophysical sources of gravitational waves, and Appendix C provides a physical discussion of interferometer evolution and possibilities for enhanced measurement sensitivity.

Volume 2, **Phase-A Design and Construction Implementation**, addresses the requirements derived from Volume 1 and presents a conceptual design description, a construction implementation plan, and a cost analysis for LIGO.

II. PHYSICS OF GRAVITATIONAL WAVES, SOURCES, AND DETECTORS

This section presents, in brief, the scientific justification and goals of the LIGO Project. For greater detail and references to the literature, see Appendix A.

A. The Physics of Gravitational Waves and Interferometric Detectors

Gravitational waves are predicted by general relativity theory and by all other relativistic theories of gravity; all the theories agree—in rough order of magnitude—on the strengths of the waves to be expected from astrophysical sources. However, the theories disagree on a wave's propagation speed (from which one can infer the rest mass of the gravitons that carry the wave) and on its polarization properties (from which one can infer the gravitons' spin). In general relativity, the propagation speed is the same as that for light (the graviton has zero rest mass), and the wave's force field is transverse to its propagation direction and has quadrupolar symmetry (the graviton has spin two). The two polarization states of general relativity's wave are called + ("plus") and \times ("cross") and are characterized by two dimensionless fields h_+ and h_\times .

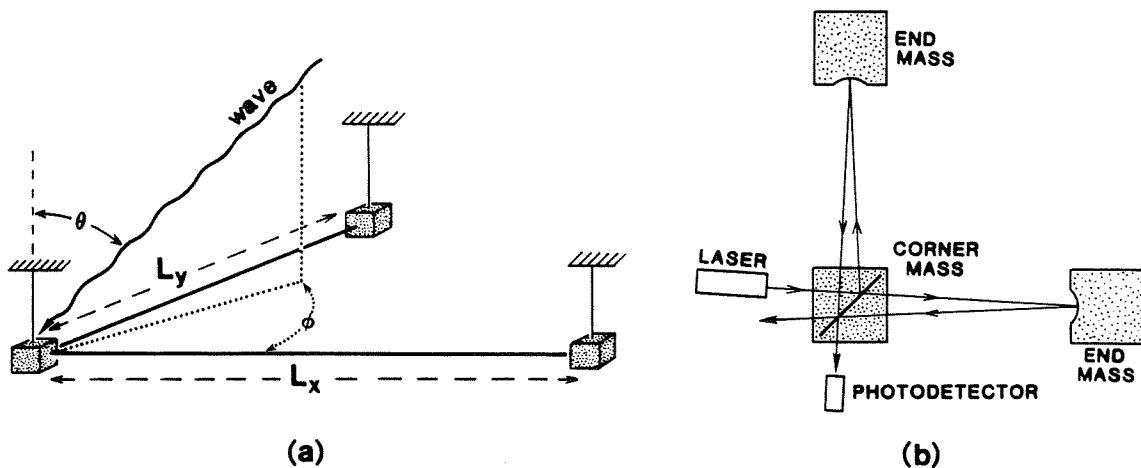


Figure II-1 Schematic diagrams of a laser interferometer gravitational wave detector, showing (a) the arrangement of three masses in an "L" configuration that responds to an incoming wave, and (b) interferometric determination of the motion of the test masses.

A *laser interferometer gravitational-wave detector*, in its simplest conceptual variant, consists of three masses hung by wires from overhead supports at the corner and ends of an "L" (Figure II-1a). A gravitational wave pushes the masses back and forth relative to each other, changing the difference $L_x - L_y$ in the length of the detector's two arms by an amount ΔL that is proportional to arm length, $L \simeq L_x \simeq L_y$, and to a linear combination of h_+ and h_\times :

$$\frac{\Delta L}{L} = [(1/2)(1 + \cos^2 \theta) \cos 2\phi]h_+ + [\cos \theta \sin 2\phi]h_\times \equiv h \quad (\text{II.1})$$

Here (θ, ϕ) is the wave's propagation direction. By laser interferometry one directly reads out $\Delta L/L$ and from its time evolution, the combination (called h) of $h_+(t)$ and $h_\times(t)$ in Equation (II.1). This h is sometimes called the *gravitational-wave strain* because it is the direct producer of the strain $\Delta L/L$ in the detector.

Laser interferometry—in its simplest theoretical variant—is performed as follows. Light from a laser shines on a beam-splitting mirror that rides on the corner mass (Figure II-1b). The beam splitter directs half the light toward each of the two end masses, and mirrors on those masses return beams to the splitter where they recombine. The gravity-wave-induced change in the arm-length difference ΔL produces a relative phase shift in the recombining beams, affecting the amounts of light received by the photodetector or returned to the laser. The photodetector output, therefore, varies in direct proportion to ΔL and thus proportionally to the combination of $h_+(t)$ and $h_\times(t)$ appearing in Equation (II.1). In realistic variants of such a detector (Section III), the ΔL -induced phase shift is increased by placing mirrors on the corner mass as well as on the ends, and bouncing the light back and forth many times in each arm (“delay-line interferometer”) or operating each arm as a giant Fabry-Perot cavity (“Fabry-Perot interferometer”).

For an optimized number of bounces¹ (and because ΔL is proportional to L), longer arms result in larger relative phase shifts for the beams that propagate down the arms, and thus a more sensitive interferometric detector. That is why we are planning to upgrade from our present prototype interferometers with $L \leq 40$ m to a full-scale LIGO with $L = 4$ km.

By cross-correlating the outputs of several interferometers with different orientations and different locations on Earth, i.e., by using them as a detector network, one can read the full information carried by a gravitational wave: the direction (θ, ϕ) of its source and the time evolution of its two waveforms $h_+(t)$ and $h_\times(t)$. One can also read the spatial pattern of the forces that act on the detector's masses and from it infer the wave's polarization properties and thence the graviton's spin. If the wave's source is, e.g., a supernova that is also seen with electromagnetic detectors (such as optical, radio, or X-ray telescopes) a measure of the delay between the electromagnetic and gravitational signals can be used to determine whether gravitons propagate at the same speed as photons; if they do, gravitons have zero rest mass.

The gravitational waveforms $h_+(t)$ and $h_\times(t)$ carry detailed information about the waves' sources. Because the strongest sources in the LIGO's broad frequency band ($10 \text{ Hz} \lesssim f \lesssim 10^4 \text{ Hz}$) are likely to be neutron stars and black holes, the waveforms can bring us detailed information about the dynamical behaviors of

¹ See Appendix B.

these objects in such violent events as their births and collisions (cf. Figure A-3 in Appendix A). Detection of a stochastic background of gravitational waves from the big bang could bring us detailed information about the earliest moments of the universe; coalescing, compact binary stars could act as standard candles for measuring the large-scale structure of the universe in later epochs (see Appendix A for details).

Gravitational and electromagnetic waves differ greatly. Gravitational waves should be emitted by coherent bulk motions of matter (e.g., collapsing stellar cores) and coherent, nonlinear vibrations of spacetime curvature (e.g., collisions of black holes). By contrast, astronomical electromagnetic waves are usually incoherent superpositions of emission from individual atoms, molecules, and charged particles. Gravitational waves are emitted most strongly in regions of spacetime where gravity is relativistically strong, whereas electromagnetic waves come almost entirely from weak-gravity regions, since strong-gravity regions tend to be obscured by surrounding matter. Because of these differences, the information carried by gravitational waves is almost “orthogonal” to that carried by electromagnetic waves and our present electromagnetically based understanding of the universe is inadequate to predict with confidence the strengths of the gravitational waves bathing the Earth. Conversely, if gravitational waves are detected and studied, they may create a revolution in our view of the universe comparable to that wrought by radio astronomy.

B. Scientific Payoff from the LIGO Project

From the above discussion and the details in Appendix A, we select the following list of scientific payoffs that might come from the LIGO Project. The project is designed and managed, so far as possible, to maximize the likelihood that some or most of these payoffs will be achieved.

1. Possible payoffs for physics

- The direct verification of the existence of gravitational waves.
- Measurement of the propagation speed and polarization properties of the waves, and from them the rest mass and spin of the graviton: do they agree with general relativity’s predictions, $m = 0$ and $s = 2$?
- Verification (by comparing theoretical and observed wave forms) that black holes exist and that their dynamics are as predicted by general relativity. By this, test general relativity for the first time in the domain of highly nonlinear, dynamic gravity.

2. Some possible payoffs for astronomy and astrophysics

- Open up a new window on the universe, one almost certain to bring surprises and that may bring a revolution comparable to that which came from the radio window in the 1950s and 60s.

- Study the behavior of neutron stars in highly dynamical situations. By this, extract information about the uncertain physics that governs neutron stars.
- Use the waves from the coalescence of black-hole and neutron-star binaries as “standard candles” for the determination of the Hubble expansion rate and deceleration parameter of the universe (see Appendix A).
- Detect primordial gravitational waves from the big bang and from them extract information about the initial conditions and earliest stages of evolution of the universe.

C. Estimates of the Strengths of the Waves at Earth and Comparison With Anticipated LIGO Sensitivities

When these payoffs can be achieved will depend on when detectors in the LIGO can reach the required sensitivities. Figure II-2 gives some indication of the prospects for this by comparing the wave strengths from various hypothesized burst sources with several benchmarks for detector sensitivity. (For the details underlying Figure II-2, and for similar figures for periodic and stochastic waves, see Appendix A.)

The most certain of the sources is coalescence of neutron-star binaries. Estimates based on pulsar statistics in our own galaxy suggest that to see three such events per year one should look out to 100_{-40}^{+100} Mpc distance. (See Appendix A for further details on this and all sources). For supernovae, the event rate is known to be roughly one each 40 years in our own galaxy (10 kpc distance) and several per year in the Virgo cluster (10 Mpc), but the amount of radiation emitted is very uncertain. For black-hole births, both the wave-emission efficiency and the distance to which one must look are highly uncertain.

The upper solid curve and stippled region in Figure II-2 indicate the best sensitivity achieved to date by our 40-meter prototype. The middle solid curve and stippling indicate the sensitivity of an early detector that might operate in the LIGO. The concept for this early detector is described in Section V.A. Once the early detector has been operated near the sensitivity of the middle curve, a succession of ever-improving detectors will evolve, continually pushing the sensitivity level down (to smaller h) and left (to lower frequencies, f). As a rough indication of where this might lead after a few years, we show (lower solid curve and stippling) the sensitivity of an “advanced detector” based on concepts given in Section V.B and Appendix C.

It is reasonable to expect, in later years of the LIGO, improvements beyond this advanced detector, as indicated by the arrows labeled “improved seismic isolation,” “improved thermal noise,” “improved recycling,” and “squeezed light” (see Appendix C). The only limit of principle on detector sensitivities in the LIGO is the “quantum limit” (solid line); with cleverness, ways of circumventing it might be developed.

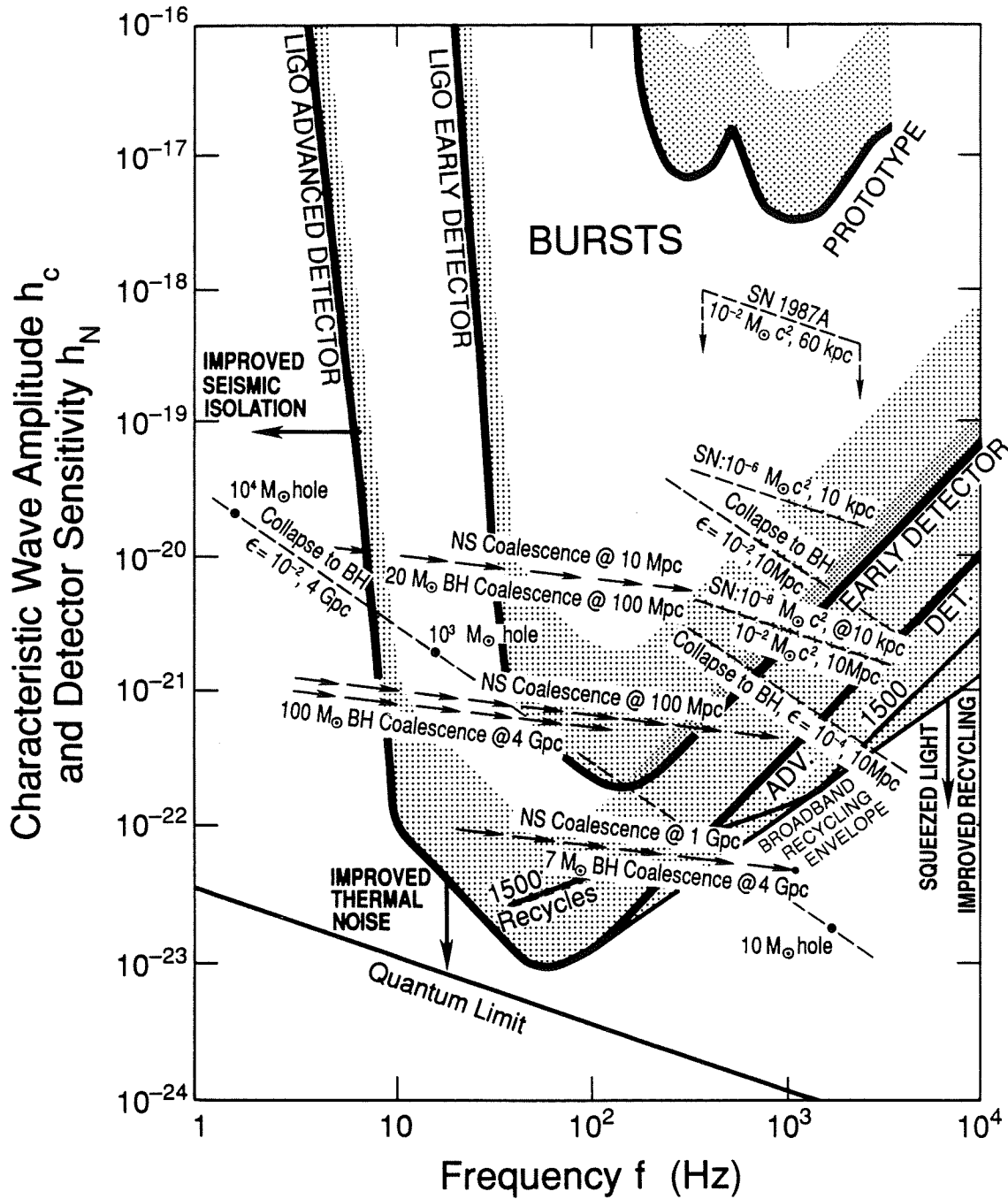


Figure II-2 A comparison of the strengths of gravitational waves (characteristic amplitude h_c and frequency f) for burst signals from various sources (dashed lines and arrows), and benchmark sensitivities h_N (solid curves and stippled strips atop them) for interferometric detectors today (*prototype*) and in the proposed LIGO (*early detector*, *advanced detector*). See the caption of Figure A-4a (a duplicate of this figure) and the associated discussion in Appendix A for more details.

By comparing the benchmark sensitivities with the source strengths in Figure II-2 (burst sources) and in Figures A-4b and c (periodic and stochastic sources) of Appendix A, one sees that *the first detector in the LIGO will have significant possibilities for detecting waves:*

- It could have detected the initial wave burst from Supernova 1987A if that burst carried $\sim 10^{-4}$ solar masses of energy or more. (This amount could easily have been the result if the collapsing stellar core were rotating rapidly enough to produce a 0.5 millisecond pulsar, as is suggested by observation.)

- It could detect the low-frequency radiation (< 300 Hz) in bursts from supernovae that have rapidly rotating cores and that fragment during the collapse—this at a distance of the Virgo cluster of galaxies.

- It could detect the coalescence of a neutron-star binary out to 30 Mpc distance (three times the distance of the Virgo cluster of galaxies).

- It could detect periodic waves from the Crab pulsar if the wave amplitude exceeds 1/10 of the current limit, which is based on the rate of spindown of the pulsar.

- It could detect a stochastic background of gravitational waves between 50 Hz and 150 Hz, if that background carries more than 2×10^{-7} of the energy required to close the universe. (This is close to the level expected from non-superconducting GUT cosmic strings, if they exist.)

If waves are not detected by the LIGO's first detector, *they probably will be detected by a subsequent detector with sensitivity somewhere between the "early detector" and "advanced detector" sensitivities of Figure II-2.* Examples that illustrate the *high* probability of detection at the "advanced detector" sensitivity are:

- The "advanced detector" could detect a supernova in our galaxy that puts out 10^{-8} solar masses of energy at frequencies of 1 kHz and less, or a supernova in the Virgo cluster that puts out 10^{-2} solar masses at 1 kHz and less.

- It could detect a neutron-star coalescence out to almost 1 gigaparsec (1/4 the Hubble distance)—within which distance there are expected to be many coalescences per year.

- It could detect the coalescence of equal-mass binary black holes throughout the observable universe, so long as the hole masses are between 10 and 1000 times the mass of the Sun.

- It could detect the Crab and Vela pulsars if they are as strong as the current (highly unreliable) best guess.

- It could detect a stochastic background between 30 Hz and 90 Hz if that background carries an energy exceeding 10^{-10} of the energy required to close the universe.

D. Other Methods of Detecting Gravitational Waves

The above discussion provides a basis for comparing the LIGO Project with other methods of detecting gravitational waves.

There is a rich potential for gravitational-wave astronomy at frequencies below the LIGO's 10-Hz cutoff, but such frequencies probably cannot be reached with Earth-based detectors. The best long-term promise in the band from 1 Hz to 10^{-5} Hz lies with interferometric detectors in space, which will rely in considerable measure on experience with the LIGO; and below 10^{-5} Hz the best promise lies with timing of pulsars and measurements of anisotropy of the cosmic microwave radiation.

In the LIGO's frequency band, Earth-based bar detectors have been under development since the early 1960s, a decade longer than interferometric detectors. Room-temperature bars achieved an h -sensitivity for bursts of 3×10^{-17} in the mid 1970s (before the Caltech and MIT prototypes were operational); by cooling to 4K, they (Stanford and Rome/CERN) are now at 1×10^{-18} . For the foreseeable future, bars will remain an important component of the world's gravitational-wave research effort and they may well improve into the vicinity of 10^{-20} , which is adequate for the detection of rare events in our own galaxy or the Magellanic clouds, but inadequate for extragalactic astronomy, the realm of large event rates.

Bar detectors cannot be lengthened to kilometer scales with an accompanying large sensitivity improvement (recall: $\Delta L \sim hL$), because they rely on sound waves (speed ~ 1 m/ms) rather than light (speed 300 km/ms) for coupling their two ends. As a result, it is unlikely they will reach the LIGO's projected sensitivity region of $\sim 10^{-21}$ to $\sim 10^{-23}$ (the realm of extragalactic astronomy) (cf. Figure II-2). Also, bar detectors have difficulty achieving large bandwidths, and correspondingly can extract only limited information from any waves they discover. At present, their bandwidths are $\Delta f/f \sim 0.01$ at $f \simeq 900$ Hz, and there is hope in the future of reaching $\Delta f/f \sim 0.2$. By contrast, the present prototype interferometers have $f_{\max}/f_{\min} \sim 10$, and the LIGO is projected to have $f_{\max}/f_{\min} \sim 1000$ (Figure II-2)—adequate for essentially full information extraction.

III. LASER INTERFEROMETERS

A. General Characteristics and Noise Effects

This section presents a brief discussion of the general characteristics of laser interferometers and of limits to the interferometers' sensitivity. For details of calculations and references to the literature, see Appendix B.

1. Gravitational-wave detection using interferometers

The sensitivity of an interferometric gravitational-wave detector— $h = \Delta L/L$ (Section II.A, Equation (II.1))—can be increased by making its arms longer, up to one-fourth the wavelength of the signal. For example, a detector optimized for 100-Hz waves would be 750 km long. Although this is prohibitively long for Earth-based detectors, interferometers several kilometers in length are realizable.

Interferometric detectors have two arms. A single, long, resonant cavity consisting of two mirrors excited by a stable laser can be used to measure motion of the cavity mirrors, motion that might be caused by gravitational waves. However, such a single-arm detector does not distinguish between a gravitational wave and frequency fluctuations in the light. A second arm is necessary to eliminate the effect of fundamental frequency fluctuations associated with all practical light sources; the maximum sensitivity is achieved when the arms are orthogonal.

2. Fabry-Perot interferometers for gravitational-wave detection

The response of an interferometer to changes in arm length can be increased by folding the optical path, thereby increasing the time that light is stored between the mirrors, until a storage time of about one-half the gravitational-wave period is reached. We have chosen to store the light by making each arm a resonant Fabry-Perot cavity.¹ Each cavity is composed of two mirrors with low-loss reflective coatings. The input mirror has a small transmission, and the end mirror is coated for highest reflectivity. The light is stored between the mirrors for a time $\tau_s \approx 2L/cT_1$, where T_1 is the intensity transmission of the input mirror. The light-transit time from one mirror to the other is $\tau_t = L/c$; one can think of the beam going back and forth between mirrors $2/T_1$ times before it reemerges from the input mirror.

One arrangement of Fabry-Perot cavities for a gravitational-wave detector is shown in Figure III-1. In their quiescent state, the cavities are in resonance² with the laser light. The incident laser light is split evenly by the beam splitter (BS) and reflects from both cavities with a phase shift of 180 degrees before returning to the splitter. There the beams are again divided. The beam returning from

¹ The theory of the Fabry-Perot cavity as an optical storage element for gravitational-wave detectors is given in Appendix B.

² The cavity length L equals a half-integral multiple of the laser wavelength.

cavity 1 (top) is in part reflected back toward the laser and in part transmitted to the photodetector (D1) at the antisymmetric port of the beam splitter. The beam returning from cavity 2 (right) is in part transmitted back toward the laser and in part reflected (with an additional 180-degree phase shift) toward the photodetector at the antisymmetric port. The two beams incident on the photodetector interfere destructively; in other words, the interferometer operates on a minimum intensity “dark fringe.”

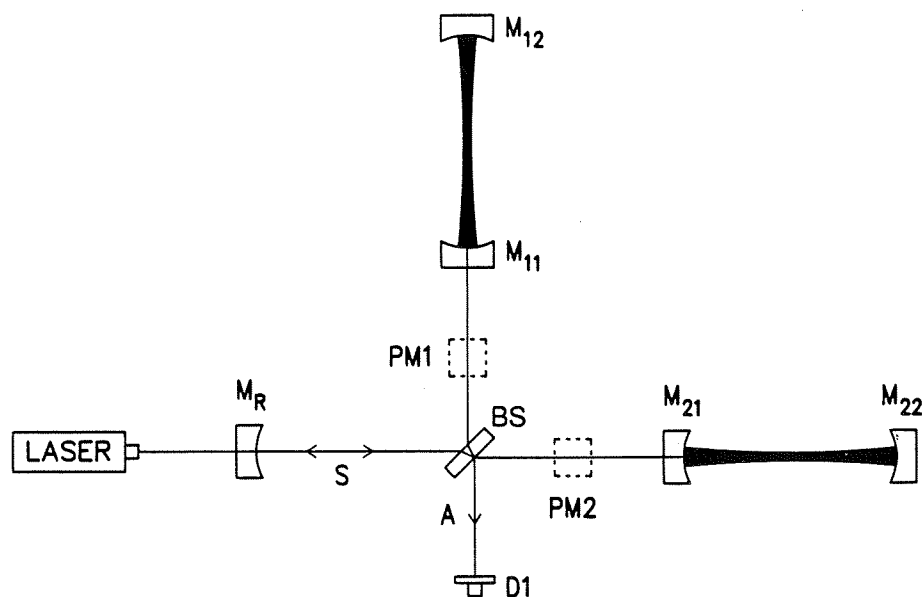


Figure III-1 Schematic of a recombined Fabry-Perot interferometer that includes a mirror, M_R , for broad-band recycling. Cavity 1 is formed by mirrors M_{11} and M_{12} , Cavity 2 by M_{21} and M_{22} . Other components include a beam splitter (BS), phase modulators (PM1 and PM2), and a photodetector (D1). The symmetric and antisymmetric ports are designated by “S” and “A”.

Assume that a gravitational wave is incident normal to the plane of the interferometer and has a polarization that stretches cavity 1 and shrinks cavity 2. When it travels through the detector, it disturbs the resonance by causing small phase shifts in the light reflected from the cavities. In the interaction with the gravitational wave, the reflected light from cavity 1 experiences, say, a positive phase shift, ϕ_1 , and the reflected light from cavity 2 has a negative phase shift, $\phi_2 = -\phi_1$. The destructive interference at the photodetector is no longer complete; a signal is developed that is proportional to the difference in phase between the two cavities, which in turn is proportional to ΔL and hence to the gravitational-wave strain, h .

The interference of the beams returning toward the laser at the symmetric port of the beam splitter is constructive (the “bright fringe”) and, if the optical losses in the interferometer are small, most of the incident light returns in this direction.

The returned light can be reused by placing a partially transmitting mirror, M_R , between the splitter and the laser. By selecting the transmission and controlling the location of this mirror, the interference is adjusted so that no light returns to the laser and the light in the cavities is enhanced.³ This technique is broad-band and has the same frequency response as the non-recycling interferometer; the only change is an increase in effective light power.

After processing, the signal from the photodetector is applied as a feedback force to cavity mirror M_{12} to hold the interferometer on the dark fringe. This use of feedback reduces sensitivity to laser amplitude noise and improves system linearity; it also makes recycling possible. The gravitational-wave signal appears at the output of the amplifier that is connected to the force transducer controlling M_{12} .

An interferometer which gives a large enhancement in sensitivity over a limited bandwidth around a chosen frequency can be obtained by arranging that the optical signal is magnified by resonance in a coupled-cavity system, in what is known as a resonant recycling interferometer. A related modification to broad-band recycling, known as dual recycling, has been proposed recently. This is a flexible optical configuration, which enables a single interferometer to be adjusted to operate over a range of modes all the way from broad-band recycling to narrow-band resonant recycling.⁴

The optical phase modulators PM1 and PM2 impress a small phase dither on the light at radio frequencies, translating the optical phase information from frequencies in the gravitational-wave band to signals at radio frequencies. This technique reduces the interferometer sensitivity to low frequency amplitude noise in the light and electronics. The optical phase modulators are also used to provide fast control of optical phase in order to stabilize the feedback loops that hold the optical fringes.

The optical components in the interferometer are suspended by wires, so above the resonance frequency of the suspensions (on the order of 1 Hz) they are effectively free in inertial space and responsive to the gravitational-wave strain. The suspensions also help isolate the optical components from seismic noise and provide a means for system alignment.

The foregoing description of a laser interferometric gravitational-wave detector gives only the basic concepts. Actual implementation of such a system involves many more components; more detailed descriptions are given in Sections III.B and V.A.

³ This "recycling" interferometer is, in effect, a resonant cavity in which the circulating power has been increased by approximately the reciprocal of the optical losses in the non-recycling interferometer.

⁴ These interferometer systems are discussed in more detail in Appendix C.

3. Noise sources and sensitivity

Sources of noise that can limit the sensitivity of an interferometric gravitational-wave detector are of three types. First, there are random processes *intrinsic* to the measurement. Examples are shot noise in the light, "quantum noise" associated with the uncertainty principle, and thermal fluctuations in masses, mirrors, suspension wires and other physical elements, that induce motions of the optical surfaces. These intrinsic noise sources give calculable theoretical limits to the detector performance.

A second source is noise induced by the *environment*; examples include the transmission of random seismic motions to the optical components, as well as random forces on the optical components due to fluctuating, Newtonian gravitational-field gradients. These influences can be reduced by good design and experiment strategy; nevertheless, they present a background that becomes increasingly important as the detector sensitivity is improved.

A third group of noise sources are *technical*. These are nonfundamental effects—those whose influence can be reduced by care and by advances in the technology. Examples are interferometer phase fluctuations resulting from instability of laser-beam geometry, phase fluctuations from residual gas along the transmission paths, and scattering of light by mirrors and tube walls.

Noise sources that have been identified, estimated, and in many cases measured in the laboratory, are listed in Table III-1. This table classifies the noise sources into two groups: those that influence the strain measurement (sensing noise), and those that impose random forces on the interferometer end points. In general, the influence of random forces is reduced linearly by increasing the interferometer arm length while the various types of sensing noise decrease as different powers of arm length.

TABLE III-1
IDENTIFIED AND ESTIMATED NOISE SOURCES

Noise terms influencing the strain measurement (various dependencies on L)

- Photon shot noise
- Laser amplitude noise
- Laser frequency fluctuations
- Scattering of light by
 1. Moving surfaces
 2. Stationary surfaces
- Laser beam fluctuations in position and angle
- Fluctuations in forward scattering of light that are caused by residual gas

Random forces on interferometer end points (all scale as $1/L$)

- Seismic noise
- Thermal noise in the suspension
- Thermal noise driving mirror modes
- Fluctuations in radiation pressure on the mirrors
- Fluctuating external gravitational gradients
- Fluctuating electric and magnetic fields⁵
- Cosmic-ray air showers⁶
- The quantum limit

⁵ Fluctuating magnetic and electric fields are not expected to be significant in the initial interferometers, but will have to be considered in the design of advanced interferometers operating below ~ 100 Hz. Electric field fluctuations ranging from 10^{-3} to 10^{-2} volts/cm arise from fluctuating charges on the surface of dielectrics and the "patch" effect (changes in the work function of conducting surfaces due to thermal migration of crystal faces or to fluctuations in the gas adsorbed on the surface). Magnetic field fluctuations ranging from 10^{-5} to 10^{-3} gauss may come from currents in wires driven by seismic noise, thermally driven polarization fluctuations in magnetic materials, or geomagnetic fluctuations, thunderstorms, magnetospheric phenomena, or transients in the power net. These fields can disturb the test masses through interaction with the much stronger electric or magnetic fields that might be used to control the position of the test masses. Shielding and careful design should bring these random forces below the level of other sources of noise.

⁶ The dominant source of noise will be the momentum transferred to test masses by secondary muons from energetic primary cosmic ray protons hitting the upper atmosphere. Individual muon events are not as significant as showers that could illuminate an entire building. The showers are not expected to give correlated events at two widely separated sites but could increase the singles rate. One scintillation detector per building will be used to monitor these events.

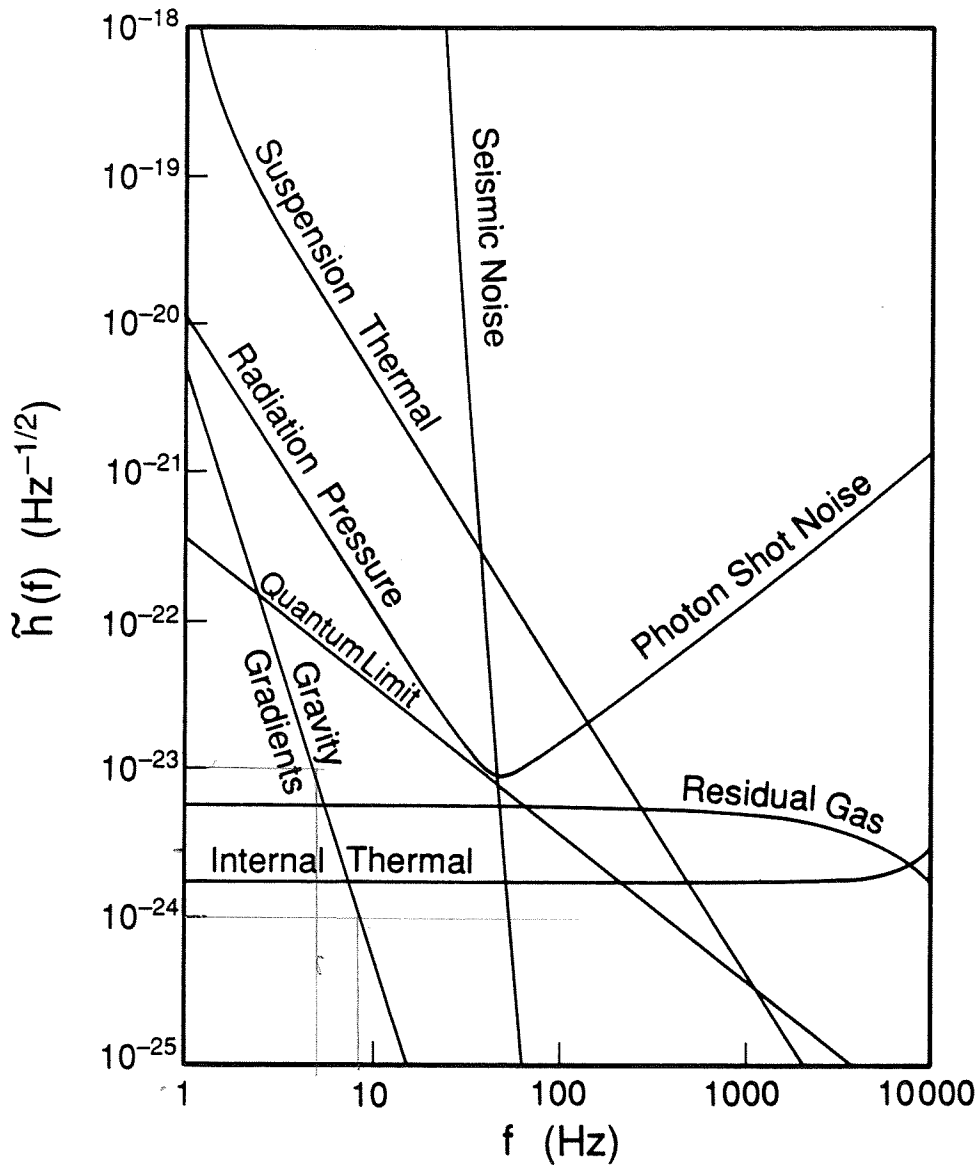


Figure III-2 Individual spectra for noise sources that can limit the performance of LIGO interferometers. They are plotted in terms of the equivalent amplitude spectral density of gravitational waves, $\tilde{h}(f)$, which has units of strain/ $\sqrt{\text{Hz}}$ and is defined in Appendix E. The expression $\tilde{h}(f)$ characterizes the instrument performance and corresponds to the rms noise amplitude normalized to an averaging time of order one second (1 Hz bandwidth). The comparison to the strength of signals depends on the signal waveform and the measurement duration (see Appendices A and E for details). The parameters used to illustrate the various noise sources are those of the initial interferometer described in Section V.A of this volume, and Section IV.B of Volume 2. The line for “photon shot noise” and “radiation pressure noise” is for a Fabry-Perot interferometer with a power buildup of 30 times (achieved with recycling), and 1 W of effective laser power (including inefficiencies). The sensitivity at the changeover from shot noise to radiation pressure noise is the quantum limit. See Appendix B for details on the other noise sources in the figure. At any frequency, the total noise level is approximately equal to the largest contributor at that frequency.

Figure III-2 shows illustrative spectra for the more important contributions to the interferometric gravitational-wave detector noise budget. In the remainder of this section we shall discuss the most important of these noise sources. Further details are given in Appendix B and references therein.

a. Photon shot noise. The ability to measure the optical phase difference at the output of the interferometer is limited by the quantum fluctuations of the light. The equivalent gravitational-wave strain noise that results from these phase fluctuations is proportional to $\sqrt{\lambda/P}$, where λ is the laser wavelength and P is the light power in the bright fringe. This photon-counting, or shot noise, depends on the gravitational-wave frequency f , and is expected to dominate the noise budget at high gravitational-wave frequencies. It also depends on the storage time τ_s ; the optimum storage time in a recycled system is $\tau_s = 1/4\pi f$. The shot noise in a broad-band recycling interferometer scales as $1/L^{1/2}$.

b. Frequency fluctuations of the laser. Laser frequency fluctuations produce phase noise if the two Fabry-Perot cavities have different storage times, τ_s . The resulting gravitational-wave strain noise spectrum is

$$\tilde{h}(f) \approx (\Delta\tau_s/\langle\tau_s\rangle)\nu(f)/\nu_0 \quad (\text{III.1})$$

where $\nu(f)$ is the spectrum of the laser frequency fluctuations and ν_0 is the laser frequency. The noise from this source is reduced by stabilizing the frequency of the laser, by balancing the two cavities, and by electronically subtracting the frequency noise common to the two arms.

Frequency noise can also enter the system through the phase fluctuations introduced by the interference between the principal beams and scattered beams that have taken different paths. The noise from stationary scatterers is reduced by using frequency stabilization. Frequency noise is not considered a major noise contributor to the initial LIGO interferometer and does not appear in Figure III-2.

c. Noise from residual gas. Residual gas in the vicinity of the test masses can produce noise by damping the suspensions (see the discussion of thermal noise, below) and by providing acoustic coupling to the outside world. These sources of noise are sufficiently reduced by operating at pressures less than 10^{-6} torr in the chambers enclosing the test masses.

A high vacuum in the long beam tubes is required to reduce the optical phase noise resulting from fluctuations in the number of residual gas molecules residing in the optical beam. The gravitational-wave strain noise spectrum is shown for an illustrative residual gas pressure (10^{-7} torr of H_2O) in Figure III-2. This noise depends on the molecular polarizability and the mass of the molecular species. Phase noise resulting from residual gas scales as $1/L^{3/4}$.

d. Thermal noise. The LIGO interferometers will operate at room temperature, and thermal excitation of mechanical elements may be a significant source

of noise. The spectrum of thermal motions depends on the frequency, mass, and the internal losses in the mechanical systems. Mechanical resonances are chosen to be outside of the gravitational-wave band. The pendulum suspensions for the optical components are designed to have resonances below the band, and the internal resonant modes of the optical components have resonances above the band.

The residual gas in the LIGO is specified to be low enough so that it does not contribute to the dissipation of the mechanical systems. The principal sources of thermal noise are expected to be dissipation in the flexure of the suspension-support elements and the internal dissipation of the normal modes of the cavity mirrors. Representative curves of the equivalent gravitational-wave strain noise, using modest-size masses and currently realized material dissipation, are shown in Figure III-2. Thermal noise is projected to be important in the noise budget of the initial interferometer at mid-frequencies; it scales as $1/L$.

e. Seismic noise. At low frequencies, an interferometer will be dominated by seismic noise transmitted through the suspension system. The amplitude of the seismic-noise spectrum varies from site to site, depends on wind conditions, and, in built-up areas, on the amount of human activity. A reasonable approximation of the noise spectrum (which we have measured at candidate sites) is given by

$$\tilde{x}(f) = 10^{-7} \left(\frac{\text{Hz}}{f} \right)^2 \text{ m}/\sqrt{\text{Hz}} \quad (\text{III.2})$$

for frequencies above 10 Hz, and as a constant $10^{-9} \text{ m}/\sqrt{\text{Hz}}$ for frequencies from 1 to 10 Hz. At frequencies above a few Hz, the seismic noise at points separated by 4 km is mostly uncorrelated; the equivalent gravitational-wave strain noise is $\tilde{h}(f) \approx 2\tilde{x}(f)/L$.

This noise level is reduced by many orders of magnitude by several cascaded spring-mass isolators, working multiplicatively with the isolation provided by the final suspension, for each test mass. Figure III-2 shows a representative noise spectrum of attenuated seismic noise⁷ for the type of multistage isolation system discussed in Appendix D. The contribution to the equivalent gravitational strain noise from seismic motions scales as $1/L$.

f. Fluctuating Newtonian gravitational gradients. Fluctuating gravitational-field gradients that arise because of moving masses in the neighborhood of the test masses may limit the performance at very low frequencies. Naturally occurring sources are the density variations in the Earth from seismic waves

⁷ This projection is not the best that can be done; seismic-noise isolation will continue to be an area in which cunning and elegance of new concepts will improve the performance of the interferometers at low frequencies. Examples of such techniques are active isolation systems and auxiliary interferometers (see Appendix C).

and in the atmosphere from sound waves. The fluctuating gravitational-field gradients are primarily uncorrelated at frequencies above a few Hertz, so the equivalent gravitational-wave strain noise from this source also scales as $1/L$. The calculated noise level is shown in Figure III-2.

g. Radiation-pressure noise and the standard quantum limit. Radiation pressure associated with the light trapped between the interferometer mirrors imparts a steady force on the mirrors, and fluctuation in the pressure driven by a fluctuating laser intensity is not expected to be a limiting factor in the LIGO performance. Additional intrinsic uncorrelated fluctuations in the radiation pressure on the cavity mirrors results from quantum fluctuations in the light.⁸ These are the source of the standard quantum limit for the interferometric gravitational detector and a macroscopic example of the application of the Heisenberg microscope. The fluctuations are uncorrelated between the cavities. Figure III-2 shows a representative estimate of the equivalent gravitational-wave strain noise from this radiation pressure source.

The radiation-pressure fluctuations are $\propto \sqrt{P}$, while the sensing shot noise is $\propto \sqrt{1/P}$. Consequently, there is an optimum circulating optical power in the interferometer that minimizes the total noise. When the interferometer operates at this power, the noise is at the standard quantum limit given by

$$h(f)_{\text{opt}} = \sqrt{4/\pi} \left(\frac{2\pi\hbar}{\eta^{1/2}m} \right)^{1/2} \frac{1}{2\pi fL} \quad (\text{III.3})$$

where $2\pi\hbar$ is Planck's constant, η the quantum efficiency of the photodetector, and m is the mass of the test mass. Figure III-2 shows the standard quantum limit for the representative system. The quantum limit is not a concern for the initial interferometers; however, it may be a fundamental limit to sensitivity and, like all other sources of random force, argues for a large detector length L .

⁸ A physically satisfying description was first given by Caves, who visualized the process by considering the fluctuating radiation pressure on the cavity mirrors as arising from the interference between the laser electric field and vacuum fluctuations entering the interferometer from the "output" (antisymmetric) port of the beam splitter.

B. 40-Meter Prototype Interferometer

The 40-meter prototype interferometer (Figure III-3), located on the Caltech campus, is the product of many years of effort in developing a laser interferometric gravitational-wave detector which uses Fabry-Perot cavities. The prototype interferometer demonstrates the feasibility and reliability of many of the proposed LIGO techniques (e.g., seismic isolation, positioning control, electro-optical servo systems), and has prepared the LIGO team to further enhance the technology. Its performance is comparable to the best existing gravitational-wave detectors. In the future, the prototype facilities⁹ will be used to identify and solve experimental problems that may arise in improving detector sensitivity, and will be used to develop and test the subsystems of full-scale LIGO interferometers.

Figure III-3 (facing page) The LIGO prototype interferometer, as of May 1989. The beam from the upper of the pair of argon-ion lasers in the foreground enters the vacuum system through a viewport on one end of a short section of vacuum tubing containing the input filter cavity. (The lower laser acts as a backup for interferometer operation, and is also used for other experiments.) The chamber in the center of the photograph houses electro-optical elements that modulate and control the phase of the beam. The beam is split in the chamber at the intersection of evacuated tubes that stretch 40 m to the ends of the corridors. (Photograph by A. Abramovici)

1. Description

The central part of the interferometer consists of two orthogonal Fabry-Perot cavities, 40 meters in length, with mirrors affixed to test masses. The chambers housing the test masses are linked by two sets of vacuum tubes: a lower pair of 20-cm-diameter tubes for the main interferometer beam, and an upper pair of 10-cm-diameter tubes for an auxiliary interferometer (under development) that will optically link the tops of the suspension wires of the test masses. Gate valves at the ends of the tubes allow the chambers to be individually vented to atmosphere without breaking vacuum in the tubes; a system of bellows compensates for atmospheric force. A cryopump maintains the vacuum at $2 \cdot 10^{-5}$ torr.

The control systems required to keep the masses precisely oriented and positioned, as well as the laser-stabilization and beam-conditioning systems, include approximately 20 separate servo loops that must function together. The interferometer has run for hour-long stretches completely unattended, even during the increased vibration levels of peak traffic, and has demonstrated the capability to operate around the clock with minimal intervention.

⁹ A second vacuum system for laser interferometers of 5-meter arm length has been constructed on the MIT campus and will be used by the LIGO team for development in parallel with the 40-meter system.

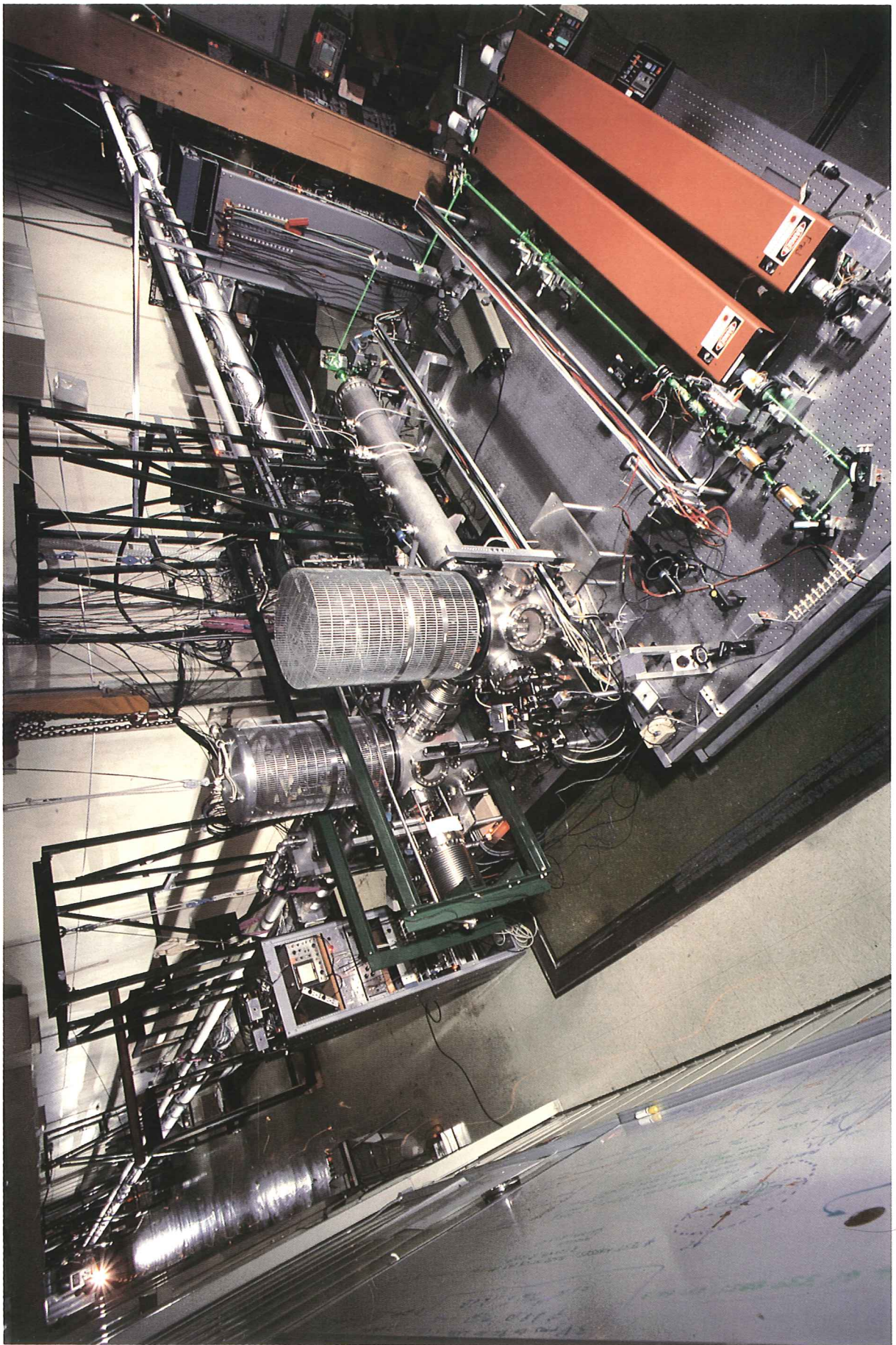


Figure III-4 shows the operational principles of the prototype interferometer, including the two-stage control of laser light frequency and phase. The optical path starts at a large-frame, argon-ion laser (Coherent I-100/20) capable of producing 5 W of single-frequency, single-transverse-mode green (514-nm) light. The beam enters an input Fabry-Perot cavity which is used as the reference for a first stage of laser frequency stabilization.¹⁰ This cavity also acts as a “mode cleaner” which filters out spatial fluctuations in the beam [III-1]. The Stage 1 frequency-control circuit causes the laser to track the mode cleaner’s length, keeping the laser in resonance with the mode cleaner at all times.

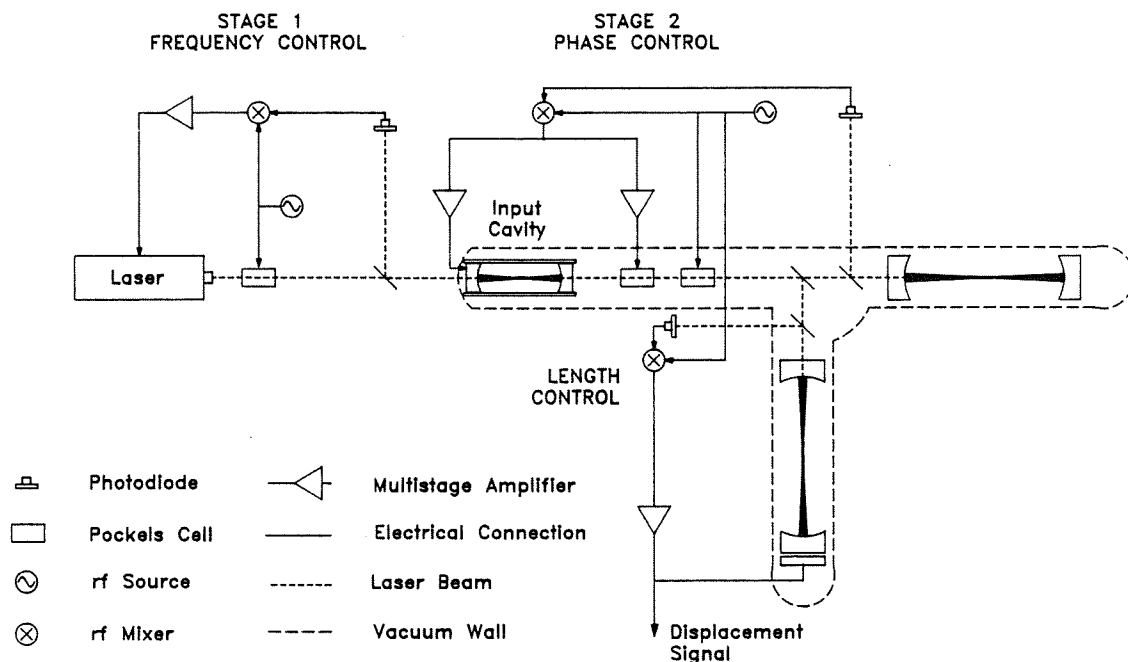


Figure III-4 The optical and electronic configuration of the 40-meter prototype interferometer, as of October 1989. Three servo loops operate to keep the input cavity and the interferometer arms on resonance. First (*Stage 1*), the laser wavelength is compared to the input cavity length by RF modulation of the optical phase via a Pockels cell. The correction signal is extracted from the reflected beam and fed back to the laser to control its frequency. Next (*Stage 2*), the light transmitted through the input cavity is stabilized to the upper interferometer arm with Pockels cells for modulation and for phase correction, and a piezo-electric transducer to adjust the length of the input cavity for frequency control. Finally (*Length Control*), the length of the other interferometer arm is controlled by pushing on the lower mass, keeping this arm in resonance with the stabilized light. The signal fed back to the mass is proportional to the length difference between the cavity arms, and hence contains the interferometer’s response to gravitational waves.

¹⁰ We thank Dr. A. Brilliet of the University of Paris-Sud, Orsay, France for providing the mechanical design of a fast piezoelectric controller for the laser frequency stabilization.

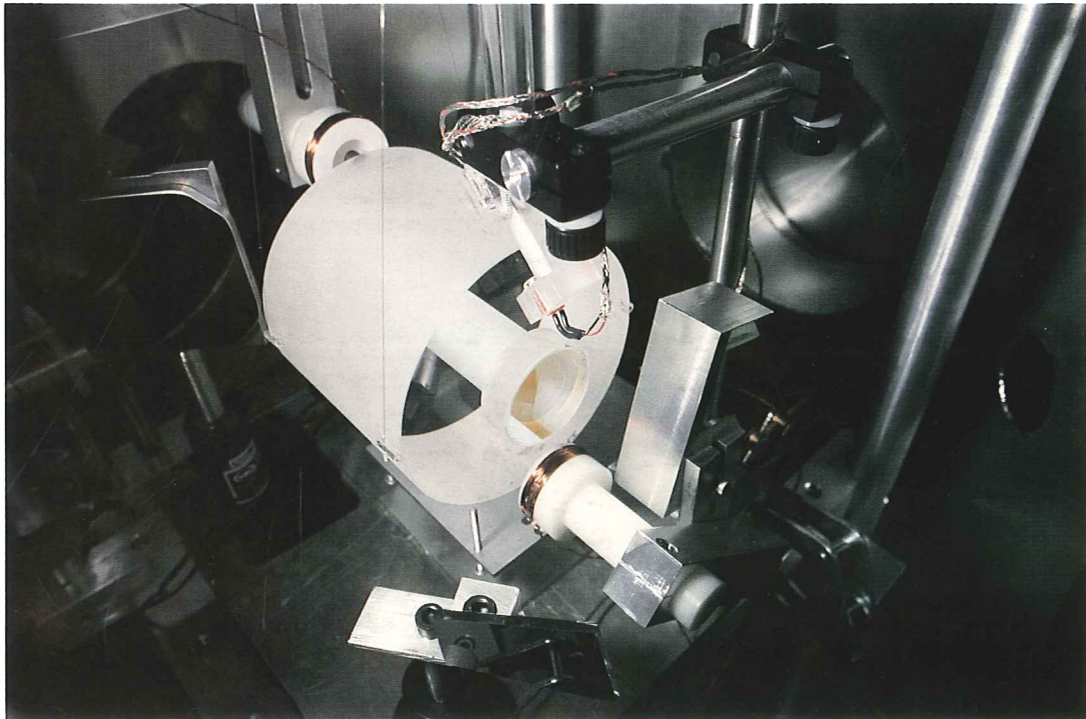
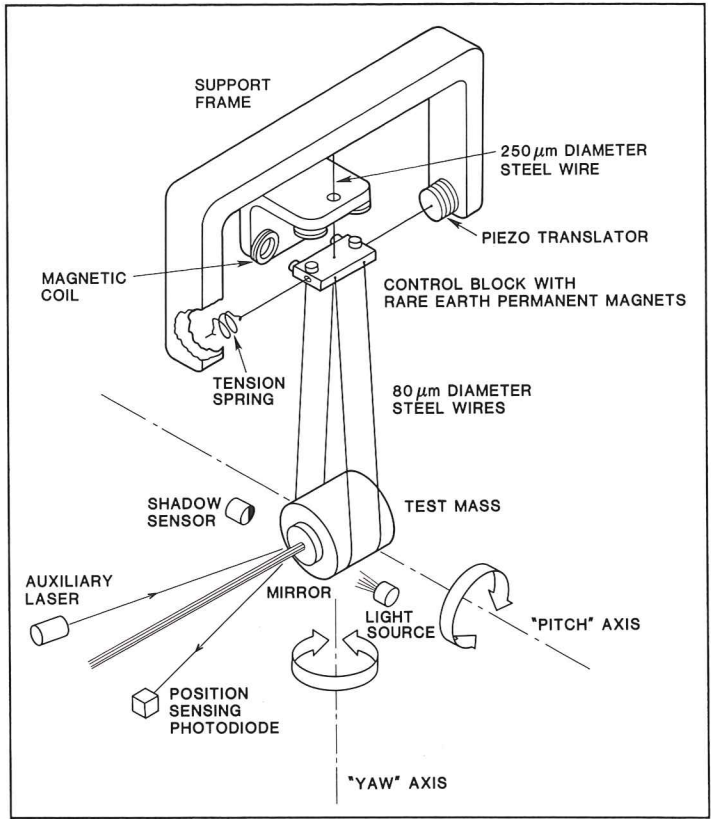
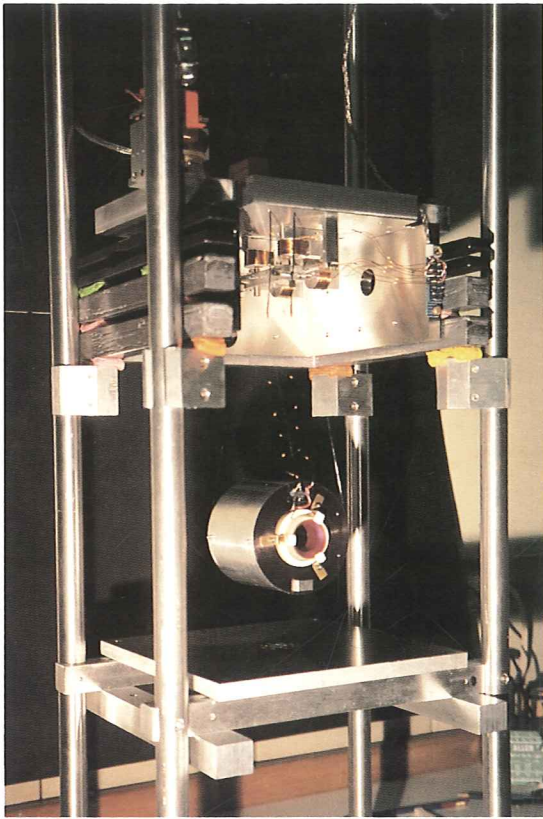
Most of the laser power passes through the input cavity to an auxiliary chamber containing Pockels cells for phase modulation and frequency stabilization. The beam is expanded by lenses to match the geometry defined by the 40-meter cavities, and directed to a beam splitter in the corner chamber.

The beam splitter divides the light between the two 40-meter-long cavities, which are operated somewhat differently from the generalized configuration described in Section III-A. Instead of being recombined optically, the output light from each cavity is detected separately.

In Stage 2, noise from frequency fluctuations in the beam exiting the mode cleaner is reduced by stabilizing this beam to the *first* arm cavity—the cavity that uses light transmitted through the beam splitter. The interference between this beam and the light stored in the cavity is detected by a photodiode and converted to an electrical signal. After amplification and filtering, the signal is used to adjust the frequency of the input light by feedback to a length-controlling element on the mode cleaner and to a phase-correcting¹¹ Pockels cell.

The Stage 2 feedback of the first arm reduces frequency fluctuations to the shot noise level defined by the arm. At the same time, it transfers information about the motion of the masses, as might be caused by a gravitational wave, to frequency changes in the light. The *second* arm—the one that uses light reflected off the beam splitter—is made to follow the frequency of the light by detecting the interference of the input light reflected by the cavity input mirror with the light leaking back from the cavity, and then using the resulting signal to adjust the length of the arm. The feedback to control the second arm contains the length difference between the arms that is the gravitational-wave signal. Length changes of the first arm contribute to the signal via the light frequency; length changes of the second arm contribute directly to the signal. A vertically-traveling gravitational wave changes the arm lengths equally and oppositely, and the resulting feedback signal is double that of the signal that would result from motion of just one of the arms. The test masses and mirrors that comprise the cavities are sufficiently well isolated from external disturbances at kilohertz frequencies that noise-induced fluctuations in the lengths of the cavities are smaller than shot noise in the light.

¹¹ The phase correction provided by the Pockels cell complements the frequency control; the Pockels cell has a faster response, but less range than the piezoelectric transducers on the mode cleaner. The two acting together track the arm length and precisely maintain the resonance condition.



2. Test masses and mirrors

Four test masses with attached cavity mirrors are housed in three 45-cm-diameter chambers: two masses in the corner chamber, and one each in end chambers at the far ends of the laboratory. Figure III-5 shows test masses with attached cavity mirrors and associated controls. The masses are cylinders of fused silica, 10 cm in diameter by 9 cm long. Their lowest internal resonance is 28 kHz, with a mechanical quality factor Q of 9×10^4 . The masses are suspended from 30-cm-long, 80- μ m-diameter steel wires, and move freely in the longitudinal direction of the interferometer beams in response to those forces which vary faster than the 1-s pendulum period. Shadow sensors, coupled with piezoelectric feedback to the suspension points of the wires, are used to damp the pendulum motion. The suspension wires serve as the final stage of seismic isolation; most of the isolation in the kHz-range occurs in three-layer stacks of lead and rubber between the top of the suspension wires and the supporting structure fixed to the vacuum chamber wall.

Figure III-5 (facing page) Details of prototype interferometer test mass and associated mirror, including wire suspension, orientation control, and seismic-isolation stacks. *Upper left:* a previous-generation aluminum test mass (ca. 1986), the magnet coils used to control orientation, and a lead and rubber seismic-isolation stack, seen edge on. *Upper right:* a schematic drawing showing the optical lever used for sensing rotation ("yaw") and tilt ("pitch") of the mass, and the permanent magnets that interact with the coils. The beam from an auxiliary laser at the far end of the tube strikes the cavity mirror and returns to a two-axis position-sensing photodiode. The electrical signal is sent to magnet coils, which twist and tilt the control block to keep the mass aligned. (The separation between the coils and magnets is exaggerated for clarity; in practice the spacing is adjusted to keep the applied torques insensitive to ground motion). Also shown are the shadow sensor and piezo-electric translator that damp longitudinal pendulum motions. A modulated beam from a light emitting diode is partially obscured by the edge of the mass, producing a spot of light on the photodetector proportional in intensity to the displacement of the mass. This signal is filtered, amplified, and applied to a piezo-electric translator at the top, damping the pendulum without adding thermal noise associated with passive viscous damping. *Bottom:* a test mass with mirror joined by optical contacting. Coils front and rear apply balanced forces to permanent magnets affixed to the test mass for high-gain control of its longitudinal position.

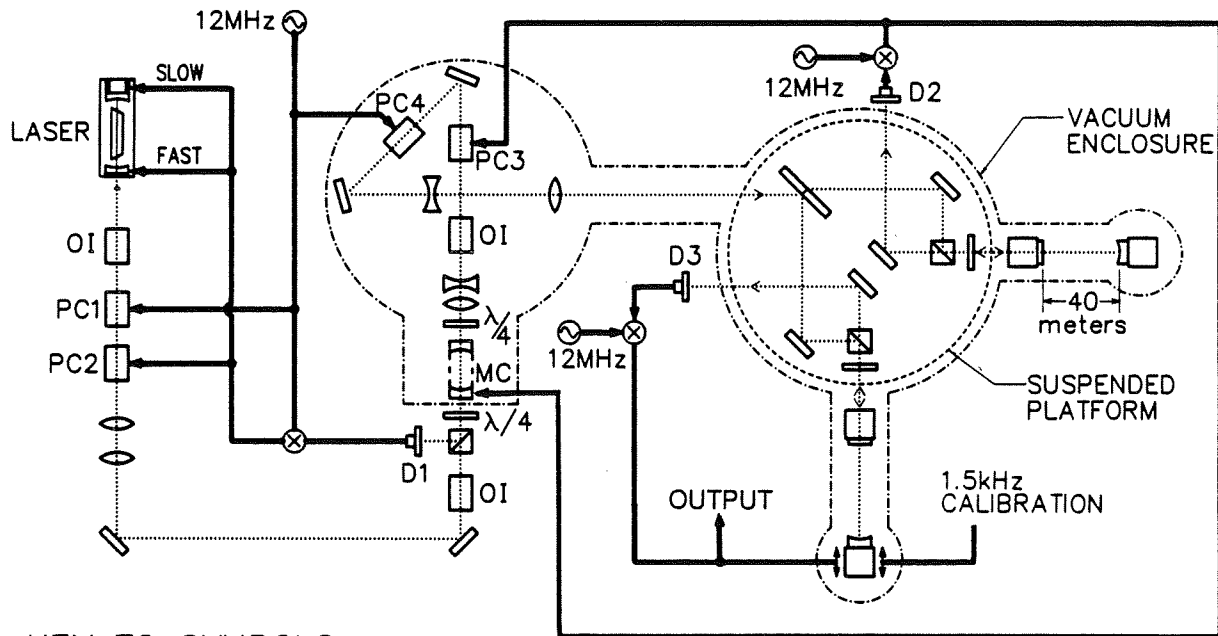
Angular orientation of the test masses is sensed by 40-meter optical levers based on low-power, helium-neon lasers. Four beams directed from the region of the central test masses traverse the vacuum tubes and are reflected from the cavity mirrors at the far ends. Similarly, beams from the ends reflect off the central masses. The return beams are sensed by two-axis, position-sensitive photodetectors which feed signals back to the mass suspensions to adjust and stabilize their angular orientations.

The interferometer mirrors are made from fused-silica substrates, 3.8 cm in diameter by 1 cm thick, polished to sub-angstrom-average surface roughness and joined by optical contacting (molecular bonding) to the test masses. The beam split-

ter output rays pass through 2.5-cm-diameter holes in the corner masses, through the planar mirror substrates, and on to the multilayer dielectric reflective coating, manufactured to transmit 450 parts per million (ppm) of the incident intensity. The mirrors at the far ends are ground with a 62-meter radius of curvature, and are coated for maximum reflectivity. The fractional energy loss due to scattering from and absorption by the mirror surfaces is less than 100 ppm per mirror.

3. Details of interferometer operation

Selected details of the operation of the current 40-meter prototype interferometer are illustrated in Figure III-6.



KEY TO SYMBOLS

Beam-splitting Polarizer	Quarter-wave plate	rf mixer
Pockels Cell	Optical Isolator	rf source
Test Mass with mirror	Photodiode	Electronic lines
Lenses		Laser beams

Figure III-6 Schematic of the 40-meter prototype interferometer, showing laser stabilization and cavity-locking servo loops. The input mode-cleaner cavity (MC) tracks the upper 40-meter arm, and the laser tracks the MC.

The first optical element in the vacuum system is the input mode-cleaner cavity (MC), made from a pair of mirrors with 50-cm-radius curvature. These mirrors are affixed to the ends of a 92-cm quartz spacer which is suspended by springs mounted on rubber-isolated blocks. Piezoelectric-transducer (PZT) elements between the

mirrors and the spacer are used to adjust the mirror separation. MC serves three purposes:

- (1) *Reduction of fluctuations in beam geometry.* The mirrors of the input cavity define a stable geometry that determines the direction and size of the output beam. Fluctuations in the beam pointing or wavefront which originate either in the laser or in the air path are suppressed by a factor of several hundred.
- (2) *Reduction of time-varying amplitude fluctuations.* The cavity acts as a passive low-pass filter against fluctuations in amplitude and wavelength that occur on timescales shorter than its storage time of 2.4×10^{-6} s.
- (3) *Frequency stabilization.* For fluctuations with timescales of about 1 ms, the cavity provides a length reference to stabilize the laser wavelength. The signal fed back to the laser reduces the fluctuations to $0.04 \text{ Hz}/\sqrt{\text{Hz}}$, compared to approximately $1000 \text{ Hz}/\sqrt{\text{Hz}}$ without active stabilization.

The modulation technique for laser frequency control [III-2] is also used on the 40-meter interferometer arms, and will be used on the LIGO. The Pockels cells PC1 and PC4 modulate the optical phase with an amplitude of approximately one radian at a frequency of 12 MHz. The phase modulation adds sidebands to the laser beam, spaced 12 MHz from the optical frequency (6×10^{14} Hz). The input cavity and 40-meter arms store the light energy for times, $\tau_s = 1/4\pi f_s$, corresponding to frequencies ($f_s = 70$ kHz and 1 kHz respectively) that are much lower than the modulation frequency. Consequently, the cavities reject the sidebands, and the light striking the photodiodes (D1 for the input cavity, D2 and D3 for the 40-meter arms) is the vector sum of two components: (1) the modulated beam reflected by the cavity input mirror; and (2) the unmodulated cavity output beam which passes back out through the input mirror. For an arm in resonance, the input and output beams have opposite phase, and the intensity on the photodiode is a minimum. If the mirror separation or the wavelength of the input beam moves slightly away from the resonance condition, the 12-MHz component of the photocurrent increases linearly. This error signal is coherently demodulated by an RF mixer which is referenced to the same oscillator that applies the phase modulation to the Pockels cell, PC4. The mixer signal from D2 is amplified, filtered, and fed back to the PZT elements and PC3 to keep the MC in resonance with the first arm. The signal from D3 is fed back to the end mass of the second arm to keep it in resonance with the light entering the beam splitter and is the output of the interferometer.

The light strikes the main beam splitter on the suspended platform after passing through two stages of stabilization. The frequency fluctuations at this point are reduced by the product of the gains in the MC loop and the first 40-meter arm loop (the upper arm in Figure III-6). This overall gain is adequate to reduce the frequency noise to the level defined by the shot noise on the light in the 40-meter arms.

4. Performance

The best gravitational-wave amplitude sensitivity achieved to date is shown in Figure III-7. Near 1.3 kHz, the sensitivity \tilde{h} is $8 \cdot 10^{-20} / \sqrt{\text{Hz}}$. The demonstrated performance corresponds to a sensitivity of position measurement of the test masses and mirrors of $3 \cdot 10^{-18} \text{ m} / \sqrt{\text{Hz}}$, corresponding to a displacement sensitivity of $\sim 10^{-16} \text{ m}$ for a 1 ms gravitational-wave burst. This sets upper limits to several sources of noise that might have been important, including thermal noise, seismic noise,¹² and noise from strain release in the suspension wires or in the masses themselves. Most of these potential sources of noise are below threshold at frequencies of $\approx 1 \text{ kHz}$ at this level of sensitivity. If the displacement sensitivity were maintained at this level in a 4-km system, the gravitational-wave sensitivity would be $8 \cdot 10^{-22} / \sqrt{\text{Hz}}$, or $4 \cdot 10^{-20}$ for a 1-ms gravitational-wave burst.

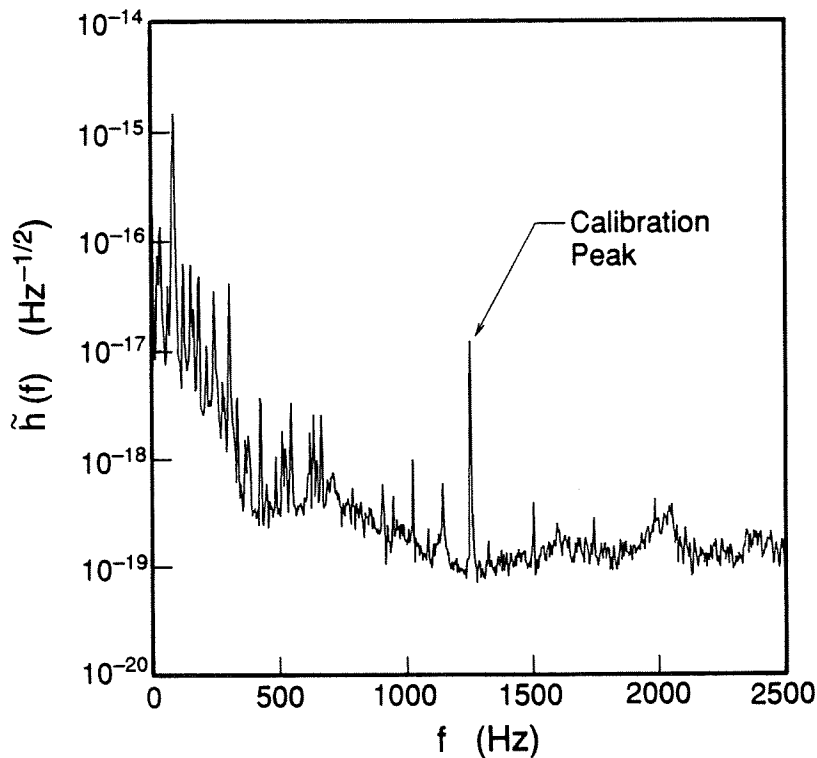


Figure III-7 Sensitivity of the 40-meter prototype interferometer. The “calibration” peak is the effect of a 10^{-15} -meter RMS sine wave motion on one of the test masses (given the 4.7-Hz bandwidth of this measurement, the calibration corresponds to 5×10^{-16} meter / $\sqrt{\text{Hz}}$). The collection of peaks below 500 Hz is in part from mechanical resonances in the beam-splitter support structure.

¹² Consistent with measurements of the isolation stacks that indicate seismic noise is at least a factor of 10 below the observed noise.

5. Future use

In addition to testing the fundamental limitations to sensitivity, the prototype apparatus is evolving to become more like the interferometers needed for LIGO operations. Many of the working units in the prototype, including much of the servo electronics, can be used in full-scale interferometers after some re-engineering. It has been demonstrated that the electronics used to stabilize laser frequency provide adequate gain, even for an interferometer with higher sensitivity than has been achieved with the prototype. Increasing the length by a factor of 100 should make possible a 100-fold decrease in equivalent gravitational strain noise from forces on the test masses, the likely dominant contributors at low frequency. Improvements now being tested show promise of higher sensitivity which can be exploited in early LIGO interferometers.

TABLE IV-1
LIGO SCIENCE CAPABILITIES

Facilities	Measurement Capability	Science Capability
I. 2 U.S. Sites	$(ah_+ + bh_x), \theta$	<p>1. <i>Physics</i>:</p> <ul style="list-style-type: none"> • Confirmation of existence of gravitational waves • Propagation speed of gravitational waves (from periodic sources, or from burst sources if event also observed in electromagnetic band) • Graviton spin (from periodic sources) • Existence of Black Holes (if sufficient number of events) <p>2. <i>Astrophysics</i>:</p> <ul style="list-style-type: none"> • Classification of signals • Statistics on types of sources (burst, periodic, semi-periodic...) • Distances and mass information for spiralling binaries • Source location on cone (from "time of flight") • Search for stochastic background
II. 2 U.S. + 1 abroad or 3 U.S.	h_+, h_x, θ, ϕ	<p>All of I, plus</p> <p>1. <i>Physics</i>:</p> <ul style="list-style-type: none"> • Graviton spin (from polarization of waves) • Test of general relativity in strong-gravity, high-speed regime (via Black Hole waveforms) <p>2. <i>Astrophysics</i>:</p> <ul style="list-style-type: none"> • Source location (θ, ϕ) • Waveforms give information on sources: e.g., core dynamics of supernovae, pulsar deformations, starquakes • Sky survey of sources
III. 2 U.S. + several abroad	h_+, h_x, θ, ϕ	All of II, but at higher sensitivity; more accurate source locations

IV. LIGO CONCEPT

A. Requirements

The Laser Interferometer Gravitational Wave Observatory (LIGO) will support a nationwide program in gravitational-wave astronomy over a period of decades. Resource constraints and other considerations prescribe a phased implementation of the project; we plan an orderly progression from startup of operations to the ultimate achievement of the LIGO capabilities.

The LIGO conceptual design has been guided by two goals: (1) maximizing the probability of detecting gravitational waves, and (2) extracting maximum information from the waves. The proposed design also provides the ability to maintain a continuous gravitational-wave monitoring program while allowing simultaneous development of enhanced-sensitivity and increased-bandwidth LIGO detectors. Specifically, the LIGO is designed to accommodate three primary objectives:

- *Observation* – the ability to monitor gravitational waves continuously (a “gravitational-wave watch”).
- *Development* – the capacity for final development and full functional testing of new and advanced interferometer-based detector concepts. Initial development of component parts will take place in campus R&D facilities.
- *Special Investigations* – the ability to accommodate specialized detectors to carry out scientific investigations of particular phenomena.

The LIGO design will allow the three primary missions to be conducted without mutual interference.

While the proposed LIGO, even in its initial phases, allows the unambiguous identification of gravitational waves and the pursuit of a number of physics and astrophysics objectives (see Table IV-1), one or more additional detectors at other sites are required to extract full waveform information ($h_+(t), h_\times(t)$) and source location (θ, ϕ). Present planning assumes the construction of one or more laser interferometer facilities in Australia, Europe, Japan, or elsewhere (see Section X.A). In the very unlikely event that none of these should be constructed, it may be appropriate to build a third facility in the U.S.; the decision to do this is not required as a prerequisite for discovering gravitational waves.

The design goals dictate the following essential features of the LIGO:

- (1) Two widely separated sites under common management.
- (2) Vacuum systems to accommodate interferometer arm lengths of up to 4 km at each site.
- (3) The ability to operate several interferometric detectors at each site simultaneously and without mutual interference.
- (4) The ability to accommodate interferometers of two different arm lengths, at

least at one site.

- (5) A vacuum tube with a clear optical aperture of approximately 1 meter for the full length of the arms.
- (6) The ability to produce a vacuum of order 10^{-9} torr of hydrogen and 10^{-10} torr of other gases.
- (7) A minimum 20-year lifetime of the facilities.
- (8) Adequate support instrumentation.

Discussion of these essential features follows:

1. Two detectors at widely separated sites under common management

a. Detector requirements. At least two detectors located at widely separated sites are essential for unequivocal detection of gravitational-wave bursts. The only means to eliminate the large set of external noise sources which includes seismic and acoustic noise as well as internal phenomena such as laser fluctuations, sudden strain release in wire suspensions, and residual gas bursts is to operate two or more detectors with comparable sensitivities at separations sufficiently large so that the noise at the two locations is uncorrelated over the time resolution of the detector pair. Gravitational-wave signals, by contrast, would be correlated.¹ Also, the detectors should be sufficiently far apart to give source location information from time-of-flight measurements. Distances of the order of the continental size of the United States meet these requirements.

b. Common management. We consider it essential that the design, construction, and gravitational-wave searches of a two-site LIGO be conducted under a single management (as opposed to, for example, a multinational consortium). The LIGO technology is not "mature;" it is a first time effort. Design and development decisions embrace considerable latitude, and there must be a project director vested with the power to make decisions. Single management is needed during construction to: (1) optimize design tradeoffs, (2) assure a common completion schedule for both facilities, and (3) guarantee overlap of operating frequencies and sensitivity.² During operations, single management can effectively balance the conflicting requirements of maintaining maximum observatory "live-time," carrying

¹ Note that *periodic* source emissions, in principle, can be detected with a single-site detector, taking advantage of the frequency modulation given to the signal by the Doppler shift due to Earth's motion relative to the source. We believe it to be unwise, however, to initiate a search for gravitational waves with periodic sources as the only targets. Burst sources are likely to be stronger than periodic ones, in terms of signal-to-noise ratio; and the only source for which the strength estimates are fairly reliable is a burst source (coalescence of binary neutron stars). Moreover, there is value in having a second site, even in a periodic search, to help separate periodic signals of local origin from periodic gravitational waves.

² To the first order, the least sensitive detector sets the threshold for discrimination against spurious events and thus for successful detection.

out systematic investigations of the noise in the interferometers, and continuing development of the instruments.

2. Arm lengths of 4 kilometers

The choice of interferometer arm length is a complex tradeoff between achievable sensitivity and cost. A “first-order” version of the tradeoff is as follows (see Appendix B for details). In the frequency range $f \lesssim 100$ Hz, where the anticipated signal-to-noise ratios are expected to be the largest and the only fairly reliable source (coalescing binary neutron stars) resides, the dominant noise is likely to be random forces on the test masses (seismic, acoustic, thermal noise, and local gravity gradients). For distant sources, the gravitational-wave event rate (or probability of detection) scales with detector sensitivity as h_N^{-3} (h_N = equivalent detector-noise-strain amplitude). Because h_N scales with arm length as L^{-1} in this regime, the event rate scales $\propto L^3$. The coalescence of neutron-star binaries in distant galaxies is one of the most promising sources for detection, and an arm length of 4 km is required for sensitivity adequate to yield a good chance of seeing this source (see Section II, Figure II-2).

Practical considerations also favor arm lengths of about 4 km. For arm lengths $L \lesssim 4$ km, the fixed costs of the facilities (including buildings and vacuum facilities for optics) are much larger than the length-dependent costs (tubes); it is cost effective to maximize tube length for maximum sensitivity. Estimates of LIGO construction funding exclude placing the vacuum tubes in subterranean tunnels; more economical surface or open-ditch construction is mandated. Topographical data from a search for sites in the U.S. revealed a dramatic dropoff of possibilities at a range of 4 to 5 km. The choice of 4-km arms is a compromise between gravitational-wave-strain sensitivity, cost, and site availability.

3. Capability for several simultaneous interferometer systems at each site

The facilities will be designed to support three detector systems between the two sites, allowing the simultaneous pursuit of observations, detector development, and special investigations without mutual interference. The ability to support more than one detector system is required because (1) gravitational-wave bursts are believed to be relatively rare events, thus requiring continuous monitoring, and (2) the development and testing of interferometers that are new, more sensitive, or have different frequency ranges require unrestricted access to the LIGO facilities for periods of months or years.

4. Interferometers of different arm lengths

One of the two U.S. sites will be configured to accommodate interferometers with both 2 and 4-kilometer arm lengths acting together as a single detector system. The fact that gravitational-wave signals are proportional to arm length can be exploited to discriminate between them and local noise, which generally is not proportional to the interferometer length. In addition, the operation of any additional interferometer, whether full or partial length, will improve the rejection of accidental coincidences. Such rejection of spurious signals will be essential for unequivocal identification of gravitational-wave bursts (see Section VII).

The availability of a dedicated paired interferometer at the same site also will provide a useful diagnostic tool in interferometer development, particularly in rejecting noise sources not detected by the environmental, facility, and interferometer monitoring systems.

A gravitational-wave *detector* unit thus consists of one full-length (4 km) interferometer at each of the two sites and a half-length interferometer (2 km) at one site. Providing this additional capacity at only one site saves costs and at present appears adequate for initial operation.

5. Vacuum-tube clear aperture approximately 1 meter in diameter

The choice of beam-tube³ diameter is an irreversible decision once the facilities are constructed. The clear aperture must accommodate not only the initial goals, but also the plans for full-facility utilization including a wide range of interferometer designs and optical technologies that eventually may be required.

A clear aperture of 1-meter diameter has been chosen because it will accommodate up to six Fabry-Perot interferometers, using 0.5 μm light, without significant diffraction loss or scattering by the tube walls. This aperture includes room for auxiliary beams for orientation control of the test masses and for monitoring the seismic motion of their suspension points. The 1-meter aperture would also be filled by a single delay-line Michelson interferometer operating at 1 μm .

6. Vacuum level of order 10^{-9} torr

The vacuum system will be designed so that fluctuations in the index of refraction of the residual gas in the interferometer arms (see Appendix B) will not become a limiting noise source. The ultimate sensitivity goals require residual gas pressures of less than about 10^{-9} torr for hydrogen and 10^{-10} torr for nitrogen or water. These pressures can be achieved through a combination of selection and preparation of materials, bakeout, and pumping strategy (see Volume 2, Section IV.D). The sensitivity of the first LIGO detector in broad-band operation (Figure V-3) may tolerate higher pressures, but the attainable vacuum cannot be allowed to limit sensitivities of this or of advanced interferometers in any mode of operation.

³ The "beam tube" provides the vacuum envelope for the 4-km interferometer arms.

7. Minimum 20-year lifetime of the facilities

The LIGO facilities are expected to support the evolution of gravitational-wave detectors with sensitivities that continually improve. Specialized interferometers will be developed with enhanced sensitivities for specific frequency bands or waveforms. As with other kinds of astronomical observatories, scientific productivity will be dependent in large measure on improvements in instrumentation over a period of many years.

The 20-year lifetime requirement is intended as a guide for design tradeoffs that balance capital costs against operating costs. The total life-cycle costs will be minimized. The facilities will maintain flexibility to deal with a variety of possible future situations (e.g., quick discovery of strong waves or a long span with no evidence of even weak waves).

The goals for the LIGO include not only the discovery of gravitational waves, but also opening of the field of gravitational-wave astronomy and a long-range program of scientific exploration.

8. Support instrumentation

The LIGO facilities will include instrumentation to monitor environmental disturbances (e.g., acoustic, seismic, electromagnetic interference, and cosmic rays) for possible correlation with interferometer signals.

B. Implementation

1. Phased construction

The LIGO is being designed to give a high probability of detecting gravitational-wave signals and thereby establish the field of gravitational-wave astronomy. A less ambitious goal would be incommensurate with the costs and scientific efforts expended. It is clearly not sufficient to plan the LIGO as only an extension of the technology development and demonstration now being carried out in prototype research.

Prototype design and development for laser interferometric gravitational-wave detectors has been underway for close to two decades. The next epoch of development requires arm lengths that cannot be accommodated on a university campus. Large facilities in remote areas are needed. There would be no significant cost savings in constructing intermediate sized facilities (e.g., interferometers of 1-km arm length); on the contrary, the long-range schedule delays and cost impacts of such a strategy would be negative. Stepping up to the ultimate, 4-km facility is, therefore, a prudent and logical initial course of action.

Similarly, the postponement of some costs by delaying construction of the second site would be far outweighed by the penalties of being unable to discriminate between noise and gravitational waves using correlations between widely separated sites. The initial construction of a two-site observatory, therefore, is both prudent and cost effective.

The only parameter that allows cost-saving compromises for the initial construction and startup periods, with tolerable impact upon subsequent capability to expand the system, is that of the number of interferometric detectors provided. The full LIGO system incorporates three detectors that allow concurrent observation, development, and special investigations. An optimal startup system would have two detectors, i.e., six interferometers distributed over two sites, four at Site 1 and two at Site 2. This would assure the most efficient progress towards the detection of gravitational waves by allowing the use of one detector in the dedicated observation mode while permitting the development of a next-generation, more-powerful system, in the second detector facility.⁴ Such a system, however, would exceed the funds expected to be available for the initial construction phase considered in this proposal.

We propose, therefore, an evolution of the LIGO in three phases.⁵

- *Phase A, The Exploration/Discovery Phase*, provides a *one*-detector facility that allows the conduct of observation *or* development. The facility has full capability for the discovery of gravitational waves and for early observatory operations, but progress will be limited by the competition between dedicated observations and advanced detector development. In particular, if the (yet unknown!) strength of gravitational-wave signals should fall below the sensitivity of the initial detector, the distribution of time between observation and development will present a serious judgmental challenge. However, at the very least, LIGO/Phase A will allow a full confirmation of the design performance of the LIGO system and will provide the basis for evaluation and decisions on future enhancements of the LIGO system.
- *Phase B, The Discovery/Observation Phase*, provides a *two*-detector facility⁶ that allows concurrent observation *and* development or specialized search.

Should gravitational waves have been discovered in Phase A, then Phase B, with its enhanced two-detector capability, will allow the continued collection of data via the dedicated observation detector while allowing the development of more advanced detectors with enhanced performance in strain sensitivity, gravitational-wave frequency coverage, and optimization for source types on the second LIGO detector.

Should the initial Phase-A detector demonstrate design performance but not have detected gravitational-wave signals, it might be prudent to introduce the enhanced capability of Phase B to accelerate the discovery of gravitational

⁴ While the campus laboratory facilities will allow some engineering development of more advanced interferometers, the LIGO facilities will be needed for full development.

⁵ Note that this proposal asks for approval of Phase A only. The Phase-A design accommodates subsequent implementation of Phases B and C, to be proposed at a future time.

⁶ It is possible, of course, to implement Phase B in steps, e.g., with the installation of the vacuum enclosures for one additional interferometer at a time. Described here is the end goal of Phase B.

waves.

- *Phase C, The Observatory Phase*, provides a *three-detector* facility that allows concurrent observation, development, special investigations, and optimal access for the scientific community at large. It completes the LIGO evolution to its presently conceived full-design capability.

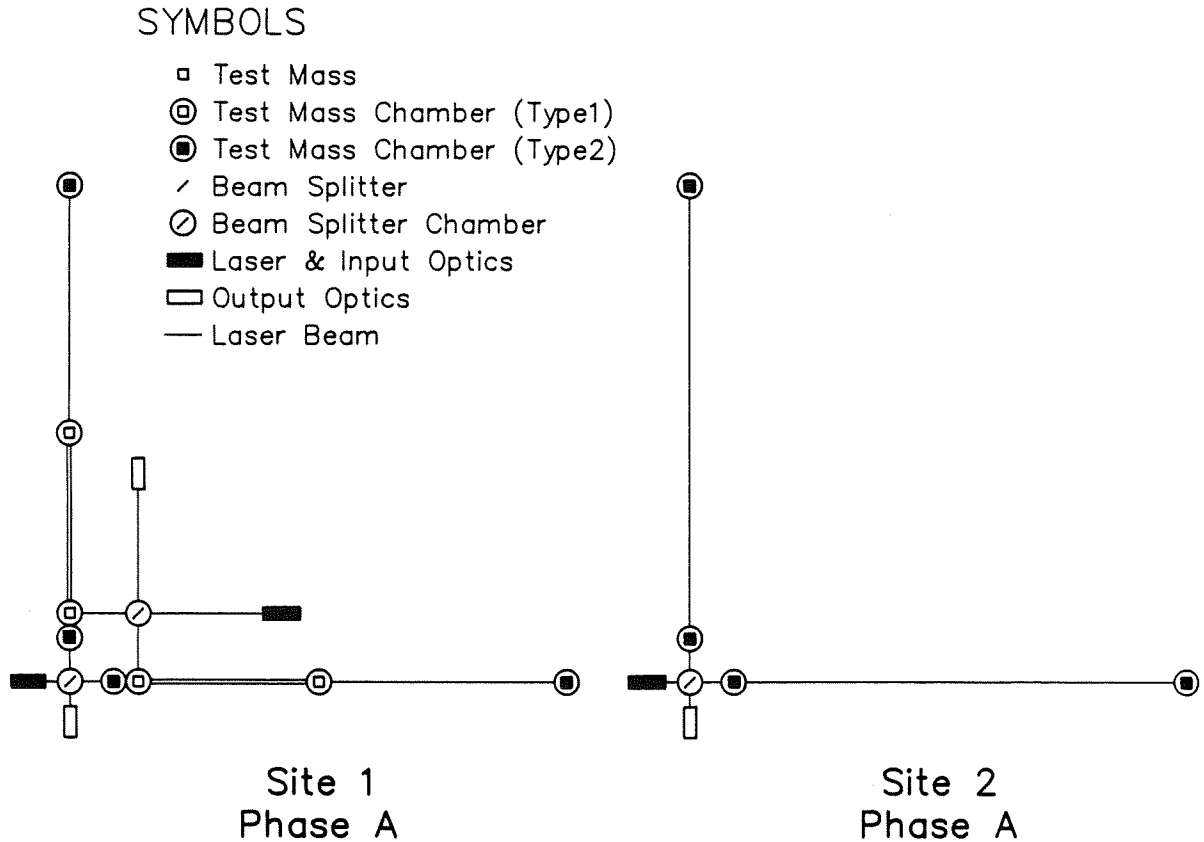


Figure IV-1 LIGO Phase A configuration at Sites 1 and 2. (See Volume 2, Section IV.C for descriptions of the two types of test mass chambers.)

a. LIGO configuration in Phase A. The LIGO Phase-A configuration is schematically illustrated in Figure IV-1. Phase A accommodates two Fabry-Perot interferometers at Site 1, of nominally a full-length and a half-length configuration;⁷ Site 2 accommodates one full-length interferometer. The three interferometers, the full- and half-length pair at Site 1 and the full-length version at Site 2, form a single detector. The facility is designed so that test masses, beam splitters, and all other in-vacuum components of the half-length interferometer at Site 1 can be introduced

⁷ It is possible to convert the half-length interferometer into a full-length version by transfer of its test mass from the mid length test- mass chamber to the end test mass chamber, but with some restrictions on the size of individual masses.

or removed from the vacuum system at will, without breaking the vacuum of the full-length interferometer or interrupting its operation, and vice versa.

Phase A thus has adequate facilities to support an initial observation and development program, and to conduct triple coincidence searches for gravitational waves to the ultimate sensitivity of the interferometers. The main limitation of this system is that full-scale LIGO detector development and testing is mutually exclusive with observation.

The Phase-A system is designed to allow expansion to Phase B without extensive interruption of operations.

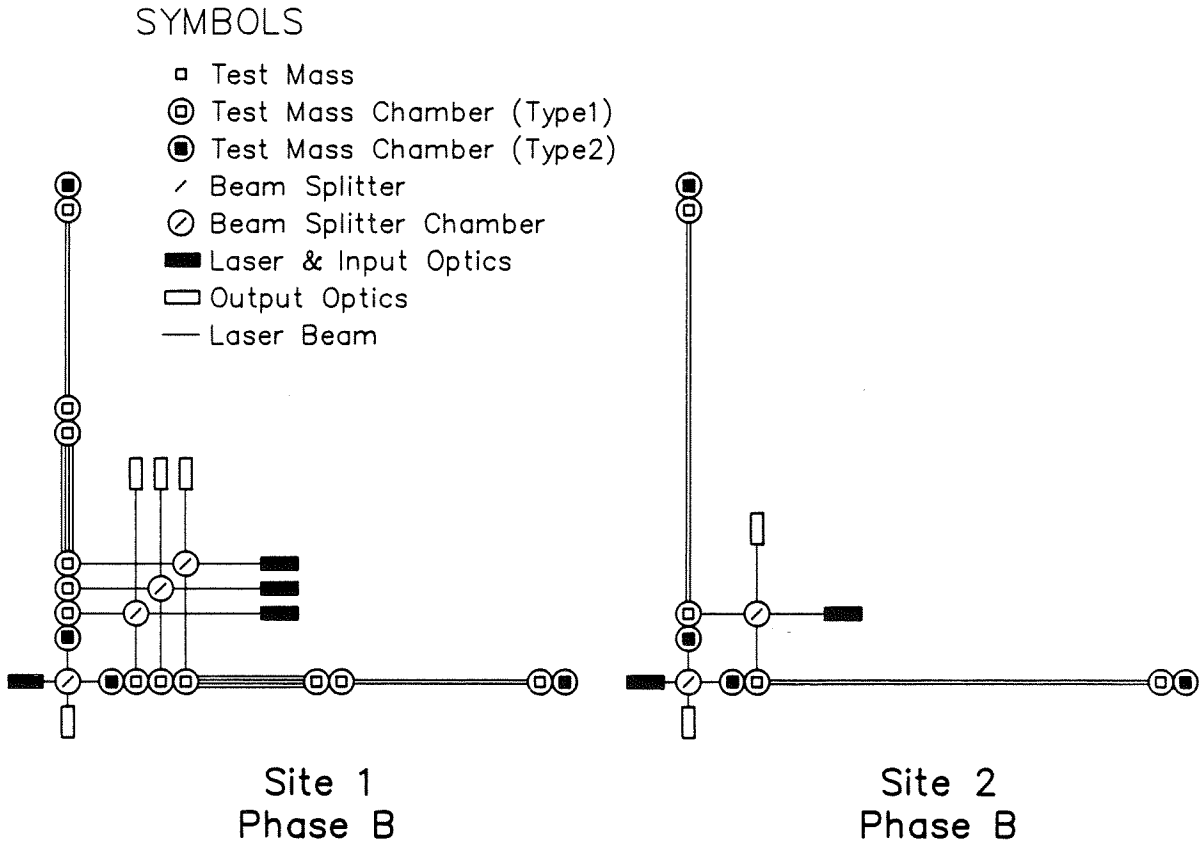


Figure IV-2 LIGO Phase B configuration at Sites 1 and 2.

b. LIGO configuration in Phase B. Phase B (Figure IV-2) doubles the capacities of Sites 1 and 2. It accommodates four Fabry-Perot interferometers at Site 1, that is, two full-length and two half-length configurations. Site 2 accommodates two full-length interferometers. This increased capacity allows the operation of two complete triple-coincidence detectors, each consisting of a full-length plus a half-length interferometer at Site 1 and a full-length interferometer at Site 2. The facility is designed so that the detectors (e.g., a development and an observation detector) can

be operated independently and without mutual interference. Test masses and optical components of any of the interferometers can be introduced or removed from the vacuum system without breaking vacuum and without interrupting operation of the others.

Phase B thus has adequate capacity to support, concurrently, observation and development of two independent observations, to the ultimate design limit of the facility.

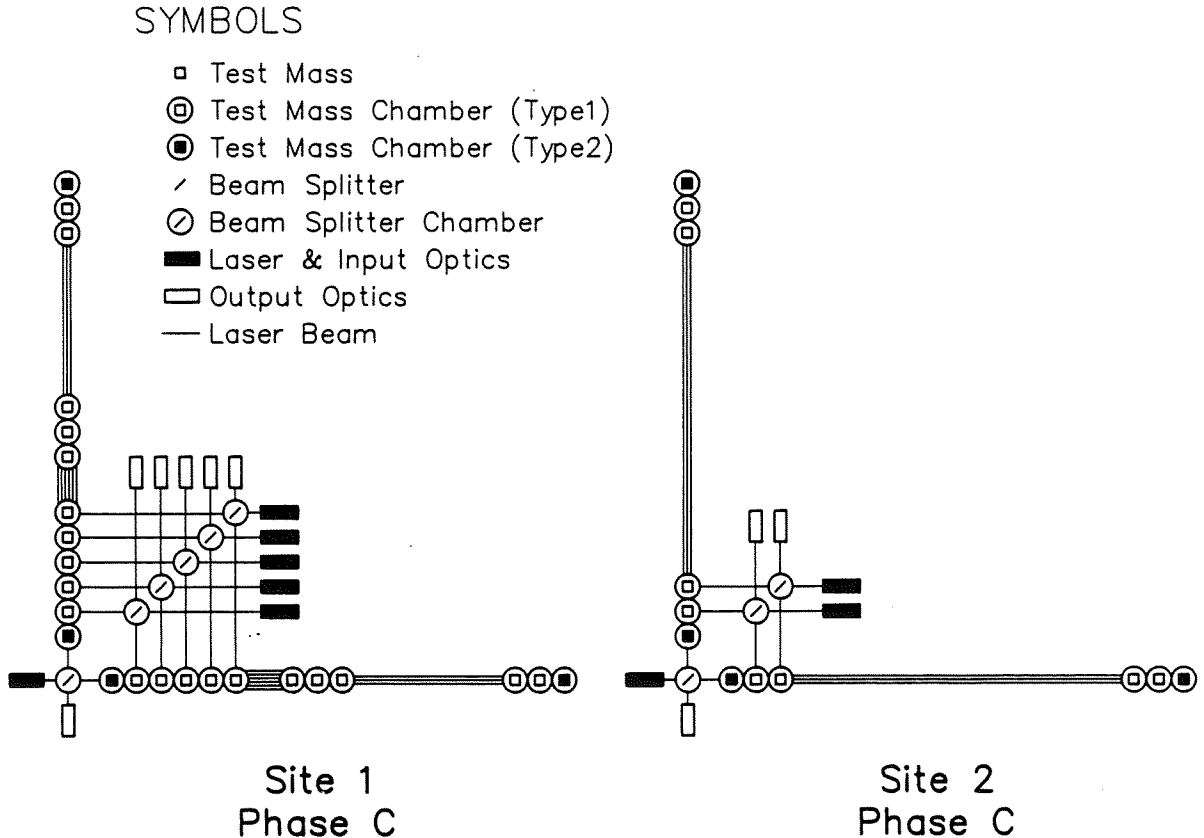


Figure IV-3 LIGO Phase C configuration at Sites 1 and 2.

c. **LIGO configuration in Phase C.** Phase C (Figure IV-3) will add a third interferometric detector port, providing for *special investigations* and opening up the facility for optimal access to the scientific community at large (see Section VI.B).

Phase C, as currently envisaged, is our present best concept for the evolution of the LIGO. In practice, the discoveries in Phases A and B will guide further development. Once gravitational waves have been observed, scientific needs will determine the best design for subsequent phases, as will considerations driven by the (then presumably existing) international network of gravitational-wave interferometric facilities.

2. Laser strategy

Gravitational-wave laser interferometers require extremely stable, single-mode, continuous-wave lasers. Our present prototypes use commercial large-frame argon-ion lasers operating at 514 nm wavelength. These lasers have been rebuilt in our laboratories for improved vibration isolation and have been further stabilized with high-gain control loops (see Section III.B). Their maximum light output is about 5 W single line. They consume about 55 kW of electrical power, plus about 25 kW for cooling.

The performance expected of the initial LIGO interferometers (Figure V-3) can be met with one such laser per interferometer. Higher power performance could be achieved by coherent addition of several argon-ion lasers, although at significant power costs.

We have adopted the following strategy: each LIGO installation will be configured to provide about 320 kW of power for all lasers on site. This allows the simultaneous operation of four interferometers with one argon-ion laser per interferometer, or the operation of a single interferometer with four coherently added lasers, at a total laser light output of 20 W. We consider this arrangement satisfactory for the initial LIGO operation.

To provide for future requirements, we have begun a collaboration with Professor Robert Byer's laboratory at Stanford University to develop solid-state Nd:YAG lasers for LIGO operations. The lasers will be frequency doubled to a wavelength of 530 nm, close enough to the argon-ion wavelength to allow replacement without major configuration changes. We expect these new lasers to be available for the LIGO before the need for higher power levels becomes serious. In fact, there is good reason to believe that these lasers will be available before or shortly after startup of LIGO operations.

Nd:YAG lasers are about 100 times more efficient than argon-ion lasers, and a single Nd:YAG laser is expected to deliver on the order of 100 W of power. This power is adequate for the most advanced detector designs under consideration; therefore, contingent on the success of the laser development program, the planned power capacity of the LIGO will accommodate the requirements of advanced interferometers.

3. Site strategy

Two sites are essential for the unambiguous detection of gravitational waves. Site selection and development depend on considerations discussed in the following paragraphs (for details, see Section V.C).

a. Scientific considerations.

i. *Interferometer alignment.* If the interferometers at the two sites are "co-aligned" (the alignment of the arms coincides when projected onto the bisecting plane), the instruments are optimally sensitive to the same polarization state, and the probability of wave detection in coincidence is maximized. If one of the interfer-

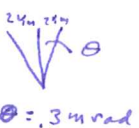
ometers, instead, is rotated 45 deg relative to co-alignment, the two are most sensitive to orthogonal polarizations and together extract the most information from the waves. We have chosen co-alignment to optimize the probability of discovery.

ii. *Distance between sites.* Optimization of the chance of discovery dictates that the sites be much farther apart than the correlation lengths of the various noise sources that can affect the interferometers; for this, 300 km is estimated to be adequate. Optimal determination of source directions, via time-of-flight between sites dictates a separation between sites as large as possible. If the site separation exceeds about 4500 km, then the overlap of the two beam patterns of interferometers at the two sites is significantly debilitated, and the detector's sensitivity is correspondingly reduced.

iii. *Direction between sites.* The probability of detection is not significantly sensitive to the geographic locations of two sites, but the accuracy of position determination via time-of-flight between sites will be direction sensitive when there is a network of three or more detectors. Optimal directionality requires a minimum of four detectors at the corners of a tetrahedron of maximum volume; failing that, there should be at least three detectors at the corners of a triangle of maximum area. The American sites will be chosen to contribute significantly to the area of an America-America-Europe triangle and to the volume of a global tetrahedron.

b. Local specifications for U.S. sites. The allowable tolerances on positioning an interferometer vacuum system at a site (such as tolerances on the 4-km nominal arm length and on the 90-deg angle between arms) have been chosen to optimize scientific returns but are constrained by construction costs. They are listed in Volume 2, Sections II and V.

An important consideration is the requirement that the LIGO arms be installed level within a few milliradians. This restriction is dictated by the fact that the "free" character of an interferometer's inertial test masses is generally brought about by a pendulum suspension. The isolation of pendulum suspensions from vibration and thermal noise is most effective when the optical axis of the interferometer is normal to the local gravity vector. The slope of the arm compromises this isolation. Note that the curvature of Earth over 4 km imposes an irreducible angle of 0.6 milliradians between the direction of the local gravity vectors at each end.



c. Site selection. Site accessibility, availability, topography, and geophysical nature are variables that may affect possible scientific return and construction costs.

We have undertaken a broad survey of potential sites in both the western and eastern United States. A smaller set of the more promising sites (Volume 2, Section V) has been further investigated for geotechnical and environmental features.

We propose to present to the National Science Foundation a short list of potential east- and west-coast sites, with detailed discussions of their properties. We hope to generate, together with NSF, a list of final candidates. Final selection will depend on the results of remaining geotechnical surveys (which can be conducted

only with permission of the land owners) and on our ability to negotiate satisfactory use permits with the owners.

V. DESIGN AND SITING OF INTERFEROMETERS

A. Conceptual Design of the Initial LIGO Interferometers

The general features of the initial LIGO interferometers are described in this section. Their detailed conceptual design will be initiated in the near future, and will reflect future research and development activities on the 5-meter and 40-meter interferometer prototypes. A design freeze for most subsystems of the initial interferometers will occur about 1 year after construction start, i.e., 2 years before completion of the first LIGO vacuum facility.

1. Comparison of prototype and initial LIGO interferometers

The initial LIGO interferometers will be based on the concepts being developed in the prototypes and on scaled-up versions of many of the prototype subsystems now in use. Table V-1 compares the parameters of the current prototype interferometer to those of the planned, fully evolved initial LIGO interferometer.

TABLE V-1
PARAMETERS OF PROTOTYPE AND LIGO INTERFEROMETERS

PARAMETER		PROTOTYPE	INITIAL LIGO
Optical Power:	Laser Output	5 W	5 W
	Bright Fringe	0.10 W	1 W
Main Cavities:	Configuration	Separately detected Fabry-Perot	Optically recombined Fabry-Perot
	Length	40 m	4 km
	Beam waist w_0	0.2 cm	1.5 cm
	Mirror Diameter	3.7 cm	20 cm
	Storage time	1 msec	2 msec
	Recycling factor	1 (no recycling)	30
Auxiliary Cavities			
Input/Output Cavities:	Number		2
	Length		12 m
Filter and Reference Cavities:	Number	1	2
	Length	1 m	1 m
Test Masses:	Material	Fused Silica	Fused Silica
	Mirror Interface	Optical Contact	Monolithic
	Mass	1.6 kg	10 kg
Central Mass		Complex	Beam splitter only

Figure V-1 shows the conceptual design of the optical system to be used in an initial LIGO interferometer. The initial interferometer has several features in common with the 40-meter prototype, and the following differences:

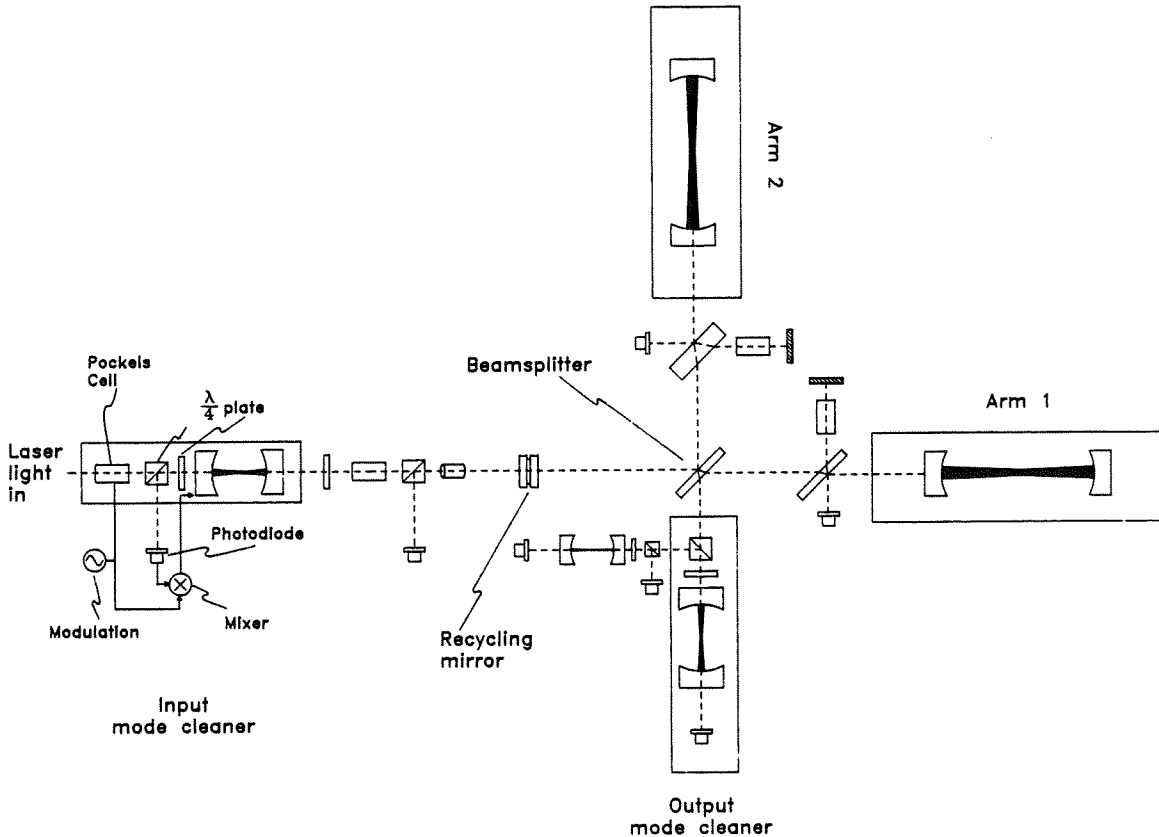


Figure V-1 Principal elements of the optical system planned for initial interferometers. The modules are: (1) *Input mode cleaner*, similar in purpose and operation to the prototype Reference Cavity described in Section III.B; (2) *Output mode cleaner*, to suppress the effects of scattered light; (3) *Arm 1 and Arm 2*, the 4-km (2-km for half-length interferometers) optical cavities. The modulation and feedback, shown explicitly for the input mode cleaner, are implicitly associated with the other photodiodes. Key components include the main *Beam splitter*, which divides the light evenly between the interferometer arms, and the *Recycling mirror*, which in its simplest form has fixed transmission of a few percent. Also shown are plates downstream from the beam splitter oriented 45 deg to the arms; these are almost transparent (99% transmitting) pick-offs that reflect a small amount of light into side arms containing optical phase modulators. The modulators impress side bands onto the light for detection of (1) the cavity resonances, and (2) the gravitational wave output at the antisymmetric port of the beam splitter. The small cavity adjacent to the output mode cleaner extracts a signal to control the beam-splitter position. Several chambers and connecting tubes (see Volume 2, Section IV.C) comprise a contiguous vacuum system enclosing all the optical components shown. The recycling mirror and output mode cleaner might be omitted from the first operational interferometer.

- (1) The main optical cavities are 100 times longer. Consequently, the diffraction-limited beam diameter is 10 times larger, and the pointing precision required is also 10 times higher. The laboratory research program addresses these issues by the development of larger diameter optics, and of a hierarchical alignment system, using computer controlled automatic alignment in the final stage.
- (2) The design calls for constructing each mirror/test mass of a single monolithic piece of fused silica, rather than optically contacting a mirror to a larger block of fused silica as in the prototype. Research we have carried out shows that fused silica with sufficient optical homogeneity and low enough birefringence to meet the goals of the initial interferometer can be manufactured. The development and testing of techniques for polishing and coating monolithic mirrors are part of the proposed research program.
- (3) Low-loss optics will be used throughout, increasing the overall optical throughput and detection efficiency to 20% and making the total effective power available at the main photodetector (the “bright light fringe” power) 1 W.
- (4) The light beams will recombine at the splitter, so there is one principal optical output. (In the prototype, the arms are monitored by separate outputs.) Some methods for recombining the light in a Fabry-Perot interferometer involving monitoring beams at the input to the main cavities were suggested early [V-1]; and these and others have been demonstrated by Glasgow University, Scotland and University of Paris-Sud, Orsay, France [V-2]. Currently research is being carried out by the LIGO Project to recombine the interferometer with a technique using an optical subcarrier. The optical system is shown in Figure V-1. This operation is described below in Section V.A.2.
- (5) A recycling mirror, with associated modulation and servo systems, makes optimal use of low-loss mirrors and long arms by building up the power within the arms. Recycling of the light in an interferometer has been demonstrated at the Max Planck Institute for Quantum Optics (MPQ) [V-3], Garching, Germany and the University of Paris-Sud, Orsay [V-2]. The specific technique shown in Figure V-1 will be tested as part of the proposed LIGO laboratory research program.
- (6) An output “mode-cleaner” cavity suppresses the effects of scattered light on the output photodiode.
- (7) Several auxiliary subsystems, such as a filter cavity on the output to separate the signal used to control the beam splitter position, are added to the prototype design. The four auxiliary cavities listed in Table V-1 include a reference cavity, mode cleaners on the input and output, and a filter cavity.
- (8) Separately suspending the main mirrors and other components reduces noise in an interferometer and facilitates the alignment of the system [V-4]. The research plan for the 40-meter system includes separately suspending all critical optical components before completion of the final engineering design of the ini-

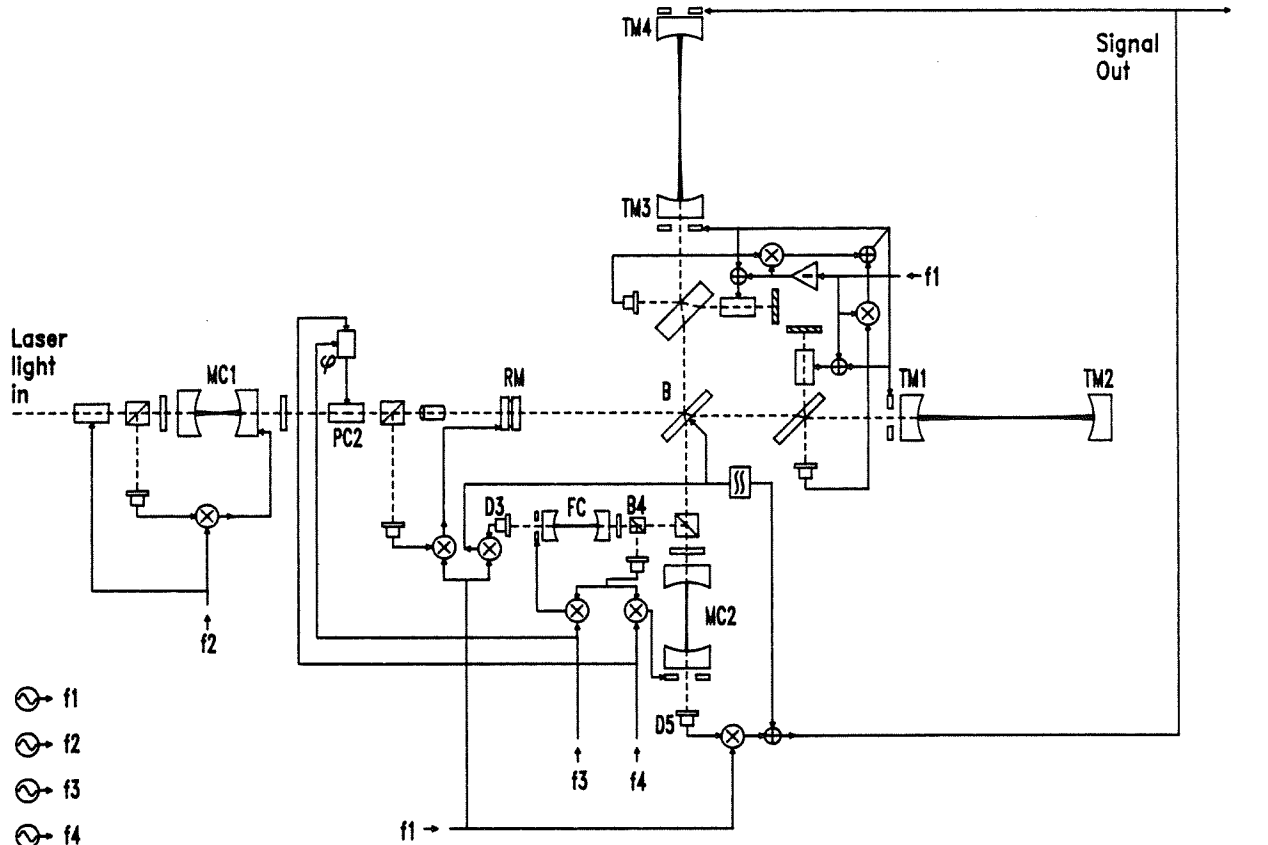
tial LIGO interferometer. The increased sensitivity demands for LIGO interferometers, together with the increased complexity of LIGO optical systems, require many more suspended optical components than have been used in the prototype to date. Modularized controllers that can be mass produced to suspend many similar components have been designed. Suspended components are discussed further in Volume 2, Section IV.B.

2. Details of interferometer operation

The initial LIGO interferometer will be developed according to the design shown in Figure V-2. This design uses eight separate radio-frequency modulated and stabilized cavity signals. Auxiliary components such as steering mirrors, isolators, and pick-offs—essential for a working implementation but not for a conceptual description—are not shown. Similarly, the optics and electronics necessary for alignment control and for a prestabilizing mode cleaner are omitted from the figure for clarity.

We describe here the main features of the design. The two optical cavities defined by the mirrors TM1, TM2 and TM3, TM4 lie along the 4-km-long arms. The light reflected by the cavities on resonance is recombined at the beam splitter, B. The light carrying the difference in phase of these two beams is incident on photodetector D5; the light carrying the sum of the phases is brought to the recycling mirror, RM. The transmission and position of the recycling mirror are adjusted so that the light emerging from the interferometer and the reflected laser light destructively interfere at the recycling mirror. This serves to match the laser light to the losses inside the interferometer and, thereby, maximizes the power circulating in the interferometer.

In addition to the primary parts of the interferometer, there is a set of auxiliary feedback systems. Light is picked off in front of the main cavities into side-arm cavities containing electro-optical phase shifters. These impress FM sidebands on the optical beams to accomplish several tasks: (1) to lock the two long Fabry-Perot cavities on resonance, (2) to hold the recycling mirror at the correct location, and (3) to maintain equal distance between the beam splitter and the input mirrors of the main cavities. External to the main interferometer are three resonant cavities and an additional electro-optical phase modulator. Cavity MC1, at the input to the system, is used to provide spatial and temporal filtering of the laser light and is a secondary frequency reference for the frequency stabilization of the input light. Electro-optical phase modulator PC2 impresses small amplitude subcarriers on the input light at frequencies (typically on the order of 500 MHz) chosen to be resonant with the recycling cavity composed of RM, TM1, and TM3, but out of the band accepted by the main cavities. The subcarriers and associated sidebands generated within the interferometer are used to control the position of the beam splitter. These subcarriers are stripped from the main beam by the filter cavity FC, and brought to photodetector D3. The final cavity, MC2, transmits the FM sidebands and the main beam to the antisymmetric detector D5. MC2 has a free spectral range equal





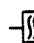





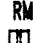





- | | | | | | | | |
|---|------------------|---|--|---|----------------------------|---|------------------|
|  | FARADAY ROTATOR |  | POLARIZING BEAMSPLITTER + QUARTER-WAVE PLATE |  | DOUBLE INTEGRATOR |  | SUMMING JUNCTION |
|  | MIRROR |  | POCKELS CELL |  | ELECTRONIC PHASE MODULATOR |  | PHOTODIODE |
|  | RECYCLING MIRROR |  | TEST MASS/CAVITY MIRROR |  | INVERTER |  | RF SOURCE |
|  | BEAMSPLITTER | | | | |  | DEMODULATOR |

Figure V-2 Optical and electronic design for the initial LIGO interferometer. Laser beams are represented by dashed lines; electrical connections are solid. Representative values for the four modulation frequencies f_1 through f_4 are 12, 14, 30, and 500 MHz, respectively. Details of electronic amplifiers and filters, and the orientation systems are omitted for clarity.

to f_1 (approximately 12 MHz). This cavity rejects light scattered by the optics and the 4-km beam tubes, and reflects the subcarriers to the filter cavity.

3. Performance

The noise spectrum of the initial interferometer, shown in Figure V-3, is estimated by using the parameters given in Table V-2 and by the theory discussed in Section III.A and Appendix B. The dominant contributions shown are photon shot noise, thermal noise, and seismic noise.

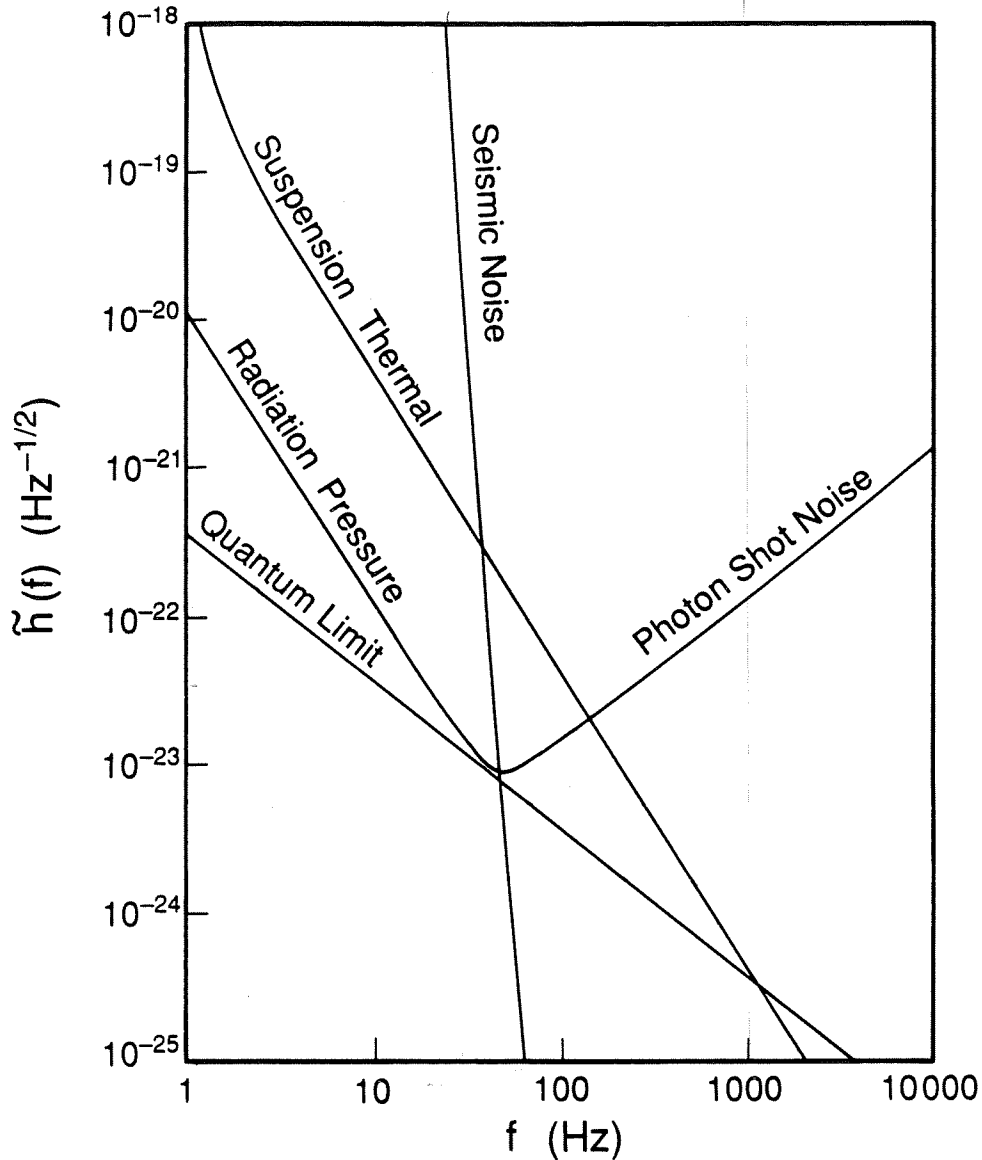


Figure V-3 Projected sensitivity of early LIGO interferometers in broad-band operation, in terms of strain amplitude spectral density, $\tilde{h}(f)$. The sensitivity at a given frequency is determined by the noise source that dominates at that frequency.

a. Photon noise. Performance at high frequency is limited by photon shot noise. The dependence of shot noise on mirror parameters and laser power is indicated in Appendix B.4.a. In estimating the shot noise in initial interferometers, the laser system is assumed to produce 5 W of light at a wavelength of 514 nm, as may be achieved with lasers similar to those used in prototype work. Allowing for inefficiencies in transmitting the light into and out of the interferometer and in the process of photodetection, $P \approx 1$ W of effective laser power (including inefficiencies).

Sensitivity at high frequencies improves as $(Pb)^{\frac{1}{2}}$, where b is the recycling factor; the photon noise in Figure V-3 corresponds to $b = 30$ recycles. Mirrors are readily available that would, in principle, allow several hundred recycles before losses in the coatings and substrates limited performance; other inefficiencies, especially in matching the wavefronts from the arms, may limit the recycling factor achievable in early interferometers to $b \simeq 30$. The recycling factor may be improved later by control of the figure of the pick-off plate between the beam splitter and TM3 in Figure V-2, which can perform the functions of a compensating plate. At low frequencies, the other form of photon noise—fluctuations in the radiation pressure on the test masses—dominates over shot noise. These fluctuations increase with the time that light is stored between the mirrors of the interferometer arms. In initial interferometers, radiation-pressure noise is not likely to be important, as thermal and seismic noise are substantially larger.

b. Thermal noise. The dominant thermal noise is expected to arise from mechanical losses in the simple pendulum mode of the suspended test masses. Because the restoring force in the pendulum comes mostly from gravity, losses sufficient to make a wire, by itself, a low Q oscillator have a much smaller effect in the complete pendulum.¹

The estimate of thermal noise shown in Figure V-3 assumes that the wire's bending loss is independent of frequency. Testing this assumption will be done as part of our research to develop improved configurations and materials (e.g., ribbon suspensions and lower loss materials) for pendulum suspensions.²

c. Seismic noise. The seismic noise is estimated by using the average of seismic displacement spectra measured at candidate sites (indicated in Table V-2), and multiplying by the isolation provided by a five-layer stack of encapsulated-elastomer springs and masses. The final stage of isolation is the wire suspension of the test masses.

The resonant frequency for horizontal motion of a single layer of the five-layer stack is 7 Hz. The vertical resonant frequency is higher—about 15 Hz. This anisotropy results in the vertical noise giving a bigger contribution than the hori-

¹ In initial interferometers, the ratio of the spring constant from the wires to the total spring constant of the pendulum will be smaller than 10^{-3} .

² Measurements of unstressed quartz fibers have shown $Q \approx 10^6$ in bending modes at 100 and 600 Hz.

Not
True
 $\frac{1}{2}$
revised
to $\frac{1}{2}$
for this case

zontal noise. In the high frequency limit, the vertical isolation of the stack in series with a 6-Hz vertical resonance in the pendulum is poorer than the horizontal isolation by a factor of about 3.6×10^4 . The interferometer's rejection of vertical test mass motion is, at best, equal to the angle of the optic axis with the horizontal.³ Thus, for the specified parameters, the vertical isolation sets the limit on the noise. A more sophisticated model of the isolator performance includes the imbalances that cause cross-coupling, making the amplitude of horizontal motion closer to that of vertical motion than this analysis suggests.

The seismic noise curve in Figure V-3 includes the effect of horizontal and vertical resonances in the suspension system; it is calculated by methods explained in Appendix D. The estimate represents the sum of direct horizontal motion and 1% of the vertical motion of the test masses, converted to horizontal motion by cross-coupling in the stacks.

The suspension system of the initial LIGO interferometer will be designed to accommodate additional auxiliary interferometers to monitor the suspension points of the main interferometer's mirrors (see Appendix C). These may be used later to reduce low-frequency seismic noise.

³ Because of the curvature of the earth, the minimum value for this angle is 3×10^{-4} .

TABLE V-2
PARAMETERS AFFECTING
INITIAL INTERFEROMETER SENSITIVITY

Parameter	Value	Notes
PHOTON SHOT NOISE		
Available Laser Power	5 W	Single argon ion laser = $5 \cdot 10^{-5}$ power loss per reflection, achieved in prototype. 40% efficiency in the optical chain; 50% modulation efficiency. Limited by matching the arms, not by mirror coatings.
Cavity Mirror Coating Loss	50 ppm	
Optical Efficiency	0.2	
Recycling Factor	30	
THERMAL NOISE		
Suspended Mass	10 kg	Fused silica monolithic mirror-masses.
Mechanical Q	10^7	Pendulum Q this high has been obtained [V-5].
SEISMIC NOISE		
Input Noise Spectrum	$10^{-7} \text{m} \left(\frac{1\text{Hz}}{f} \right)^2 \text{Hz}^{-1/2}; (f > 10\text{Hz})$	
Intra-vacuum Isolation ¹	x: $\left[\frac{f}{7\text{Hz}} \right]^{-2 \times 5} \times \left[\frac{f}{1\text{Hz}} \right]^{-2 \times 1}$ y: $\left[\frac{f}{15\text{Hz}} \right]^{-2 \times 5} \times \left[\frac{f}{6\text{Hz}} \right]^{-2 \times 1}$	

¹ The seismic noise intra-vacuum isolation is specified for horizontal (x) and vertical (y) motion of the test masses. Each of the five layers of the isolation stack, as well as the final pendulum suspension, provides multiplicative isolation proportional to f^{-2} (see Appendix D).

B. Evolution of LIGO Interferometers

To detect gravitational waves, the use of high performance detectors in extended observational runs is necessary. Development of better detectors that enhance our ability to make new discoveries is also vital. A continuing detector development program is planned to improve LIGO capabilities. The design of the first LIGO interferometer emphasizes simplicity, so that we may place a detector in service as rapidly as possible; succeeding generations of interferometers will more fully exploit the unique capabilities of the LIGO.

A conceptual outline of the development program is summarized in Table V-3. The effort will have three main themes: (1) to lower the photon shot noise, (2) to expand to lower frequencies the band in which measurements can be made at or near the shot noise level, and (3) to develop the techniques required to improve sensitivity for special classes of signals, such as narrow-band waves.

Detector evolution will be coordinated with the observational program. As a general rule, a detector in development will replace the previous operational detector as soon as it can provide a significant scientific advantage, even if further development could bring it closer to the performance limits of its design. Consequently, new detector development will sometimes involve pushing an earlier design closer to its performance limits, while at other times it will entail developing entirely new detector designs.

1. Joint observation and detector development in the initial facility

We are committed to perform gravitational-wave searches with the LIGO at the earliest possible time. The initial operations and the proposed strategy for installation and test of the initial interferometers in the LIGO are described in Section VI.

The initial Mark I detector, consisting of three interferometers (full-length and half-length at Site 1, and full-length at Site 2), will be brought on line as early as possible, conceivably with poorer sensitivity than the design level.

We will start a program of performance improvement, adjusting the development schedule to maximize observation time, as soon as the first detector becomes operational.

Development will proceed incrementally in carefully planned stages. Whenever the developmental interferometer is not disabled for testing or installing modifications, its data stream can provide data for observations. The development program will start with small modifications to the interferometer for diagnostic purposes, evolving into use as a test bed for the second-generation LIGO detector.

TABLE V-3
EVOLUTION OF DETECTOR CAPABILITIES

Performance Improvement	Scientific Benefit	Technical Developments
Better broad-band sensitivity in the original frequency band ($f \geq 200$ Hz), by reduction of shot noise	Deeper search for: <ul style="list-style-type: none"> • Supernovae • Late stages of binary neutron star coalescence • Low-mass black hole events • Millisecond pulsars 	<ul style="list-style-type: none"> • Higher power lasers • Improved broad-band or dual recycling • Operation of interferometer and optics at higher power • Use of "squeezed light" techniques • Reduction of other noise sources as they appear
Extend signal band to lower frequencies	Ability to see: <ul style="list-style-type: none"> • More massive black holes • Much larger fraction of pulsar population Better sensitivity to binary neutron star coalescence	<ul style="list-style-type: none"> • Improved seismic isolation (including active systems) • Lower thermal noise • Lower noise test mass damping and control systems • Reduction of other noise sources as they appear
Better sensitivity in narrow frequency range	<ul style="list-style-type: none"> • Allows deeper searches for particular periodic sources • Improved sensitivity to broad-band stochastic background 	<ul style="list-style-type: none"> • Implement resonant recycling or dual recycling • Reduction of other noise sources as they appear

2. Development of the second-generation LIGO detector

While the Mark I detector is going into operation, campus development of the second-generation LIGO detector, Mark II, will be proceeding. The Mark II design will include options not incorporated in Mark I and improvements based on the experience gained from operating Mark I. The advantages of new technology, made available after the Mark I design freeze, will be evaluated.

3. Development of advanced broad-band and narrow-band detectors with higher sensitivity

Development of advanced broad-band detectors will concentrate on two efforts: (1) reducing shot noise, which limits performance at higher frequencies; and (2) overcoming obstacles, such as vibration and thermal noise, which limit interferometer performance at low frequencies. Progress is expected to come both from research

in the LIGO campus facilities and from collaborative work with other groups.

a. Improved sensitivity above 200 Hz. Above 200 Hz the principal noise source in the interferometers is expected to be photon shot noise. Improving performance at these frequencies will require increasing the optical power in the interferometers.

Powerful and efficient solid-state lasers are expected to be incorporated, at the latest, into the second- or third-generation LIGO detectors. Currently, Prof. R. Byer of Stanford University is collaborating with the LIGO Project to develop Nd:YAG laser technology for use in gravitational-wave interferometers. This effort will concentrate on producing high power output with high efficiency and on stabilizing the light to LIGO specifications. The stabilization techniques will be similar to those already developed in prototype work with argon-ion lasers.

In addition to improving the light source, sensitivity can be increased by improving recycling efficiency. The number of times that light can be recycled in an interferometer is limited by absorption, scattering, depolarization, and distortion of the wavefronts by imperfections in the optics.⁴ Improved recycling efficiency may require the development of better optics. This effort will be supported and coordinated with industry through the campus Optics Test Facility (see Section VIII.B). It is likely that certain interferometer configurations in which light is exchanged between the main cavities will be relatively insensitive to optical deformations. Promising techniques for this are dual recycling and resonant recycling. Work in this area has been done at Glasgow University. We plan further work on new optical systems of these and other types.

Employing "squeezed light" [V-6, 7, 8] may make it possible to reduce the influence of shot noise at a given power level (see Appendix C). Eventually such techniques will be employed, if they prove suitable, but an R&D effort in this area is not currently being pursued.

b. Improved sensitivity below 200 Hz. The low-frequency limit to sensitivity is set by mechanical noise, principally seismic noise and thermal noise. Seismic isolation will be improved by the development of more sophisticated passive filters and by the implementation of schemes for active seismic isolation. Both of these approaches are being pursued by the LIGO team, as well as by scientists elsewhere.⁵

Passive isolation can be improved by increasing the number of resonant stages

⁴ Thermal distortion in mirrors made from conventional materials limits the maximum optical power usable in advanced interferometers. We will address this problem by a program to develop low-absorption coatings and substrate materials that can handle larger heat loads. We will also investigate interferometer geometries that are less susceptible to thermal distortion effects, as discussed in Appendix C. Still another strategy is to exploit the current development of optics and coatings in the near infrared where losses are substantially smaller than in the visible.

⁵ We have recently formed a collaboration on vibration-isolation systems with Professors P. Bender and J. Faller at the University of Colorado (see Section VI.B and Appendix K).

[V-9, 10, 11, 12] or by reducing the resonant frequency of each stage. The engineering challenges are substantial, as the springs need to be soft, roughly isotropic, compatible with high vacuum, and well damped. The isolation systems need to be designed and assembled to avoid cross-coupling of the different degrees of freedom.

Active systems use feedback to reduce the seismic noise transmission within the servo bandwidth. One such system, the suspension-point interferometer (see Appendix C), is an option in the initial LIGO interferometer design. Other active systems involve using the test mass as an inertial reference to which its own suspension point is locked [V-13, 14, 15, 16, 17].

Reduction of thermal noise associated with test-mass suspensions is accomplished by reducing the mechanical loss and by increasing the mass for a fixed level of loss (the LIGO test-mass chambers can accommodate up to 1-ton test masses and their associated isolation systems, although 10-kg masses will be used in the first interferometers). Thermal noise in low-loss pendulums has been analyzed theoretically, but no accurate measurements have yet been made. We have begun a research effort to learn more about the dissipation mechanisms, as well as to find what materials, processing methods, pendulum geometries, and clamping or welding procedures will yield the lowest level of noise.

c. A candidate advanced broad-band interferometer. The noise spectrum shown in Figure V-4 represents the possible performance of an advanced broad-band interferometer, after development is done as previously described. The high-frequency noise is shot noise from 60 W of green light, recycled 100 times. The thermal noise is that in a pendulum of 1-ton mass, with losses which correspond to a Q of 10^9 . The seismic noise is filtered through a passive five-layer isolation stack, with single-layer resonant frequencies of 2 Hz.

4. Specialized searches

A substantial part of our development effort will be directed toward techniques that allow detectors to be optimized for particular sources.

a. Searches with narrow-band detectors. In addition to improving sensitivity in broad-band detectors, searches can be conducted with interferometer configurations that enhance sensitivity in a narrow frequency band. Two methods of accomplishing this, resonant recycling and dual recycling, are described in Appendix C. These methods require modifications to the recycling optics in the beam-splitter chamber, although for dual recycling these may be fairly small. While the basic concepts for these techniques have been worked out for incorporation into the vacuum system design, prototype development will be required before such techniques are implemented.

The clearest advantage of using narrow-band detectors arises in searching for periodic sources. Figure A-4b of Appendix A shows the dramatic increase in search capability expected in a selected frequency band. If a periodic source is discovered in a broad-band search, a narrow-band detector would be quickly deployed for more

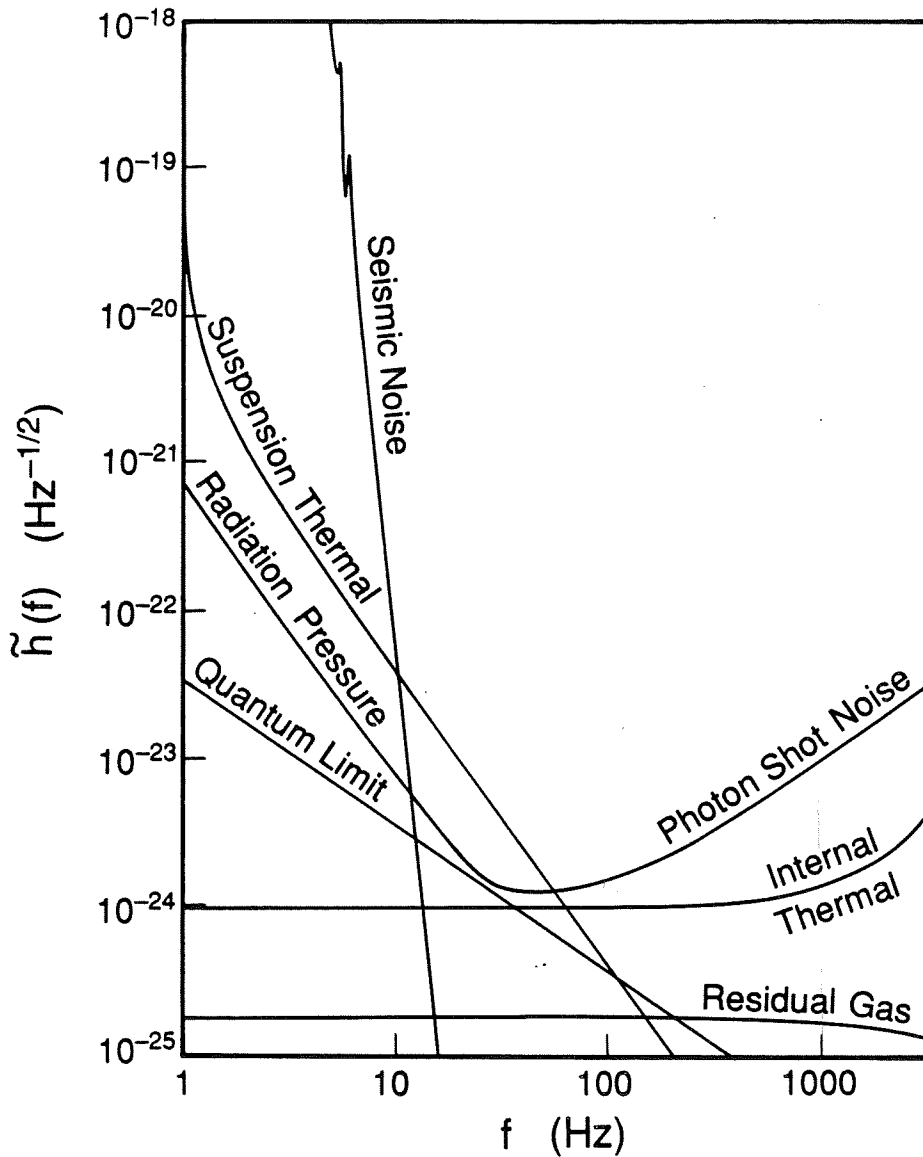


Figure V-4 Projected sensitivity of a possible advanced LIGO interferometer, in terms of strain amplitude spectral density, $\tilde{h}(f)$. The parameters that set the level of the various sources of noise are as follows: 4-km arms, 1-ton test masses of fused silica with mechanical $Q = 10^6$, 60 W of bright-fringe power, broad-band recycling with 100 recycles, suspension $Q = 10^9$, residual gas = 10^{-9} torr hydrogen or 10^{-10} torr water.

detailed observations. At other times, the use of narrow-band detectors is planned to search for periodic sources too weak for detection with previously developed broad-band detectors. Such searches will be guided by whatever insights are provided by radio, optical, and X-ray observations.

Whenever information on the power spectrum of a specific type of burst source exists, either from data or theoretical prediction, the frequency and bandwidth of a

narrow-band detector can be suitably adjusted. Thus, narrow-band detectors can also be used advantageously to search for nonperiodic sources.

b. Stochastic-background searches. A search will be made for a stochastic background of gravitational waves by cross-correlating [V-18] the outputs of different interferometers. Data from the most suitable of the interferometers developed for other searches will be analyzed with cross-correlation algorithms.

The smallest spectral density signal of stochastic gravitational waves detectable by this technique is proportional to $h_N(f)/(\Delta f t_{int})^{1/4}$ where $h_N(f)$ is the equivalent gravitational strain noise in the interferometer due to noise sources other than the gravitational waves, Δf is the bandwidth over which the cross-correlation is done and t_{int} is the integration time of the observation. The strong dependence on the interferometer noise and the weak dependence on the bandwidth give advantages to narrow-band interferometers (resonant- or dual-recycled) in such a search.

Occasional searches for a stochastic background at low frequencies, in the outputs of two interferometers at different sites, will be carried out as a special project, as workforce and schedules permit. It may even be useful to set limits by cross-correlating the outputs of two interferometers at the same site if their noise spectra do not appear correlated.

C. LIGO Sites: Scientific Aspects

LIGO Sites will be chosen to maximize the chance of discovering gravitational waves and to ensure the power of LIGO as an astrophysical observatory. The choice of sites also has an important bearing on the ability of the LIGO to form part of an effective international network for the extraction of scientific information from gravitational-wave signals.

1. Physical attributes of the sites

The environmental noise at a site affects the sensitivity of the interferometers and, thereby, both the depth and reliability of the search for gravitational-wave signals. Important considerations in a site choice are the levels of the local intrinsic and wind-driven seismic noise and the spectrum of man-made noise, including varying Newtonian gravitational gradients. The extent to which man-made noise is likely to increase over the lifetime of the LIGO due to local development is another consideration. Seismic noise is especially important for detectors designed to search for gravitational waves at low frequency, where noise levels are generally higher and isolation is more difficult.

Another criterion for site selection is that the plane defined by the interferometer arms should be level. Pendulum suspensions generally exhibit more noise for motion along the vertical than the horizontal. A site that is not level couples vertical noise to the sensitive optic axis of the interferometer. The Earth's curvature sets a limit to the orthogonality which can be achieved. This limit is 3 mrad for a separation of 4 km; all interferometer layouts with slope less than this are roughly equivalent.

2. Separation and relative orientation of sites

Separation of the two LIGO sites is important for the detection of gravitational waves and for the extraction of information from the signals. The LIGO strategy for the identification of gravitational waves is discussed in Section VII; here we concentrate on the influence of site separation in determining astrophysical information.

The discrimination of gravitational waves from environmental noise is satisfied by site separations of hundreds of kilometers or more. We choose to separate the sites by continental distances, thereby enhancing our ability to determine the position of sources in the sky. Because of the broad sensitivity pattern of an interferometer, we will use the difference in arrival time of the wave at different sites to learn the position of a source of gravitational waves. To get the most accurate position determination, the individual interferometers should be as far apart as possible, but limited to a distance such that the response patterns (discussed below) overlap sufficiently. This maximum desirable distance is approximately 4500 km because of the curvature of the Earth.

Several considerations enter into choosing the relative orientations of interferometers at separate sites. The response of a pair of interferometers operated in coincidence gives the highest probability of detection for an isotropic distribution of sources when the arms, projected into the plane that bisects the two detector planes, are aligned.⁶ We have chosen this “coincidence projection” alignment, at the cost of the loss of some information concerning the polarization of the waves.

Because a minimum of three sites must function together to extract complete wave information, LIGO site locations need to be planned with a view toward an international network. The quality of time-delay information from a three-site network is maximized by arranging the sites in a triangle of the largest possible area.⁷ Ratios of the signals at different interferometers will give both polarization states as a function of time. Gürsel and Tinto [V-20] have shown that three interferometers would suffice to uniquely determine all the wave properties, provided the signal-to-noise ratio is sufficiently high. Even an optimal three-site network, however, does not provide full sky coverage with good spatial resolution (see discussion below). Complete astronomy requires a fourth site. With four sites, the figure of merit is the volume of the enclosed tetrahedron. Thus not only the distance between the two LIGO sites will be considered, but also their arrangement with respect to the other possible sites in Europe and elsewhere.

3. Precision of source position determinations

An estimate of the precision obtainable in determining the position of a gravitational-wave burst is presented using a network of three sites.

For near-overhead sources, the uncertainty $\Delta\Theta$ in a burst source’s position is approximately [V-21]

$$\Delta\Theta = \left[\frac{8}{\pi A \cos\theta} \right]^{1/2} \left[\frac{c}{2\pi f S/N} \right] = 10 \text{ arcmin} \frac{1}{\sqrt{\cos\theta}} \frac{10}{S/N} \left[\frac{0.22 R_{\text{Earth}}^2}{A} \right]^{1/2} \frac{1 \text{ kHz}}{f}. \quad (\text{V.1})$$

Here Θ is the angle between the source direction and the normal to the plane of the three sites, A is the area of the triangle defined by the three sites, f is the characteristic frequency of the signal, and S/N is the signal-to-noise ratio. R_{Earth} is the radius of the Earth, and $0.22 R_{\text{Earth}}^2$ is the value of the detector triangle’s area A for a network with one detector in California, one in Germany, and one near the east coast of the United States.

⁶ In a two-site observatory, Schutz and Tinto [V-19] have analyzed the sensitivity of a coincidence search for burst sources in the Virgo cluster of galaxies and shown that there is a preferred relative orientation which differs from that for sources distributed isotropically over the sky. This “Virgo-optimized” alignment differs from the isotropic-optimized coincidence projection alignment by only 10 deg, and results in less than 5% change in sensitivity.

⁷ We have defined a figure of merit, the area factor, given by $A_M = \frac{|\vec{a} \times \vec{b}|}{R_{\oplus}^2}$ where \vec{a} and \vec{b} are vectors between the sites and R_{\oplus} is the Earth’s radius.

This order of magnitude estimate has been confirmed by the detailed numerical simulations of Gürsel and Tinto [V-20]. Figure V-5 shows some results of these simulations for a one-cycle, circularly polarized signal with characteristic frequency 1 kHz, impinging on detectors in the Western and Eastern United States and Western Europe. The signal-to-noise ratio would have been 45 if the source had been overhead at a given detector but is less for sources not overhead. The two graphs in the figure are for different values of the angle θ between the source location and the normal to the plane formed by the three detectors. Each graph shows the magnitude $\Delta\Theta$ of the vectorial angular error in the algorithm's estimate of the source direction, for a sequence of simulations with varying azimuthal angle ϕ around the normal to the three-detector plane. Notice that when the source is nearly overhead [Figure V-5 (a), $\theta = 9$ deg], the rms angular error is rather small: about 3 arcmin. When the source is near the three-detector plane [Figure V-5 (b), $\theta = 99$ deg], the rms error is at least 1 deg.

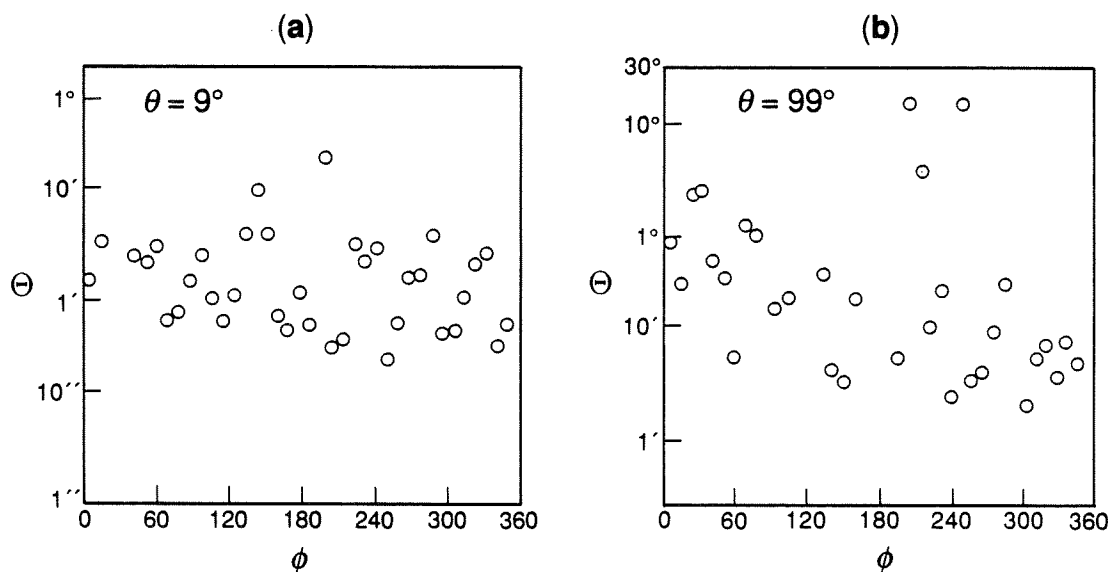


Figure V-5 The angular errors in the estimated source location as computed in simulation tests of a computer code [V-20] developed to extract the source direction and wave form from noisy data from a three-detector network. The plots give the angle, Θ , between the computed and known source locations as functions of azimuth, ϕ , for (a) sources nearly overhead relative to the three-detector plane, and (b) sources nearly in the three-detector plane. A signal-to-noise ratio of 45 (for sources directly overhead) is assumed.

The reduction in angular accuracy near the three-detector plane embodied in the $\cos\theta$ and S/N factors in Equation (V.1) and demonstrated in Figure V-5 shows the importance of having a network of four sites in order to get good full-sky coverage. The best coverage will result from a network whose four detectors are at the corners of a tetrahedron of maximum volume. Adding a detector in western Australia to the network formed by detectors in Europe and on the east and west coasts of the United States would provide an especially large tetrahedral volume.

VI. LIGO OPERATIONS

A. Evolution of Facilities

A successful initial science strategy for the LIGO must cope with uncertainty in the amplitudes, frequency spectra, and rates of the gravitational waves reaching Earth (see Section II). To deal with these uncertainties and to assure an orderly evolution, the LIGO concept includes a staged construction of facilities (Phase A, B, and C, see Section IV) with milestones for reviews and decision making.

Resource limitations dictate the start of operations with the one-detector Phase-A configuration instead of the preferred two-detector Phase-B system (which would allow concurrent observation and development). Although this will reduce the initial operating efficiency, it will not delay the discovery of gravitational waves if their strengths fall within the sensitivity range of the initial detector. The Phase-A design also permits upgrading to the ultimate sensitivity, although at a slower pace than the Phase-B design.

As discussed in Section IV, an important goal is the early expansion of the LIGO capabilities to the Phase-B configuration. This should be implemented as soon as LIGO Phase A has demonstrated satisfactory performance. A continuing program to develop detectors, working in parallel with uninterrupted observations (the "gravitational-wave watch"), is a necessity. Given the pioneering character of the operation, the detector-development program is needed whether or not the initial observations find gravitational waves. If no signals are observed with the first detectors, there will be an urgent need for new detector designs with increased sensitivity and spectral coverage. This development will be carried out in part in facilities on the Caltech and MIT campuses, and in part within the full-scale LIGO facilities themselves. The scaling from short to long baselines is an important factor in detector development, especially as some of the proposed methods to enhance the sensitivity in second-generation detectors cannot be adequately tested on small baselines. Therefore, we are designing the LIGO to enable both development and observation with a minimum of interference. We will plan smooth transitions from one observing detector system to the next iteration of an enhanced detector system that has been technically qualified in the LIGO.

If gravitational waves are detected in the initial observing program, the dual capability for observation and development is just as important. There will be multiple demands on the facilities as the field moves from a discovery phase to an investigative one. The success of the field will doubtless engender enough interest so that a much larger part of the scientific community, both observers and instrument developers, will want to join the new science. At this stage in the LIGO project it would be appropriate to upgrade the LIGO to its Phase-C configuration, enabling the use of the LIGO for many different and concurrent observing programs.

Once waves have been detected, we expect to be operating in concert with gravitational-wave observatories abroad in an international network (see Section V.C and Section X).

B. National Context

We envision the LIGO as an initial quasi-experimental project, focused upon the invention, development, verification, and first use of technologies for laser interferometer gravitational-wave astronomy, with a gradual transition to a mature facility. The early stages of evolution will be conducted primarily by the Caltech/MIT LIGO team, followed by a gradual transition to broader-based national and international participation.

Caltech and MIT, with the principal support of the National Science Foundation (NSF), have invested close to two decades of effort in developing a laser interferometer for gravitational-wave astronomy. The two institutions are committed to continuing a vigorous program leading to the establishment of the LIGO and gravitational-wave astronomy, and subsequently developing, operating, and maintaining LIGO under NSF sponsorship in the interest of the scientific community.

Completion of the LIGO, bringing it to operational readiness in the course of the early search for gravitational waves and, ultimately, conversion to a broadly accessible facility, will require the full commitment and expertise of the Caltech/MIT team. It is expected that once a firm NSF commitment towards construction and operation of the LIGO exists, a broader-based national scientific community will be interested in participation. Early indications of such efforts are an existing collaboration between Stanford University (Professor R. Byer) and the LIGO project in the development of Nd-YAG lasers for LIGO, and collaborative studies with the University of Colorado at Boulder (Professors P. Bender and J. Faller) towards the development of extremely low-frequency ($\lesssim 10$ -Hz) antivibration platforms for laser interferometers. With increasing maturity, the LIGO program will be able to evolve new modes of participation with the scientific community. It is to be expected that the Caltech/MIT LIGO team will continue to provide operations support and maintenance, and that it will conduct a basic gravitational-wave watch and development of advanced interferometers, either alone or in collaboration with others. There will also be outside users who will provide their own hardware and operate their own interferometer systems in the LIGO, as well as users who analyze data from the gravitational-wave watch program. It is proposed that the LIGO director will then work with a national advisory committee that will participate in experiment selection and planning.

C. Operations Plan

The operations phase starts upon completion of Site 1 construction when the facilities become available for installation and operation of interferometers. Although the details of early LIGO operations will depend on what is encountered after startup, there are certain principal lines of progress that will dominate the planning.

1. Phase A: early LIGO operations

The main goal of Phase A is to install and operate LIGO detectors at a sensitivity and duty cycle that will give a significant probability for the detection of gravitational waves. The scenario described below is likely to extend over a period of years (see also Figure XII-1):

a. Task 1 (upon completion of vacuum facility at Site 1):

- i. Shakedown of Site 1 facilities.
- ii. Installation and shakedown of full-length interferometer at Site 1.
- iii. Installation and shakedown of half-length interferometer at Site 1.

b. Task 2 (Site 2 vacuum system completed):

- i. Shakedown of Site 2 facilities.
- ii. Installation and shakedown of full-length interferometer at Site 2.

c. Task 3:

- i. Completion of control and data system for observatory operations: Sites 1 and 2 operating in triple coincidence mode.¹
- ii. Tests of interferometers in coincidence between the two sites.
- iii. Start of observatory operations. First detector (Mark I) committed to search for gravitational waves.²
- iv. Startup of major effort in data analysis.
- v. On-campus development of Mark II interferometer.

d. Task 4:

- i. Alternating operation of Mark I detector in observation or development (sensitivity enhancements) modes.
- ii. Qualification of LIGO performance for Phase B.

2. Phase B/C: regular LIGO operations

Regular LIGO operations will follow the implementation of the Phase-B or Phase-C capability enhancements as discussed in Section IV. In particular, these enhancements include the capability to conduct a gravitational-wave watch, detector development, and special investigations concurrently and without mutual interference.

¹ While we expect to conduct observations of burst sources in the multi-coincidence mode, single or paired interferometers may also be used to search for periodic sources or stochastic background as appropriate.

² The Mark I detector will be committed to the first gravitational-wave search as soon as it performs at a sensitivity of about an order of magnitude better than other preceding extended-time search detectors.

D. LIGO Staff

The organization of the fully operational LIGO is illustrated in Figure VI-1.

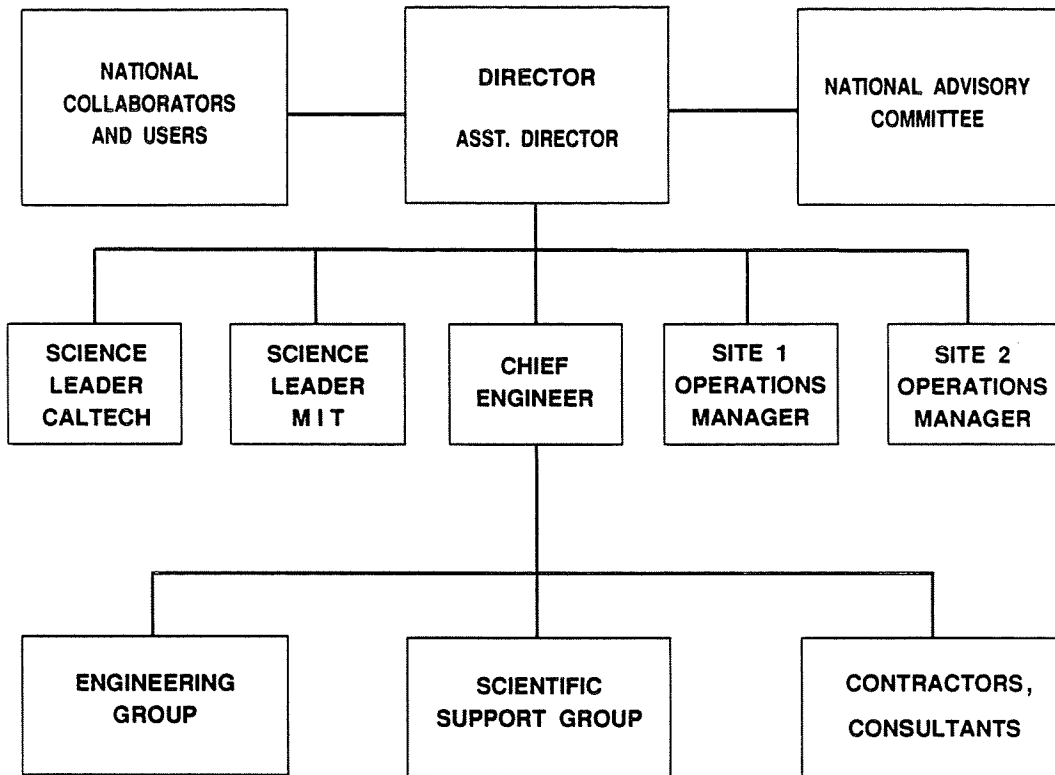


Figure VI-1 Organization of staff to support Phase-C operations.

1. Site operations staff

Each site will have a resident operations staff that is responsible for providing operations support, facilities maintenance and upgrade, and assistance to visiting scientists in their use of the facilities. The operations staff will consist typically of about a dozen persons per site: a resident scientist and site manager, secretary, operators (5), computer analyst, electronics technician, mechanical/vacuum technician, physical plant technician, and custodian.

Five operators will be required to staff the control room for round-the-clock operations (168-hour week). The other technical support staff will be assigned a day shift of 8 hours.

The resident technical staff will be augmented, as needed, by campus scientists and engineers on a detached-duty basis. In addition, visiting scientists will frequently be on site for the installation of new interferometers, trouble-shooting, and real-time data-taking operations.

2. Engineering staff

A core engineering group will be collocated with the director at Caltech. In addition to planning, designing, and implementing maintenance and changes to the LIGO facilities, this group will be instrumental in the development, construction, qualification, and installation of new, advanced interferometers. Meeting these responsibilities will require, typically, the services of the following staff: digital electronics engineer, analog electronics engineer, facilities/vacuum engineer, mechanical engineer, optics engineer, and software engineer. The engineering group activity will be led by a chief engineer who will be a de facto member of the director's office.

3. Scientific staff

At the conclusion of the construction phase, the LIGO science groups (expected to number about six professorial faculty, a dozen scientists, ten graduate students, a varying number of undergraduate students, plus technical and clerical support personnel) will be relieved of their construction support duties and will be able to concentrate fully on observation, data analysis, and detector research and development. The establishment of the LIGO will also create a fruitful environment for a number of postdoctoral research associates, additional graduate students, and additional junior professorial faculty.

E. Coordination of Campus and LIGO Site Activities

The distribution of work among campus and LIGO site facilities will be optimized in an integrated operation.

The LIGO installations will serve three principal objectives: (1) observation, (2) development, and (3) special investigations, in a continuous mode and without mutual interference (see Section IV). The sites will be equipped with all facilities necessary to support the installation, debugging, operation, and scientific diagnosis of gravitational-wave interferometers. These include small mechanical and electronic shops, laser maintenance clean rooms, environmental monitoring and diagnostic equipment, computers, and data-handling equipment.

Because the home university campuses cannot accommodate the testing and final development of the km-size interferometers, the LIGO systems themselves will have dedicated access ports for this purpose. However, the design and early development of interferometers, and the testing and qualification of complete interferometer subsystems, will take place on the home campuses. This approach takes advantage of the home locations of personnel, allows for the most intensive participation of students, and assures minimum interference with the field observing program.

VII. STRATEGY FOR IDENTIFICATION OF GRAVITATIONAL WAVES

We are designing the LIGO for the direct observation of gravitational radiation. Because the gravitational-wave sources have uncertain strengths, rates, and character, we must adopt a multifaceted strategy for the verification of their signals. An essential part of the LIGO concept, especially important early on, is high confidence that the signals observed are indeed gravitational waves and not instrumental or other terrestrial noise.

Should the signals be strong and of recognizable form, the wave shapes themselves can provide information to help identify them as gravitational waves. A good example is the chirp signal arising from the coalescence of a binary neutron star or black-hole system (Figure A-3 in Appendix A). Another example is the characteristic frequency and amplitude changes associated with a periodic source observed from the rotating and orbiting Earth.

Because we cannot count on these signatures, the LIGO design will include tests to assure that the signals are consistent with gravitational waves and inconsistent with spurious phenomena. The verification strategy includes the following elements:

- (1) *The operation of interferometers at widely separated locations.* Burst gravitational waves produce signals that are coincident in separated interferometers (except for a delay due to travel-time). If the interferometers are far enough apart, there is only a small probability of correlations from environmental and instrumental noise. Separated interferometers are also useful in identifying continuous gravitational-wave sources.
- (2) *The operation of an environmental and instrument monitoring system.* The signals that are due to gravitational waves must not correlate with measured perturbations in the environment or the instrument.
- (3) *The operation of interferometers of different length.* With two interferometers at the same site but of different lengths, the signals must be in the ratio of the lengths to qualify as gravitational waves.

All three elements of this strategy are required because no one by itself is sufficient to give the confidence needed for an unambiguous detection. Furthermore, each element contributes in other ways to the research program, as will be discussed below.

A. Statistical Characteristics of the Noise

The noise estimated in Sections III.A, V.A, and V.B is due to continuous random processes (shot noise, thermal noise, and the average seismic noise) and is a good predictor of the detector performance in a search for such continuous signals as periodic and stochastic-background gravitational-wave sources. The data used for a burst search have two components: (1) a Gaussian distribution of pulses

from continuous random processes and (2) a non-Gaussian distribution of pulses that occur infrequently but may have a large amplitude. An impulse given to a test mass from a sudden release of strain in a suspension wire is an example of a mechanism that can contribute to the non-Gaussian distribution. Experience with operating single interferometers in long-duration runs shows that the non-Gaussian noise can be described by a flat distribution of pulse amplitude versus the frequency of occurrence.

B. Noise Suppression and Signal Confirmation

We plan to use coincidence techniques between interferometers and veto information from the environmental and instrument monitoring systems to bring the sensitivity of a pulse search to the level of the Gaussian noise. The noise in widely separated interferometers is expected to have a low probability of correlation. Interferometers sharing the same site have a higher probability of correlated noise, but have the advantage that the gravitational-wave signal amplitudes will have well-defined ratios if the interferometers are of different length. We are proposing that the optimal broad-band LIGO detector will consist of three interferometers operating in coincidence: a full-length interferometer at Site 2, and a full-length/half-length pair of interferometers at Site 1.¹

1. Multiple interferometer coincidence detectors

In principle, it is possible to search for bursts using just two interferometers, one at each site, and operating the pair in coincidence. The simplest method would be to note whenever an event occurs (the interferometer output exceeds a preset threshold value) in either interferometer, and then look for coincidences between events from the two interferometers. If an event occurs at time t_0 in interferometer 1, then the double-coincidence criterion is true if an event occurs in interferometer 2 at time $t_0 \pm \tau_W/2$, where τ_W is the duration of the acceptance window. This two-fold coincidence method will work provided the rate of spurious double coincidences is sufficiently low.

For double-coincidence operation of two interferometers, the rate of spurious coincidences due to the noise is given by

$$R_{12} = \tau_W R_1 R_2 \quad (\text{VII.1})$$

where R_1 , R_2 are the singles rates (the rate of noise pulses) for interferometers 1 and 2, respectively. To allow detection of a pulse of duration τ_P , we set

$$\tau_W = \tau_P + 2l/c \quad (\text{VII.2})$$

¹ A full-length interferometer has test masses at each end of the 4-km vacuum tubes. A half-length interferometer has its central masses in the corner building and its end test masses in mid-station buildings located near the middle of each 4-km tube.

where l is the separation between the interferometers and c is the speed of light. The term $2l/c \simeq 20 \text{ ms} \cdot (l/3000\text{km})$ accounts for gravitational waves coming from all directions.

The rate of spurious coincidences can be greatly reduced by operating in triple-coincidence mode with a third interferometer at one of the two sites. In this case the spurious coincidence rate is given by

$$R_{123} = (\tau_P + 2l/c)\tau_P R_1 R_2 R_3 \quad (\text{VII.3})$$

where R_3 is the third interferometer's singles rate and l is the separation between the sites. Table VII-1 gives the allowable rate of noise events in each interferometer (assuming $R_1 = R_2 = R_3$) to achieve a spurious coincidence rate of 0.1 /yr if the noise is uncorrelated between the interferometers.

TABLE VII-1
CONSTRAINTS ON COINCIDENCE DETECTION¹

Number of Interferometers in Coincidence	Separation l	Tolerable Noise Event Rate/Interferometer	
		$\tau_P = 1\text{ms}$	$\tau_P = 10\text{ms}$
2	4000 km	1.2/hr	1.2/hr
2	0 km	6.4/hr	2.0/hr
3	$l_{12} = 0 \text{ km}$ $l_{13} = 4000 \text{ km}$	175/hr	74/hr

¹ Constraints on single interferometer noise event rates to achieve a spurious coincidence rate of 0.1/yr.

We see from Table VII-1 that triple-coincidence detection affords approximately two orders of magnitude better suppression of noise events than a double coincidence between two sites. This analysis assumes that the interferometer outputs are statistically independent. Some local correlation in the noise of the interferometers at Site 1 can be tolerated, depending on the singles rate R_2 at Site 2. Locally correlated noise increases the accidental triple-coincidence rate by

$$\Delta R_{123} = R_{c1} R_2 (\tau_P + 2l/c) \quad (\text{VII.4})$$

where R_{c1} is the rate of correlated noise events at Site 1. For example, in a search for millisecond bursts the accidental triple-coincidence rate increases by 0.1/yr for R_{c1} of order 1/day, assuming $R_2 = 20/\text{hr}$ (comparable to the observed unvetoes singles rate in gravitational-wave searches using prototype interferometers). One can measure the degree of local correlation by comparing the coincidence rate between Site

1 interferometers with the prediction of Equation (VII.1). If locally correlated noise is a problem, it must be diagnosed and eliminated. One cannot test for globally correlated noise statistically, because a triple coincidence is itself a characteristic of a gravitational wave.

Past experience suggests that, at least during the early stages of LIGO operations, the singles rates will be high enough to require the simultaneous operation of three independent interferometers. If the singles rates can be adequately reduced, the option of using two interferometers for searches, and thereby freeing up the third interferometer for development, will become available.

2. Auxiliary diagnostic/veto monitors

Besides the interferometer output signal, there are many other other signals (such as laser power, pointing control, beam position, and mass damping controls) within the interferometer that will be monitored for correlations with the output signal. In addition, each LIGO site will have auxiliary instrumentation to monitor the physical environment of the interferometers. Representative phenomena to be monitored are given in Table VII-2. These monitors will be used to veto spurious pulses in burst searches,² reducing the singles rate of spurious pulses without affecting sensitivity.

3. Wave amplitude tests with collocated interferometers of different lengths

The ratio of the amplitudes of the signals developed in two interferometers of different length—specifically, one half the length of the other—at the same site is useful in discriminating gravitational waves from sources of noise. The basis of this discriminant is that gravitational-wave signals will be in the ratio of the interferometer lengths. This is the only element in the strategy that has the attribute of giving a positive signature for the gravitational waves from all classes of sources. A half-length interferometer also measures the effect of noise sources by a method qualitatively different from the environmental monitoring system. It provides discrimination against noise in general, independent of the generating mechanism. Thus, the combination of two interferometers can reject spurious events that bypass the auxiliary monitors. Moreover, it provides additional and qualitatively different diagnostic information on noise sources. This information can be especially useful when there is no correlation between the interferometer output and the auxiliary monitors.

There is a slight sensitivity penalty in configuring three interferometers as two full-length and one half-length, compared with using three full-length interferometers. The triple-coincidence sensitivity depends on the separation of the interferometers, their relative sensitivities, and the frequency band of the signals. For typical

² The monitors may also be useful in reducing noise in continuous wave searches, if the monitored quantities correlate with the interferometer output.

TABLE VII-2
ENVIRONMENTAL PARAMETERS TO BE MONITORED

PHENOMENON	MONITOR
Seismic Noise	Translation and rotation: $f < 10$ Hz; 1 seismometer/building $f > 10$ Hz; 3 accelerometers/test mass tank
Acoustic Noise	Microphones at test mass tanks and critical optical components
Magnetic Field Fluctuations	Low frequency: 1 magnetometer/building High frequency: 3 coils/test mass tank
Radio Frequency Interference (RFI)	Multilevel receiver to record rms noise in selected channels, one per building
Cosmic Rays	Shower detector, one per building
Electrical Power	Transient monitor, one per building
Fluctuations in Residual Gas Column Density in Beam Tubes ¹	UV absorption spectroscopy
Housekeeping Data From Facility Control	Temperatures, wind velocity, ion pump currents, etc.

¹ Although not planned for installation at the outset, a monitor for gas may be required based on experiences with the system. The standard vacuum measuring gauges are not sensitive enough to detect column density changes that would be interpreted as gravitational wave signals. A system using UV absorption spectroscopy on the gas column in the beam tubes has been devised which should have sufficient sensitivity to veto gas bursts at the level required to match the sensitivities of the advanced detectors being planned for the LIGO. The gas bursts, should they occur, will have a characteristic pulse signature that depends on the tube diameter and the pumping speed. There is no information that such gas bursts occur, however, the LIGO will be exploring a new measurement regime.

LIGO sites, and for the half-length interferometer operating with half the signal-to-noise ratio of the full-lengths, the sensitivity to kHz-band signals is reduced by at most 30%. This result applies to Gaussian noise, with the optimal setting for trigger thresholds of 4.9 and 6.5 times the rms Gaussian noise level in the full- and half-length interferometers, respectively.

C. Data Strategy

1. Requirements and essential features

We do not yet have a detailed design for data archiving and analysis; this will become a high-priority effort during the proposed grant period. We present here essential features of a design, based on our experience in gravitational-wave searches and on projected LIGO data recording and analysis requirements.

Appendix G describes five separate analyses from three data runs made between 1983 and 1987. The runs were conducted with prototype detectors at Caltech and MIT, at sensitivities insufficient to detect plausible astrophysical sources. The most recent (1987) data collection was a coincidence run complete with atomic standard time keeping at both sites. Conventional low-density recording techniques were used so data were taken for only a few days. Nevertheless, these searches provided useful experience in recording and analyzing data streams similar to what are expected from LIGO.

The data archiving and analysis strategy will be tailored to the following attributes of LIGO operations:

- Interferometers have a large bandwidth (10 Hz to 10 kHz, except for specialized narrow-band detectors) and nearly omnidirectional response to gravitational waves.
- Observations will use two or three interferometers operated in coincidence, along with auxiliary monitors.
- LIGO data will be used to search for and measure signals from a wide variety of sources in postdetection analysis, including burst waveforms, and periodic and stochastic-background signals.
- LIGO detectors will be used to conduct extended-duration searches with near 100% live time.

The total quantity of data accumulated will be large compared to most other physics experiments and astronomical observations, and high-density recording techniques are required. Even so, special techniques are needed to reduce the total amount of data recorded, especially from wide-bandwidth auxiliary measurement systems (see Volume 2, Section IV.F).

2. Types of signals and characteristic bandwidths

The signals to be recorded fall into three categories.

a. High-bandwidth, continuous. The most critical signals, including the interferometer output and perhaps one or two monitor channels, will be recorded continuously and with full bandwidth—approximately $2 \cdot 10^4$ 2-byte samples/s, for a data rate of 40 kbytes/s/interferometer. These signals place the largest demands on the capacity of the recording and archiving system.

b. High-bandwidth, sporadic. Many auxiliary monitor signals—such as the intensity of laser beams at several parts in the optical chain, servo signals, and acoustic monitors—have inherently high bandwidth. Continuous archiving of these signals could overwhelm the data recording system; if necessary, they will be recorded on the basis of infrequent triggers, described below.

c. Low-bandwidth, continuous. A large number of low-bandwidth signals, including filtered forms of alignment servo signals, temperature monitors, and “alarm” signals that indicate out-of-range conditions for critical optical and electronic components, will be recorded. Continuous recording, at rates ranging from less than 1 to approximately 100 samples/s (depending on the signal), presents an aggregate load on the data system that is smaller than that of the high-bandwidth continuous signals.

The precise distribution, trigger rate, and bandwidth for these signals is yet to be determined. The overall average rate of recording, however, is constrained by the capacity of foreseen recording and archiving systems, and is expected to be approximately $5 \cdot 10^9$ bytes/day per interferometer. Even with 1989 technology, data at this rate can be stored by writing approximately two 8-mm video cassettes per day.

3. Archiving of data

a. Shakedown/development phase. During the diagnostic phase of interferometer installation and shakedown, all the signals will be useful. Our experience with the prototypes shows that the initial noise spectrum of a new interferometer is usually far from the theoretical limits. The process of reducing the instrument noise exploits the ancillary interferometer signals and other monitors to pinpoint the most performance-critical parts. Troubleshooting and development will rely on cross-correlating many pairs of available signals within one interferometer—such as the pointing servos against the interferometer output—and, when available, the outputs from different interferometers. Selected data from this phase of operations will be archived and made available for subsequent analysis in the improvement of the operating interferometer and to guide the development of advanced interferometers. The data from both sites will be sent to the university campuses for analysis.

b. Searches with broad-band detectors. The most important information is in the interferometer output that carries the gravitational-wave signal. These data will be filtered to whiten the spectrum and reduce the recording dynamic range requirements. Additional filtering will remove aliasing associated with the limited sampling rate. The archive will include time tags with a precision of $1 \cdot 10^{-6}$ s., UT.

A limited amount of real-time analysis will be performed on the interferometer output³ and on some of the monitor signals. One possible method is to pass the interferometer output through several specialized filters, arranged in parallel, each providing enhanced signal-to-noise ratio for a specified waveform. A flag will be raised whenever a candidate source is identified in the main output, or when a significant effect is reported by the auxiliary monitors. A time buffer will store auxiliary-monitor data that precede the identified event, so that bursts of data at full bandwidth may be recorded along with the interferometer output.

A simple set of processors—for example, bandpass filters covering several frequency bands—will reliably set flags on events that are large compared to the Gaussian noise level. More specific filters will potentially catch smaller events. Selection of the best filter function and threshold depends on the instrument's noise spectrum, which will be determined during instrument and facility shakedown. Because the gravitational-wave output from each interferometer in a search detector is continuously archived, it can be reanalyzed if developments in theoretical astrophysics predict new waveforms, or if new information about specific sources becomes available.

c. Searches with narrow-band detectors. The output of initial interferometers will be inherently broad-band, and bandwidth reduction to search for periodic or semiperiodic sources will be accomplished by specialized algorithms for off-line data analysis. Interferometers with resonant recycling, on the other hand, will have useful output over only narrow bands of frequencies; the required recording rate for these data will be reduced. Furthermore, several monitor signals from each interferometer can be recorded in narrow frequency bands around the search frequency and its subharmonics, without exceeding the capacity of the recording system. As with searches for bursts, the ultimate discrimination against false signals in periodic searches will be provided by a comparison of the outputs of separate interferometers.

4. Analysis of archived data

a. A search for coincident burst events. Candidate events can be processed by passing the flagged data through a set of specialized pulse-filter templates to improve the signal-to-noise ratio and then recording the pulses in a time-ordered list of events for each interferometer. The lists from each interferometer are next compared for coincidence. The pulses that fall into a coincidence window determined by the interferometer separations are studied one by one. An additional discriminant is provided by matching the pulse waveforms from each interferome-

³ Current planning for initial LIGO operations does not include real time links between sites for on-line analysis of coincident events. Once the field is established, and especially after a network (three or more) of gravitational-wave detectors is operating to give positional information, it will be advantageous to carry out on-line analysis of burst events in order to alert the astrophysical community to their occurrence. The communications technology for this service exists now and need not be developed.

ter.

b. A search for periodic sources. The continuous data stream from the interferometer output of any one interferometer can be analyzed for periodic sources. The techniques used initially are expected to be similar to those developed for searches made with the prototypes in which the optimal filter was a Fourier transform. The data for this analysis need not retain the full amplitude range of the original data stream but only enough (4 bits) to preserve information on the FM and AM components of the sources when averaged over periods of hours to months. Livas [VII-1] showed that a search for periodic signals over the complete bandwidth of the interferometer, optimized for a specific location in the sky, is within the capabilities of present supercomputers. A search for all frequencies, over the entire sky, would pose a formidable challenge and could require the development of dedicated hardware or new search algorithms.

One of the requirements for a search for periodic sources is separating spectral peaks originating in the environment or the instrument (e.g., low-amplitude oscillations of suspension wires) from those due to gravitational-wave sources. The principal discriminants available are the Doppler shift and the amplitude modulation of the signal from the motion of Earth relative to the wave. The LIGO offers an additional dimension in solving this observational problem through the operation of two sites. Cross-correlation of the analyzed power spectra will be a powerful tool in discriminating local mechanical oscillations (especially those that may wander in frequency) from astrophysical sources.

c. A search for a stochastic background. The signature of a stochastic background would be correlated broad-band noise in two interferometers, used in much the same manner as electromagnetic radiometers.⁴ The gravitational-wave stochastic background, if white over the interferometer response, grows against the uncorrelated noise as the quarter power of the product of the detector bandwidth and the correlator integration time; see Section V.B and Equation (A.20) of Appendix A. The computational requirements for this search are well within reach of present computers and do not require additional hardware development.

⁴ The techniques have already been used in an early search for gravitational-wave stochastic background with broad-band bar detectors. [V-18]

VIII. CAMPUS RESEARCH AND DEVELOPMENT IN SUPPORT OF LIGO

A. Results from Prior NSF Support

Almost two decades of research activity on laser interferometric gravitational-wave detectors form the supporting basis for this proposal. The highlights of this work are summarized here. Appendix H reports in greater detail progress during the most recent grant period.

1. Development of new concepts in gravitational-wave detection using laser interferometry

a. New concepts for gravitational-wave detection. Many of the key concepts and techniques of laser interferometer gravitational-wave detectors have been introduced and developed by members of the LIGO team.¹ LIGO team members were responsible for the invention and original development of two principal variants of interferometric detectors: the “optical delay line” (or “Michelson”) variant [VIII-1, 2, 3] in which the laser beam makes many discrete passes in each arm of the interferometer, and the Fabry-Perot variant [VIII-4, 5], in which each arm is operated as a very long Fabry-Perot cavity.

In the Fabry-Perot system, the wavelength of the light from the laser source has to be controlled to very high precision, and a new technique for doing this was conceived and developed [III-2]. This involves modulating the phase of the laser light at a high radio frequency, and monitoring light reflected from the cavity input mirror. This laser stabilization method, now one of the most precise known, has subsequently been widely applied in laser physics and atomic spectroscopy laboratories.

Practical development of these techniques has proceeded over many years. Special techniques, such as use of feedback systems and modulation methods to shift gravitational-wave induced phase changes to higher frequencies where the laser light is quiet, are used to achieve interferometer performance at the level limited only by photon shot noise. New technical concepts and strategies have been introduced to overcome noise sources of various kinds as they were identified, and to gradually improve performance and sensitivity to the levels achieved to date. Advances in displacement sensitivity have exposed phenomena unobservable by other techniques. Examples are the broad-band, thermal noise vibration spectra of mechanical structures at room temperature, and subtle noise effects associated with various methods of bonding mirrors to test masses.

¹ Although all the work described was done by members of the LIGO team, some of it preceded or was done outside the NSF-supported groups at Caltech and MIT.

b. More advanced concepts to enhance interferometer sensitivity. Work with the 40-meter Fabry-Perot prototype interferometer led to the demonstration that mirrors made by techniques developed for laser gyroscopes were capable of storing light in a cavity for times longer than the periods of the gravitational waves being sought—and could give quality factors for cavity resonances of more than 10^{12} , hitherto unprecedented in optics. Consideration of what could be possible with large-scale systems of this type led to the invention of the techniques for enhancing efficiency and performance of interferometers now known as *broad-band recycling* and *resonant recycling* [V-1]. In the first of these the whole interferometer is turned into a large optical cavity, in which resonant build-up of the laser light can give a significantly improved shot-noise limit to sensitivity. In the second the optical signal from a gravitational wave builds up by resonance in a system of coupled cavities, which enhances further the sensitivity for periodic sources. These concepts are opening a new area in optical techniques for gravitational-wave research.

2. Technological developments

a. Experience acquired in construction and operation of prototype interferometers. Since 1972, members of the LIGO team have been engaged in construction and operation of gravitational-wave detectors of various types. This effort has involved experimental study of noise sources and development of experimental techniques. From this work experience has been gained in the following areas:

- The use of interferometer mirrors mounted to suspended test masses free at frequencies above the suspension resonance (approximately 1 Hz)—a departure from conventional interferometry, in which all components are rigidly mounted to a solid monolithic base.
- The development of systems to control the interferometer [VIII-6]. This includes the many servo systems for control of position and orientation of optical components and for optimization of cavity parameters relative to the input light beam.
- The development of simple but highly effective vibration-isolation stacks to suppress transmission of seismic noise into the interferometer [VIII-6].
- The use of spatial and temporal filters, such as optical fibers and mode-cleaning cavities, to reduce fluctuations in the frequency and spatial geometry of optical beams.
- The use of simple, high mechanical Q, test-mass structures employing optically contacted mirrors to reduce noise from thermal excitations.
- The use of optical cavities of very high finesse,² and multi-loop wide-band servo systems to lock lasers to them.
- The development of techniques to rebuild high-power lasers to operate with

² Finesse $F \approx \pi / (1 - \sqrt{R_1 R_2})$ where R_i is the intensity reflectivity of mirrors.

low levels of spatial and frequency fluctuations.

- The successful application to interferometry of advances in optical polishing and coatings which have provided low-loss components.
- The development of techniques to phase-modulate light with random noise and pseudo-random pulse sequences to control the effects of scattering in equal-path-length Michelson interferometers.

Based in part upon this experience with the prototypes, a Fabry-Perot design was adopted as the basis of the initial LIGO interferometer. The 40-meter prototype, described in Section III.B, began operation as a Fabry-Perot interferometer in 1983. Figure VIII-1 illustrates successive improvements in sensitivity in the working interferometer as various technical advances were introduced.

b. Implications for design of LIGO interferometers. Besides the demonstration of interferometric detection techniques, operation of the 40-meter prototype has led to the development of prototype designs for LIGO subsystems and has identified problems which require further research.

The 40-meter prototype is the longest interferometric gravitational-wave detector in existence. The high-precision mirror-alignment system developed for this baseline will guide the development of similar systems for LIGO. A 5-meter baseline vacuum system for a prototype interferometer with LIGO-scale test masses has also been constructed. The combination of the 5 and 40-meter prototypes will serve to investigate length-dependent effects for extrapolation to LIGO conditions.

The electro-optical technique for servo-locking lasers to optical cavities, described in Section III.B, can serve as a general purpose building block throughout the LIGO. This system has achieved suppression of laser frequency fluctuations by more than 2×10^8 over millisecond timescales, with more than an order of magnitude electronic gain in reserve. This technique is adaptable to various laser systems, including those operating at high power. This experience has uncovered no fundamental limitation in achieving the frequency control required for LIGO.

The 40-meter prototype has demonstrated that light can be stored in Fabry-Perot cavities for sufficiently long times to optimize LIGO interferometers for sensitive detection of gravitational waves at all frequencies above about 1 Hz. The heating of optical components by absorption of light has been identified as a problem associated with high input power and long storage times. Thermal distortion effects in Fabry-Perot cavities have been observed. Preliminary analysis suggests that the distortion is due to thermal lensing in the mirror substrates driven by optical power absorption in the mirror coatings. Based partly on these findings, an optical test facility is being established to develop and evaluate optical components that meet the high-power and large-aperture requirements of LIGO interferometers.

The best sensitivity achieved to date with the 40-meter prototype has established that our techniques for construction of test masses, suspension systems, and vibration-isolation systems are sufficient to achieve an equivalent displacement noise

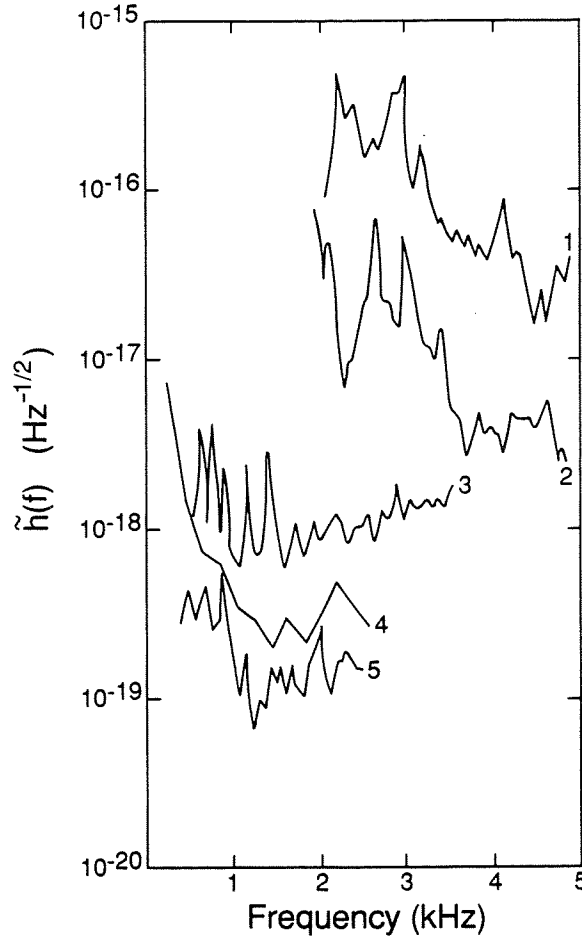


Figure VIII-1 Sensitivity improvements in the 40-meter prototype interferometer. The spectra show the increasing sensitivity from the time of first operation in May 1983 (1), to the best performance achieved to date (5). The improvements shown are attributable in part to the following changes: (1) to (2)—the installation of low-loss cavity mirrors for increased storage time; (2) to (3)—the replacement of complex test masses containing several optical components by simpler masses backing the cavity mirrors alone; (3) to (4)—the installation and rebuilding of a high-power argon-ion laser, and the refinement of electronic servos maintaining resonance in the interferometer; (4) to (5)—the installation of fused-silica test masses and an in-line mode cleaner.

of $\leq 3 \times 10^{-18} \text{m}/\sqrt{\text{Hz}}$ at 1.5 kHz. A 4-km-baseline LIGO interferometer—if limited by mirror displacements of this magnitude—would exhibit a strain sensitivity of $\tilde{h} \leq 8 \times 10^{-22}/\sqrt{\text{Hz}}$ at 1.5 kHz.

3. Analytical developments

Members of the LIGO team have carried out theoretical work to assess the likely strengths and event rates for various types of gravitational-wave sources [VIII-7]. Team members have also developed computer algorithms for extracting source direction (θ, ϕ) and waveforms $(h_+(t), h_\times(t))$ from the data of networks of three or

more detectors. This work has influenced siting of the LIGO facilities and demonstrated that for many sources a three detector network can provide accurate source positions; see Section V.C. Specialized data analysis strategies for burst, chirp, and periodic sources have been developed and refined through test operations of the prototypes (see Appendix G). This research has led to criteria for the data system as discussed in Section VII.

Interferometer noise mechanisms have been modeled and their relative importance has been determined. A description of the most important noise sources is included in Section III.A and Appendix B, and the resulting estimates of sensitivity are presented in Section V and Appendix A. We have analyzed the general problem of discriminating between gravitational-wave bursts and intermittent spurious pulses, and have modeled multiple coincidence detectors using interferometers with different baselines. This work has led to the strategy for identification of gravitational waves described in Section VII.

4. Current status of campus research facilities

The LIGO project has several special-purpose experimental facilities at Caltech and MIT:

- (1) A 40-meter prototype gravitational-wave interferometer described in Section III.B.
- (2) A 5-meter vacuum system, completed in 1988, with large chambers and connecting tubing appropriate for constructing a new prototype and for testing LIGO-scale components.
- (3) A vacuum facility to test suspensions and seismic isolation systems, including an electromagnetic shaker.
- (4) A facility to measure total losses in mirrors by determining the Q of optical cavities.
- (5) A facility to measure the angular distribution of light scattered by mirrors.
- (6) A vacuum test facility to measure the outgassing properties of vacuum enclosures and components.

5. Conceptual design

Based on the progress described above, as well as several dedicated studies made over the past 5 years, a conceptual design for the LIGO has been formulated. The basic LIGO concept and operations plan has been developed and is described in Sections IV and VI, respectively. We have decided to pursue a phased construction approach to deliver, at the earliest time, a system capable of directly detecting gravitational waves and exploiting the observations for physics and astrophysics. Later evolution of the facilities will enhance the scientific capabilities of LIGO and allow broad participation in this new field. We have identified a simultaneous search and development capability, with minimum interference between these

missions, as the optimum strategy to ensure successful LIGO operation. This has defined requirements for three distinct detector types (observation, development, and special investigation detectors), and a flexible modular vacuum system capable of supporting simultaneous operation of multiple interferometers.

The scientific functional requirements have been specified and documented for the LIGO facilities, including requirements on sites, vacuum systems, interferometer design, data and control systems, and support facilities. Preliminary designs for the facilities and hardware have been developed to meet these requirements, and the interaction between them to identify key driving parameters has been studied. The resulting design is described in Volume II.

B. Future Activities

Campus R&D activity during the period covered by this proposal will be divided into five areas:

- (1) The continuing development of the prototype interferometers to test techniques and designs that will be used in the initial LIGO system. This will guide the initial LIGO interferometer design toward improved sensitivity and reliability.
- (2) The development of subsystems for the prototypes—with application to the initial LIGO interferometer for automated operation and detailed investigations of noise sources.
- (3) The development and use of specialized facilities for R&D in optics and vibration-isolation systems to support both prototype and LIGO development.
- (4) Scientific planning and support of the LIGO engineering and construction, including the design, fabrication, and testing of the initial LIGO interferometer and the development of data analysis strategies and software.
- (5) A continuing basic research program to develop and test new interferometer concepts to enhance the sensitivity and frequency coverage of LIGO detectors.

1. Prototype development of techniques for Mark I interferometer

Conceptual design of the initial LIGO interferometer is in progress and will continue through the first two years of the proposal period. By early CY 1992, we expect to have a complete design, based partly on current concepts and partly on the results of the proposed research and development program. Specifying much of the design requires operating the prototypes at the very lowest noise levels we can achieve. This is necessary to uncover unanticipated problems with the conceptual design of the Mark I LIGO interferometers, and will lead to a higher performance in their final version. As described in Appendix H, we are currently reconfiguring our light-stabilization scheme and beam-splitting optics on the 40-meter prototype to develop the techniques to be used in the initial LIGO interferometers. Experimental parameters of the prototypes such as optical power, finesse, and modulation method will be chosen to simulate operating conditions in the LIGO.

a. Development of techniques to recombine the beams in a Fabry-Perot interferometer. In the full-scale LIGO interferometers, the light reflected by the two 4-km-long Fabry-Perot cavities will be recombined at the beam splitter. Recombination compares the signals from the two orthogonal arms optically rather than electronically, and should result in superior common-mode subtraction and better shot-noise-limited performance. It is also a prerequisite for recycling the light.

i. Preliminary development of recombination techniques in a stationary interferometer. We have constructed a stationary interferometer (Figure VIII-2) and are using it for the development of recombination and recycling techniques without the additional complications of suspended components. This initial development should be completed by the beginning of the proposed grant period. Coordinated recombination and recycling development will then be transferred to suspended-mass interferometers in the 5-meter baseline vacuum system and the 40-meter prototype, where it will continue through the design freeze for the Mark I LIGO detector.

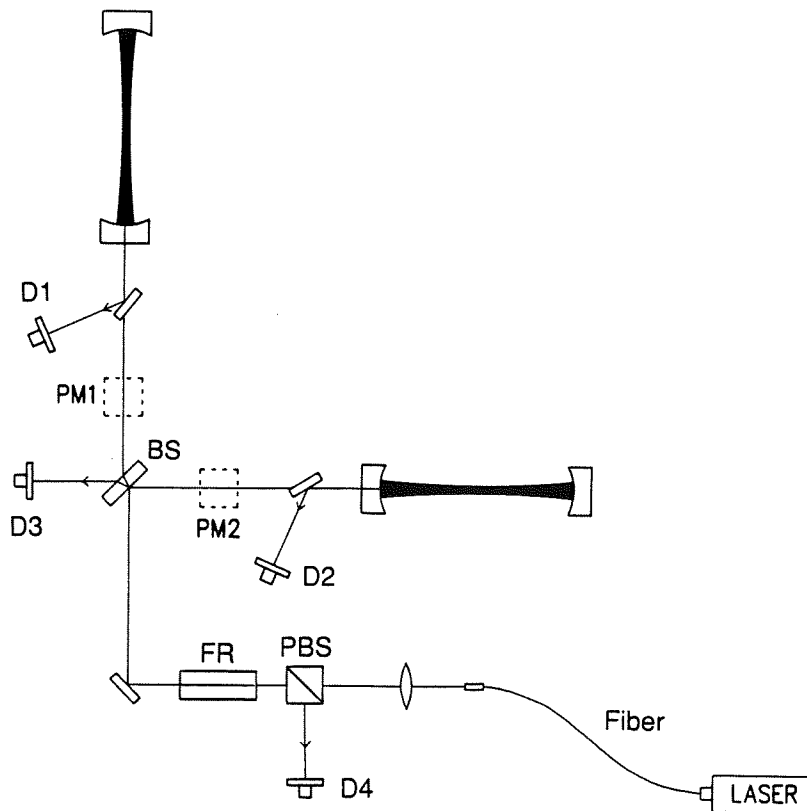


Figure VIII-2 Schematic diagram of stationary recombined interferometer. Photodetectors D1 and D2 monitor the Fabry-Perot cavities; D3 and D4 monitor the antisymmetric and symmetric outputs, respectively. PM1 and PM2 refer to modulation functions in the two arms of the interferometer. These functions are accomplished either by in-line Pockels cells, or by Pockels cells in a side-arm configuration. Other components include a beam splitter (BS), Faraday rotator (FR), polarizing beam splitter (PBS), and mode-matching optics.

The most straightforward recombination configuration entails placing electro-optic phase modulators in the main beams between the beam splitter and the cavity input mirrors. The modulators are used both to impress RF sidebands on the light

and for optical phase control to hold the dark fringe³ at the antisymmetric output. The Fabry Perot cavities are individually maintained on resonance by optical signals derived from pickoff plates and photodetectors in front of each cavity. This scheme is being tested in the stationary prototype as a preliminary step; its use in the initial LIGO interferometer with recycling would require development of higher power modulators because it places the electro-optic phase modulators in high-power beams.

We will next test the method proposed for the initial LIGO interferometer by placing the optical phase modulators in side arms outside of the main high-power beam, where they modulate approximately 1% of the light. This method, described in Section V.A., requires research to test the modulation efficiency and fringe phase control and to develop the additional servo systems required to control the side-arm cavity.

ii. Recombination studies in suspended interferometers. After the basic recombination technology is developed, we will conduct noise studies in suspended interferometers. This will occur after the 5-meter prototype's optical components have been suspended, and after completion of the initial development of broad-band recycling. Eventually, technical developments on the 5-meter prototype will be incorporated into the 40-meter prototype for operation at higher resolution and for length-dependence tests.

The method for controlling the spacing between the beam splitter and the main-cavity input mirrors in the initial LIGO interferometer, described in Section V.A., will be evaluated as part of the recombination studies with the suspended interferometer.

b. Tests of interferometer performance at high power. The Mark I design requires several watts of laser power delivered with fairly high efficiency. Until the design freeze, we will gradually increase the power levels used in the 40-meter prototype to uncover and characterize any problems associated with operation at these higher power levels. During this period, we will convert the 40-meter prototype to operation as a recycling, recombined interferometer.

The 40-meter prototype currently operates with much higher finesse than anticipated to be needed for the longer-baseline Mark I design. For some experimental tests, we intend to reduce the finesse of the 40-meter prototype to the value we will use in the Mark I interferometer. This will allow us to uncover problems that might be associated with high phase sensitivity, and are independent of displacement noise, or the effects of high circulating power in the cavities.

³ In LIGO designs, several electro-optic servo loops operate together to keep a large number of coupled and separate cavities in resonance. Throughout, sine-wave phase modulation is used to generate an error signal, and broad-band feedback is used to maintain the "dark-fringe" resonance—the condition where the detected signal at the modulation frequency is a minimum. The same type (and in some cases the identical unit) of electro-optic modulator serves both functions.

c. Development of broad-band recycling. Broad-band recycling is included in the Mark I design. We plan experimental work on recycling in the stationary interferometer this year. This effort will determine the number of recycles achievable in practice and how this limit is related to optical properties of materials inside the recycled interferometer. The electronics necessary to recycle a suspended interferometer will be developed on the 5-meter prototype and then transferred to the 40-meter prototype for final evaluation before the design freeze.

d. Development of the suspension-point interferometer. As mentioned in Section V.A., the Mark I design includes the option of a suspension-point interferometer to monitor and reduce the effect of vibrational perturbations (see Appendix C). We do not require this feature to function at the startup of operations, although it would be desirable. We intend to complete development work on the suspension-point interferometer at the 40-meter prototype before the design freeze.

2. Development of prototype subsystems for use in the LIGO

a. Development of position sensors and controllers. A substantial systems engineering task associated with the initial LIGO interferometer is the engineering design and fabrication of the optical position sensors and controllers that will be used on suspended optical components. The large number of these sensors and controllers required in LIGO interferometers sets requirements on the pumping capacity of the vacuum chambers, the number and type of vacuum feedthroughs, and the architecture of the data- and control-instrumentation system. Our effort will be directed toward small-scale mass production and the requirements of automated operation and control. During the proposal period, we will develop engineering specifications and a plan for the manufacture and testing of commercially produced position sensors, controllers, and associated electronics.

i. Sensors. The sensors used in damping and positioning servo loops in the initial interferometer need a position sensitivity of better than 10^{-9} cm/ $\sqrt{\text{Hz}}$ at frequencies between a fraction of a hertz and several hundred hertz, and a dynamic range of a few millimeters. The main-cavity mirrors impose the most stringent requirements on the sensors; requirements on other suspended components may be relaxed substantially.

Three types of sensors have been developed by LIGO scientists during the course of prototype research: a single-axis shadow detector, a reflective two-dimensional detector, and a fiber-optic interferometric detector. Each has properties particularly suited for a specific purpose.

ii. Controllers. Controllers apply forces to damp and position the suspended optical components. A magnetic controller,⁴ consisting of a permanent magnet mounted on the suspended object, and a stationary driving coil, is currently used in the 40-meter prototype. An electrostatic controller system is being developed for critical applications where the magnetic system might be a source of noise. Depending on its state of readiness at the time of the design freeze, the electrostatic controller may be used in the initial LIGO interferometer. It could be particularly useful in advanced detectors at lower frequencies.

b. Instrumentation system and automated operation. The prototypes have made use of computers for data acquisition and, in a more limited way, for interferometer control and monitoring. Both the 40-meter and 5-meter prototypes will be increasingly tied to computers, with the goal of developing single-console automated operation and data retrieval as planned for the initial LIGO interferometer. Instrumentation of the prototypes with state-of-the-art computers, instrumentation interfaces, and archival storage capability will become more important as the prototypes grow in complexity.

i. Control development. Although the plan for developing the control system is not yet well formulated, the steps required are clear. The early steps will be passive: monitoring, the display of instrument state, and archiving of operating parameters. Active computer control of interferometers will be introduced gradually. The low bandwidth control signals, such as the position and orientation of components in the optical train, the gain and filter properties of servo loops, and the compensation for drifts, will be automated. Procedures for fringe acquisition will be automated, and systems for automatic optimization of cavity mirror position and alignment will be introduced. The diagnostic tests and procedures used to optimize system performance, such as perturbations of beam position and angle and the introduction of AM and FM noise sidebands, will also come under computer control.

ii. Software development. Full utilization of the proposed monitoring and control system requires extensive software development. Basic software for data handling and communications can be purchased, whereas software to produce graphic representations of the instrument state must be custom designed. The software for analysis of instrument performance, such as cross-correlation studies of instrument parameters and transfer-function measurements, can be adapted from available, general computer "toolbox" programs for data analysis, statistics, and hypothesis testing.

3. Supporting R&D in special campus facilities

a. Optics research and development. The Optics Test Facility now being developed will be used throughout the proposed grant period to study special optics problems pertinent to the LIGO, but problems that do not require the full

⁴ A magnetic control system was developed first by the gravitational-wave research group at the MPQ, Garching, Germany, who kindly provided us with a sample of a coil and sensor of their system.

capabilities of a working prototype interferometer. This facility will support LIGO in several areas.

i. Research and development on mirrors and beam splitters. The initial LIGO interferometers will require mirrors and beam splitters of much larger aperture than those in the current prototypes. Early in the proposed grant period, we plan to acquire and test large-aperture optics for use in these interferometers. Our preliminary data on thermal distortion in fused-silica optics indicate that this material is suitable for LIGO interferometers operating with a few watts of injected power, i.e., at levels sufficient to perform significant gravitational-wave searches. In addition, fused-silica substrates and test masses of sufficient size can be produced with current technology.

Our current research effort in optics is focused on a systematic study of thermal distortion effects in Fabry-Perot cavities. As discussed in Appendix H, we have recently observed such effects in a variety of cavities and have developed a theoretical model consistent with preliminary observations. Our first goal is to refine this preliminary work. The thermal lensing model we are currently using has firm predictive power once the input data—thermal coefficient of refractive index, thermal expansion coefficient, thermal conductivity of substrate, and absorption coefficient of mirror coating and substrates—are known. These parameters are well known except those for absorption by the mirror coatings and substrates. We plan to measure the optical power absorbed by cavity mirrors and to correlate these data with the onset of thermal distortion effects.

Assuming the measurements confirm that the primary heating is due to absorption by the coatings, we plan to coordinate work with industry to produce mirror coatings that are less absorbing. A proven physical model will also help us to evaluate different substrate materials for advanced LIGO interferometers. Preliminary work indicates that high thermal conductivity and low thermal coefficients of expansion and refractive index change are achievable in improved substrates. Sapphire is one candidate material. We also intend to experiment with cavity geometries that are less susceptible to thermal distortion effects (see Appendix C). We expect that this work will continue throughout the period covered by this proposal.

ii. Preliminary investigations of interferometer noise mechanisms. The Optics Test Facility will be used to support investigations of noise mechanisms using the prototypes and for preliminary investigations of noise associated with optical parameters (e.g., phase noise induced by fluctuations in optical beam geometry). Methods to measure and reduce noise, including new monitors and electronic subsystems, will be developed in the test facility. These will then be added to the prototypes for further high-resolution studies.

iii. Evaluation and development of new lasers for LIGO. Development of new laser systems for LIGO will be done by outside groups in collaboration with LIGO personnel (see Section X). In addition to requiring high-power output and high efficiency, LIGO laser beams ideally are stable in amplitude, frequency and geometry.

The Optics Test Facility will provide the capability to measure intrinsic noise of new lasers and to develop any required stabilization techniques.

iv. Research and development related to scattering by optical components. The scattering of light by optical components degrades interferometer performance both by reducing the efficiency of light use, with a resulting poorer shot-noise limit per watt of input light, and by subsequent interference of the scattered light with the main optical beams. The Optics Test Facility will be used to evaluate scattering from optical components and to coordinate the development of low-scatter optics. In addition, we plan extensive theoretical simulation of noise contributed from scattered light in the LIGO, using test data as input.

v. Optical component testing and quality assurance. We will develop programs to test and evaluate the many optical components required for LIGO interferometers. A first task will be to set technical specifications and identify suppliers for the components of initial LIGO interferometers. We anticipate that most of the components will be stock items provided by the optics industry, but these must be certified to be reliable for long-term use under vacuum at LIGO power levels. For other components, in particular electro-optic modulators, Faraday isolators, and single-mode optical fibers, we may find it advantageous to support industrial development of components optimized for the LIGO. We will also establish routine quality assurance procedures for newly acquired optics and routine screening tests for components in use.

b. Vibration isolation and thermal noise studies. The Vibration and Thermal Noise Test Facility will be used throughout the proposed grant period for tests of vibration-isolation stacks and suspensions for optical components. We anticipate that initial characterization and modeling of key concepts for the isolation system design will be completed before the beginning of the proposed grant period. More detailed testing will be pursued during the detailed interferometer design. This will entail construction of a working model of the candidate vibration-isolation stack for measurements of transfer function, drift, and cross-coupling between different degrees of freedom.

We have begun studies of the intrinsic damping and low-loss clamping techniques for candidate materials used in the pendulum suspension of LIGO test masses. We plan to investigate fundamental dissipation mechanisms and to determine the materials, processing methods, and geometries that are likely to result in the lowest thermal noise. Basic research in this area should enhance future LIGO capabilities to observe gravitational-wave sources at low frequencies (see Section V.B.).

4. Science design and planning

A significant effort in science planning and design will continue throughout the proposed grant period. Major efforts will be devoted to:

- Analysis and modeling in support of the engineering design of facilities and

interferometers.

- Analytic studies of the scaling of the interferometer optical and servo systems from 40 m to 4 km.
- Scientific strategy and systems engineering for control of beam position and orientation and fringe acquisition.
- Development of data-analysis strategies.
- Support of LIGO interferometer fabrication and testing.
- Coordination of collaborative R&D programs with outside groups.

5. R&D activity after the initial interferometer design effort

During CYs 1993 and 1994, activity will shift toward interferometer fabrication, subsystem testing, and installation of an interferometer at Site 1. At the same time, we intend to maintain research activity on the campuses. Part of this effort will be devoted to solving unforeseen technical problems and developing and testing subsystems for the initial interferometers. Another part will be development of the more advanced interferometers. We will also maintain a core effort of basic research directed at laying the foundation for improvements in future interferometer systems. This effort will be crucial to the evolution of future LIGO detectors, discussed in Section V.B.

6. Improvements to campus facilities

The 40-meter prototype currently operates in its original (with slight modifications) vacuum system. As this system will not be adequate to support LIGO operations, the vacuum envelope will be rebuilt with larger vacuum chambers and beam tubes.

The recently completed 5-meter vacuum system has a sufficiently large envelope for LIGO support, and we plan no extensive renovation of this facility during the proposed grant period. We will install a new laser system to upgrade the 5-meter prototype to high-power operation.

We will upgrade the instrumentation of both campus facilities to improve their capability for LIGO support. The new instrumentation will enhance the efficiency of prototype operations and expand our capability to test LIGO components.

IX. ORGANIZATION AND MANAGEMENT

The LIGO project is an integrated, collaborative effort between scientists at the California Institute of Technology (Caltech) and the Massachusetts Institute of Technology (MIT). The proposed organization of the project throughout the construction phase of the LIGO is shown in Figure IX-1. It differs from the existing organization in the provision for an external design review board, which will be constituted upon NSF approval of this proposal, and in the designation of an Assistant Director, who will take on tasks and responsibilities as delegated by the Director.

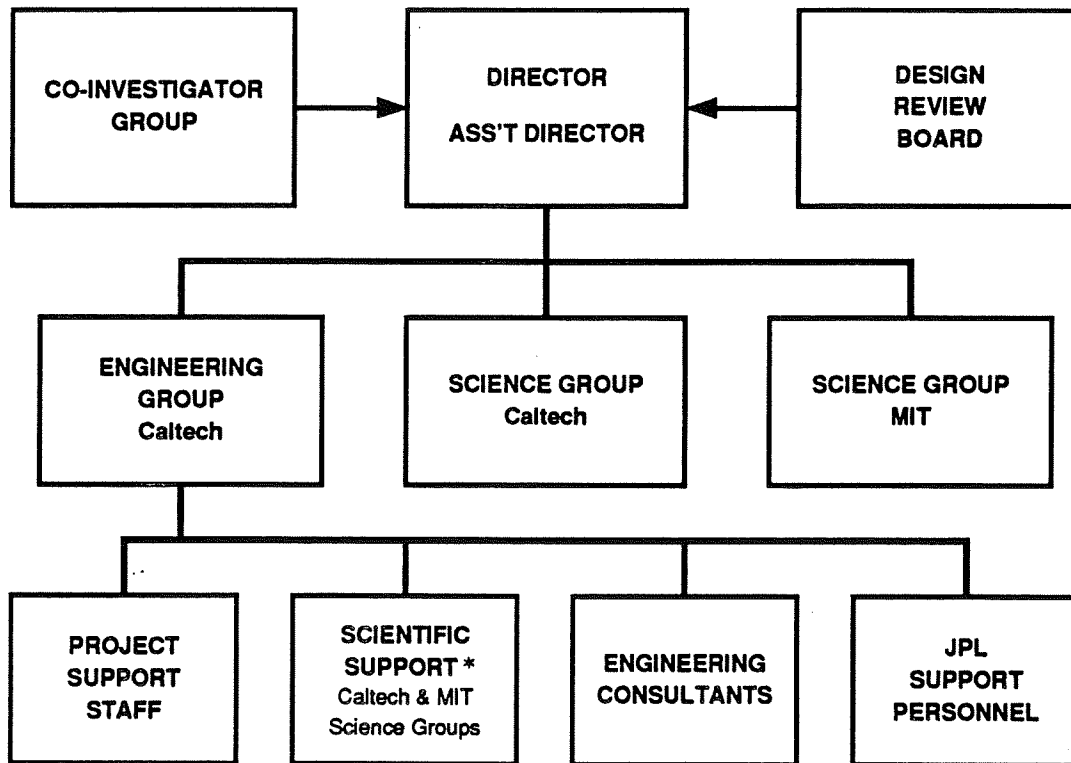


Figure IX-1 Organization and management of the LIGO project. (* Members of the science groups serve in two capacities: (1) the conduct of research and development, and (2) the support of engineering tasks.)

The Project Director and Principal Investigator has overall responsibility for all aspects of the LIGO Project. He reports administratively to the Provost of Caltech. His administrative contacts at MIT are the Chairman of the Department of Physics and the Director of the Center for Space Research.¹ Caltech serves as the prime contractor for the LIGO Project with the National Science Foundation

¹ See Appendix K, Memorandum of Understanding on the LIGO Project between Caltech and MIT.

(NSF); the activities of the MIT science group are supported under a subcontract from Caltech to MIT. The LIGO activities at MIT are coordinated by one of the Co-Investigators, Professor R. Weiss. The Project Director, Professor R. Vogt, and the other three Co-Investigators, Professors Drever, Raab, and Thorne, are resident at Caltech.

During the proposed construction phase, the science group will conduct interferometer research and development, provide science support to the engineering group, participate in the design, construction, installation, and operation of the LIGO interferometers, and conduct data analysis. The project's science staff includes, in addition to the Co-Investigators, eight scientists, six graduate students, and a varying number of undergraduates. We plan to strengthen the present science staff by about four physicists. We also expect to add another professorial faculty member (at MIT) in the near future. The number of graduate students on the project is expected to increase to about a dozen. The scientists will accomplish their work in task groups, whose leaders report to the director. Professor Thorne, a theoretical physicist/astrophysicist, and selected members of his research group² will provide analytical support to the project, as needed.

The engineering group is headed by a Chief Engineer, W. Althouse, who reports to the director. Its membership will increase from the current 12 to about 20 engineers, programmers, technicians, and programmatic support staff,³ counting personnel resident at both Caltech and MIT. During the construction phase, the engineering group, with close support from the science groups, will be responsible for overseeing the detailed engineering design and construction of the LIGO facilities. It also will implement the design and construction of interferometers and support equipment. The project will continue to take advantage, as needed, of engineering support from Caltech's Jet Propulsion Laboratory (JPL).

² The theoretical astrophysics activities are supported under separate grants.

³ Additional details on the engineering organization are provided in Volume 2, Section VI.B.

X. INTERNATIONAL AND DOMESTIC COLLABORATION

A. International

This proposal asks for construction in the United States of a two-site observatory, the minimum facility required for gravitational-wave event verification, diagnostics, and detector development (See Section VII). The LIGO, as proposed, cannot by itself extract the complete waveform information contained in a gravitational-wave burst. We will rely for full information upon an international network of observatories, to be established in a collaborative arrangement with scientists in Europe, Australia, and Japan.¹ At the present, there are serious proposals pending to establish two multi-kilometer-size observatory sites in Europe (British-German and French-Italian collaborations) and one in Australia. Participation of the United States LIGO in an international network will save the United States the construction costs for the third and fourth sites and assure an observing network with higher spatial resolution. Experience of radio astronomers with the VLBI (Very Long Baseline Interferometry) network has shown that such an undertaking can be executed successfully and at the same time provides information on how such a collaboration could be further improved.

A collaboration of the European and United States teams was officially initiated in Paris at a February 1989 meeting, convened by the NSF and attended by representatives of all European and United States gravitational-wave groups and their funding agencies. A number of working groups² has been established for efficient exchange of information on research topics of common interest.

B. Domestic

United States collaboration will be tightly focused and coordinated. Before and during the LIGO construction phase, collaborations will concentrate mainly upon the development of LIGO subsystems, such as lasers (Professor Byer, Stanford University; see Appendix K) and vibration isolation platforms (Professors Bender and Faller, University of Colorado at Boulder; see Appendix K). We expect that after the NSF makes a visible commitment to the construction of LIGO, other United States experimenters will want to establish collaborative arrangements with the

¹ As discussed in Sections II and V.C, the full information carried by a gravitational wave consists of the direction (θ, ϕ) to its source and its two waveforms $h_+(t)$ and $h_\times(t)$. For gravitational-wave bursts, extraction of their full information requires a minimum of three widely separated interferometers operating in coincidence. For better position resolution and waveform accuracy, especially for sources that lie in the plane defined by the three interferometers, it is important to have a minimum of four interferometers, distributed over the Earth so that they form a tetrahedron with large volume.

² Working group topics include Data Analysis, Data Acquisition, Lasers, Vibration Isolation, Mirrors, Vacuum, and Control Systems.

LIGO project on scientific and technical topics. We intend to maintain an effective interchange with the interested national community through publications, seminars, workshops, and visiting scientists; by the time LIGO becomes a fully operational facility, there will be considerable depth in the United States scientific community for participation in the observational and technical development program. During the LIGO operational phase, scientists from other than Caltech or MIT are expected to become users of LIGO both by (1) installing, cooperatively or independently, detector systems in the LIGO facilities and (2) engaging in the analysis of data derived from the Caltech/MIT "gravitational-wave watch" detectors.

We expect that a number of graduate students and postdoctoral fellows, who will be trained by the LIGO project, will enter the national scientific community to become LIGO outside users.

XI. REFERENCES

- I-1. C. M. Will, *Theory and Experiment in Gravitational Physics*, (Cambridge Univ. Press, Cambridge, 1981), chapt. 10.
- III-1. A. Rüdiger, R. Schilling, L. Schnupp, W. Winkler, H. Billing and K. Maischberger, *Optica Acta* **28**, 641, (1981).
- III-2. R.W.P. Drever, J. L. Hall, F. V. Kowalski, J. Hough, G. M. Ford, A. J. Munley, and H. Ward, *Appl. Phys.* **B31**, 97, (1983).
- V-1. R.W.P. Drever, "Interferometric Detectors for Gravitational Radiation," *Gravitational Radiation*, NATO Advanced Physics Institute, Les Houches, ed. N. Deruelle and T. Piran, (North Holland Publishing, 1983), 321.
- V-2. C. Man, A. Brillat, D. Shoemaker, "Ultra-high sensitivity interferometric techniques for the detection of gravitational waves," International Quantum Electronics Conference, Tokyo, July 1988.
- V-3. K. Maischberger, A. Rüdiger, R. Schilling, L. Schnupp, W. Winkler, and G. Leuchs, "Status of the Garching 30 meter prototype for a large gravitational wave detector," in *Experimental Gravitational Physics*, P. F. Michelson, H. En-ke, and G. Pizzella, eds., (World Scientific Publ., Singapore, 1988), p. 52.
- V-4. D. Shoemaker, R. Schilling, L. Schnupp, W. Winkler, K. Maischberger, *Phys. Rev.* **D38**, 423, (1988).
- V-5. W. Martin, "Experiments and Techniques for the Detection of Gravitational and Pulsed Electromagnetic Radiation from Astrophysical Sources," Ph.D. Thesis, University of Glasgow, 1978.
- V-6. C. M. Caves, *Phys. Rev.* **D23**, 1693, (1981).
- V-7. H. P. Yuen, *Phys. Rev.* **A13**, p. 2226, (1976).
- V-8. J. Gea-Banacloche, G. Leuchs, *J. Modern Opt.*, **34**, 793 (1987).
- V-9. C. A. Cantley, N. A. Robertson, and J. Hough, "A Suspension System for Use in a Laser Interferometric Gravitational Wave Detector," contributed talk, 12th Int. Conf. on Gen. Rel. and Grav., Boulder, (2-8 July 1989).
- V-10. R. Del Fabbro, A. di Virgilio, A. Giazotto, H. Kautzky, V. Montelatici, and D. Passuello, *Phys. Lett.* **A124**, 253, (1987).
- V-11. J. Kovalik, P. Saulson, M. Stephens, "The Performance of a Double Pendulum Vibration Isolation System," contributed talk, 12th Int. Conf. on Gen. Rel. and Grav., Boulder, (2-8 July 1989).
- V-12. R. Del Fabbro, A. di Virgilio, A. Giazotto, H. Kautzky, V. Montelatici, D. Passuello, *Phys. Lett.* **A132**, 237, (1988) and *Phys. Lett* **A133**, 471, (1988).
- V-13. J. E. Faller, R. L. Rinker, *NBS Dimensions*, **63**, 25, (1979).
- V-14. N. A. Robertson, R.W.P. Drever, I. Kerr, and J. Hough, *J. Phys. E. Sci. Instr.* **15**, 1101, (1982).
- V-15. P. R. Saulson, *Rev. Sci. Instr.*, **55**, 1315, (1984).

- V-16. A. Giazotto, D. Passuello, A. Stefanini, *Rev. Sci. Instr.* **57**, 1145, (1986).
- V-17. R. T. Stebbins, P. L. Bender, J. E. Faller, D. B. Newell, and C. C. Speake, "A 1-to-10 Hz Prototype Isolation System for Gravitational Wave Interferometers and Thermal Noise Measurements," contributed talk, 12th Int. Conf. on Gen. Rel. and Grav., Boulder, (2-8 July 1989).
- V-18. J. Hough, J. R. Pugh, R. Bland, R.W.P. Drever, *Nature* **254**, 498, (1975).
- V-19. B. Schutz and M. Tinto, *Monthly Notices of the Royal Astronomical Society*, **224**, 131, (1987).
- V-20. Y. Gürsel and M. Tinto, "A Near Optimal Solution to the Inverse Problem for Gravitational Wave Bursts," *LIGO preprint 89-1*, accepted for publication in *Phys. Rev. D*.
- V-21. B. F. Schutz, "Sources of Gravitational Radiation," in *Gravitational Wave Data Analysis*, B. F. Schutz, ed., (Kluwer Academic, 1989), p. 3.
- VII-1. J. Livas, "Broadband Search Techniques for Periodic Sources of Gravitational Radiation," in *Gravitational Wave Data Analysis*, B. F. Schutz, ed., (Kluwer Academic, 1989), p. 217.
- VIII-1. R. Weiss, *Quartr. Progr. Rep. Res. Lab. Electr. MIT*, **105**, 54, (1972).
- VIII-2. J. Livas, R. Benford, D. Dewey, A. Jeffries, P. Linsay, P. Saulson, D. Shoemaker, R. Weiss, "The M.I.T. Prototype Gravitational Wave Detector," in *Proc. Fourth Marcel Grossman Mtg. on Gen. Rel.*, R. Ruffini, ed. (Elsevier Science Publishers, 1986) p. 591, (1985).
- VIII-3. P. S. Linsay, D. H. Shoemaker, *Rev. Sci. Instr.* **53**, 1014, (1982).
- VIII-4. R.W.P. Drever, G. M. Ford, J. Hough, I. M. Kerr, A. J. Munley, J. R. Pugh, N. A. Robertson, and H. Ward, "A Gravity-Wave Detector Using Optical Sensing," in *Proceedings of the Ninth International Conference on General Relativity and Gravitation (Jena 1980)*, ed. E. Schmutzer (VEB Deutscher Verlag der Wissenschaften, Berlin, 1983), 265.
- VIII-5. R.W.P. Drever, J. Hough, A. J. Munley, S.-A. Lee, R. Spero, S. E. Whitcomb, J. Pugh, G. Newton, B. Meers, E. Brooks III, Y. Gürsel, "Gravitational-Wave Detectors Using Laser-Interferometers and Optical Cavities," in *Quantum Optics, Experimental Gravity, and Measurement Theory* ed. P Meystere and M.O. Scully, (Plenum Publishing, 1983), 503.
- VIII-6. S. Whitcomb, D. Z. Anderson, R.W.P. Drever, Y. Gürsel, M. Hereld, R. Spero, "Laser-Interferometer Experiments at Caltech," in *Proc. Third Marcel Grossman Mtg. on Gen. Rel.*, Hu Ning, ed., (Science Press and North-Holland Publishing Co., 1983), p. 1399.
- VIII-7. K. S. Thorne, "Gravitational radiation," in *300 Years of Gravitation*, S. W. Hawking and W. Israel, eds., (Cambridge Univ. Press, Cambridge, 1987), p. 330.

XII. SCHEDULE AND BUDGET

This section presents an overview of the LIGO Project schedule and costs. Details may be found in Volume 2, Section VI and Section VII.

A summary project schedule is shown in Figure XII-1. The design and construction activities span the 4-year interval covered by this proposal. Engineering design of the LIGO facilities will proceed upon the availability of funds, estimated to be at the beginning of calendar year 1991. The engineering design is estimated to take 18 months. Procurement of some long-lead items will be initiated during this period. Construction at the first site, which may commence after completion of the first year of the design activity, is estimated to take about two years. Construction at the second site, also estimated to take about two years, starts one year after the start of construction at Site 1 to allow use of the same contractors at both sites and take maximum advantage of the experience gained at Site 1. At the end of the proposed 4-year period, construction at both sites will be completed, the first Mark I interferometer will be installed, and we should be ready to begin operations at Site 1. Operations at Site 2 will start 1 year later after completing checkout and acceptance testing of the Site 2 facilities and installation of a Mark I interferometer there.

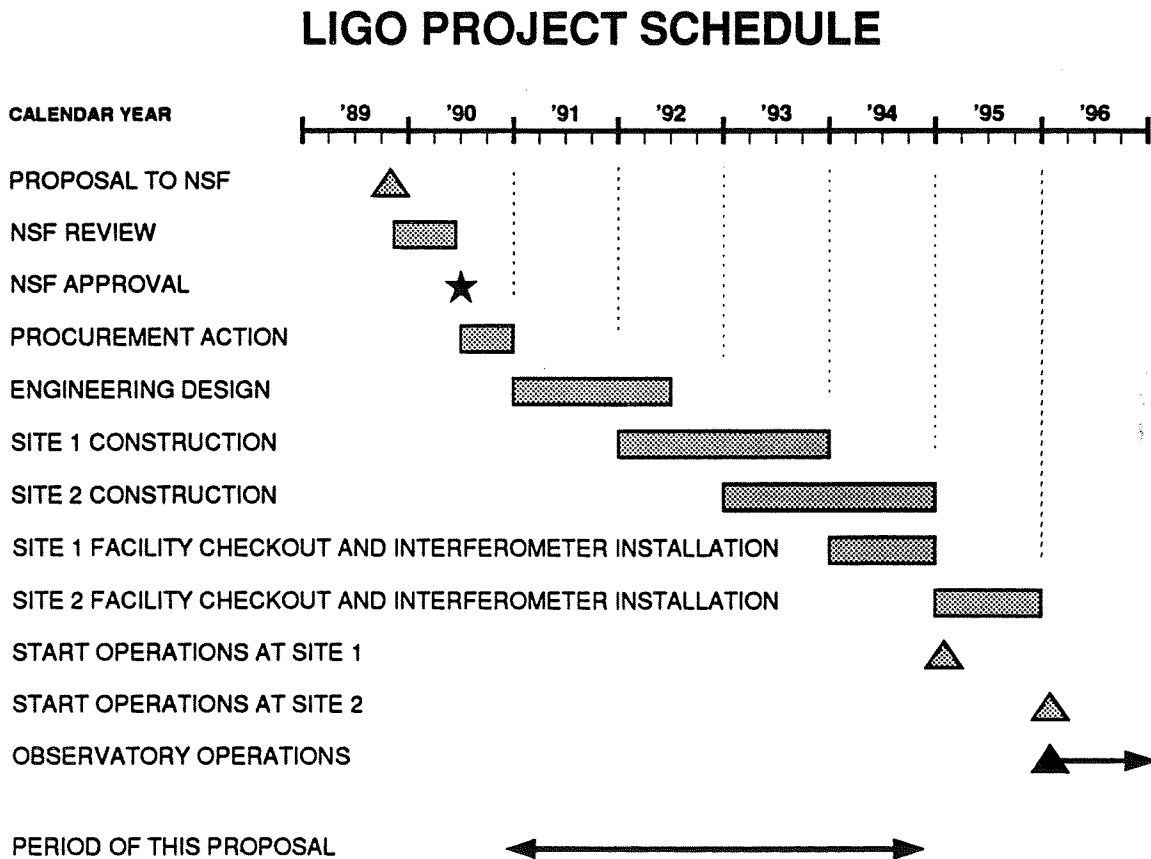


Figure XII-1 LIGO project schedule.

The total estimated cost of the LIGO Project during the construction phase is summarized in Table XII-1. The research and development item covers the estimated cost of LIGO team salaries, supplies, expenses, and equipment required to support the effort described in Section VIII.B. The amount for "LIGO Design and Construction" covers the total estimated cost of the LIGO facilities and initial interferometers, including in-house scientific, engineering, and management support of the construction project. "Remote Site Operations" covers the cost of on-site manpower, facility, and equipment maintenance, and utilities costs for the first site, the operation of which will commence in the fourth year of the proposed construction period. All costs are given in 1989 dollars. An inflation allowance, computed at a rate of 5% per year, is separately computed and added to the annual 1989 amounts shown. The total amount requested is \$193.8 million in FY'89 dollars.

TABLE XII-1
LIGO PROJECT—TOTAL COST SUMMARY
FY89 \$M

	1991	1992	1993	1994	TOTAL	Note:
Research and Development	3.0	3.0	3.0	3.0	12.0	1
LIGO Design and Construction	44.6	49.4	48.1	37.7	179.8	2
Remote Site Operations				2.0	2.0	3
TOTAL ESTIMATED COST, FY89 \$M	47.6	52.4	51.1	42.7	193.8	
Inflation allowance @ 5%/yr, FY89 base	4.9	8.3	11.0	11.8	36.0	
TOTAL ESTIMATED COST, ESCALATED \$M	52.5	60.7	62.1	54.5	229.8	

Note 1: Caltech/MIT on-campus research and development effort
Note 2: Total cost of remote LIGO installations including initial interferometers, excluding ~\$7.0M in local sales taxes pending decision on ownership of LIGO facilities (government or private)
Note 3: LIGO remote site operations cost for first year, Site 1

RESPONSE TO NSF NOTICE NO. 107

A. Education and Development of Human Resources

Interferometric gravitational-wave detection is a unique, developing discipline that does not yet fit the patterns of established research in physics and astrophysics. It provides training for scientists, primarily undergraduate and graduate students, in experimental skills associated with the design, construction and operation of sophisticated and precise electronic, optical, and mechanical systems. Scientists trained in this field acquire a deep understanding of experimental techniques that span several fields—an opportunity now rare in much of physics. These scientists often become consummate experimental physicists, employed by industry, government laboratories, and university research groups.

The *academic* career path for scientists in this discipline has been difficult and will continue to be so until the LIGO comes to fruition. The technically intensive nature of this work in its early stages does not match the criteria established for university hiring and promotions. Typically, physics faculties must gamble that gravitational-wave astronomy will become “scientifically” productive on a reasonable time scale. Other fields in physics, such as high-energy physics and space research, also have long-term technical phases, but these are established fields with virtually guaranteed scientific results. They also have a substantial network of laboratories and research centers that permit an academic researcher the mobility to remain in the field. The LIGO Project is obliged to recognize these facts in the recruitment and employment of tenure-track faculty and postdoctoral associates.

During the design and construction phase, research will be even more technically intensive than it is now. The major part of the effort will be focused on bringing the facilities and first interferometers into operation. This will require professional scientists, graduate students, and undergraduates working with engineers. The opportunities for training scientists in the LIGO Project will improve as the project proceeds. There will be a role for postdoctoral scientists willing to assume such technical research and development as interferometer subsystem development, analysis and testing, and development of software for data analysis. These efforts, however, will most likely not result in many scientific publications, and the project will employ the majority of additional scientists in longer-term staff positions.

Once the LIGO is operating, the opportunities for junior scientists will change dramatically. Many of the scientists who have worked through the design and construction phase then become the leaders of a new field. The expectation is that the initial observations will be scientifically important and publishable, even if only to set significant upper limits to the gravitational-wave flux. The data will be analyzed in many ways and in different types of independent investigations, limited only by the creativity of the individuals working with it. There will be continuing opportunities for students and junior scientists with technical interests

in the development of advanced interferometers. They will have the opportunity to work in a setting that is closer to “small science” than “big science.”

In the observation phase, the LIGO will offer opportunities for training and development of junior experimental scientists in the disciplinary styles of physics (the development of sophisticated, fundamental measurement techniques and technologies) and astronomy (astrophysical observation, analysis, and modeling).¹

Once the LIGO exists, any investigation will break new ground in terms of astrophysical sensitivity. It is very likely that other universities will then become involved and the academic opportunities for young scientists in this field will expand. The style of gravitational-wave research will then resemble that of other productive areas in physics and astrophysics.

In summary, we foresee a gradual evolution in the training and development pattern of scientists as the LIGO progresses. During the construction phase, there will be opportunities for undergraduates to get their first exposure to research, or for graduate students to do thesis work. Junior scientists will have only limited opportunities to establish credentials; their careers will be better served by longer term scientific staff appointments than by short-term postdoctoral appointments. Beginning with the observation phase, opportunities for undergraduates, graduate students, and postdoctoral trainees will become abundant.

B. P. I.: Biography

(See Key Personnel: Vitae)

C. P. I.: List of (5) Publications Relevant to Proposed Research

None (P.I. took on duties of director of LIGO Project in Fall 1987).

D. P. I.: List of (5) Other Publications

“Electrons in the Primary Cosmic Radiation,” (with P. Meyer), *Phys. Rev. Letters*, **6**, 193 (1961).

“The Isotopic Composition of Solar Flare Accelerated Neon,” (with R. A. Mewaldt, J. D. Spalding, and E. C. Stone), *Ap. J. (Letters)*, **231**, L97 (1979).

“Voyager 1: Energetic Ions and Electrons in the Jovian Magnetosphere,” (with W. R. Cook, A. C. Cummings, T. L. Garrard, N. Gehrels, E. C. Stone, J. H. Trainor, A. W. Schardt, T. Conlon, N. Lal, and F. B. McDonald), *Science*, **204**, 1003 (1979).

“Energetic Charged Particles in Saturn’s Magnetosphere: Voyager 1 Results,” (with D. L. Chenette, A. C. Cummings, T. L. Garrard, E. C. Stone, A. W. Schardt, J. H. Trainor, N. Lal, and F. B. McDonald), *Science*, **212**, 231 (1981).

¹ The LIGO will also offer, during both the development and operations phases, opportunities for applied research, including control systems and computation.

“Elemental Composition of Solar Energetic Particles,” (with W. R. Cook and E. C. Stone), *Ap. J.*, **279**, 827 (1984).

E. P. I.: Names of Graduate Students and Postdoctoral Scholars Sponsored During Past Five Years

None (P.I. has held administrative and science management positions since 1975).

F. P. I.: Total Number of Graduate Students Advised and Postdoctoral Scholars Sponsored

Advisor or co-advisor to 21 Ph.D students

Sponsor or co-sponsor of ~ 12 postdoctoral scholars

G. P. I.: Collaborators or Associates During Past 48 Months

Members of LIGO team, including

Prof. R. Drever, Caltech

Prof. F. Raab, Caltech

Prof. K. Thorne, Caltech

Prof. R. Weiss, MIT

Collaborators:

Prof. P. Bender, JILA, Boulder

Prof. J. Faller, JILA, Boulder

Prof. R. Byer, Stanford University

H. P. I.: Graduate Advisors

Prof. P. Meyer, University of Chicago

Prof. J. Simpson, University of Chicago

KEY PERSONNEL: VITAE

William E. Althouse

Born: December 2, 1942, Los Angeles, California
U.S. Citizen

Present

Position: Member of the Professional Staff, Caltech

Education: 1968-B.S.E.E. California State Polytechnic University

Positions: 1963-1964 Electronics Technician, Caltech
1964-1965 Junior Engineer, Caltech
1965-1969 Associate Engineer, Caltech
1969-1972 Electronics Engineer, Caltech
1972-1979 Senior Engineer, Caltech
1979-1981 Technical Manager, Caltech
1981-1987 Chief Engineer, Space Radiation Laboratory, Caltech
1987-present Chief Engineer, Caltech/MIT Laser Interferometer
Gravitational Wave Observatory (LIGO) Project

Research:

Developed, managed, supervised and/or participated in gamma-ray astronomy and high energy charged particle experiments: Team Leader, balloon-borne gamma-ray imaging observations of SN1987a; engineering supervisor, Heavy Ion Counter experiment, Galileo Project; engineering supervisor, Gamma-Ray Imaging Payload Project; Experiment Manager, Comprehensive Particle Analysis System, International Solar Polar Mission; Experiment Manager, Heavy Isotope Spectrometer Telescope experiment, International Sun-Earth Explorer Project; Deputy Experiment Manager, Cosmic Ray Subsystem, Voyager Project; Project Manager, Electron-Isotope Spectrometer, Interplanetary Monitoring Platforms 7 and 8; Project Engineer, Galactic Cosmic Ray Experiment, Orbiting Geophysical Observatory Project.

Other

Activities: Assistant Chairman, Nuclear Science Symposium, 1979-1985

Professional Societies: Institute of Electrical and Electronics Engineers
IEEE Nuclear Sciences and Plasma Society
IEEE Computer Society
IEEE Instrumentation and Measurement Society
IEEE Lasers and Electro-Optics Society

Ronald William Prest Drever

Born: October 26, 1931, Scotland
British Citizen

Present
Position: Professor of Physics, Caltech

Education: 1953–B.S. Glasgow University
1958–Ph.D. Glasgow University

Positions: 1956–1960 Research Fellow, Glasgow University
1960–1967 Lecturer, Glasgow University
1960–1961 Research Fellow, Harvard University
1967–1973 Senior Lecturer, Glasgow University
1973–1975 Reader, Glasgow University
1975–1979 Titular Professor, Glasgow University
1977–1978 Visiting Associate, Caltech
1979–1984 Professor of Physics, Part-time, Caltech
1979–1984 Professor of Physics, Part-time, Glasgow University
1984–present. Professor of Physics, Caltech

Research:

Ph.D. and post-doctoral work in experimental nuclear physics and low energy beta spectroscopy, including experiments relevant to neutrino mass, and on spectrum and half-life of rhenium 187 setting limits to change of fine structure constant with geological time. Experiments on anisotropy of inertial mass by nuclear free precession in the earth's magnetic field. Work on Mossbauer effect, at Harvard; on studies of cosmic rays by atmospheric Cerenkov radiation, at Harwell; on pulse radio astronomy and other astronomical experiments.

Work on gravitational radiation experiments since 1972. Development of wide-band gravity-wave bar detectors and first extensive searches for pulses; stochastic background radiation with them. Developed laser interferometer gravity wave detection techniques using optical cavities, at the University of Glasgow and at Caltech.

Other
Activities: 1968–1972 Consultant and Vacation Assistant, Atomic Energy Research Establishment, Harwell (U.K. Atomic Energy Authority)
1972–1974 Member of the Astronomy Policy and Grants Committee, (U.K. Science Research Council)
1972–1976 Council Member of the Royal Astronomical Society
1973–1976 Vice President of the Royal Astronomical Society
1974 Consultant, National Science Foundation
1974–1976 Royal Astronomical Society Assessor to the Astronomy I Committee
1979 Morris Loeb Lectureship in Physics, Harvard University
1985 Ernest Guptill Memorial Lecturer, Dalhousie University, Canada

Professional
Societies: Fellow of the Royal Society of Edinburgh
Member of the International Society of General Relativity on Gravitation

Frederick J. Raab

Born: October 14, 1951, New York City, New York
U.S. Citizen

Present
Position: Assistant Professor of Physics, Caltech
Affiliate Assistant Professor of Physics
University of Washington

Education: 1973-B.S. Physics, Manhattan College, N.Y.
1975-M.A. Physics, S.U.N.Y. Stony Brook, N.Y.
1980-Ph.D. Physics, S.U.N.Y. Stony Brook, N.Y.

Positions: 1980-1984 Postdoctoral Research Associate
University of Washington
1984-1986 Research Associate
University of Washington
1986-1988 Research Assistant Professor
University of Washington
1988-present Assistant Professor of Physics, Caltech

Research:
Pulsed laser development.
Atomic and molecular spectroscopy.
Precision measurements of fundamental symmetries: Time Reversal Non-invariance, Local Lorentz Invariance, Equivalence Principle.
Searches for intermediate range forces.
Laser interferometric gravity wave detector development.

Professional
Societies: American Physical Society

Honors: NBS Precision Measurements Grant Award, 1986.

Kip S. Thorne

Born: June 1, 1940, Logan, Utah
U.S. Citizen

Present Positions: The William R. Kenan, Jr., Professor, and Professor of Theoretical Physics, Caltech
Adjunct Professor Physics, University of Utah
Andrew D. White Professor at Large, Cornell University

Education: 1962 B.S. California Institute of Technology
1963 A.M. Princeton University
1965 Ph.D. Princeton University

Positions: 1965–1966 Postdoctoral Fellow in Physics, Princeton
1966–1967 Research Fellow in Physics, Caltech
1967–1970 Associate Professor of Theoretical Physics, Caltech
1970–present Professor of Theoretical Physics, Caltech
1971–present Adjunct Professor of Physics, University of Utah
1981–present The William R. Kenan, Jr., Professor, Caltech
1986–present Andrew D. White Professor at Large, Cornell

Research: Theoretical physics, gravitation physics, astrophysics.

Other Activities: International Committee on General Relativity and Gravitation, 1971–1980
Committee on US-USSR Cooperation in Physics, 1978–1979
Advisory Board, Institute for Theoretical Physics, Santa Barbara, 1978–1980
Space Science Board, 1980–1983
Advisory Board, Institute for Theoretical Physics, University of Florida, 1989–present

Honors: Fulbright Lecturer in France, 1966
Alfred P. Sloan Foundation Research Fellow in Physics, 1966–1968
John Simon Guggenheim Fellow, 1967–1968
AIP–U.S. Steel Foundation Science Writing Award in Physics and Astronomy, 1969
Fellow, American Academy of Arts and Sciences, 1972–present
Member, National Academy of Sciences, 1973–present
Honorary Doctor of Science, Illinois College, 1979
Doctoris Honoris Causa, Moscow University, 1981

Professional Societies: American Astronomical Society
International Astronomical Union
American Physical Society, Fellow
American Association for the Advancement of Science, Fellow

Rochus E. Vogt

Born: December 21, 1929, Germany (FRG)
U.S. Citizen

Present Position: R. Stanton Avery Distinguished Service Professor and
Professor of Physics, Caltech
Director, Caltech/MIT Laser Interferometer Gravitational
Wave Observatory (LIGO) Project

Education: 1952—cand. phys. Technische Hochschule Karlsruhe, FRG
Universität Heidelberg, FRG
1957—S.M. University of Chicago
1961—Ph.D. University of Chicago

Positions: 1953—1961 Research Assistant, Enrico Fermi Institute for
Nuclear Studies, University of Chicago
1961—1962 Research Associate, Enrico Fermi Institute for
Nuclear Studies, University of Chicago
1962—1965 Assistant Professor of Physics, Caltech
1965—1970 Associate Professor of Physics, Caltech
1970—present Professor of Physics, Caltech
1975—1977 Chairman of the Faculty, Caltech
1977—1978 Chief Scientist, Jet Propulsion Laboratory (JPL),
Caltech
1978—1983 Chairman, Division of Physics, Mathematics and
Astronomy, Caltech
1980—1981 Acting Director, Owens Valley Radio Observatory,
Caltech
1982—present R. Stanton Avery Distinguished Service Professor,
Caltech
1983—1987 Vice President and Provost, Caltech
1987—present Director, Caltech/MIT Laser Interferometer
Gravitational Wave Observatory (LIGO) Project
1988—present Visiting Professor of Physics, Massachusetts
Institute of Technology

Research:

Research on astrophysical aspects of cosmic radiation and in gamma-ray astronomy.
Gravitational Wave Astronomy.
Co-investigator (1962—1969) and Principal Investigator (1969—1983) on NASA grant supporting space research at Caltech. Principal Investigator on NASA's Voyagers 1 and 2 missions (1972—1984). Co-investigator on cosmic ray experiments on NASA's OGO-6, IMP 7 and 8, HEAO-3, ISEE-3 missions. Principal Investigator on NSF grant supporting the Caltech/MIT LIGO project (1988—present).

Other	1963–present	Various consultantships with government and industry
Activities:	1971–1973	Panel on Alternate Approaches to Graduate Education (Council of Graduate Schools in the US)
	1973–1976	Physical Sciences Committee (NASA)
	1984–present	Member of the Board of Directors, International Rectifier Corporation
	1985–1987	Vice Chairman of the Board of Directors, California Association for Research in Astronomy
	1985–1989	Princeton University Physics Department Advisory Council
	1986–present	Member, UC Scientific & Academic Advisory Committee for Los Alamos and Lawrence Livermore National Laboratories
Professional	American Physical Society (Fellow)	
Societies:	American Association for the Advancement of Science	
Honors:	Member, Studienstiftung des deutschen Volkes (1950–1953)	
	Fulbright Fellow (1953–1954)	
	Professional Achievement Award (1981), University of Chicago Alumni Association	
	NASA Exceptional Scientific Achievement Medal (1981)	
	R. Stanton Avery Distinguished Service Professor, Caltech (1982)	

Rainer Weiss

Born: September 29, 1932, Berlin, Germany
U.S. Citizen

Present

Position: Professor of Physics, MIT

Education: 1955–B.S. Massachusetts Institute of Technology
1962–Ph.D. Massachusetts Institute of Technology

Positions: 1960–1961 Instructor of Physics, Tufts University
1961–1962 Assistant Professor of Physics, Tufts University
1962–1964 Research Associate in Physics, Princeton University
1964–1967 Assistant Professor of Physics, MIT
1967–1973 Associate Professor of Physics, MIT
1973–present Professor of Physics, MIT

Research:

Experimental Atomic Physics, Atomic Clocks, Laser Physics, Experimental Gravitation, Millimeter and Sub-millimeter Astronomy, Cosmic Background Measurements, Major Projects: Atomic Clock development, Balloon program to measure Cosmic Background Radiation, COBE satellite program, Laser Interferometer Gravitational-Wave Observatory (LIGO)

Professional Societies: American Association for the Advancement of Science
American Physical Society

Other

Activities: NASA Physical Science Committee, 1970–1974
National Academy Summer Study on Outer Planet Exploration, 1972
NASA Management Operations Working Group for Shuttle Astronomy, 1973– 1976
NASA Management Operations Working Group for Airborne Astronomy, 1973– 1986
Chairman, NASA Panel on Experimental Relativity and Gravitation, 1974–1976
NCAR Scientific Ballooning Advisory Panel, 1971–1978
Chairman, NCAR Scientific Ballooning Advisory Panel, 1974–1978
Members' Representative to NCAR from MIT, 1974–1982
Chairman, NSF Subcommittee on Gravitational Physics, 1978
NASA SSSC Committee, 1979–1982
NASA Infrared Detector Panel, 1978
NASA Space and Earth Science Advisory Committee, 1982
National Academy Space Science Board, 1983–1986
Panel Chairman on Fundamental Physics and Chemistry, National Academy Summer Study, Major Directions for Space Research 1995–2015, 1984–86
Panel for the Joint Institute of Laboratory Astrophysics, Board on Assessment of NBS Programs, National Academy of Sciences, 1985–present

KEY PERSONNEL: PUBLICATIONS

This section contains a listing of publications by key LIGO personnel (see VITAE) (ordered alphabetically).

William E. Althouse

Publications

1. "A Solar and Galactic Cosmic Ray Satellite Experiment", (with E. C. Stone, R. E. Vogt, and T. H. Harrington), *IEEE Trans. on Nuclear Science*, **NS-15**, 229 (1968).
2. "A Cosmic Ray Isotope Spectrometer", (with A. C. Cummings, T. L. Garrard, R. A. Mewaldt, E. C. Stone, and R. E. Vogt), *IEEE Trans. on Geoscience Electronics*, **GE-16**, 204 (1978).
3. "The Voyager Cosmic Ray Experiment", (with D. E. Stilwell, W. D. Davis, R. M. Joyce, F. B. McDonald, J. H. Trainor, A. C. Cummings, T. L. Garrard, E. C. Stone, and R. E. Vogt), *IEEE Trans. on Nuclear Science*, **NS-26**, 513 (1979).
4. "A Balloon-Borne Imaging Gamma-Ray Telescope", (with W. R. Cook, A. C. Cummings, M. H. Finger, T. A. Prince, S. M. Schindler, C. H. Starr, and E. C. Stone), *Conf. Papers*, 19th International Cosmic Ray Conference, La Jolla, CA, **3**, 299 (1985).
5. "Balloon-Borne Video Cassette Recorders for Digital Data Storage", (with W. R. Cook), *ibid*, **3**, 395 (1985).
6. "First Flight of a New Balloon-Borne Gamma-Ray Imaging Telescope", (with W. R. Cook, A. C. Cummings, M. H. Finger, D. M. Palmer, T. A. Prince, S. M. Schindler, C. H. Starr, and E. C. Stone), *Conf. Papers*, 20th International Cosmic Ray Conference, Moscow, USSR, **1**, 84 (1987).

Ronald W.P. Drever

Publications

1. "K-Capture in the Decay of Chlorine-36", (with A. Moljk), *Phil. Mag. (7th Series)*, **46**, 1336 (1955).
2. "Neutron Activation Applied to Potassium-Mineral Dating", (with A. Moljk and S. C. Curran), *Rev. Sci. Inst.*, **26**, 1034 (1955).
3. "Measurement of Tritium as Water Vapour", (with A. Moljk), *Rev. Sci. Inst.*, **27**, 650 (1956).
4. "Ratio of K-Capture to Positron Emission in Flourine-18", (with A. Moljk and S. C. Curran), *Nucl. Inst. and Meth.*, **1**, 41 (1957).
5. "L/K Capture Ratio of Germanium-71", (with A. Moljk), *Phil. Mag. (8th Series)*, **2**, 427 (1957).
6. "Proportional Counters for Demonstration Experiments", (with A. Moljk), *Amer. J. Phys.*, **25**, 165 (1957).
7. "The Background of Counters and Radiocarbon Dating", (with A. Moljk and S. C. Curran), *Proc. Roy. Soc.*, **A239**, 433 (1957).
8. "Studies of Orbital Electron Capture Using Proportional Counters", Ph.D. Thesis, University of Glasgow (1958).
9. "Proportional Counters for Low Activity Measurements", (with A. Moljk and S. C. Curran), (*Proceedings of the 1st UNESCO International Conference, Paris, 1957*), *Radioisotopes in Scientific Research*, **II**, 596 (1958).
10. "Upper Limit to Anisotropy of Inertial Mass", *Phil. Mag. (8th Series)*, **5**, 409 (1960).
11. "A Search for Anisotropy of Inertial Mass Using a Free Precession Technique", *Phil. Mag. (8th Series)*, **6**, 683 (1961).
12. "Effect of Hydrostatic Compression on the 14.4 keV Gamma Ray from Iron-57", (with R. V. Pound and G. B. Benedek), *Phys. Rev. Lett.*, **7**, 405 (1961).
13. "The L/K Capture Ratio of Argon-37", (with P. W. Dougan and K.W.D. Ledingham), *Phil. Mag. (8th Series)*, **7**, 475 (1962).
14. "The Decay of Chlorine-36 to Sulphur-36", (with P. W. Dougan and K.W.D. Ledingham), *Phil. Mag. (8th Series)*, **7**, 1223 (1962).
15. "The Ratio of K-Capture to Positron Emission in the Decay of Nitrogen-13", (with K.W.D. Ledingham and J. A. Payne), *Proceedings of the International Conference on Role of Atomic Electrons in Nuclear Transformations, Warsaw, 1963*, ed. D. Berenyi, **II**, 359 (1956).

16. "Search for High Energy Gamma-Rays from Pulsar CP 1133", (with W. N. Charman, J. V. Jelley, P. R. Orman and B. McBreen), *Nature*, **220**, 565 (1968).
17. "A Technique for Removing Pile-Up Distortion in High Precision Pulse Height Spectroscopy", (with M.D.C. Williams), *Proceedings of the International Symposium on Nuclear Electronics*, Versailles (1968).
18. "Further Search for High Energy Gamma-Rays from CP 1133", (with W. N. Charman), *Nature*, **224**, 567 (1969).
19. "A Search for Periodic High Energy Gamma-Rays from Pulsars", (with W. N. Charman and J. V. Jelley), *Proceedings of the 11th International Conference on Cosmic Rays*, Budapest, 1969; *Act Phys. Acad. Sci. Hungary*, **29**, Suppl. 1, 63 (1970).
20. "The Ratio of K-Capture to Positron Emission in the Decay of Carbon-11", (with J. L. Campbell, W. Leiper and K.W.D. Ledingham), *Nucl. Phys.*, **A96**, 279 (1967).
21. "Upper-Air Fluorescence as a Tool in X-Ray Astronomy and Searches for X-Rays from CP 0532 and Other Pulsars", (with W. N. Charman, J. H. Fruin and J. V. Jelley), in *Non Solar X- and Gamma-ray Astronomy*, ed. L. Gratton, Int. Astron. Union, (1970).
22. "Spaced Receiver Observations of Radio Pulses", (with W. N. Charman, J. H. Fruin, J. V. Jelley, E. R. Hodgson, P. F. Scott, J. R. Shakeshaft, G. A. Baird, T. Delaney, B. G. Lawless, W.P.S. Meikle, R. A. Porter and R. A. Spencer), *Nature*, **228**, 346 (1970).
23. "A Search for Isolated Radio Pulses from the Galactic Centre at 151.5 MHz.", (with W. N. Charman, J. H. Fruin, J. V. Jelley, R. F. Haynes, E. R. Hodgson, P. F. Scott, J. R. Shakeshaft, G. A. Baird, T. Delaney, B. G. Lawless and W.P.S. Meikle), *Nature*, **232**, 177 (1971).
24. "A Precision Sidereal Telescope Drive", (with J. H. Fruin and J. V. Jelley), *Observatory*, **91**, 203 (1971).
25. "K-Electron Capture to Positron Emission Ratio in the Decays of Oxygen-15 and Neon-19", (with W. Leiper), *Phys. Rev.*, **C6**, 1132 (1972).
26. "A Search for Isolated Radio Pulses from the Crab Nebula at 151.5 MHz.", (with W.P.S. Meikle, R. F. Haynes, J. R. Shakeshaft, W. N. Charman and J. V. Jelley), *Mon. Not. Astro. Soc.*, **160**, 50 (1972).
27. "Proportional Counters for the Localization of Ionizing Radiation", (with J. Hough), *Nucl. Instr. and Meth.*, **103**, 365 (1972).
28. "Contribution to Open Discussion on Gravitational Radiation Experiments", *Proceedings of the 6th Texas Symposium on Relativistic Astrophysics*, Ann. New York Acad. Sci., ed. J. H. Hegyi, **224**, 103 (1973).
29. "Weber's Waves", *Nature*, **243**, 553 (1973).

30. "Search for Short Bursts of Gravitational Radiation", (with J. Hough, R. Bland and G. W. Lessnoff), *Nature*, **246**, 340 (1973).
31. "An Experiment to Search for Prompt Emissions from Supernovae at Microwave Frequencies", (with J. V. Jelley, W.P.S. Meikle, G.G.C. Palumbo, F. Bonoli, H. Smith and T. Delaney), *Proceeding of the International Conference on Supernovae and Supernovae Remnants, Lecce, May, 1973*, ed. C.G. Cosmovici, **61**, (D. Reidel Publishing Co., 1974).
32. "Experiments and Observations with Wide Band Gravity-Wave Detectors", (with J. Hough, R. Bland, G. W. Lessnoff), *Colloque Internationaux du Centre National de la Recherche Scientifique (Ondes et Radiations Gravitationnelles, June, 1973): CNRS Report*, ed. Y. Choquet-Bruhat, **220**, 113 (Paris, 1974).
33. "Gravitational-Wave Experiments", *Proceedings of the 1973 School for Young High Energy Physicists, Rutherford Laboratory*, ed. H. Muirhead. Rutherford Lab. Report RL-74-038, VIII-1 (1974).
34. "Searches for Ionospheric Effects of X-Ray Bursts, and for Bursts of Radio Emission, Gravitational Radiation and Microwave Emission from Astronomical Sources", (with W.P.S. Meikle, J. Hough, R. Bland, G. W. Lessnoff; in association with J. V. Jelley, T. Delaney and G.G.C. Palumbo), *Proceedings of the Conference on Transient Cosmic Gamma and X-ray Sources*, Los Alamos, September, 1978, ed. I. Strong, LA-5505-C Conference Proceedings UC-34B (1974).
35. "A Search for Isolated Microwave Pulses from the Perseus Clusters of Galaxies", (with T. Delaney, G. A. Baird, H. Smith, J. V. Jelley, J. H. Fruin, W.P.W. Meikle, G. Morigi, G.G.C. Palumbo and R. G. Partridge), *Astronomy and Astrophysics*, **36**, 83 (1974).
36. "Contribution to Panel Discussion on Gravitational-Waves", *Proceedings of the 7th International Conference on General Relativity and Gravitation, Tel-Aviv, June 1974*, ed. G. Shaviv and J. Rosen, 243-298 (1975).
37. "A Search for VHF Radio Pulses in Coincidence with Celestial Gamma-Ray Bursts", (with G. A. Baird, T. Delaney, B. F. Lawless, D. J. Griffiths, J. R. Shakeshaft, W.P.S. Meikle, J. V. Jelley and W. N. Charman), *Astrophysics J. Lett.*, **196**, L11 (1975).
38. "Search for Continuous Gravitational Radiation", (with J. Hough, J. R. Pugh and R. Bland), *Nature*, **254**, 498 (1975).
39. "An Upper Limit to Microwave Pulse Emission at the Onset of a Supernova", (with W.P.S. Meikle, G. A. Baird, T. Delaney, J. V. Jelley, J. H. Fruin, G.G.C. Palumbo, G. Morigi and R. B. Partridge), *Astronomy and Astrophysics*, **46**, 477 (1976).
40. "Gravitational-Wave Astronomy", *Quarterly J. Roy. Astr. Soc.*, **18**, 9 (1977).
41. "Gravitational-Wave Detectors Using Optical Interferometry", (with J. Hough,

- W. Edelstein and W. Martin), *Gravitazione Sperimentale*, (Accademia Nazionale dei Lincei, Rome), ed. B. Bertotti, 365 (1977).
42. "Upper Limits for the Microwave Pulsed Emission from Supernova Explosions in Clusters of Galaxies", (with G.G.C. Palumbo, N. Mandolesi, G. Morigi, G. A. Baird, T. Delaney, W.P.S. Meikle, J. V. Jelley, J. H. Fruin and B. Partridge), *Astrophysics Space Science*, **54**, 355 (1978).
 43. "Gravity-Wave Detection: A Tough Challenge", (with J. Hough), *New Scientist*, **79**, 464 (1978).
 44. "Quantum Nondemolition Measurements of Harmonic Oscillators", (with K. S. Thorne, C. M. Caves, M. Zimmermann and V. D. Sandberg), *Phys. Rev. Lett.*, **40**, 667 (1978).
 45. "The Quantum Limit for Gravitational Wave Detectors and Methods of Circumventing It", (with K. S. Thorne, C. M. Caves, V. D. Sandberg and M. Zimmermann), *Sources of Gravitational Radiation*, ed. L. Smarr, 49 (1979).
 46. "On the Measurement of a Weak Classical Force Coupled to a Quantum Mechanical Oscillator", (with C. M. Caves, V. D. Sandberg, K. S. Thorne and M. Zimmermann), *Rev. Mod. Phys.*, **52** (2), 341 (1980).
 47. "Optical Cavity Laser-Interferometers for Gravitational Wave Detection", (with J. Hough, A. J. Munley, S.-A. Lee, R. Spero, S. E. Whitcomb, H. Ward, G. M. Ford, M. Hereld, N. A. Robertson, I. Kerr, J. Pugh, G. P. Newton, B. Meers, E. D. Brooks III and Y. Gürsel), *Proceedings of the 5th International Conference on Laser Spectroscopy (VICOLS)*, Jasper, Canada, **33**, (1981).
 48. "Interferometric Detectors for Gravitational Radiation", *Gravitational Radiation*, NATO Advanced Physics Institute, Les Houches, ed. N. Deruelle and T. Piran, 321-337, (1983).
 49. "Laser-Interferometer Gravitational Radiation Detectors", *Science Underground, American Institute of Physics*, Conference Proceedings No. 96, 336-346 (Los Alamos, 1982).
 50. "Passive and Active Isolation for Gravitational Radiation Detectors and Other Instruments", (with N. A. Robertson, I. Kerr and J. Hough), *Phys. E. Sci. Instr.*, **15**, 1101-1105 (1982).
 51. "The Search for Gravitational-Waves", *Engineering and Science*, 6-9; 24-26 (Caltech, 1983).
 52. "Gravitational-Wave Detectors Using Laser-Interferometers and Optical Cavities: 1. Ideas, Principles, and Prospects", (with J. Hough, A. J. Munley, S.-A. Lee, R. Spero, S. E. Whitcomb, J. Pugh, G. Newton, B. Meers, E. Brooks III and Y. Gürsel), in *Quantum Optics, Experimental Gravity, and Measurement Theory*, ed. Pierre Meystere and Marlan O. Scully, 503-514 (Plenum Publishing, 1983).
 53. "Gravitational-Wave Detectors Using Laser-Interferometers and Optical Cav-

- ities: 2. Some Practical Aspects and Results”, (with J. Hough, A. J. Munley, S.-A. Lee, R. Spero, S. E. Whitcomb, J. Pugh, G. Newton, B. Meers, E. Brooks III and Y. Gürsel), in *Quantum Optics, Experimental Gravity, and Measurement Theory*, ed. Pierre Meystere and Marlan O. Scully, 515–524 (Plenum Publishing, 1983).
54. “Contribution on the Millisecond Pulsar”, *Proceedings of the Meeting of the Royal Astronomical Society, (December, 1982), The Observatory*, **103**, 118 (June 1983).
 55. “Laser Phase and Frequency Stabilization Using an Optical Resonator”, (with J. L. Hall, F. V. Kowalski, J. Hough, G. M. Ford, A. J. Munley and H. Ward), *Applied Physics*, **B31**, 97–103 (1983).
 56. “A Gravity-Wave Detector Using Optical Cavity Sensing”, (with G. Ford, J. Hough, I. Kerr, A. J. Munley, J. Pugh, N. Robertson and H. Ward), *Proceedings of the 9th International Conference on General Relativity and Gravitation, 1981*, ed. E. Schmutzer, 265–267, (Veb Deutscher Verlag der Wissenschaften, DDR-1080, Berlin, 1983).
 57. “Direct Observational Upper Limit to Gravitational Radiation from Millisecond Pulsar PSR 1937 + 214”, (with J. Hough, H. Ward, A. J. Munley, G. Newton, B. Meers, S. Hoggan and G. A. Kerr), *Nature*, **303**, (5941), 216–217 (May, 1983).
 58. “Laser-Interferometer Experiments at Caltech”, (with S. E. Whitcomb, D. Z. Anderson, Y. Gürsel, M. Hereld and R. Spero), *Proceedings of the Third Marcel Grossman Conference on General Relativity*, Shanghai, China 1982, ed. Hu Ning, 1399 (1983).
 59. “Developments in Laser-Interferometer Gravitational-Wave Detectors”, (with S. Hoggan, J. Hough, B. J. Meers, A. J. Munley, G. P. Newton, H. Ward, D. Z. Anderson, Y. Gürsel, M. Hereld, R. Spero and S. E. Whitcomb), *Proceedings of the Third Marcel Grossman Conference on General Relativity*, Shanghai, China 1982, ed. Hu Ning, 739–753 (1983).
 60. “The Caltech Gravitational-Wave Detector”, (with R. Spero, D. Z. Anderson, Y. Gürsel, G. Gutt, M. Hereld, K. Kaufman and S. E. Whitcomb), in *General Relativity and Gravitation, Proceedings of the 10th International Conference on General Relativity and Gravitation*, Padua, July 1983, eds. B. Bertotti, F. de Felice, and A. Pascolini, 930–932 (1984).
 61. “Development of Long Baseline Laser Interferometer Gravitational Radiation Detectors Using Resonant Optical Cavities”, (with H. Ward, J. Hough, A. J. Munley, G. P. Newton, B. J. Meers, S. Hoggan and G. A. Kerr), in *General Relativity and Gravitation, Proceedings of the 10th International Conference on General Relativity and Gravitation*, Padua, July 1983, eds. B. Bertotti, F. de Felice, and A. Pascolini, 939–941 (1984).

Frederick J. Raab

Publications

1. "Improvements to a Home-Built Nitrogen Laser", (with M. Feldman, P. Lebow and H. Metcalf), *Appl. Opt.*, **17**, 774 (1978).
2. "Measurement of g-factors by Quantum Beats in the OH Free Radical", (with P. Lebow and H. Metcalf), *Phys. Rev. Lett.*, **42**, 85 (1979).
3. "Quantum Beat Spectroscopy of the $A^2\Sigma$ State of the OH Free Radical", (with T. Bergeman, D. Lieberman and H. Metcalf), *Opt. Lett.*, **5**, 427 (1980).
4. "Precision Study of the $A^2\Sigma$ State of the OH Radical", (with T. Bergeman, D. Lieberman and H. Metcalf), *Phys. Rev.*, **A24**, 3120 (1981).
5. "Search for a Permanent Electric Dipole Moment on the ^{129}Xe Atom", (with T. G. Vold, B. Heckel and E. N. Fortson), *Phys. Rev. Lett.*, **52**, 2229 (1984).
6. "Optically-Pumped Atoms: A Tool for Fundamental Physics", *Satellite Workshop on Atomic Tests of General Physical Principles, Ninth Int. Conf. Atomic Phys.*, (1984).
7. "Search for a Permanent EDM on Atoms and Molecules", in *Atomic Physics 9*, R. S. Van Dyck and E. N. Fortson, eds., World Scientific, Singapore, (1984).
8. "Search for Electric Dipole Moments and Space Anisotropy", *Bull. Am. Phys.*, **30**, 715 (1985).
9. "Time Reversal Noninvariance and Electric Dipole Moments of Atoms", in *Advances in Laser Science I*, W. C. Stwalley and M. Lapp, eds., AIP Conf. Proc. No. 146, New York, (1986).
10. "Atomic Physics Tests of Gravity and the Equivalence Principle", *Bull. Am. Phys.*, **31**, 778 (1986).
11. "New Limits on Spatial Anisotropy Using Optically-Pumped Hg(201) and Hg(199)", (with S. K. Lamoreaux, J. P. Jacobs, B. R. Heckel and E. N. Fortson), *Phys. Rev. Lett.*, **57**, 3125 (1986).
12. "Search for an Intermediate Range Interaction", (with C. W. Stubbs, E. G. Adelberger, J. H. Gundlach, B. R. Heckel, K. D. McMurray, H. E. Swanson and R. Watanabe), *Phys. Rev. Lett.*, **58**, 1070 (1987).
13. "Search for Time Reversal Noninvariance in Atoms", in *Search for New and Exotic Phenomena*, J. Tran Thanh Van, ed., Proc. VIIth Moriond Workshop, Editions Frontieres, France, (1987).
14. "Search for an Intermediate Range Interaction: Results of the Eot.-Wash. I Experiment", in *Search for New and Exotic Phenomena*, J. Tran Thanh Van, ed., Proc. VIIth Moriond Workshop, Editions Frontieres, France, (1987).

15. "New Constraints on Composition-Dependent Interactions Weaker than Gravity", (with E. G. Adelberger, C. W. Stubbs, W. F. Rogers, B. R. Heckel, J. H. Gundlach, H. E. Swanson and R. Watanabe), *Phys. Rev. Lett.*, **59**, 849 (1987).
16. "New Constraints on Time-Reversal Asymmetry from a Search for a Permanent Electric Dipole Moment of ^{199}Hg ", (with S. K. Lamoreaux, J. P. Jacobs, B. R. Heckel and E. N. Fortson), *Phys. Rev. Lett.*, **59**, 2275 (1987).
17. "Limits on Composition-Dependent Interactions Using a Laboratory Source: Is There a "Fifth Force" Coupled to Isospin?", (with C. W. Stubbs, E. G. Adelberger, B. R. Heckel, W. F. Rogers, R. Watanabe and J. H. Gundlach), *Phys. Rev. Lett.*, **62**, 609 (1989).
18. "Optical Pumping Technique for Measuring Small Nuclear Quadrupole Shifts in 1S_0 Atoms and Testing Spatial Isotropy," (with S. K. Lamoreaux, J. P. Jacobs, B. R. Heckel, and E. N. Fortson), *Phys. Rev. A*, **39**, 1082 (1989).

Kip S. Thorne

Partial List of Publications

TECHNICAL BOOKS CO-AUTHORED

1. "Gravitation Theory and Gravitational Collapse," (with B. K. Harrison, M. Wakano, and J. A. Wheeler), *University of Chicago Press, Chicago, 1965*, 177 pp.
2. "High Energy Astrophysics, Vol. 3" (with A.G.W. Cameron), eds. C. DeWitt, E. Schatzman, P. Veron, *Gordon and Breach, New York, 1967*, 449 pp.
3. "Gravitation," (with C. W. Misner and J. A. Wheeler), *W. H. Freeman & Co., San Francisco, 1973*, 1279 pp.
4. "Black Holes: The Membrane Paradigm," (with R. H. Price and D. M. Macdonald), *Yale University Press, New Haven, Conn., 1986*, 367 pp.
5. "Gravitational Radiation: A New Window Onto the Universe," *Cambridge University Press, Cambridge, England, 1990*, in press.

SELECTED PUBLICATIONS ON GRAVITATIONAL RADIATION

6. "Gravitational Radiation Damping," *Physical Review Letters*, **21**, 320–323 (1968).
7. "Nonradial Pulsation of General Relativistic Stellar Models. III. Analytic and Numerical Results for Neutron Stars," *Astrophysical Journal*, **158**, 1–16 (1969).
8. "Gravitational-Wave Astronomy," (with W. H. Press), *Annual Review of Astronomy and Astrophysics*, **10**, 335–374 (1972).
9. "How to Test Gravitation Theories by Means of Gravitational-Wave Measurements," *Colloque Internationaux C.N.R.S. No. 220, "Ondes et Radiations Gravitationnelles"*, Institut Henri Poincaré, Paris, 214–223 (1974).
10. "The Generation of Gravitational Waves. I. Weak-Field Sources," (with S. Kovacs), *Astrophysical Journal*, **200**, 245–262 (1975).
11. "Gravitational-Wave Bursts from the Nuclei of Distant Galaxies and Quasars: Proposal for Detection Using Doppler Tracking of Interplanetary Spacecraft," (with V. B. Braginsky), *Astrophysical Journal*, **204**, L1–L6 (1976).
12. "Recent JPL Work on Gravity Wave Detection and Solar System Relativity Experiments," (with H. D. Wahlquist, J. D. Anderson, and F. B. Estabrook), *Gravitazione Sperimentale*, Proceedings of September 1976 Pavia Conference, ed. B. Bertotti (Rome: Accademia Nazionale dei Lincei), 335–350 (1977).
13. "The Generation of Gravitational Waves. IV. Bremsstrahlung," (with S. Kovacs) *Astrophysical Journal*, **222**, 62–85 (1978).

14. "The Generation of Gravitational Waves: A Review of Computational Techniques," *Topics in Theoretical and Experimental Gravitation Physics*, eds V. De Sabbata and J. Weber (Plenum Press, New York and London) 1-61 (1977).
15. "Quantum Nondemolition Measurements of Harmonic Oscillators," (with R.W.P. Drever, C. M. Caves, M. Zimmermann, and V. D. Sandberg), *Physical Review Letters*, **40**, 667-671 (1978).
16. "The Quantum Limit for Gravitational-Wave Detectors and Methods of Circumventing It," (with C. M. Caves, V. D. Sandberg, M. Zimmermann, and R.W.P. Drever), *Sources of Gravitational Radiation*, ed. L. Smarr (Cambridge: Cambridge University Press), 49-68 (1979).
17. "Quantum Non-demolition Measurements," (with V. D. Braginsky and Y. I. Vorontsov), *Science*, **209**, 547-557 (1980). Reprinted as Chapter VI.8 of "Quantum Theory and Measurement," ed. J. A. Wheeler and W. H. Zurek (Princeton University Press, Princeton, N.J.) 749-768 (1983).
18. "On the Measurement of a Weak Classical Force Coupled to a Quantum Mechanical Oscillator. I. Issues of Principle," (with C. M. Caves, R.W.P. Drever, V. D. Sandberg, and M. Zimmermann), *Reviews of Modern Physics*, **52**, 341-392 (1980).
19. "Multipole Expansion of Gravitational Radiation," *Reviews of Modern Physics*, **52**, 299-340 (1980).
20. "Gravitational-Wave Research: Current Status and Future Prospects," *Reviews of Modern Physics*, **52**, 285-298 (1980).
21. "The Gravitational Waves that Bathe the Earth: Upper Limits Based on Theorists' Cherished Beliefs," (with M. Zimmermann), *Essays in General Relativity. A Festschrift for Abraham Taub*, ed. F. Tipler (Academic Press, New York) 139-155 (1980).
22. "The Theory of Gravitational Radiation: An Introductory Review," *Gravitational Radiation*, eds. N. Dereulle and T. Piran (North Holland, Amsterdam), 1-57 (1983).
23. "Skyhook Gravitational Wave Detector," (with V. B. Braginsky), *Nature*, **316**, 610-612 (1985).
24. "Gravitational-Wave Bursts with Memory and Experimental Prospects," (with V. B. Braginsky), *Nature*, **327**, 123-125 (1987).
25. "Gravitational Radiation," *Three Hundred Years of Gravitation*, ed. S. W. Hawking and W. Israel (Cambridge: Cambridge University Press), 330-458 (1987).
26. "Light Scattering and Proposed Baffle Configuration for the LIGO," (1989); to be submitted to *Physical Review*.

Rochus E. Vogt

Publications in High Energy Astrophysics

1. "Electrons in the Primary Cosmic Radiation", (with P. Meyer), *Phys. Rev. Letters*, **6**, 193 (1961).
2. "The Primary Cosmic Ray Electron Flux during a Forbush-Type Decrease", (with P. Meyer), *J. Geophys. Res.*, **66**, 3950 (1961).
3. "Flux and Energy Spectra of Primary Cosmic Ray Protons from 70 to 400 MeV", *J. Phys. Soc. Japan*, **17**, SA-11, 436 (1962).
4. "Some Properties of Primary Cosmic Ray Electrons", (with P. Meyer), *J. Phys. Soc. Japan*, **17**, SA-III, 5 (1962).
5. "Primary Cosmic Ray and Solar Protons", *Phys. Rev.*, **125**, 366 (1962).
6. "High Energy Electrons of Solar Origin", (with P. Meyer), *Phys. Rev. Letters*, **8**, 387 (1962).
7. "Primary Cosmic Ray and Solar Protons II", (with P. Meyer), *Phys. Rev.*, **129**, 2275 (1963).
8. "Changes in the Primary Cosmic Ray Proton Spectrum in 1962 and 1963", (with P. Meyer), *Proc. 8th Int. Conf. on Cosmic Rays*, **3**, 49 (1963).
9. "A Solar and Galactic Cosmic Ray Satellite Experiment", (with W. E. Althouse, T. H. Harrington, and E. C. Stone), *IEEE Trans.*, NS-15, 229 (1968).
10. "Long-Term Variations of the Primary Cosmic Ray Electron Component", (with J. L'Heureux, P. Meyer, and S. D. Verma), *Can. J. Phys.*, **46**, 896 (1968).
11. "Flux of Cosmic Ray Electrons between 17 and 63 MeV", (with M. H. Israel), *Phys. Rev. Letters*, **20**, 1053 (1968).
12. "Cosmic Ray Negatron and Positron Spectra between 12 and 220 MeV", (with K. P. Beuermann, C. J. Rice, and E. C. Stone), *Phys. Rev. Letters*, **22**, 412 (1969).
13. "Characteristics of the Diurnally Varying Electron Flux near the Polar Cap", (with M. H. Israel), *J. Geophys. Res.*, **74**, 4714 (1969).
14. "Cosmic Ray Negatron and Positron Spectra Observed near Fort Churchill in 1968", (with K. P. Beuermann, C. J. Rice, and E. C. Stone), *Acta Physica Academiae Scientiarum Hungaricae*, **29**, Suppl. 1, 173 (1970).
15. "Interplanetary Deceleration of Solar Cosmic Rays", (with S. S. Murray and E. C. Stone), *Phys. Rev. Letters*, **26**, 663 (1971).
16. "The Isotopes of H and He in Solar Cosmic Rays", (with T. L. Garrard and E. C. Stone), *High Energy Phenomena on the Sun Symposium Proceedings*, edited by R. Ramaty and R. G. Stone, GSFC Preprint X-693-73-193, 341 (1973).

17. "The Energy Spectrum of 0.16 to 3 MeV Electrons during Solar Quiet Times", (with G. J. Hurford, R. A. Mewaldt, and E. C. Stone) *Conf. Papers*, 13th Int. Cosmic Ray Conf., Denver, **1**, 324 (1973).
18. "Observations of the Ratio of Low-Energy Cosmic Ray Positrons and Electrons during Solar Quiet Times", (with G. J. Hurford, R. A. Mewaldt, and E. C. Stone), *ibid*, **1**, 330 (1973).
19. "Observations of Low Energy Hydrogen and Helium Isotopes during Solar Quiet Times", (with G. J. Hurford, R. A. Mewaldt, and E. C. Stone), *ibid*, **1**, 93 (1973).
20. "Measurements of the Cosmic Ray Be/B Ratio and the Age of Cosmic Rays", (with J. W. Brown and E. C. Stone), *ibid*, **1**, 484 (1973).
21. "The Elemental Abundance Ratios of Interstellar Secondary and Primary Cosmic Rays", (with J. W. Brown and E. C. Stone), *ibid*, **1**, 556 (1973).
22. "Interstellar Electron Spectrum from the Galactic Non-Thermal Radio Emission", (with A. C. Cummings and E. C. Stone), *ibid*, **1**, 335 (1973).
23. "Evidence for Primary Interstellar Cosmic Ray Electrons", (with A. C. Cummings and E. C. Stone), *ibid*, **1**, 340 (1973).
24. "Interplanetary Diffusion Coefficients for Cosmic Rays", (with A. C. Cummings and E. C. Stone), *ibid*, **2**, 772 (1973).
25. "Analytic Approximations in the Study of the Solar Modulation of Electrons", (with A. C. Cummings and E. C. Stone), *ibid*, **2**, 765 (1973).
26. "Solar Modulation of Cosmic Ray Protons and He Nuclei", (with T. L. Garrard and E. C. Stone), *ibid*, **2**, 732 (1973).
27. "Relation of the Radial Gradient of Cosmic Ray Protons to the Size of the Solar Modulation Region", (with T. L. Garrard and E. C. Stone), *ibid*, **2**, 1336 (1973).
28. "Measurements of the Flux of Low-Energy Solar-Flare Positrons", (with G. J. Hurford, R. A. Mewaldt, and E. C. Stone), *ibid*, **2**, 1613 (1973).
29. "The Energy Spectrum of 0.16 to 2 MeV Electrons During Solar Quiet Times", (with G. J. Hurford, R. A. Mewaldt, and E. C. Stone), *Ap. J.*, **192**, 541 (1974).
30. "Particles and Fields in the Outer Solar System", (with G. L. Siscoe), *Icarus*, **24**, 333 (1975).
31. "The Isotopic Composition of Hydrogen and Helium in Low Energy Cosmic Rays", (with R. A. Mewaldt and E. C. Stone), 14th International Cosmic Ray Conf., Munich, Germany, *Conf. Papers*, **1**, 306 (1975).
32. "Isotopic Composition of the Anomalous Low Energy Cosmic Ray Nitrogen and Oxygen", (with R. A. Mewaldt, E. C. Stone, and S. B. Vidor), *ibid*, **1**, 349 (1975).

33. "The Elemental Composition of 4–30 MeV/nuc Cosmic Ray Nuclei with $1 \leq Z \leq 8$ ", (with R. A. Mewaldt, E. C. Stone, and S. B. Vidor), *ibid*, **2**, 798 (1975).
34. "Implications of Time Variations for the Origin of Low Energy Cosmic Ray Nitrogen and Oxygen Nuclei", (with R. A. Mewaldt and E. C. Stone), *ibid*, **2**, 804 (1975).
35. "Observations of Hydrogen and Helium Isotopes in Solar Cosmic Rays", (with G. J. Hurford and E. C. Stone), *ibid*, **5**, 1624 (1975).
36. "A Search for Solar Flare Positrons", (with R. A. Mewaldt and E. C. Stone), *ibid*, **5**, 1668 (1975).
37. "Observations of Low Energy Interplanetary Electrons", (with R. A. Mewaldt and E. C. Stone), *ibid*, **2**, 758 (1975).
38. "The Quiet Time Flux of 0.16–1.6 MeV Cosmic Ray Positrons", (with R. A. Mewaldt and E. C. Stone), *ibid*, **1**, 401 (1975).
39. "The Quiet Time Spectra of Low Energy Hydrogen and Helium Nuclei", (with R. A. Mewaldt and E. C. Stone), *ibid*, **2**, 774 (1975).
40. "Enrichment of Heavy Nuclei in ^3He Rich Flares", (with G. J. Hurford, R. A. Mewaldt, and E. C. Stone), *Ap. J.*, **201**, L95 (1975).
41. "Splash Albedo Protons Between 4 and 315 MeV at High and Low Geomagnetic Latitudes", (with K. P. Wenzel and E. C. Stone), *J. Geophys. Res.*, **80**, 3580 (1975).
42. "The Isotopic Composition of Hydrogen and Helium in Low Energy Cosmic Rays", (with R. A. Mewaldt, and E. C. Stone), *Ap. J.*, **206**, 616 (1976).
43. "Observations of Jovian Electrons at 1 AU", (with R. A. Mewaldt and E. C. Stone), *J. Geophys. Res.*, **81**, 2397 (1976).
44. "Isotopic and Elemental Composition of the Anomalous Low Energy Cosmic Ray Fluxes", (with R. A. Mewaldt, E. C. Stone, and S. B. Vidor), *Ap. J.*, **205**, 931 (1976).
45. "Neutral Particle Background in Cosmic Ray Telescopes Composed of Silicon Solid State Detectors", (with R. A. Mewaldt and E. C. Stone), *Space Science Instrumentation*, **3**, 231 (1977).
46. "Cosmic Ray Investigation for the Voyager Missions; Energetic Particle Studies in the Outer Heliosphere—and Beyond", (with E. C. Stone, F. B. McDonald, B. J. Teegarden, J. H. Trainor, J. R. Jokipii, and W. R. Webber), *Space Science Review*, **21**, 355 (1977).
47. "Simultaneous Observations of Cosmic Ray Particles in Corotating Interplanetary Structures at Different Solar Distances between 0.3 and 1.0 AU from HELIOS 1 and 2 and IMP 7 and 8", (with H. Kunow, G. Wibberenz, G. Green, R. Müller-Mellin, R. Witte, E. Hemp, E. C. Stone, and R. Mewaldt), 15th International Cosmic Ray Conference, Plovdiv, Bulgaria, *Conf. Papers*, **3**, 227,

(1977).

48. "A Cosmic Ray Isotope Spectrometer", (with W. E. Althouse, A. C. Cummings, T. L. Garrard, R. A. Mewaldt, and E. C. Stone), *IEEE Trans. on Geoscience Electronics*, **GE-16**, 204 (1978).
49. "The Radial Diffusion Coefficient of 1.3–2.3 MeV Protons in Recurrent Proton Streams", (with R. A. Mewaldt and E. C. Stone), *Geophys. Res. Ltrs.*, **5**, 965 (1978).
50. "Characteristics of the Spectra of Protons and Alpha Particles in Recurrent Events at 1 AU", (with R. A. Mewaldt and E. C. Stone), *Geophys. Res. Ltrs.*, **6**, 589 (1979).
51. "The Isotopic Composition of Solar Flare Accelerated Neon", (with R. A. Mewaldt, J. D. Spalding, and E. C. Stone), *Ap. J. (Letters)*, **231**, L97 (1979).
52. "The Voyager Cosmic Ray Experiment", (with D. E. Stilwell, W. D. Davis, R. M. Joyce, F. B. McDonald, J. H. Trainor, W. E. Althouse, A. C. Cummings, T. L. Garrard, and E. C. Stone), *IEEE Trans. on Nuclear Science*, **NS-26**, 513 (1979).
53. "Voyager 1: Energetic Ions and Electrons in the Jovian Magnetosphere", (with W. R. Cook, A. C. Cummings, T. L. Garrard, N. Gehrels, E. C. Stone, J. H. Trainor, A. W. Schardt, T. Conlon, N. Lal, and F. B. McDonald), *Science*, **204**, 1003 (1979).
54. "Voyager 2: Energetic Ions and Electrons in the Jovian Magnetosphere", (with A. C. Cummings, T. L. Garrard, N. Gehrels, E. C. Stone, J. H. Trainor, A. W. Schardt, T. F. Conlon, and F. B. McDonald), *Science*, **206**, 984 (1979).
55. "Satellite Measurements of the Isotopic Composition of Galactic Cosmic Rays", (with R. A. Mewaldt, J. D. Spalding, and E. C. Stone), 16th International Cosmic Ray Conference, Kyoto, Japan, *Conf. Papers*, **12**, 86 (1979).
56. "The Elemental Composition of Quiet Time Low Energy Cosmic Rays Measured on the Voyager Spacecraft", (with W. R. Webber and E. C. Stone), *ibid*, **5**, 357 (1979).
57. "Elemental Composition of Solar Energetic Particles in 1977 and 1978", (with W. R. Cook, E. C. Stone, J. H. Trainor, and W. R. Webber), *ibid*, **12**, 265 (1979).
58. "High Resolution Measurements of Galactic Cosmic Ray Neon, Magnesium and Silicon Isotopes", (with R. A. Mewaldt, J. D. Spalding, and E. C. Stone), *Ap. J. (Letters)*, **235**, L95 (1980).
59. "The Isotopic Composition of Galactic Cosmic Ray Iron Nuclei", (with R. A. Mewaldt, J. D. Spalding, and E. C. Stone), *Ap. J. (Letters)*, **236**, L121 (1980).
60. "Elemental Composition of Solar Energetic Nuclei", (with W. R. Cook and E. C. Stone), *Ap. J. (Letters)*, **238**, L97 (1980).

61. "The Isotopic Composition of Solar Flare Accelerated Magnesium", (with R. A. Mewaldt, J. D. Spalding, and E. C. Stone), *Ap. J. (Letters)*, **243**, L163 (1981).
62. "Energetic Charged Particles in Saturn's Magnetosphere: Voyager 1 Results", (with D. L. Chenette, A. C. Cummings, T. L. Garrard, E. C. Stone, A. W. Schardt, J. H. Trainor, N. Lal, and F. B. McDonald), *Science*, **212**, 231 (1981).
63. "High Resolution Measurements of Solar Flare Isotopes", (with R. A. Mewaldt, J. D. Spalding, and E. C. Stone), 17th International Cosmic Ray Conference, Paris, France, *Conf. Papers*, **3**, 131 (1981).
64. "The Isotopic Composition of Low Energy Cosmic Rays", (with R. A. Mewaldt, J. D. Spalding, and E. C. Stone), *ibid*, **2**, 68 (1981). Erratum, *ibid*, **11**, 431 (1981).
65. "The Isotopic Composition of Cosmic Ray B, C, N, and O Nuclei", (with R. A. Mewaldt, J. D. Spalding, and E. C. Stone), *Ap. J. (Letters)*, **251**, L27 (1981).
66. "Energetic Charged Particles in Saturn's Magnetosphere: Voyager 2 Results", (with D. L. Chenette, A. C. Cummings, T. L. Garrard, E. C. Stone, A. W. Schardt, J. H. Trainor, N. Lal, and F. B. McDonald), *Science*, **215**, 577 (1982).
67. "Elemental Composition of Solar Energetic Particles" (with W. R. Cook and E. C. Stone), *Ap. J.*, **279**, 827 (1984).

Rainer Weiss
Publications

1. "Magnetic Moments and Hyperfine Structure Anomalies of Cs₁₃₃, Cs₁₃₅, and Cs₁₃₇", (with H. H. Stroke, V. Jaccarino, and D. S. Edmonds), *Physical Review*, **105**, 590 (1957).
2. "Molecular Beam Electron Bombardment Detector," *Review of Scientific Instruments*, **32**, 397 (1961).
3. "A Search for a Frequency Shift of 14.4 KeV Photons on Traversing Radiation Fields," (with L. Grodzins), *Physics Letters*, **1**, 342 (1962).
4. "Stark Effect and Hyperfine Structure of Hydrogen Fluoride", *Physical Review*, **131**, 659 (1963).
5. "The Cesium Fountain Experiment: The Paucity of Slow Atoms", Festschrift, for J. R. Zacharias (1965).
6. "A Gravimeter to Monitor the ${}_0S_0$ Dilational Mode of the Earth", (with B. Block), *J. Geophys. Res.*, **70**, 5615 (1966).
7. "Experimental Test of the Freundlich Red-Shift Hypothesis, (with G. Blum), *Physical Review*, **155**, 1412 (1967).
8. "Electric and Magnetic Field Probes," *Journal of Applied Physics*, **35**, 1047 (1967).
9. "Laser-induced Fluorescence in a Molecular Beam of Iodine", (with S. Ezekiel), *Physical Review Letters*, **20**, 91 (1968).
10. "A Measurement of the Isotropic Background Radiation in the Far Infrared", (with D. Muehlner), *Physical Review Letters*, **24**, 742 (1970).
11. "Electromagnetically Coupled Broadband Gravitational Antenna", *Quarterly Progress Report*, Research Lab. of Electronics, MIT, **105**, 54 (1972).
12. "Balloon Measurements of the Far Infrared Background Radiation", (with D. Muehlner), *Physical Review D*, **7**, 326 (1973).
13. "Further Measurements of the Submillimeter Background at Balloon Altitude", (with D. Muehlner), *Physical Review Letters*, **30**, 757 (1973).
14. "Measurements of the Phase Fluctuations in a He-Ne Zeeman Laser", (with D. K. Ownes), *Review of Scientific Instruments*, **45**, 1060 (1974).
15. "The Oldest Fossil", *Technology Review*, **78**, 56 (1975).
16. "A Large Beam Sky Survey at Millimeter and Submillimeter Wavelengths Made from Balloon Altitudes", (with D. Owens and D. Muehlner) *Astrophysical Journal*, **231**, 702 (1979).
17. "Gravitational Radiation—The Status of the Experiments and Prospects for the Future," in *Sources of Gravitational Radiation*, Cambridge University Press, Cambridge, England (1979).

18. "Measurements of the Cosmic Background Radiation", *Annual Review of Astronomy and Astrophysics*, **18**, 489 (1980).
19. "The COBE Project", *Physica Scripta*, **21**, 670 (1980).
20. "Monolithic Silicon Bolometers", (with P. M. Downey, F. J. Bachner, J. P. Donnelly, W. T. Lindley, R. W. Mountain and D. J. Silversmith), *Journal of Infrared and Millimeter Waves*, **1** (1980).
21. "Monolithic Silicon Bolometers", (with P. M. Downey, A. D. Jeffries, S. S. Meyer, F. J. Bachner, J. P. Donnelly, W. R. Lindley, R. W. Mountain, and D. J. Silversmith), *Applied Optics*, **23**, 910 (1983).
22. "A Search for the Sunyaev-Zel'dovich Effect at Millimeter Wavelengths", (with S. S. Meyer and A. D. Jeffries), *The Astrophysical Journal Letters*, **271**, L1 (1983).
23. "Measurements of the Anisotropy of the Cosmic Background Radiation and Diffuse Galactic Emission at Millimeter and Submillimeter Wavelengths", (with M. Halpern, R. Benford, S. Meyer, D. Muehlner), *The Astrophysical Journal*, **332**, 596 (1988).

Conference Reports

24. "The MIT Prototype Gravitational Wave Detector", (with J. Livas, R. Benford, A. Jeffries, P. Linsay, P. Saulson, D. Shoemaker), in *Proceedings of the Fourth Marcel Grossman Meeting on General Relativity*, ed. R. Ruffini, 591 (1985).
25. "Interferometric Gravitational Wave Detection at MIT", (with R. Benford, M. Burka, N. Christensen, M. Eisgruber, P. Fritschel, A. Jeffries, J. Kovalik, P. Linsay, J. Livas, and P. Saulson), *13th Texas Symposium on Relativistic Astrophysics*, ed. M. Ulmer, Singapore: World Scientific, 15 (1986).
26. "Progress on the MIT 5-Meter Interferometer", (with R. Benford, M. Burka, N. Christensen, M. Eisgruber, P. Fritschel, A. Jeffries, J. Kovalik, P. Linsay, J. Livas, and P. Saulson) *International Symposium on Experimental Gravitational Physics*, Guangzhou, China, ed. P. Michelson, Singapore: World Scientific, 312 (1987).

Reports

27. "Report of the Sub-Panel on Relativity and Gravitation", (with P. Bender, C. Misner, and R. V. Pound), Management and Operations Working Group for Shuttle Astronomy, NASA Headquarters, (Sept., 1976).
28. "Study Report for the Cosmic Background Explorer", (with S. Gulikis, M. Hauser, J. Mather, G. Smoot, and D. Wilkinson), Goddard Space Flight Center, (Feb. 1977).
29. "Report of the Detector Study Panel NASA", (with P. Richards, Chairman) (1979).

30. "A Study of a Long Baseline Gravitational Wave Antenna System", (with P. Linsay and P. Saulson) (1983).
31. "Task Group on Fundamental Physics and Chemistry", (with P. Bender, A. Berlad, R. Donnelly, F. Dyson, W. Fairbank, G. Homsy, J. Langer, J. Nauge, R. Pellat, J. Reynolds, R. Ruffini, D. Saville, and R. Schrieffer), National Academy of Sciences Report on Gravitational Physics, (1987).

APPENDIX A

THE PHYSICS OF GRAVITATIONAL WAVES, AND COMPARISON OF SOURCE STRENGTHS WITH DETECTOR SENSITIVITIES

This appendix presents a detailed discussion of the issues raised in Sections II.A, II.B, and II.C of the proposal (for still greater detail see Reference [A-1]).

1. The Physics of Gravitational Waves

Gravitational waves are predicted by general relativity theory and by all other relativistic theories of gravity, and all the theories agree, in rough order of magnitude, on the strengths of the waves to be expected from astrophysical sources. Although gravitational waves have not yet been observed directly, the effect of the back-action of gravitational-wave emission on one source (the orbital decay of the binary pulsar PSR 1913+15) has been measured and agrees with general relativity's predictions to within the experimental error of several percent [A-2]. The primary goals of the LIGO Project are to detect gravitational waves directly, and use them to test the fundamental laws of physics and to open a new window onto the astrophysical universe.

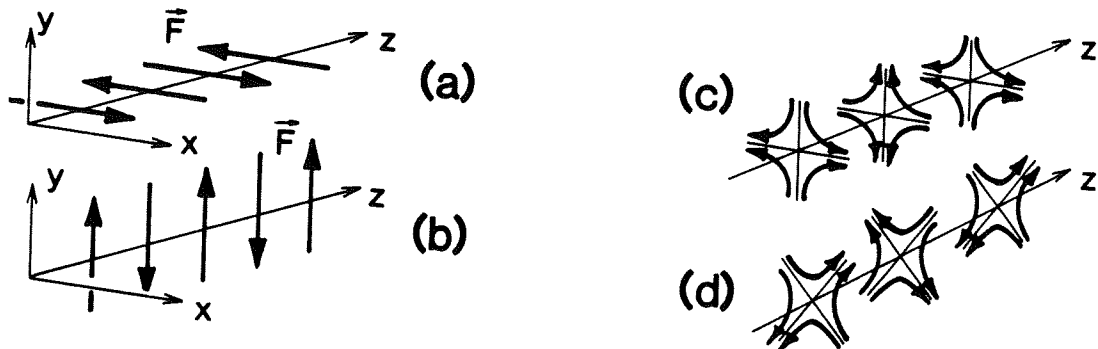


Figure A-1 Left half: The forces produced on charged particles by an electromagnetic wave propagating in the z direction: (a) for x -polarization, and (b) for y -polarization. Right half: The forces on massive particles produced by a gravitational wave propagating in the z direction: (c) for $+$ polarization, and (d) for \times polarization.

a. The forces produced by gravitational waves. Just as an electromagnetic wave pushes a charged particle that initially is at rest back and forth in a direction transverse to the wave's propagation (Figure A-1 (a) and (b)), so also a gravitational wave pushes a massive particle, initially at rest, back and forth transversely (Figure A-1 (c) and (d)). The figures show the lines of force as measured in a local "proper reference frame", whose time coordinate t is equal to the proper time ticked by physical clocks and whose orthogonal spatial coordinates (x, y, z) measure proper (physical) distance. For a gravitational wave the force on a particle

of mass m at location (x, y, z) is the sum of contributions from two polarizations: the + (“plus”) polarization (Figure A–1 (c)) with force

$$\vec{F} = \frac{1}{2}m\ddot{h}_+(x\vec{e}_x - y\vec{e}_y) \quad (\text{A.1a})$$

and the \times (“cross”) polarization (Figure A–1 (d)) with force

$$\vec{F} = \frac{1}{2}m\ddot{h}_\times(y\vec{e}_x + x\vec{e}_y). \quad (\text{A.1b})$$

Here dots denote time derivatives, \vec{e}_x and \vec{e}_y are unit basis vectors in the x and y directions, and h_+ and h_\times are dimensionless *gravitational-wave fields*, which propagate in the z -direction at the speed of light

$$h_+ = h_+(t - z/c), \quad h_\times = h_\times(t - z/c). \quad (\text{A.2})$$

Notice that the gravitational force fields (Equations (A.1a,b)) are quadrupolar and are transverse to the waves’ propagation direction.

If a test particle at (x, y, z) is unconstrained by other forces, then it will accelerate by an amount $\delta\vec{x} = \vec{F}/m$ in response to the gravitational wave, and its resulting displacement will be

$$\delta x = \frac{1}{2}h_+x, \quad \delta y = -\frac{1}{2}h_+y, \quad \delta z = 0 \quad (\text{A.3a})$$

for the + polarization and

$$\delta x = \frac{1}{2}h_\times y, \quad \delta y = \frac{1}{2}h_\times x, \quad \delta z = 0 \quad (\text{A.3b})$$

for the \times polarization. Since the displacement is proportional to the separation of the particle from the origin of the local proper reference frame, with proportionality factor h_+ or h_\times , one can regard h_+ and h_\times as dimensionless “strains of space.”

b. Effect of the wave on an interferometric detector. Figure A–2 is a simplified schematic diagram of an interferometric detector of the type to be operated in the LIGO. Three masses hang by wires from overhead supports at the corner and ends of an “L”. We shall denote by $L \equiv (L_x + L_y)/2 \simeq L_x \simeq L_y$ the mean length of the (nearly equal) arms of the “L” and shall place the origin of a proper reference frame at the corner mass as shown. If a gravitational wave propagates vertically (z -direction), and has its + polarization axes parallel to the detector’s arms, and has a frequency f high compared to the 1-Hz pendulum frequency of the masses, then the wave will move the end masses back and forth relative to the corner mass in just the same manner as if the end masses were free (the pendulum restoring force does not have time to act). The resulting wave-induced changes in the x -arm and y -arm lengths (Equation (A.3a)) will be $\delta L_x = \frac{1}{2}h_+L$ and $\delta L_y = -\frac{1}{2}h_+L$; i.e., they will be equal and opposite. These changes are monitored by

laser interferometry: laser beams, sent from the center mass down the two arms and reflected off mirrors on the end masses, will return to the corner with a relative phase change $\Delta\Phi$ that is proportional to the difference in arm lengths,

$$\Delta\Phi = 2\pi\Delta L/\lambda_l, \quad \text{where } \Delta L \equiv \delta L_x - \delta L_y = h_+(t)L. \quad (\text{A.4})$$

Here λ_l is the light's wavelength. By interfering the beams one can monitor this phase change and thence monitor the gravitational-wave field $h_+(t)$.¹

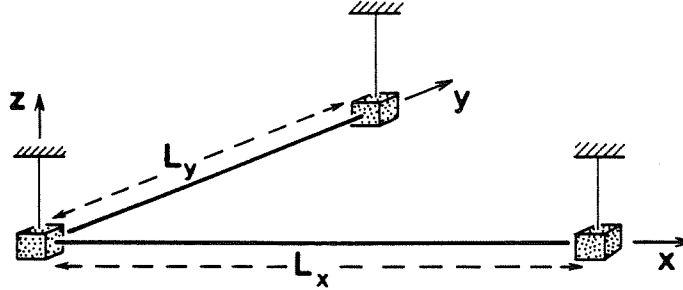


Figure A-2 Schematic diagram of a laser interferometer gravitational wave detector.

If the wave, instead of coming in vertically, comes in from a direction with polar angles (θ, ϕ) relative to the Cartesian coordinates of Figure A-2 (cf. Figure II-1 in Section II.A), and if we take one of the $+$ state's polarization axes to be horizontal, then straightforward algebra shows that the forces (Equations (A.1a) and (A.1b)) produce the relative arm-length change

$$\Delta L/L = F_+(\theta, \phi)h_+(t) + F_x(\theta, \phi)h_x(t), \quad (\text{A.5a})$$

where F_+ and F_x are the detector's quadrupolar beam pattern functions

$$F_+ = \frac{1}{2}(1 + \cos^2 \theta) \cos 2\phi, \quad F_x = \cos \theta \sin 2\phi. \quad (\text{A.5b})$$

Note that the beam patterns are very broad. This means that the relative responses of different detectors, with different orientations, will give rather poorer information about source directions than the time-of-flight between widely separated detectors (cf. Appendix B and Section V.C).

¹ One might worry that the gravitational wave will interact with the laser beams and, thereby, alter the standard phase-change relation $\Delta\Phi = 2\pi\Delta L/\lambda_l$. Not so if one uses, as we have, a rigid, Cartesian coordinate system whose coordinate lengths are unaffected by the wave. Only if one uses "rubbery coordinates" (e.g., the "transverse-traceless coordinates" introduced in many textbooks) need one worry about interaction of the gravitational wave with the light. (This approach was taken in Appendix B to derive the frequency (and angular) response of a Fabry-Perot gravitational-wave interferometer.)

c. **Measurement of the graviton's rest mass and spin.** Quantum field theory tells us that classical waves are carried by quanta (photons for electromagnetic waves and gravitons for gravitational waves), and that the rest masses and spins of the quanta can be inferred from the propagation speeds and polarization properties of their waves.

The propagation speed will be precisely the speed of light if and only if the quanta have zero rest mass; otherwise it will be slower. Thus, one goal of the LIGO Project is to detect gravitational waves from a supernova outburst in the nearest large cluster of galaxies, the Virgo Cluster, and compare the waves' arrival time with the beginning of the optical outburst. Since the distance to Virgo is about 30 million light years, even with an optical time resolution of only one day, one could infer that the light and gravitational waves propagated with the same speed to within a fractional error of (one day)/(30 million light years) $\sim 10^{-10}$, and one, thereby, could place on the graviton rest mass a limit of $\sim 10^{-5} \times$ (the energy of a 1000 Hz graviton) $\sim 10^{-16}$ eV. If neutrinos could also be detected, the time resolution for both neutrinos and gravitational waves could be about 1 ms; and if their onsets were that close together, one would infer equal speeds to within $\sim 10^{-18}$ and corresponding rest mass limits of $\sim 10^{-20}$ eV for the graviton, and $\sim 10^{-2}$ eV for the neutrino. (This limit for the graviton is about the same as one obtains from the validity of the inverse square law for the sun's gravity as manifest in planetary orbits. Therefore, if gravitational waves were found to propagate at a different speed from light and neutrinos, we would infer that the gravitons which carry the waves are different from the gravitons which mediate the solar system's gravity—an unlikely but not impossible outcome. An alternative explanation could be that gravitons, like photons, have zero rest mass, but they propagate on the light curves of a different metric from that which governs photons [A-3].)

The spin S of the quantum that carries a classical wave determines the "return angle" of the wave's force field: rotate the force field (Figure A-1) about the wave's propagation direction. The minimum angle of rotation that brings the field back to its original orientation is its return angle θ_{ret} and is equal to $(360 \text{ deg})/S$. For the electromagnetic wave of Figure A-1 (a) and (b), θ_{ret} is 360 deg, so the photon must have spin one; for the gravitational wave of Figure A-1 (c) and (d), θ_{ret} is 180 deg, so the graviton must have spin two. Correspondingly, one goal of the LIGO project is to determine the return angle for gravitational waves by simultaneous measurements with several different detectors (in a worldwide network) that have several different orientations. Since most other relativistic theories of gravity predict a mixture of spin-two, spin-one, and/or spin-zero gravitons [A-3], such a measurement would be a powerful test of whether general relativity is correct.

d. The strengths of cosmic gravitational waves. Energy conservation dictates that the wave fields h_+ and h_\times die out as $1/(\text{distance to the source}) = 1/r$. Just as an electromagnetic wave is produced by oscillating multipole moments of a charge distribution, so also a gravitational wave is produced by oscillating multipole moments of a mass distribution. In the electromagnetic case the monopole moment cannot oscillate because it is the source's total charge and charge is conserved; and, consequently, the radiation is typically dipolar. Similarly, in the gravitational case the monopole moment cannot oscillate because it is the source's total mass and mass is conserved; moreover, the mass dipole moment cannot oscillate because its time derivative is the source's total momentum and momentum is conserved; and, consequently, gravitational radiation is typically quadrupolar. Dimensional considerations then dictate that $h_+ \sim h_\times \sim (G/c^4)\ddot{Q}/r$ where G is Newton's gravitation constant, c is the speed of light, Q is the quadrupole moment, and dots denote time derivatives. Because the quadrupole moment is of order the mass of the source times the square of its size, \ddot{Q} is of order the mass times the square of the source's internal velocities, i.e., of order the source's internal kinetic energy—or, more precisely, that part of the kinetic energy associated with oscillatory, nonspherical motions, $E_{\text{kin}}^{\text{ns}}$:

$$h_+ \sim h_\times \sim \frac{G}{c^4} \frac{E_{\text{kin}}^{\text{ns}}}{r} \sim 10^{-20} \left[\frac{E_{\text{kin}}^{\text{ns}}}{M_\odot c^2} \right] \left[\frac{10 \text{ Mpc}}{r} \right]. \quad (\text{A.6})$$

Here M_\odot is the mass of the sun and $10 \text{ Mpc} \equiv (10 \text{ megaparsecs}) = (30 \text{ M light years})$ is the distance to the Virgo Cluster of galaxies. Equation (A.6) is a correct order-of-magnitude estimate not only for general relativity, but also for other theories of gravity; and it suggests that the strongest extragalactic waves bathing the Earth are not likely to exceed $h \sim 10^{-20}$.

e. Characteristics of the strongest sources. The strongest sources are those for which the nonspherical, internal kinetic energy is largest, which means those with large masses and large internal velocities. Since the internal velocities are generated by internal gravity, large internal velocities mean large internal gravity, which means compact size. Thus it is that the strongest sources are likely to be black holes and neutron stars—e.g., the violent births of black holes and neutron stars in stellar implosions, the inspiral and coalescence of binary neutron stars and black holes in distant galaxies, and the rotation of nonaxisymmetric neutron stars (pulsars) in our own galaxy.

f. The frequencies of cosmic gravitational waves. The characteristic frequencies of vibration and rotation for neutron stars are less than or of order a few kilohertz; and those for a black hole of mass M are

$$f \sim \frac{10 \text{ kHz}}{M/2M_\odot} \quad (\text{A.7})$$

(where $2M_\odot$ is the smallest possible mass for a black hole that forms by stellar collapse). Thus, the strongest waves are likely to lie at frequencies of 10 kHz and

below. The LIGO is designed to work from 10 kHz down to the lowest frequencies at which one can isolate the detectors from earth vibrations, ~ 10 Hz—a range in which a rich variety of sources should exist. At yet lower frequencies, where there should also be interesting sources, one must use space-based detectors—the most promising of which will be LIGO-type detectors that might fly in space in the early 21st century [A-4]. The LIGO Project will provide an important base of technology and experience for those future detectors.

g. Penetrating power of gravitational waves. Because the strongest sources of gravitational waves are compact concentrations of highly dynamical mass, they typically will lie in regions obscured by surrounding matter (e.g., in the core of a supernova explosion or at the center of a galaxy or in the big-bang origin of the universe). Fortunately, gravitational waves are highly penetrating. For example, whereas neutrinos scatter many times in emerging from the center of a supernova and photons cannot get out at all, gravitational waves should emerge nearly unscathed; the total loss to scattering and absorption should be many orders of magnitude below unity. Similarly, whereas photons from the big bang (the cosmic microwave radiation) last scattered off matter when the universe was about one million years old and neutrinos last scattered when it was a few seconds old, primordial gravitational waves should have last scattered near the Planck time, $\sqrt{G\hbar}/c^5 \sim 10^{-43}$ seconds, when the initial conditions of the universe were being set by the (little understood) laws of quantum gravity [A-5].

h. Electromagnetic information as a poor predictor of cosmic gravitational waves. Electromagnetic waves studied by astronomers are almost always incoherent superpositions of the emissions from a large number of molecules, atoms, or charged particles. In contrast, cosmic gravitational waves are produced by the coherent, bulk motions of mass-energy (either in the form of matter as in neutron stars, or in the form of vibrating, nonlinear spacetime curvature as in colliding black holes). This difference of emission mechanism, together with the fact that the strongest gravitational-wave sources are probably opaque to photons, serves as a warning that our present photon-based knowledge of the universe may be a rather poor guide as to what gravitational-wave astronomy will bring. On one hand, we cannot estimate with confidence how sensitive a LIGO detector must be in order to discover waves. On the other hand, when waves are discovered, they are likely to bring surprises. Indeed, it seems likely that gravitational radiation will produce a revolution in our understanding of the universe comparable to that which came from radio waves in the 1950s and 1960s [A-6].

i. Astrophysical information carried by gravitational waves. Gravitational waves carry substantial information about their sources. The total information carried to earth is embodied in the celestial coordinates (α, δ) of the source, plus the two “gravitational waveforms” $h_+(t)$ and $h_\times(t)$ evaluated at the location of a detector. The LIGO detectors are broad-band instruments, designed to measure the waveforms in the time domain with a high-frequency cutoff around 10 kHz

and a seismic-noise-induced low-frequency cutoff, which in present prototypes is around 400 Hz and will be pushed continually downward toward 10 Hz over the coming years. A goal of the LIGO Project, in cooperation with other detectors in a worldwide network, is to extract the full information, α , δ , $h_+(t)$, and $h_\times(t)$ from the waves (cf., Section V.C); and, where possible, to cross-correlate that information with data from other kinds of radiation.

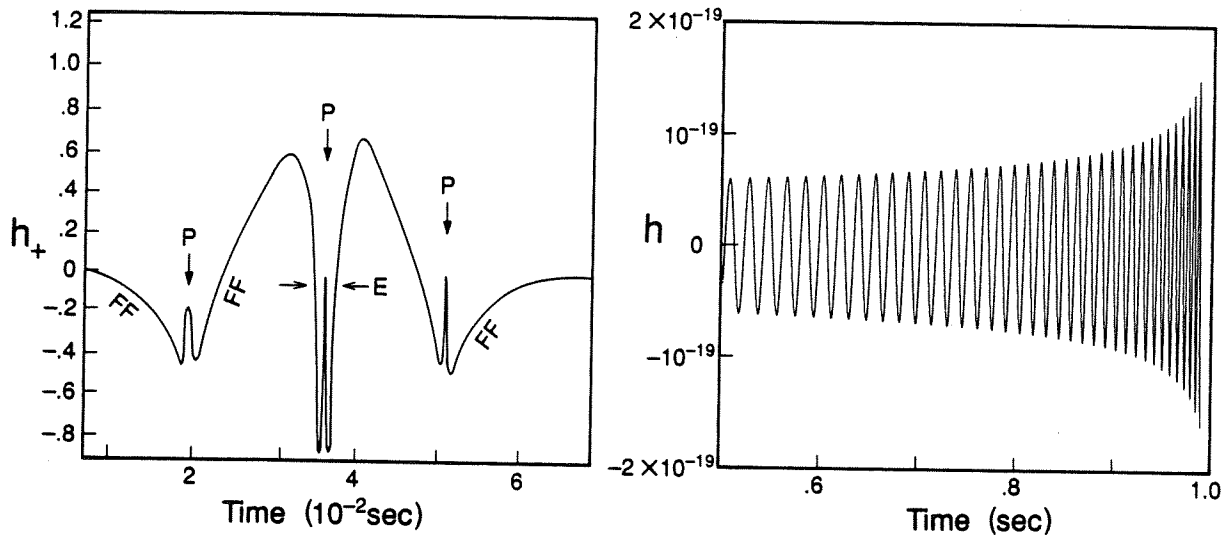


Figure A-3 Part (a): The gravitational waveform produced by one scenario for the collapse of a star to form a neutron core, as computed in a numerical simulation by Richard A. Saenz and Stuart L. Shapiro [A-7]. Part (b): The waveform produced by the inspiral, toward coalescence, of a binary system made of two $10 M_\odot$ black holes. The waveforms for black-hole and neutron-star coalescences are much the same when the objects are far apart (toward the left of the chirp) but differ substantially at the end points.

j. Extraction of information from a waveform. Figure A-3 (a) shows a waveform $h_+(t)$ computed several years ago by numerical simulation of a specific kind of source [A-7]. The associated $h_\times(t)$ is identical to this $h_+(t)$ except for an overall multiplicative factor. If these $h_+(t)$ and $h_\times(t)$ were measured by gravitational-wave detectors, one could infer the following from them: Because $h_\times(t) = \text{const} \times h_+(t)$, the source must be axisymmetric. Because the shortest time scales present in the waveform are ~ 0.5 ms, the source must be either a neutron star or a several-solar-mass black hole. Assuming, as usually will be the case, that the radiation is predominantly quadrupolar, one can double-time-integrate the waveform to get the time evolution of the source's quadrupole moment. One then notices that the segments of the waveform marked *FF* have the shapes $h_+ \propto (t - \text{const})^{-2/3}$ that one expects from nonspherical, free-fall motion; and the sharply reversed peaks marked *P* are what one expects from a sharp acceleration in the direction opposite to the free fall. The natural and correct interpretation is that these waves are from

- Detect primordial gravitational waves from the big bang, and from them extract information about the initial conditions and earliest stages of evolution of the universe.

3. Estimates of the Strengths of the Waves at Earth and Comparison with Anticipated LIGO Sensitivities

When we achieve these payoffs will depend, primarily, on when detectors in the LIGO can reach the required sensitivities. The best estimates of the required sensitivities come from astrophysical source-strength calculations. Unfortunately, those calculations, being based on our electromagnetic understanding of the universe, are very uncertain. With the single exception of binary-neutron-star coalescences (see below), for each type of source either (1) the strength of the source's waves for a given distance from earth is uncertain by several orders of magnitude, or (2) the rate of occurrence of that type of source, and thus the distance to the nearest one, is uncertain by several orders, or (3) the very existence of that type of source is uncertain.

The source strength calculations are summarized by the thin curves and lines in Figures A-4a (short bursts), A-4b (periodic waves), and A-4c (stochastic waves). For full details of the assumptions and calculations that underlie these figures and for extensive references to the literature, see Reference [A-1, Section 9.4]. Here we shall give only a brief overview.

a. Gravitational-wave bursts (Figure A-4a). Gravitational wave bursts that have been modeled by theorists last for no more than a few thousand cycles, and usually no more than five cycles. We shall describe such a burst by a characteristic frequency f (horizontal axis of Figure A-4a) and by a characteristic dimensionless amplitude h_c which is approximately equal to the amplitude of the waveform oscillations $h_+(t)$ and/or $h_\times(t)$ multiplied by the square root of the number n of cycles that the burst spends near frequency f . (The factor \sqrt{n} accounts for the ability of the detector to amplify the signal by integrating up the cycles.)³

i. Coalescing neutron-star binaries. Our one moderately (but not highly) certain source is the coalescence of a neutron-star binary system. That coalescence should produce, during the inspiral phase, a "chirp", with characteristic frequency sweeping upward through the LIGO's band from a few tens of Hertz to 1000 Hz in a time of a few minutes. The characteristic amplitude of the inspiral waves for a binary at a given distance is predicted with confidence and accuracy by general

³ h_c is defined more precisely in Reference [A-1], Equation (31) in terms of optimal signal processing of a gravitational-wave detector's output and an average over source locations.

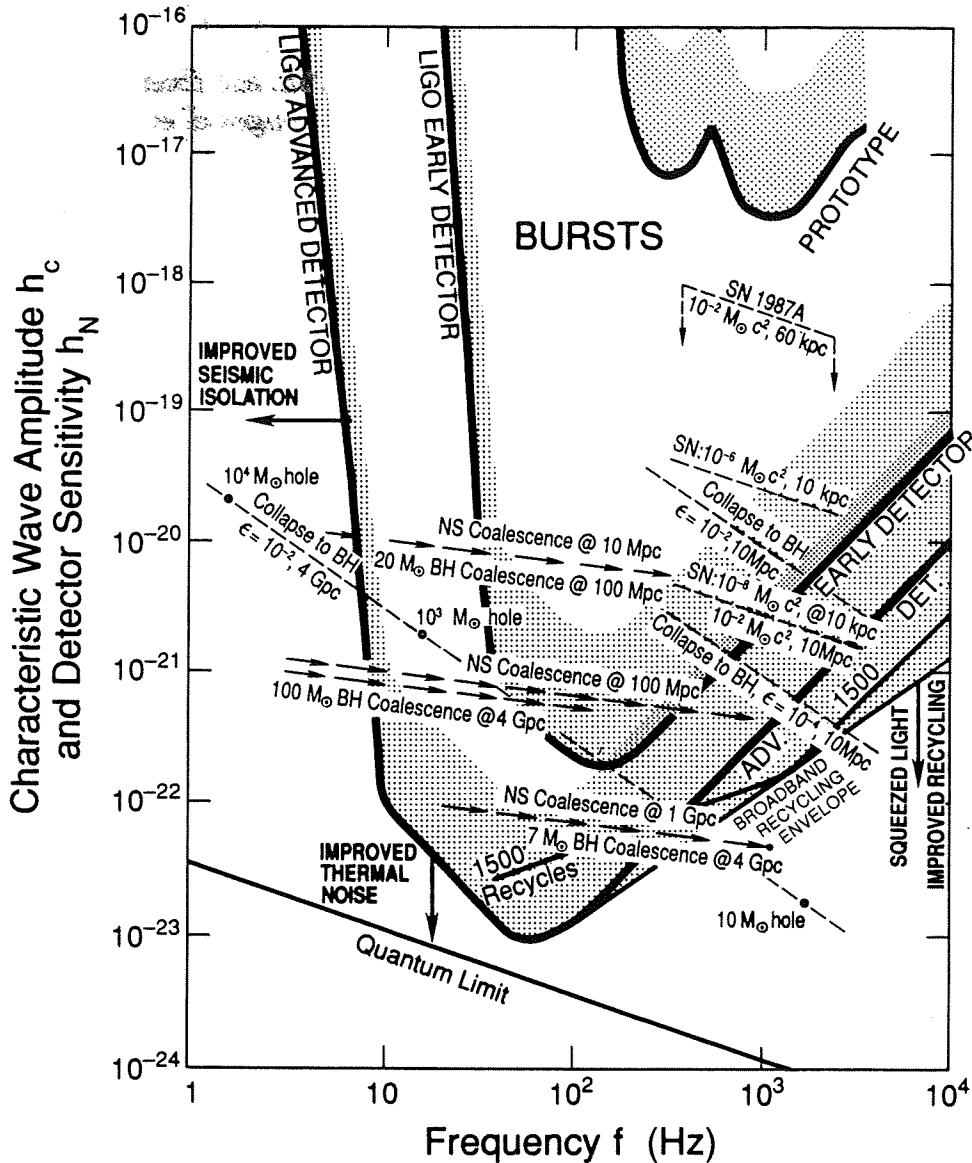


Figure A-4a The estimated characteristic amplitude $h_c \simeq h \sqrt{n}$ and frequency f for gravitational-wave bursts from various sources (dashed lines and arrows); and benchmark sensitivities $h_N \simeq \tilde{h}(f) \sqrt{T}$ (solid curves and stippled strips atop them), for interferometric detectors today and in the proposed LIGO. n is the number of cycles in the burst for which the amplitude is near h and the frequency is near f (see text) and $\tilde{h}(f)$ is the square root of the spectral density of the interferometer's noise; (see Equations (A.18), (A.19) and Appendix E). For each detector the solid curve corresponds to the characteristic amplitude of a gravitational wave burst which would be detected with unity signal-to-noise ratio, for optimal polarization and arrival direction. The top of the stippled strip corresponds to the characteristic amplitude of gravitational waves which would give significant detection of bursts occurring as infrequently as three times per year, with random polarizations and arrival directions, in detectors which are free from spurious non-Gaussian noise bursts. Stated more precisely, it corresponds to a confidence level of 90% that the signals are not false alarms caused by statistical fluctuations in Gaussian noise, in a cross-correlation experiment between two detectors at separate sites. The lowest solid line (Quantum Limit) is the limit to the sensitivity curve for the advanced detector set by the quantum limit for the test masses. "Envelope" defines the range of broad-band recycling improvements to the sensitivity, for detectors optimized for each frequency in the range shown. Abbreviations: *SN*—supernova; *NS*—neutron star; *BH*—black hole; $M_\odot c^2$ —one solar rest mass (units for energy carried by waves); ϵ —the fraction of the mass of a black hole emitted in the waves. The assumed distances to the sources include 10 kpc—10 kiloparsecs (center of our galaxy); 50 kpc (Large Magellanic Cloud); 10 Mpc—10 megaparsecs (Virgo cluster of galaxies); 4 Gpc—4 gigaparsecs (the edge of the observable universe).

relativity (Reference [A-1, Equation (46b)], with correction of a $\sqrt{2}$ error):

$$\begin{aligned}
 h_c &= 0.34 \frac{G(\mu M)^{1/2}}{c^2 r} \left(\frac{\pi G M f}{c^3} \right)^{-1/6} \\
 &= 5.8 \times 10^{-22} \left(\frac{\mu}{M_\odot} \right)^{1/2} \left(\frac{M}{M_\odot} \right)^{1/3} \left(\frac{100 \text{ Mpc}}{r} \right) \left(\frac{100 \text{ Hz}}{f} \right)^{1/6}.
 \end{aligned} \tag{A.8}$$

Here μ is the binary system's reduced mass, M is its total mass, r is its distance from Earth, and G and c are Newton's gravitation constant and the speed of light. The number of cycles spent near frequency f is

$$\begin{aligned}
 n &\equiv \frac{f^2}{\dot{f}} = \frac{5}{96\pi} \frac{M}{\mu} \left(\frac{c^3}{\pi G M f} \right)^{5/3} \\
 &= 3200 \frac{M/4}{\mu} \left(\frac{M_\odot}{M} \right)^{5/3} \left(\frac{100 \text{ Hz}}{f} \right)^{5/3}.
 \end{aligned} \tag{A.9}$$

The arrows at $h_c \sim 10^{-20}$ to 10^{-23} in Figure A-4a show the sweep of such binaries from low frequency to high, for neutron stars (abbreviated *NS* in the figure) with individual masses $1.4M_\odot$ (so $M = 2.8M_\odot$ and $\mu = 0.7M_\odot$). The distance one must look to see three such coalescences per year can be estimated from the observed statistics of pulsars in our own galaxy: Clark, Van den Heuvel and Sutantyo [A-10] compute the three per year distance 100_{-40}^{+100} Mpc with 90 percent confidence. Schutz [A-11] computes, with "very high confidence", 10 Mpc to 1 Gpc. The arrows in Figure A-4a are for 100 Mpc (best estimate), 1 Gpc (most pessimistic estimate) and 10 Mpc (most optimistic). (Recall: 1 parsec is three light years; the center of our galaxy is at 10 kpc, the Virgo cluster is 10 Mpc, and the Hubble distance is 4 Gpc.)

ii. Coalescing black-hole binaries. During the inspiral phase, coalescing black-hole binaries can be described by the same Equations (A.8) and (A.9) as neutron stars; see Figure A-3 (b). However, their final gravitational-wave burst, as their horizons coalesce and the combined hole then vibrates, will be very different. It is this final burst that will be computed with confidence using supercomputers in the next few years and that, by comparison of theory and experiment, should constitute both a firm proof of the existence of black holes and a powerful test of general relativity. Coalescing black-hole binaries should be more rare than coalescing neutron-star binaries. Most likely their event rate is somewhat larger than one per year out to the Hubble distance of ~ 4 Gpc; but they might not exist at all, and they might be as common as several per year at 100 Mpc. The characteristic amplitudes during the inspiral phase are shown in Figure A-4a for distances of 4 Gpc and 100 Mpc and for several masses.

iii. Coalescing binaries as standard candles. Notice that during the inspiral phase of any compact binary the number of cycles spent near a given frequency

(Equation (A.9)) and the characteristic amplitude (Equation (A.8)) depend on the same combination of masses, $\mu^{3/5} M^{2/5}$. Correspondingly, as Schutz [A-9] has pointed out, one can solve directly from the observational data for the distance r to the source. If one can also identify the galaxy or cluster of galaxies in which the source lies and get a redshift from its electromagnetic radiation, one therefrom can determine the Hubble expansion rate of the universe and perhaps get a handle on its deceleration parameter.

iv. Supernovae and other stellar collapses that form neutron stars. The rate of occurrence of supernovae is fairly well determined (about one every 30 years per galaxy as large as our own; several per year in the Virgo cluster). Stellar collapses that produce no bright optical display could be up to ten times more numerous, or might not occur at all. Unfortunately, the strengths of the waves from a stellar collapse at a given distance are highly uncertain. If the collapse is spherical, no waves are produced at all; if it is highly nonspherical, as much as 1 percent of the rest mass of the collapsing stellar core could come off in gravitational waves. Even the characteristic frequency of the waves is uncertain; various plausible models have given frequencies anywhere from a few hundred Hertz to 10 kHz. The characteristic amplitude h_c , as a function of the characteristic frequency f , the total energy ΔE_{GW} carried off in gravitational waves, and the distance r to the source is (Equation (37) of Reference [A-1]):

$$h_c \simeq \left(\frac{3}{2\pi^2} \frac{G\Delta E_{GW}/f}{c^3 r^2} \right)^{1/2} = 2.7 \times 10^{-20} \left(\frac{\Delta E_{GW}}{M_\odot c^2} \right)^{1/2} \left(\frac{1 \text{ kHz}}{f} \right)^{1/2} \left(\frac{10 \text{ Mpc}}{r} \right). \quad (\text{A.10})$$

Figure A-4a shows this characteristic amplitude for collapses that produce neutron stars (labeled "SN") with gravitational-wave outputs of 10^{-2} to 10^{-8} solar masses and distances of our galactic center (10 kpc), the Large Magellanic Cloud (50 kpc), and the Virgo Cluster (10 Mpc). Supernova 1987A in the Large Magellanic Cloud should have produced

$$h \simeq 5 \times 10^{-18} \left(\frac{\Delta E_{GW}}{M_\odot c^2} \right)^{1/2} \left(\frac{1 \text{ kHz}}{f} \right)^{1/2}. \quad (\text{A.11})$$

If the remnant of SN1987A is really a 1/2 ms pulsar as optical observations suggest, then the supernova's collapsing core must have been rotating very rapidly and thus have been highly nonspherical; and correspondingly, ΔE_{GW} was probably $\gtrsim 10^{-3} M_\odot$.

v. Stellar collapses that form black holes. Stellar collapses that form black holes produce short wave bursts with characteristic amplitude given by Equation (A.10) and with characteristic frequency $f \sim c^3/5\pi GM \simeq (1.3 \text{ kHz})(10M_\odot/M)$. The energy carried off can vary from $\Delta E_{GW} \sim 0.1Mc^2$ down to zero, depending on the degree of nonsphericity of the collapse. The wave strengths and frequencies

shown in Figure A-4a are for efficiencies $\epsilon \equiv \Delta E_{\text{GW}}/Mc^2$ of 10^{-2} and 10^{-4} and distances of 10 Mpc (Virgo) and 4 Gpc (Hubble).

b. Periodic gravitational waves (Figure A-4b). Periodic gravitational waves are characterized by the amplitude h of the waveforms' sinusoidal oscillations (vertical axis) and their frequency (horizontal axis). The sources shown in Figure A-4b are all *nonaxisymmetric, rotating neutron stars* in our own galaxy. The number of neutron stars in our galaxy is $\gtrsim 10^8$; but most may rotate so slowly and/or may be so axisymmetric as to be poor gravitational-wave sources. The dependence of the gravitational-wave amplitude on the neutron star's moment of inertia $I_{\bar{z}\bar{z}}$ about the rotation axis, its distance r from earth, its frequency f , and its ellipticity in the equatorial plane $\epsilon = (Q_{\bar{x}\bar{x}} - Q_{\bar{y}\bar{y}})/I_{\bar{z}\bar{z}}$ (where $Q_{\bar{j}\bar{k}}$ is a component of its quadrupole moment) is (Equation (55) of Reference [A-1])

$$h = 8\pi^2 \sqrt{2/15} \frac{\epsilon I_{\bar{z}\bar{z}} f^2}{r} = 7.7 \times 10^{-20} \epsilon \left(\frac{I_{\bar{z}\bar{z}}}{10^{45} \text{g cm}^2} \right) \left(\frac{f}{1 \text{ kHz}} \right)^2 \left(\frac{10 \text{ kpc}}{r} \right). \quad (\text{A.12})$$

This amplitude is shown (NS Rot'n) in Figure A-4b for a distance of 10 kpc (the center of our galaxy), a moment of inertia of 10^{45} (all neutron stars should be within a factor ~ 3 of this), and a range of plausible ellipticities, $\epsilon \leq 10^{-5}$. This amplitude is the relevant one for waves emitted at a frequency $f = 2f_{\text{rot}}$ where f_{rot} is the star's rotation frequency. For most neutron stars this frequency should dominate the gravitational-wave spectrum, but there may also be detectable waves at $f = f_{\text{rot}} + f_{\text{prec}}$ where f_{prec} is the star's free precession frequency, and at other frequencies. From the observed spectrum and its changes with time (e.g. in starquakes) one may be able to learn much about the physics of neutron stars.

i. Known pulsars. The large dots in Figure A-4b are known pulsars, for which the amplitudes are uncertain by ~ 5 orders of magnitude because we do not know the stars' ellipticities. For each pulsar are shown (1) a best (but highly unreliable) guess of h based on all present knowledge; and (2) an upper limit, based on the observed slow-down rate of the star's rotation and the (somewhat unlikely) assumption that the slow down is due to gravitational wave emission rather than electromagnetic emission.⁴ Present knowledge permits $h < 10^{-29}$ (off the bottom of the figure).

ii. Gravitational-spindown neutron stars. Each horizontal line (dashed) in Figure A-4b shows the h of the brightest member of a hypothesized population of rotating neutron stars that are spinning down because of gravitational radiation reaction rather than electromagnetic emission [A-12]. Each line is for a fixed mean time τ_B between births of those neutron stars; and the frequency-independent amplitude is ([A-1, Equation (57)])

$$h \simeq \left[\frac{4}{3} \frac{GI_{\bar{z}\bar{z}}}{c^3 R_G^2 \tau_B} \right]^{1/2} \sim 1 \times 10^{-25} \left(\frac{10^4 \text{ years}}{\tau_B} \right)^{1/2}. \quad (\text{A.13})$$

⁴ See Section 9.4.2b of Reference [A-1].

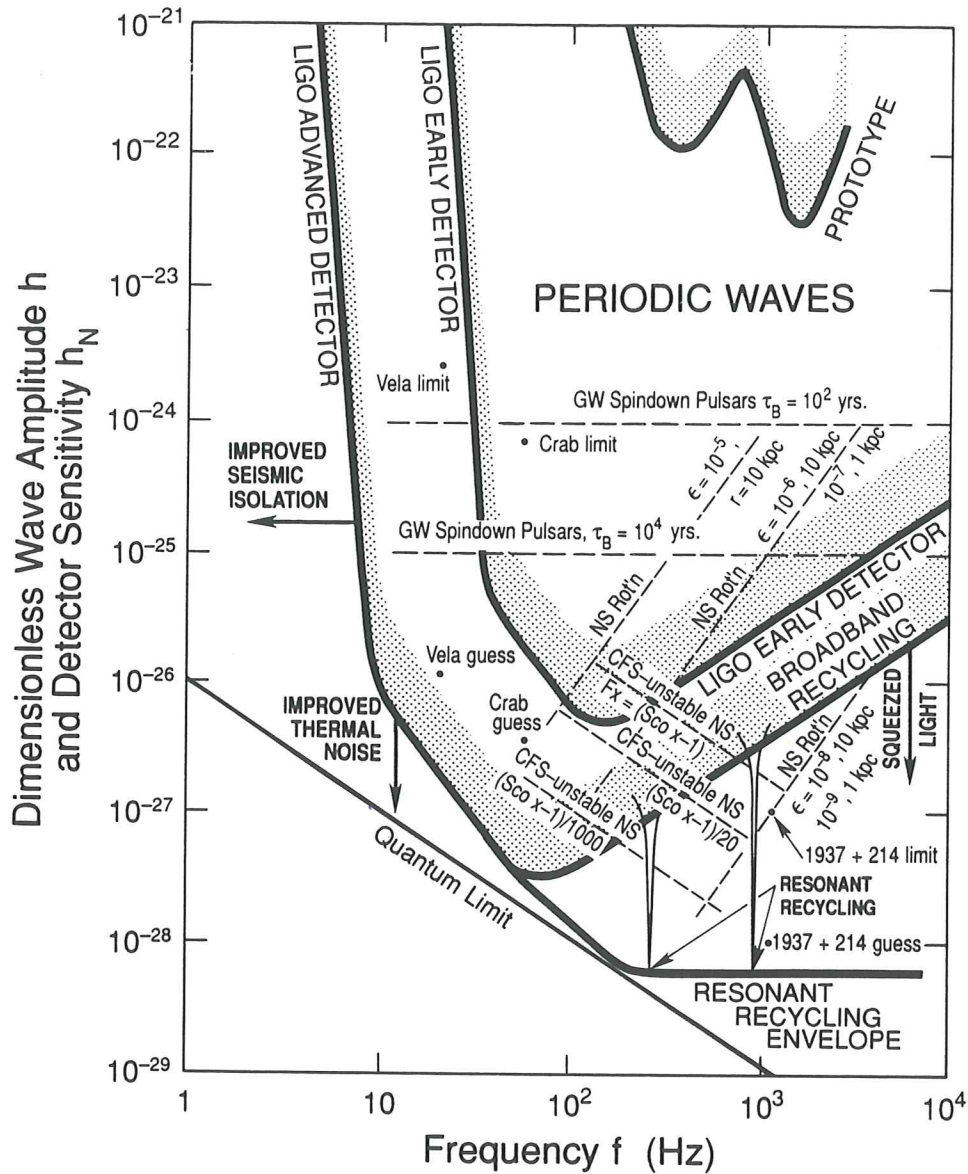


Figure A-4b The estimated dimensionless amplitude h for periodic gravitational waves from various sources (dashed lines and dots); and benchmark sensitivities (solid curves and stippled strips atop them) for interferometric detectors today and in the proposed LIGO. For each detector the solid curve corresponds to the dimensionless amplitude of a periodic gravitational wave, of previously known frequency, which would be detected at unity signal-to-noise ratio after integration for $\hat{\tau} = 10^7$ seconds, for optimal polarization and arrival direction. This amplitude, h_N , is related to the square root of the interferometer's spectral density of strain noise, $\tilde{h}(f)$, by $h_N = \tilde{h}(f)/\sqrt{\hat{\tau}}$ (see Equations (A.18), (A.19) and Appendix E). The top of the stippled strip corresponds to the dimensionless amplitude of a periodic gravitational wave of previously known frequency, with random polarization and arrival direction, which would give significant detection in 10^7 seconds. Stated more precisely, it corresponds to a confidence level of 90% that the signal is not a false alarm caused by a statistical fluctuation in Gaussian noise.

The lower right-hand part of the advanced detector curve indicates the envelope of peak responses of a resonant recycling detector when it is tuned for optimal operation at each frequency in the range shown. The slanting part of the advanced detector curve above this indicates the response of a broad-band recycling detector. The solid line near the bottom of the figure indicates limits to the advanced detector sensitivity curves set by the quantum limit for the test masses.

where $I_{zz} \sim 10^{45} \text{ g cm}^2$ is the star's moment of inertia and R_G is the radius of our Galaxy's disk.

iii. Chandrasekhar-Friedman-Schutz instability. The rightward slanted lines (labeled CFS—unstable NS) in Figure A-4b are neutron stars that have been spun up by accretion from a companion, until they became unstable against nonaxisymmetric perturbations (the “Chandrasekhar-Friedmann-Schutz” [A-13] or CFS instability). These neutron stars would now be sources of X-rays due to their accretion and gravitational waves due to their nonaxisymmetry, and their gravitational-wave amplitudes would be proportional to the square root of their X-ray luminosities, F_X ([A-14]; Equation (53) of Reference [A-1]):

$$h \simeq 2 \times 10^{-27} \left(\frac{300 \text{ Hz}}{f} \right)^{1/2} \left(\frac{F_X}{10^{-8} \text{ erg/cm}^2\text{s}} \right)^{1/2}. \quad (\text{A.14})$$

This amplitude is shown in Figure A-4b for X-ray luminosities as fractions of that of the brightest candidate for such an object, *Sco X-1*. NASA is considering flying an “X-Ray Large Array” [A-15] which, among other things, would search for X-ray modulations that might be due to the CFS instability. Any observed modulations would be cross-correlated with the outputs of gravitational wave detectors.

c. Stochastic waves (Figure A-4c). Stochastic gravitational waves are characterized in Figure A-4c by the amplitude h of the fluctuations of h_+ and h_\times in a bandwidth Δf equal to the frequency f at which one searches.⁵

i. Primordial gravitational waves. The most interesting stochastic background would be that from the *big bang*. Its strength is often described in terms of the gravitational-wave energy density $\rho_{\text{GW}}(f)$ in a band $\Delta f = f$ divided by the energy density required to close the universe,

$$\Omega_{\text{GW}}(f) \equiv \frac{\rho_{\text{GW}}(f)}{\rho_{\text{closure}}}, \quad (\text{A.15})$$

which is related to h by (Equation (65) of Reference [A-1])

$$\begin{aligned} h &= \left[\frac{4G}{\pi f^2 c^2} \Omega_{\text{GW}}(f) \rho_{\text{closure}} \right]^{1/2} \\ &= 1.3 \times 10^{-18} \left(\frac{\rho_{\text{closure}}}{1.7 \times 10^{-8} \text{ erg cm}^{-3}} \right)^{1/2} \left(\frac{1 \text{ Hz}}{f} \right) [\Omega_{\text{GW}}(f)]^{1/2}. \end{aligned} \quad (\text{A.16})$$

Lines of constant Ω_{GW} are shown in Figure A-4c. Current speculations about gravitational waves from the very early universe would place Ω_{GW} for the LIGO frequency band in the range 10^{-4} or downward. These waves almost certainly

⁵ cf., Section 9.4.3a of Reference [A-1].

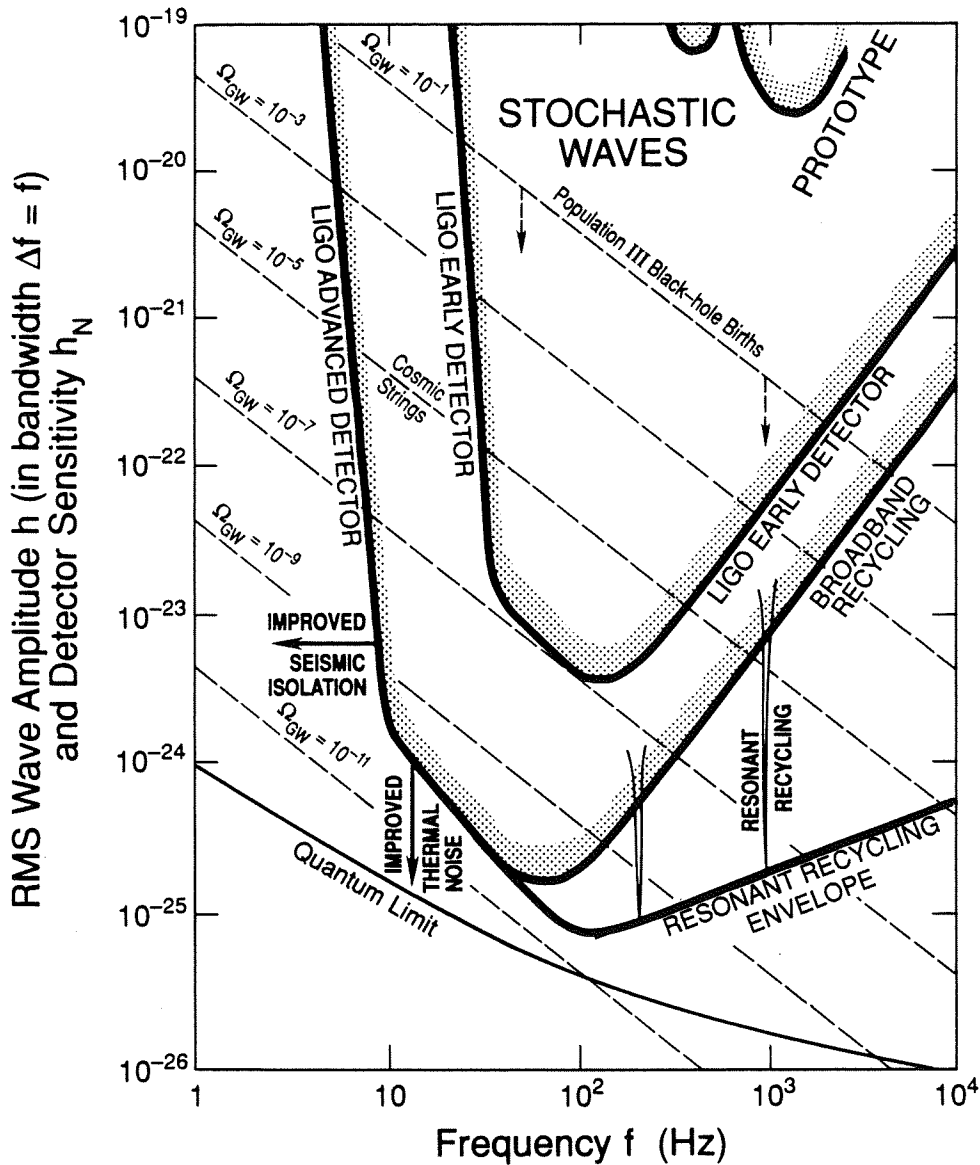


Figure A-4c The estimated rms amplitude h in a bandwidth $\Delta f = f$ for stochastic backgrounds of gravitational waves from various sources (dashed lines); and benchmark sensitivities $h_N \simeq \sqrt{5}h(f)[2f/\hat{\tau}]^{1/4}[1 + fD/c]^{1/2}$ (see Equation (A.20)) (solid curves and stippled strips atop them) for interferometric detectors today and in the proposed LIGO. For each detector the solid curve corresponds to the rms amplitude in a bandwidth equal to the frequency for a stochastic background which would be detected at unity signal-to-noise ratio in a cross-correlation experiment between two interferometers at different LIGO sites, after integration for $\hat{\tau} = 10^7$ seconds. The top of the stippled strip corresponds to the rms amplitude in a bandwidth equal to the frequency of a stochastic background which would give significant detection in 10^7 seconds. Stated more precisely, it corresponds to a confidence level of 90% that the signal is not a false alarm due to a statistical fluctuation in Gaussian noise. The lower right-hand part of the advanced detector curve indicates the envelope of peak responses of a resonant recycling detector system when tuned for optimal operation at each frequency in the range shown. Each of the resonance curves above this indicates response of a particular resonant recycling system. The solid line near the bottom of the figure indicates the limit to the advanced detector sensitivity curves set by the quantum limit for the test masses.

are not thermalized at $\sim 3\text{K}$ like primordial photons because they decoupled from matter at the Planck time, and because their interaction with background spacetime curvature is likely to have produced significant nonadiabatic, frequency-dependent amplification soon after the Planck time (e.g., during an inflationary era).⁶ Pulsar timing [A-16] has produced an observational limit $\Omega_{\text{GW}} \lesssim 10^{-6}$ at the exceedingly low frequency $f \sim 10^{-8}$ Hz, 10 orders of magnitude away from the LIGO frequency band; and the isotropy of the cosmic microwave radiation places limits $\Omega_{\text{GW}} \lesssim 10^{-12}$ at $f \sim 10^{-16}$ Hz and $\Omega_{\text{GW}} \lesssim 10^{-8}$ at $f \sim 3 \times 10^{-18}$ Hz ([A-17]; Section 9.5.5c of Reference [A-1]). A newly recognized limit comes from the time delay between different paths forming the image of a quasar deflected by the gravitational lens formed by a galaxy intervening between Earth and the quasar; $\Omega_{\text{GW}} < 10^{-8}$ at $f < 3 \times 10^{-18}$ Hz [A-18]. Standard versions of inflationary cosmology predict a unique spectrum for $\Omega_{\text{GW}}(f)$ — one which, when combined with the above limits, requires $\Omega_{\text{GW}} \lesssim 10^{-12}$ in the LIGO frequency band. However, other cosmological models permit a primordial Ω_{GW} as large as 10^{-4} in the LIGO band.

ii. Cosmic strings. Another possible source of stochastic background is the decay of nonsuperconducting, cosmic strings. If such strings, created in a GUT phase transition in the very early universe, actually exist, they are estimated [A-19] to produce

$$\Omega_{\text{GW}} \sim 10^{-7} \left(\frac{\mu}{10^{-6}} \right)^{1/2} \quad (\text{A.17})$$

throughout the LIGO frequency band and also in the band $f \sim 10^{-8}$ Hz of pulsar timing (Equation (68) of Reference [A-1]). Here μ is G/c^2 times the string's mass per unit length, and a value $\mu \sim 10^{-6}$ is suggested both by fundamental theory and by that value's success in producing from strings possible seeds for galaxy formation [A-19].

iii. Population III black-hole births. Stochastic waves could also result from a superposition of emissions from the deaths, long ago, by stellar collapse to form black holes, of a pre-galactic population of massive stars (“Population III stars”) [A-20]. Such a population has been hypothesized to help explain the observed abundances of the elements in very old stars. Figure A-4c shows an upper limit of $\Omega_{\text{GW}} \lesssim 0.1$ [A-20] in the LIGO band for the plausible strengths of such Population III waves—which, of course, might not exist at all.

d. Sensitivities of detectors in the LIGO

i. Characterization of detector sensitivities. Internal noise in an interferometric detector (discussed in more detail in Section III.A and Appendix B) causes the fractional arm length difference, $\Delta L/L$, as inferred from the detector's readout, to fluctuate stochastically in time. Those fluctuations are characterized statistically by their spectral density $S_{\Delta L/L}(f)$ (see Appendix E) as a function of frequency f .

⁶ See Section 9.4.3d of Reference [A-1] for details and references.

It is conventional in this field to denote the square root of that spectral density by

$$\tilde{h}(f) \equiv \sqrt{S_{\Delta L/L}(f)}, \quad (\text{A.18})$$

and call it the detector's *strain noise per root hertz*. The root-mean-square fluctuations of $\Delta L/L$ at frequency f and in a bandwidth Δf are

$$(\Delta L/L)_{\text{rms}} = \tilde{h}(f)\sqrt{\Delta f}. \quad (\text{A.19})$$

It is these rms fluctuations that compete with the gravitational wave (Equation (A.5a)) in the output data.

When searching for gravitational-wave bursts the relevant bandwidth is $\Delta f \sim f$; and, correspondingly, we plot the "noise amplitude" $h_N \equiv \tilde{h}(f)\sqrt{f}$ in Figure A-4a (solid curves) as a measure of detector sensitivity. A source with characteristic amplitude h_c equal to this noise amplitude and with optimal direction and polarization would produce unity signal to noise in the detector. As a second measure of the sensitivity we plot, as the top of the stippled strips, the quantity $11\tilde{h}(f)\sqrt{f}$. The factor 11 gives a 90% confidence level that wave bursts with random polarization and direction, observed three times per year, are not false alarms because of fluctuations in Gaussian noise (Equation (111) of Reference [A-1]).

When searching for periodic sources, the relevant bandwidth is $\Delta f \simeq 1/\hat{\tau}$, where $\hat{\tau}$ is the integration time; and correspondingly, we plot the noise amplitude $h_N \equiv \tilde{h}(f)\sqrt{1/\hat{\tau}}$ in Figure A-4b (solid curves) as our measure of detector sensitivity, with $\hat{\tau}$ set equal to 10^7 seconds. This corresponds to unity signal to noise for a source with optimal direction and polarization. The top of the stippled strips is $3.8\tilde{h}(f)\sqrt{1/\hat{\tau}}$. The factor 3.8 guarantees 90 percent confidence of detecting a periodic source, with previously known frequency, and with a random direction (Equation (112) of Reference [A-1]). If the period is not known in advance, the sensitivity is reduced by an additional factor 4 using conventional data processing. Computational techniques have been developed [A-21] to regain this factor if the position of the source is known. The analysis problem for sources with both unknown period and unknown position has been formulated but poses a substantial computational challenge.

When searching for a stochastic background one cross-correlates two detectors and, thereby, if one cross-correlates over a band Δf , one achieves an effective bandwidth of about $f/\sqrt{\frac{1}{2}\hat{\tau}\Delta f}$. Assuming that the background is isotropic and polarization independent (as we shall), one must use a direction-averaged sensitivity to describe the detector; this means reducing the sensitivity by a factor $\sqrt{5}$ relative to that for an optimal direction and polarization [A-1]. At low frequencies, waves from all directions excite the two detectors coherently, but at frequencies much above $c/D \simeq 75$ Hz (where $D \simeq 4000$ km is the separation of the LIGO detectors) only waves from a fraction $\simeq c/fD$ of the sky excite them coherently. The result is a

reduction in the amplitude sensitivity by a factor $\simeq \sqrt{1 + fD/c}$. By combining all these effects, we see that an isotropic background, whose rms amplitude in a bandwidth equal to frequency is h , will produce a unity signal-to-noise ratio in the cross correlation of the detectors if $h = h_N$, where

$$h_N \equiv \sqrt{5}\tilde{h}(f) \left[f / \sqrt{\frac{1}{2}\hat{\tau}\Delta f} \right]^{\frac{1}{2}} [1 + fD/c]^{\frac{1}{2}} \quad (\text{A.20})$$

Correspondingly, we plot this quantity in Figure A-4c (solid lines), with $\hat{\tau} = 10^7$ seconds and with cross-correlation bandwidth $\Delta f = f$, except in the case of resonant recycling (see below). The top of the stippled strips is 1.7 times larger than that given by Equation (A.20), corresponding to 90 percent confidence of detection of the isotropic background.

To a great extent, the choice of bandwidth and the details of the search are fixed in the data analysis. Thus, general purpose data can be collected and then analyzed in a variety of ways for a variety of sources. However, this is not entirely true: some special choices of the interferometric optics, e.g., resonant recycling, produce in the “hardware” special narrow-banding of the output, with significant gains of sensitivity at the price of a loss of frequency coverage. These issues are discussed in Appendix C and in greater detail in Section 9.5.3e of Reference [A-1] (especially Figure 9.13).

In Figures A-4 three detector sensitivity curves are shown:

(a) Prototype detector. The upper solid curve is the best sensitivity, as defined above, that has been achieved so far by our prototype detector with 40-meter arms (cf., Section III.B).

(b) LIGO early detector. The middle solid curve in each figure is the sensitivity of a possible detector that might operate soon after the LIGO is completed. The concepts for this detector are described in Section V.A and its estimated noise spectrum $\tilde{h}(f)$ is given in Figure V-3.

(c) LIGO advanced detector. Once the first detector has been operated successfully in the LIGO at something like the sensitivities of Figures A-4a, b, and c, there will follow a succession of generations of ever improving detectors, with the sensitivity levels being pushed continually downward (to smaller h) and leftward (to lower frequencies f). As a rough measure of where this might lead after a few years, we show a sensitivity curve which corresponds to an “advanced detector” whose concept is discussed in Section V.B and whose estimated noise spectrum $\tilde{h}(f)$ is given in Figure V-4.

(d) Further improvements beyond advanced detector. The LIGO “advanced detector” does not represent an ultimate limit on detector sensitivities in the LIGO. Further improvements are likely to occur in several different directions: (1) Improvements in antiseismic isolation are likely to push downward the detectors’ low-frequency cutoff (left-pointing arrows in Figures A-4). (2) Improvements in thermal

noise are likely to produce sensitivity improvements in the frequency band between 10 Hz and 50 Hz (down-pointing arrows in Figures A-4). (3) The “LIGO advanced detector” entails 100 broad-band recyclings of the light in the interferometer (cf., Section V.B and Appendix C). By increasing the number of recyclings, the broad-band sensitivity can be improved at frequencies above 100 Hz (Section 9.5.3(e) of Reference [A-1]); see, for example the sensitivity curve labeled “1500 recycles” in Figure A-4a and the curve labeled “broadband recycling envelope”, which represents the lower envelope of the sensitivities of detectors identical to the “LIGO advanced detector” except for having more recyclings. (4) The envelope can be pushed downward by improvements in mirror reflectivities, together with increases in the number of recyclings. (5) The \sqrt{N} photon shot noise, which is responsible for the limitations on sensitivity above 100 Hz, is actually produced by a superposition of laser light and quantum electrodynamical vacuum fluctuations [A-22]. The vacuum fluctuations enter the interferometer through the beam splitter from the direction of the photodetector (Figure II-1). By injecting, in place of vacuum fluctuations, “squeezed vacuum light” that is phase coherent with the laser, one can reduce the detector’s photon shot noise below the standard, Poissonian, \sqrt{N} level, and thereby improve the broad-band sensitivity in the region $f \gtrsim 100$ Hz [A-22], see Appendix C. (6) When searching for periodic sources or stochastic background one can use “resonant recycling” or “dual recycling” (see Appendix C) to improve the sensitivity over a narrow frequency band (see narrow solid curves in Figures A-4b and A-4c and lines marked “resonant recycling envelope”, which show the envelope of the achievable sensitivities with resonant recycling if one uses 100 W of laser power and mirrors whose losses are 10^{-4} per bounce.)

Quantum mechanics places an ultimate limit on the detector noise level achievable by any of the above techniques (Section 9.5.3(f) of [A-1]):

$$\tilde{h}(f) = \left[\frac{2}{\pi^2} \frac{\hbar}{mL^2 f^2} \right]^{1/2} = 4 \times 10^{-26} \left(\frac{1000 \text{ kg}}{m} \right)^{1/2} \left(\frac{1000 \text{ Hz}}{f} \right) \quad \text{for bursts.} \quad (\text{A.21})$$

This *standard quantum limit* is enforced by the fluctuations in the pressure of laser light on the detector’s masses (analog of “Heisenberg-microscope” enforcement of uncertainty principle). Figures A-4a,b,c show this limit, translated into the form of detector sensitivity (unity signal-to-noise ratio for a source of optimal polarization and direction in Figures A4-a and A4-b, and for an isotropic stochastic background in Figure A4-c). In principle this limit can be circumvented; see [A-23]. However, it might never be circumvented in practice.

e. Conclusions. By comparing the source strengths and benchmark sensitivities in Figures A-4, one sees that *the first detector in the LIGO has significant possibilities for detecting waves:*

- It could have detected the initial wave burst from Supernova 1987A if that burst carried more than $\sim 10^{-4}$ solar masses of energy (an amount that would easily be produced if the collapsing stellar core was rotating rapidly enough to produce a 0.5 ms pulsar, as is suggested by observation).
- It could detect the low frequency radiation (< 300 Hz) in bursts from supernovae that have rapidly rotating cores and fragment during the collapse at a distance of the Virgo cluster of galaxies.
- It could detect the coalescence of a neutron-star binary out to 30 Mpc distance (three times the distance of the Virgo cluster of galaxies).
- It could detect periodic waves from the Crab pulsar if the wave amplitude exceeds 1/10 of the current limit, which is based on the rate of spindown of the pulsar.
- It could detect a stochastic background of gravitational waves between 50 Hz and 150 Hz, if that background carries more than 2×10^{-7} of the energy required to close the universe. (This is close to the level expected from non-superconducting GUT cosmic strings, if they exist.)

If waves are not detected by the LIGO's first detector, then they probably will be detected by a subsequent detector with sensitivity somewhere between the "early detector" and "advanced detector" sensitivities of Figures A-4. Examples that illustrate the high probability of detection at the "advanced detector" sensitivity are:

- The "advanced detector" could detect a supernova in our galaxy that puts out 10^{-8} solar masses of energy at frequencies of 1 kHz and less, or a supernova in the Virgo cluster that puts out 10^{-2} solar masses at 1 kHz and less.
- It could detect a neutron-star coalescence out to almost 1 Gpc (1/4 the Hubble distance)—within which distance there are expected to be many coalescences per year.
- It could detect the coalescence of equal-mass binary black holes throughout the observable universe, so long as the hole masses lie between 10 and 1000 times the mass of the sun.
- It could detect the Crab and Vela pulsars if they are as strong as the current (highly unreliable) best guess.
- It could detect a stochastic background between 30 Hz and 90 Hz if that background carries an energy exceeding 10^{-10} of the energy required to close the universe.

References

- A-1. Thorne, K. S., "Gravitational Radiation," *300 Years of Gravitation*, S. W. Hawking and W. Israel (eds.), Cambridge University Press, Cambridge, England, pp. 330-458, 1987.
- A-2. Taylor, J. H., and J. M. Weisberg, *Astrophysical Journal*, Vol. 253, pp. 908-920, 1982; J. H. Taylor, *General Relativity and Gravitation*, M.A.H. MacCallum (ed.), Cambridge University Press, Cambridge, England, p. 209, 1987.
- A-3. Eardley, D. M., D. L. Lee, and A. P. Lightman, *Physical Review D*, Vol. 8, p. 3308, 1983; Will, C. M., *Theory and Experiment in Gravitational Physics*, Cambridge University Press, Cambridge, England, 1981.
- A-4. Faller, J. E., P. L. Bender, J. L. Hall, D. Hils, and M. A. Vincent, "Kilometric Optical Arrays in Space," *Proceedings of the Colloquium*, Cargese, Corsica, ESA SP-226, October 23-25 1984.
- A-5. See, e.g., Section 7.2 of Yakov B. Zel'dovich and Igor D. Novikov, "Relativistic Astrophysics, Vol. 2," *The Structure and Evolution of the Universe*, University of Chicago Press, Chicago, 1983.
- A-6. See, e.g., *Serendipitous Discoveries in Radio Astronomy*, K. I. Kellerman and B. Sheets (eds.), National Radio Astronomy Observatory, Green Bank, West Virginia, 1983.
- A-7. Saenz, R. A., and S. L. Shapiro, *Astrophysical Journal*, Vol. 221, p. 286, 1978.
- A-8. See, e.g., Nakamura, T., *Gravitational Collapse and Relativity*, H. Sato and T. Nakamura (eds.), World Scientific, Singapore, p. 295, 1987; also see the discussion and references in Section 9.3.3(e) of Reference 1.
- A-9. Schutz, B. F., *Nature*, Vol. 323, p. 310, 1986.
- A-10. Clark, J.P.A., E.P.J. van den Heuvel, and W. Sutantyo, *Astronomy and Astrophysics*, Vol. 72, p. 120, 1979.
- A-11. Schutz, B. F., "Sources of Gravitational Radiation," *Gravitational Wave Data Analysis*, B. F. Schutz (ed.), Kluwer Academic, Dordrecht, 1989.
- A-12. Blandford, R. D., unpublished work reviewed in equation (57) of Reference [A-1], and associated discussion.
- A-13. Chandrasekhar, S., *Physical Review Letters*, Vol. 24, p. 611, 1970; Friedman, J. L., and B. F. Schutz, *Astrophysical Journal*, Vol. 222, p. 281, 1978.
- A-14. Wagoner, R. V., *Astrophysical Journal*, Vol. 278, p. 345, 1984.
- A-15. Wood, K. S., P. F. Michelson, P. Boynton, M.R. Yearian, H. Gursky, H. Friedman, and J. Dieter, *A Proposal to NASA for an X-Ray Large Array (XLA) for the NASA Space Station*, Stanford, Palo Alto, CA, 1986.
- A-16. Taylor, J. H., *General Relativity and Gravitation*, M.A.H. MacCallum (ed.), Cambridge University Press, Cambridge, England, p. 209, 1987.

- A-17. Grishchuk, L. P., *General Relativity and Gravitation*, M.A.H. MacCallum (ed.), Cambridge University Press, Cambridge, England, p. 86, 1987.
- A-18. Allen, B., *Physical Review Letters*, **63**, 2017, 1989.
- A-19. Vilenkin, A., *300 Years of Gravitation*, S. W. Hawking and W. Israel (eds.), Cambridge University Press, Cambridge, England, p. 499, 1987.
- A-20. Bond, J. R., and B. J. Carr, *Monthly Notices of the Royal Astronomical Society*, Vol. 207, p. 505, 1984.
- A-21. Livas, J., "Broadband Search Techniques for Periodic Sources of Gravitational Radiation," *Gravitational Wave Data Analysis*, B. F. Schutz (ed.), Kluwer Academic, 1989.
- A-22. Caves, C. M., *Physical Review Letters*, **23**, 1693, 1981.
- A-23. Unruh, W. G., unpublished (1982); Caves, C. M., *Quantum Measurement and Chaos*, E. R. Pike (ed.), Plenum, New York, 1987.

APPENDIX B

INTERFEROMETER CONCEPTS AND NOISE

This appendix provides some analytic basis and further explanations for the concepts introduced in Section III. The subjects discussed are

1. The theory of the Fabry-Perot Cavity
2. The transfer function of an interferometric gravitational wave detector
3. Basic optical concepts including the RF phase modulation of the optical beams
4. The physical basis of some of the noise terms

There is an extensive published literature on some of these issues [B-1]. We include a discussion of them in the same format and notation as other parts of the proposal for the convenience of the reader.

1. The Theory of the Fabry-Perot Cavity.

In a gravitational wave interferometer each arm's Fabry-Perot cavity is a light storage element. The input mirror, in the interferometer corner station, is partially transmitting with an intensity transmission coefficient of $T_1 = (1 - R_1 - A_1)$. Here A_1 is the mirror's optical absorption and R_1 is its intensity reflection coefficient. The rear mirror, which is in one of the interferometer's end stations a distance L from the input mirror, is coated for high reflectivity, $R_2 = (1 - A_2) \approx 1$, i.e. for negligible transmission. The electric field reflection and transmission coefficients of each mirror, r_1, r_2, t_1, t_2 are equal to the square root of the intensity coefficients; the reflection coefficients have opposite sign depending on whether the incident beam approaches the reflecting surface from the substrate side or from the vacuum.

When an optical electric field pulse of unit amplitude is incident on the cavity input mirror, a set of pulses is returned from the cavity. Figure B-1(a) shows the time series of these pulses. The first pulse, reflected by the input mirror, returns immediately and has an amplitude of r_1 . The second pulse, reflected once by the rear mirror where it is inverted in sign, arrives a time $2L/c$ later and is reduced in amplitude to $r_2 t_1 t_1$ as a result of two transmissions through the input mirror and one reflection off the end mirror. Subsequent pulses undergo reflections from both mirrors and are delayed in time by $n2L/c$ where n is the number of round trips in the cavity. The pulses become progressively smaller and have amplitudes $t_1 t_1 r_2 (r_1 r_2)^n$. The sum of all these pulses is the cavity's "reflected electric field impulse response" (Green's function), and is given algebraically by

$$h_r(t) = \frac{E_r(t)}{E_0} = r_1 \delta(t) - t_1 t_1 r_2 \sum_{n=0}^{\infty} (r_1 r_2)^n \delta\left(\frac{t - 2L(n+1)}{c}\right). \quad (\text{B.1})$$

The response of the cavity for an arbitrary incident electric field is the convolution

of the impulse response with the incident field.

$$E_r(t) = \int_{-\infty}^t h_r(\tau) E_{inc}(t - \tau) d\tau. \quad (\text{B.1a})$$

If the input light has a sinusoidal dependence, $E_{inc}(t - \tau) = E_0 e^{i\omega(t-\tau)}$, the convolution gives the cavity's reflection transfer function:

$$\frac{E_r(t)}{E_o} = e^{i\omega t} \left[r_1 - t_1 t_1 r_2 e^{-i2\omega L/c} \sum_{n=0}^{\infty} (r_1 r_2)^n e^{-i2\omega n L/c} \right]. \quad (\text{B.2})$$

Since $|r_1 r_2| < 1$ the series can be summed:

$$\begin{aligned} \frac{E_r(t)}{E_o} &= e^{i\omega t} \left[r_1 - \frac{t_1 t_1 r_2 e^{-i2\omega L/c}}{1 - r_1 r_2 e^{-i2\omega L/c}} \right] \\ &= e^{i\omega t} \left[\frac{r_1 - r_2 (r_1^2 + t_1^2) e^{-i2\omega L/c}}{1 - r_1 r_2 e^{-i2\omega L/c}} \right]. \end{aligned} \quad (\text{B.3})$$

Figure B-1(b), a phasor diagram, shows how the convolution produces the reflection transfer function of the cavity. The resultant field is made up from the superposition of the individual waves from the multiple reflections described in Figure B-1(a). The net reflected electric field is the distance from the origin, the center of the circle, to the end point of a trajectory indicated by a progression of dots. The phase of the net reflected field is the azimuthal angle around the circle with zero degrees being to the right. Each trajectory, associated with a specific value of $x = (2\omega L/c) - (2\omega_0 L_0/c)$, begins at the point marked by * which represents the first term in the series: the initial reflection from the input mirror. Along any one trajectory the distance between dots is proportional to the magnitude of the individual reflected components. The angle of each line segment between dots, relative to the horizontal, is the phase of the individual reflected wave. The trajectory labeled $x = 0$ is the resonance case, with cavity length equal to a half-integral multiple of the laser wavelength. Going to the left one sees the individual reflections adding up coherently with the resultant field being almost equal to the incident field but shifted in phase by 180 degrees providing the cavity losses are small. In a low-loss cavity, the component of the field emerging from the cavity is almost twice the incident field. As the cavity is moved away from resonance, $x \neq 0$, by a change in length, the phase of the net reflected wave changes; this phase shift is proportional to an incident gravitational wave. The change in net phase produced by a unit change in cavity length is a maximum at resonance. At large values of x , far from resonance, the phase of the successive individual waves changes rapidly and the phase of the resultant reflected field changes little with a change in x . The entire cavity then behaves just like the input mirror without a cavity behind it.

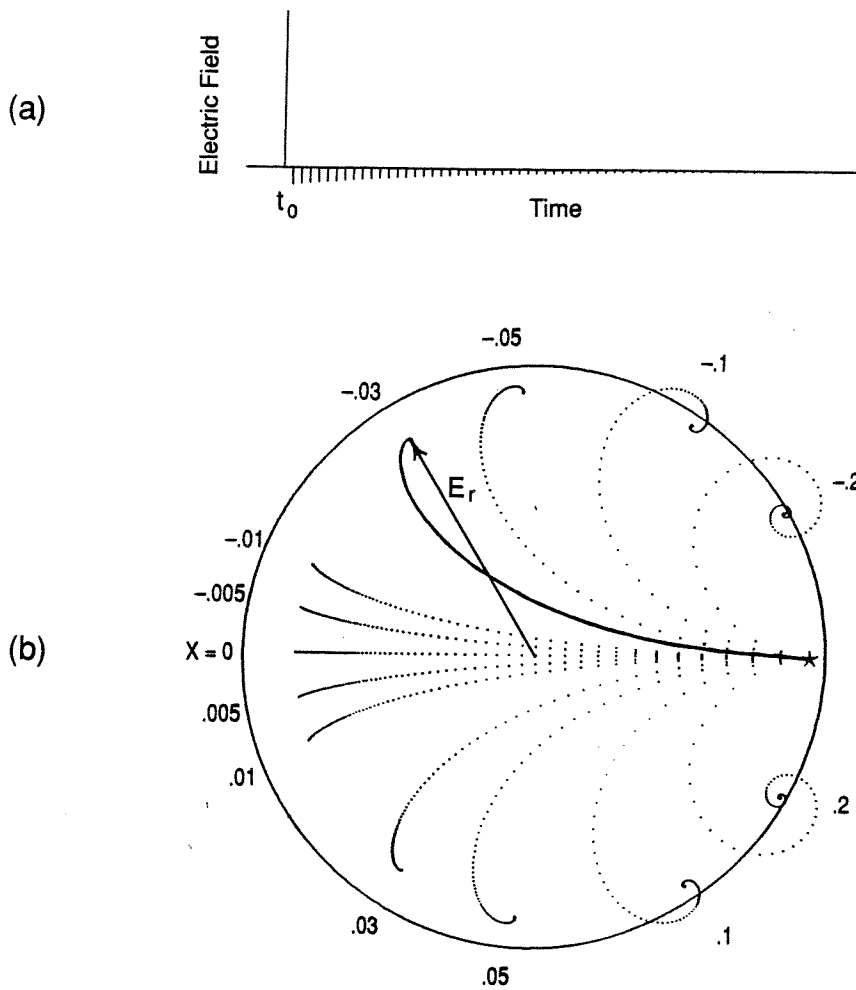


Figure B-1 (a) Time evolution of the optical response of a Fabry-Perot cavity to an input pulse. The figure is drawn for a cavity with an input mirror transmission $T = 0.1$, end mirror reflectivity $R = 1$, and 0.01 loss per pass in the cavity mirrors. The direct reflection from the input mirror occurs at time t_0 . The delayed pulses (with opposite phase from the initial one) correspond to light which enters the cavity, and reflects many times between the mirrors; a small amount of this light is transmitted upon each encounter with the input mirror. (b) Phasor diagram for light reflected from a Fabry-Perot cavity with the same properties, under continuous illumination. The radius of the circle is equal to the amplitude of the input light beam. The direct reflection from the input mirror is the vector (not drawn) from the center of the circle to the star. Each series of dots, originating at the star, represents the superposition of waves which have made different numbers of passes through the cavity, calculated for a given value of detuning between the input light and the cavity's resonance frequency. The length and direction of each line segment connecting adjacent dots corresponds to the amplitude and phase, respectively, of one of these waves. The vector from the origin to the end of the series (E_r) gives the net electric field reflected from the cavity. The vector from the star to the end of the series (not drawn) is the leakage field from the cavity.

When the cavity length, L , is tuned to resonance, the optical electric field stored in the cavity grows by resonant buildup to $\approx 2/\sqrt{T_1}$ times the incident field. The light storage time of the cavity is then

$$\tau_s = \frac{\tau_t}{1 - |r_1 r_2|} \approx \frac{2L}{cT_1} \quad (\text{B.4})$$

where $\tau_t = L/c$ is the one-way transit time in the cavity. The change in optical phase of the reflected field for a unit change in cavity length near resonance is

$$\frac{\Delta\varphi}{\Delta L} \cong \frac{-16\pi}{\lambda_o T_1 [1 - (\frac{A_1 + A_2}{T_1})^2]} \approx \frac{-8\pi}{\lambda_o} \frac{\tau_s}{\tau_t}. \quad (\text{B.5})$$

The amplitude of the net reflected field at cavity resonance is

$$\frac{E_r}{E_0} = 1 - \frac{2(A_1 + A_2)}{T_1} \quad (\text{B.6})$$

when the mirror optical losses are much smaller than the input mirror transmission.

2. The Gravitational Wave Transfer Function of the Interferometric Detector.

This section outlines the response of an interferometric gravitational-wave detector (“interferometer”) that uses Fabry-Perot cavities as the optical storage elements. We compute the responses to a sinusoidal wave incident from an arbitrary direction. The end result is the “transfer function” of the interferometer, defined as the complex ratio of the optical phase shift at the output (the antisymmetric port) of the interferometer at the gravitational wave frequency, f , to an excitation by a gravitational wave with amplitude h at frequency f .

In our calculation the interferometer masses are idealized as free (a good idealization above the resonant frequencies of the mass suspensions). The masses then travel along geodesics of the spacetime, which are distorted by the gravitational wave. We perform the calculation in “transverse traceless (TT) coordinates” [B-2]. In these coordinates the masses are forever at rest (x, y, z are constant on their geodesic world lines), and their coordinate separations are forever constant. However, the gravitational wave perturbs the metric of spacetime, thereby altering the masses’ physical separations.

One interferometer mass is located at the origin and the other two are situated a distance L on the the x and y axes. The metric tensor is

$$g_{ij} = \eta_{ij} + h_{ij}(t, \vec{r}) \quad (\text{B.7})$$

where η_{ij} is the flat spacetime Minkowski metric and $h_{ij}(t, \vec{r})$ is the metric perturbation produced by the gravitational wave. In TT coordinates h_{ij} is purely spatial ($h_{tj} = 0$), and the components that are relevant to our calculation are [B-2]

$$h_{xx} = h G_{xx} e^{(i\vec{k}\cdot\vec{r} - i\omega t)}, \quad h_{yy} = h G_{yy} e^{(i\vec{k}\cdot\vec{r} - i\omega t)} \quad (\text{B.8})$$

where

$$\begin{aligned} G_{xx} &\equiv \cos 2\Omega (\cos^2 \phi - \sin^2 \phi \cos^2 \theta) - \sin 2\Omega \sin 2\phi \cos \theta \\ G_{yy} &\equiv \cos 2\Omega (\sin^2 \phi - \cos^2 \phi \cos^2 \theta) + \sin 2\Omega \sin 2\phi \cos \theta. \end{aligned} \quad (\text{B.9})$$

Here h is the gravitational wave strain in the plane perpendicular to the propagation direction and \vec{k} is the wave vector,

$$\vec{k} = \frac{\omega}{c} (\sin \theta \sin \phi \vec{x} - \sin \theta \cos \phi \vec{y} + \cos \theta \vec{z}). \quad (\text{B.10})$$

The polarization of the wave is specified by the angle Ω . We can think of $\Omega = 0$ as being the + polarization state and $\Omega = \pi/4$ as being the \times state.

Now consider a photon traveling between the central mass and the mass located at $x = L$. The equation $ds^2 = g_{ij}dx^i dx^j = 0$, which expresses the fact that the photon travels at the speed of light, takes the following form, accurate to first order in the wave amplitude h :

$$c \frac{dt}{dx} = \pm(1 + \frac{1}{2} h_{xx}). \quad (\text{B.11})$$

By integrating this equation along the photon's world line as it travels from the central mass at time t_0 to the end mass and back, we obtain for the time t of its return to the central mass

$$t = t_0 + 2\tau_t + \frac{\tau_t h G_{xx}}{2} H(\omega, k_x) e^{-i\omega(t_0 + \tau_t)}. \quad (\text{B.12})$$

Here $\tau_t = L/c$,

$$H(\omega, k_x) = \text{sinc} \frac{1}{2}(k_x L - \omega \tau_t) e^{\frac{i}{2}(k_x L + \omega \tau_t)} + \text{sinc} \frac{1}{2}(k_x L + \omega \tau_t) e^{\frac{i}{2}(k_x L - \omega \tau_t)}, \quad (\text{B.13})$$

and $\text{sinc } z = \sin z / z$.

A similar calculation is carried out for the light leaving the central mass at time t_0 that travels back and forth along the y direction. The difference in transit time for the two paths is given by

$$\Delta t = \frac{h\tau_t}{2} [G_{xx} H(\omega, k_x) - G_{yy} H(\omega, k_y)] e^{-i\omega(t_0 + \tau_t)}. \quad (\text{B.14})$$

Because the gravitational wave has $h_{tt} = 0$ and the central mass remains always at rest in the coordinate system, this Δt is equal to the proper time difference as measured by a physical clock riding on the central mass. The optical phase shift at the antisymmetric port of the interferometer due to this time difference is

$$\Delta \phi^{(1)} = \omega \Delta t = \frac{2\pi c \Delta t}{\lambda} \quad (\text{B.15})$$

where λ is the optical wavelength.

For the Fabry-Perot cavity the procedure is applied iteratively to the terms that transit the cavity multiple times. When the cavity is on resonance the unperturbed phase shift for each transit is a multiple of 2π . The perturbed phase shifts are small enough so that $e^{i\Delta\phi^{(1)}}$ is well approximated by $1 + i\Delta\phi^{(1)}$ and can be summed over the infinite series of transits.

After some algebraic manipulation, the transfer function of the recombined Fabry-Perot interferometer is found to be given by

$$\frac{\phi(f)}{h(f)} = \frac{4\pi c\tau_t^2}{\lambda\tau_s} [G_{xx}H(\omega, k_x) - G_{yy}H(\omega, k_y)] \times \left(\frac{e^{i\omega\tau_t}}{1 - 2(1 - \tau_t/\tau_s)e^{i\omega\tau_t} \cos(\omega\tau_t) + (1 - \tau_t/\tau_s)^2 e^{i2\omega\tau_t}} \right) \quad (\text{B.16})$$

The transfer function simplifies at low gravitational wave frequencies, $f < 1/4\pi\tau_t$, and for optimal source direction ($\theta = \phi = 0$) and polarization ($\Omega = 0$). For this case it is

$$\frac{\phi}{h}(f) \approx \left(\frac{8\pi c\tau_s}{\lambda} \right) \frac{1}{(1 + (2\omega\tau_s)^2)^{1/2}}. \quad (\text{B.17})$$

At other angles of incidence the angular dependence of the interferometer is primarily determined by $G_{xx} - G_{yy}$.

Figure B-2 shows the amplitude response of an interferometric gravitational-wave detector as a function of the propagation direction of the wave relative to the plane of the detector. The response has been averaged over the wave polarization angle (Ω).

3. Basic Optical Concepts and RF Phase Modulation.

In this section a rudimentary description of the basic optical concepts of an interferometer, such as that shown in Section III, Figure III-1, is given. The analysis makes many simplifying assumptions, the most important being that only a single mode and polarization of the light are considered. The Fabry-Perot cavities are assumed to be close enough to resonance that their phase response can be linearized, and the RF modulation has small enough amplitude that it too can be linearized.

The analysis is intended to show the steps involved in the propagation of the optical wave field from the beam splitter, through the RF phase modulators, reflection from the Fabry-Perot cavities, to recombination at the second encounter with the beam splitter, and finally to the photodiode at the antisymmetric port of the interferometer, which monitors the output signal of the system.

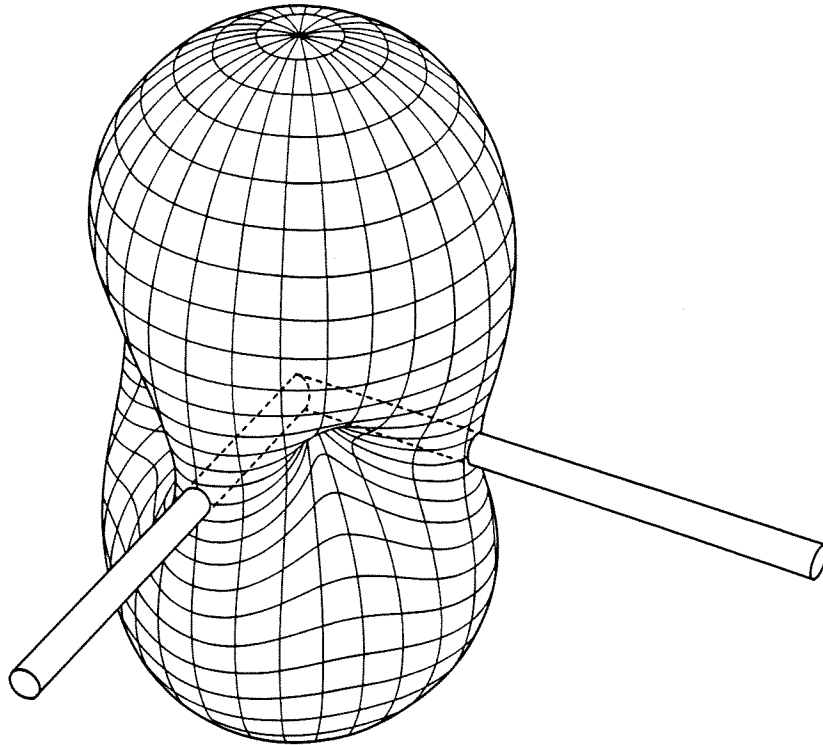


Figure B-2 The angular response pattern of an interferometer with orthogonal arms to unpolarized gravitational radiation. The tubes penetrating the response pattern surface represent the interferometer arms.

The time dependence of the input light at the beam splitter is given by

$$E = E_0 e^{-i\omega t}. \quad (\text{B.18})$$

The two waves leaving the beam splitter are

$$\begin{aligned} E_{10} &= r_s E && \text{the wave launched into arm 1,} \\ E_{20} &= t_s E && \text{the wave launched into arm 2,} \end{aligned} \quad (\text{B.19})$$

where t_s and r_s are the transmission and reflection coefficients of the beam splitter. The two waves next pass through optical phase modulators which are crystals with the property that their optical index of refraction is linearly proportional to an applied modulating field (Pockels effect). The modulating field is chosen to be at a radio frequency (RF), ω_m , sufficiently high that the laser amplitude noise and the noise in the photodetection circuitry at this frequency are close to fundamental limits. The phase modulation adds a time dependent phase to the optical beams given by

$$\phi(t) = \pm \Gamma \sin(\omega_m t), \quad (\text{B.20})$$

where the + sign is used in arm 1 and the - sign in arm 2. The wave fields after the phase modulator are

$$\begin{aligned} E_{11} &= E_0 r_s e^{i(\Gamma \sin(\omega_m t))} e^{-i(\omega t - \delta_{11})} \\ E_{21} &= E_0 t_s e^{-i(\Gamma \sin(\omega_m t))} e^{-i(\omega t - \delta_{21})} \end{aligned} \quad (\text{B.21})$$

in arms 1 and 2, respectively.

The complex exponentials with sinusoidal arguments are most conveniently expanded in terms of Bessel functions of the first kind

$$e^{i\Gamma \sin(\omega_m t)} = \sum_{n=-\infty}^{\infty} J_n(\Gamma) e^{in\omega_m t} \approx J_0(\Gamma) + J_1(\Gamma) (e^{i\omega_m t} - e^{-i\omega_m t}) + \dots \quad (\text{B.22})$$

This expansion explicitly expresses the phase modulation in terms of a set of sidebands of the main optical carrier wave. This is a useful representation with which to calculate the reflection from the Fabry-Perot cavities and is shown graphically in Figure B-3.

To first order in the modulation, the waves incident on the Fabry-Perot cavities are rewritten as

$$\begin{aligned} E_{12} &= E_0 r_s [J_0(\Gamma) + J_1(\Gamma) (e^{i\omega_m t} - e^{-i\omega_m t})] e^{-i(\omega t - \delta_{12})} \\ E_{22} &= E_0 t_s [J_0(\Gamma) - J_1(\Gamma) (e^{i\omega_m t} - e^{-i\omega_m t})] e^{-i(\omega t - \delta_{22})}, \end{aligned} \quad (\text{B.23})$$

in arms 1 and 2, respectively.

The reflection coefficients of the cavities given by Equation (B.3) are rewritten in terms of an amplitude and phase

$$r_j = A_j(\omega_j, \omega_l) e^{i\phi_j(\omega_j, \omega_l)} \quad (\text{B.24})$$

The index j takes on the value 1 or 2 indicating the cavity, ω_j is the resonance frequency of the cavity and ω_l is the frequency of the light. The gravitational wave affects the phases ϕ_j .

The waves after reflection from the cavities become

$$\begin{aligned} E_{13} &= E_0 r_s \left[J_0(\Gamma) A_1(\omega_1, \omega) e^{i\phi_1(\omega_1, \omega)} + J_1(\Gamma) \right. \\ &\quad \times \left(A_1(\omega_1, \omega + \omega_m) e^{i\phi_1(\omega_1, \omega + \omega_m)} e^{i(\omega_m t + \delta_{1+})} \right. \\ &\quad \left. \left. - A_1(\omega_1, \omega - \omega_m) e^{i\phi_1(\omega_1, \omega - \omega_m)} e^{-i(\omega_m t - \delta_{1-})} \right) \right] e^{-i(\omega t - \delta_{13})} \end{aligned} \quad (\text{B.25})$$

in arm 1 and

$$\begin{aligned} E_{23} &= E_0 t_s \left[J_0(\Gamma) A_2(\omega_2, \omega) e^{i\phi_2(\omega_2, \omega)} - J_1(\Gamma) \right. \\ &\quad \times \left(A_1(\omega_2, \omega + \omega_m) e^{i\phi_2(\omega_2, \omega + \omega_m)} e^{i(\omega_m t + \delta_{2+})} \right. \\ &\quad \left. \left. - A_2(\omega_2, \omega - \omega_m) e^{i\phi_2(\omega_2, \omega - \omega_m)} e^{-i(\omega_m t - \delta_{2-})} \right) \right] e^{-i(\omega t - \delta_{23})} \end{aligned} \quad (\text{B.26})$$

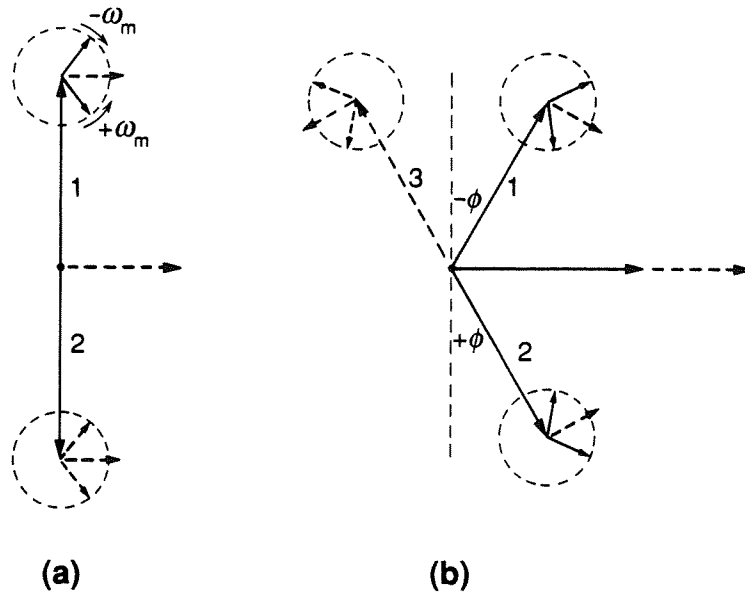


Figure B-3 Phasor diagrams for the optical fields returned by the two cavities of a Fabry-Perot interferometer, drawn in a reference system rotating at the average optical frequency, ω . The labels 1, 2, and 3 each denote a field complex composed of a stationary component (the long vectors), corresponding to a main optical field, and components rotating at $\pm\omega_m$ (the short vectors), which correspond to phase modulation sidebands. In (a) the field at the antisymmetric port is shown when cavities 1 and 2 are on resonance. The resultant field (sum of 1 and 2) is a small oscillating field due to the modulation (the dashed line). The intensity in this case has a small average value and a component at $2\omega_m$ but no component at ω_m . In (b), the interaction with a gravitational wave, produces opposing phase shifts in the two arms of the interferometer, each with magnitude ϕ . The resultant of the fields 1 and 2 is the total field at the antisymmetric output, which has both an average value (the solid line) and an oscillating component (the dashed line). The intensity now includes a term proportional to ϕ at ω_m . An additional set of vectors, labelled 3, depicts the field from arm 2 that appears at the symmetric port. The resultant of 1 and 3 is the total field at the symmetric port. When $\phi \approx 0$, the resultant field is approximately equal to the input field without modulation. This is the field that gets recycled.

in arm 2. Here δ_{1+}, δ_{1-} (or δ_{2+}, δ_{2-}) are small phase shifts that depend on the sum and difference modulation frequencies, respectively, for cavity 1 (or cavity 2).

After reflection from the cavities the waves are recombined at the beam splitter. The wave leaving the antisymmetric port of the splitter, given by $E_{\text{anti}} = t_s E_{13} - r_s E_{23}$ is detected on the output photodetector. The wave leaving the symmetric port of the splitter, given by $E_{\text{sym}} = r_s E_{13} + t_s E_{23}$ returns to the recycling mirror or laser depending on the interferometer configuration.

When the Fabry-Perot cavities are operated close to resonance, $\omega \approx \omega_j$, the reflected wave at the main optical carrier of frequency ω suffers a phase shift of $\pi \pm \phi$ (refer to Figure B-1). Here ϕ is the phase shift due to the gravitational wave; the

+ sign is associated with one cavity and the - sign with the other. The phase shift is first-order insensitive to the losses in the cavities but the reflection amplitudes at resonance are first-order sensitive to the cavity losses. The reflection amplitudes at resonance may be expressed as $A_1(\omega_1, \omega) = A_0(1 + \Delta)$, $A_2(\omega_2, \omega) = A_0(1 - \Delta)$, where A_0 is the average reflection amplitude of the two cavities at resonance and 2Δ is their difference due to any asymmetries in the cavities. The RF frequency, ω_m , is usually chosen so that the optical sidebands fall outside the cavity resonances. Then the cavity's input mirror reflects the sidebands with $A_j(\omega_j, \omega \pm \omega_m) \approx 1$ and $\phi_j(\omega_j, \omega \pm \omega_m) \ll 1$. The propagation phase shifts for the sidebands, $\delta_{k\pm}$, are assumed close to multiples of 2π , which is accomplished by a proper choice of ω_m knowing the path lengths in the interferometer.

With these assumptions the wave fields at the antisymmetric and symmetric ports become

$$\begin{aligned}
E_{\text{anti}} &= -2\sqrt{RT}E_0 \left[J_0(\Gamma)A_0(i \sin \phi + \Delta \cos \phi) - 2iJ_1(\Gamma) \sin \omega_m t \right] \\
E_{\text{sym}} &= -E_0 \left[J_0(\Gamma)A_0(\cos \phi((R + T) + \Delta(R - T)) \right. \\
&\quad \left. + i \sin \phi((R - T) + \Delta(R + T))) \right. \\
&\quad \left. - 2iJ_1(\Gamma)(R - T) \sin \omega_m t \right]
\end{aligned} \tag{B.27}$$

where $R = r_s^2$ and $T = t_s^2$ are the intensity reflection and transmission of the beam splitter. These fields are shown in Figure B-3. Terms that oscillate at the modulation frequency are shown with dashed lines.

The intensity is proportional to the envelope of the field given by $I = |E|^2$. The intensity at the output photodetector (antisymmetric port) becomes

$$\begin{aligned}
I_{\text{anti}}(t) &= 4RTE_0^2 \left[J_0^2(\Gamma)A_0^2(\sin^2 \phi + \Delta^2 \cos^2 \phi) + 2J_1^2(\Gamma) \right. \\
&\quad \left. + \text{higher order time independent terms} \right] \\
&\quad - 4RTE_0^2 \left[4J_0(\Gamma)J_1(\Gamma)A_0 \sin \phi \sin \omega_m t - 2J_1^2(\Gamma) \cos 2\omega_m t \right. \\
&\quad \left. + \text{higher order time dependent terms.} \right]
\end{aligned} \tag{B.28}$$

The interferometer output signal is the term associated with $\sin \omega_m t$, which after synchronous demodulation and for $\phi < 1$ is linearly proportional to ϕ , the gravitational wave induced phase shift. The time independent terms make up the background light on the photodetector. They are important in estimating the interferometer's photon shot noise limit. In a completely balanced interferometer with perfect contrast, $\Delta = 0$, the average background intensity becomes $2A_0^2 RTE_0^2(1 - J_0(2\Gamma))$ when $\phi = 0$. The small average intensity remaining in the dark fringe is then entirely due to the modulation: for $\Gamma \ll 1$, it is¹ $2A_0^2 RTE_0^2 \Gamma^2$.

¹ For small values of Γ the first two Bessel functions of the first kind are $J_0(\Gamma) \approx 1 - \Gamma^2/4$ and $J_1(\Gamma) \approx \Gamma/2$.

The intensity leaving the symmetric port becomes

$$\begin{aligned}
I_{\text{sym}} = & E_0^2 \left[J_0^2(\Gamma) A_0^2 \left(\cos^2 \phi ((R + T) + \Delta(R - T))^2 \right. \right. \\
& + \sin^2 \phi ((R - T) + \Delta(R + T))^2 \left. \right) \\
& + J_1^2(\Gamma) (R - T)^2 \\
& - 4J_0(\Gamma) J_1(\Gamma) A_0 \sin \phi (R - T) ((R - T) + \Delta(R + T)) \sin \omega_m t \\
& - 2J_1^2(\Gamma) (R - T)^2 \sin 2\omega_m t \\
& \left. + \text{higher order terms} \right] \tag{B.29}
\end{aligned}$$

To first order in Γ in the limit where the interferometer is symmetric, ($R = T = 0.5$, $\Delta = 0$, $\phi = 0$), the intensity leaving the symmetric port is $E_0^2 J_0^2(\Gamma) A_0^2$. This is just the input intensity degraded by the cavity loss and a small loss due to the modulation. This intensity is first-order insensitive to the modulation frequency and the gravitational-wave-induced phase shift ϕ . Figure B-3 shows this geometrically.

4. The Physical Basis of Some of the Noise Terms.

In this section we discuss the photon shot noise, the effect of laser frequency noise, the fluctuations in the forward scattering of the residual gas, the thermal noise, and the optical radiation pressure fluctuations that enforce the standard quantum limit. Seismic noise is discussed separately in Appendix D and fluctuating Newtonian gravitational field gradients are calculated in Reference [B-6].

a. Photon shot noise. Photon shot noise, which can be thought of as due to the counting statistics of the photons, dominates the estimated noise budget at high frequencies. The uncertainty in the optical phase and the uncertainty in the number of photons in a specific state of the radiation field are related by the electromagnetic uncertainty relation $\Delta\phi\Delta n > 1$. In the coherent state of single-mode laser light, the photons have a Poisson distribution: $\Delta n = \sqrt{\langle n \rangle}$. The amplitude spectral density of the photon "current" at frequency f is given by

$$\frac{dn}{dt}(f) = \left(2 \left\langle \frac{\delta n}{\delta t} \right\rangle \right)^{1/2} \tag{B.30}$$

The resultant phase fluctuations, expressed as an optical phase amplitude density at the antisymmetric output of the interferometer, is given by

$$\tilde{\phi}_n(f) = \left(\frac{2hc}{\lambda\eta\epsilon P(1 - L_{\text{opt}})G_R} \right)^{1/2} \tag{B.31}$$

Here η =detector quantum efficiency, ϵ =optical efficiency of the entire optical train, P =laser optical power, L_{opt} =total optical loss $\geq 4Ac\tau_s/L$, A =average loss per

mirror, G_R =broad-band recycling power gain $\leq 1/L_{\text{opt}}$ ($G_R = 1$ for no recycling), λ =optical wavelength, h =Planck's constant.

The interferometer's shot noise limited sensitivity expressed as an equivalent gravitational wave strain amplitude, is given from Equations (B.17) and (B.31) by

$$\tilde{h}(f) = \tilde{\phi}_n(f) \left[\frac{\phi}{h}(f) \right]^{-1} \quad (\text{B.32})$$

For a Fabry-Perot interferometer without recycling this becomes

$$\tilde{h}(f) = f_0 \left(\frac{2 h \lambda}{\eta \epsilon P (1 - L_{\text{opt}}) c} \right)^{1/2} [1 + (f/f_0)^2]^{1/2}. \quad (\text{B.33})$$

where $f_0 = 1/4\pi\tau_s$, and τ_s is the light's energy-storage time for each arm's cavity. This result includes a factor of 2 for recovery of the phase information from the RF modulation techniques used in a practical interferometer. The shot noise contribution becomes independent of the storage time at gravitational wave frequencies greater than f_0 , so there is no penalty in using large storage times.

For broad-band recycling, under the optimum assumption that all the optical loss in the system is due to the loss in the cavity mirrors, the shot noise limit is

$$\tilde{h}(f) = f_0^{1/2} \left(\frac{cA}{\pi L} \right)^{1/2} \left(\frac{2 h \lambda}{\eta \epsilon P (1 - L_{\text{opt}}) c} \right)^{1/2} [1 + (f/f_0)^2]^{1/2}. \quad (\text{B.34})$$

In a broad-band recycled system the sensitivity is optimized at a frequency f by choosing the storage time so that $\tau_s = 1/4\pi f$, i.e. so that $f = f_0$.

b. Frequency fluctuations of the laser. Fluctuations in the frequency of the laser can contribute to the interferometer's phase noise in two ways: (i) Frequency fluctuations can couple to a difference in the storage times of the two Fabry-Perot cavities to produce a gravitational-strain noise $\tilde{h}(f) = \tilde{\nu}(f)\Delta\tau/\nu\tau$, where $\tilde{\nu}(f)$ = amplitude spectrum of frequency fluctuations, ν = laser frequency, $\Delta\tau/\tau$ = fractional storage-time unbalance of the two cavities. This noise can be reduced by electronically differencing the cavity locking signals and the antisymmetric output, since frequency noise is common to them. (ii) Frequency noise can introduce relative phase fluctuations between the main beam in a cavity and scattered-light beams, thereby enhancing scattered-light noise. Methods for controlling this are discussed in Appendix F.

c. Noise from the residual gas. The residual gas can produce mechanical noise in the interferometer by damping the suspensions (see below) and by producing acoustic coupling to the outside world. This mechanical noise will be reduced to a negligible level in the LIGO by operating at pressures less than 10^{-6} torr. More serious are fluctuations in forward scattering of light by residual gas in the beam

tubes. The gravitational wave noise due to fluctuations in scattering is calculated by determining the overlap of the forward scattered fields of each molecule in the beam with the main field mode at the photodetector. The scattered field of the individual molecules appears as pulses with different amplitudes and pulse lengths depending on the molecule's position and velocity transverse to the main beam axis. The power spectrum of these pulses, when averaged over all the molecules residing in the beam with a Maxwell distribution of molecular speeds, gives a gravitational-phase noise of

$$\tilde{h}_{\text{total}}(f) = \frac{2^{5/2} \pi^{5/4} \alpha (\omega_{\text{opt}}) \rho_{\#}^{1/2}}{b^{1/2} v_0^{1/2} \lambda^{1/4} L^{3/4}} e^{-\sqrt{2\pi} f(\lambda L)^{1/2}/v_0}. \quad (\text{B.35})$$

This expression assumes that the optical beam radius is the minimum allowed by the length L of an interferometer arm. In this expression α is the polarizability of the residual gas molecule at the optical frequency ω_{opt} , $\rho_{\#}$ is the average number of molecules per unit volume, v_0 is the average thermal velocity of the molecule, λ is the wavelength of the light and b is the number of light beams (for a Fabry-Perot interferometer, $b = 1$). Figure B-4 shows the numerical results for various gas species.

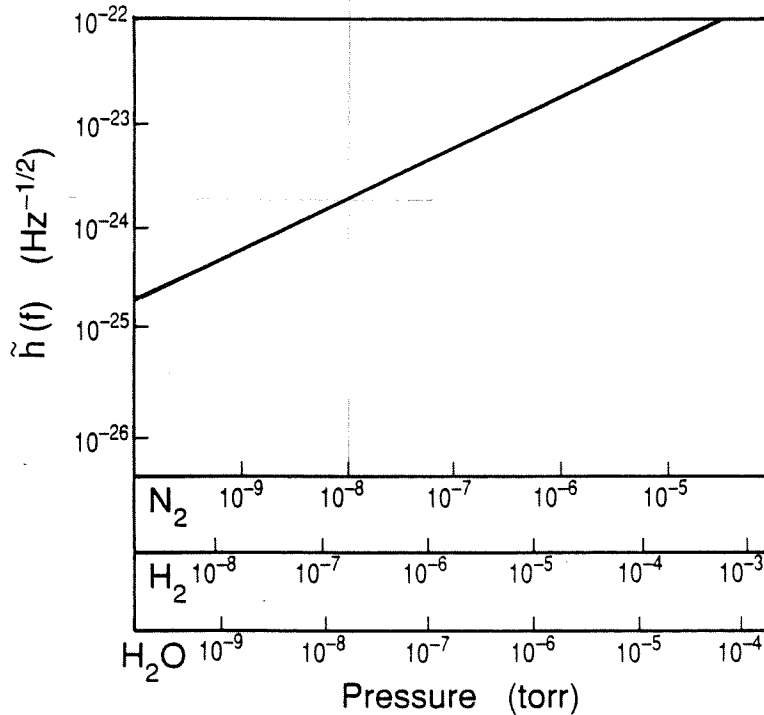


Figure B-4 Noise due to statistical fluctuations in the index of refraction of the residual gas in the LIGO beam tubes, expressed as an equivalent gravitational-wave strain amplitude spectral density $\tilde{h}(f)$. This noise is nearly independent of frequency over the LIGO's frequency band. The contribution to $\tilde{h}(f)$ is plotted as a function of partial pressure for various gas species.

d. Thermal noise. The fluctuation-dissipation theorem of statistical mechanics [B-3] asserts that the damping mechanism in a physical system produces thermally-driven random fluctuations in the system's modes of motion. The theorem is easy to understand in the case of the damping of a mechanical system by residual gas. The damping mechanism is the coherent transfer of momentum from the moving object to the residual gas particles (Doppler friction), while the fluctuations are imparted to the object by the random impacts of the residual gas particles, which are thermalized at temperature T .

The residual gas in the LIGO is specified to be low enough so that it does not contribute to the dissipation of the LIGO's mechanical elements (mirrors, masses, beam splitters, ...). The principal sources of thermal noise are expected to be dissipation in the flexure of the suspension support elements and the internal dissipation of the normal modes of the cavity mirrors.

Thermal noise in a mechanical system can be expressed as

$$F^2(f) = 4kT\alpha(f) \quad \text{dynes}^2/\text{Hz}. \quad (\text{B.36})$$

Here $\alpha(f)$ is the coherent damping coefficient (dynes sec/cm) of the mechanical system when driven at a frequency f .

The spectral representation $F^2(f)$ of the thermal noise is useful in estimating the displacement noise in the mechanical elements of the interferometer at all frequencies, providing $\alpha(f)$ is known. The frequency dependence of $\alpha(f)$ depends on the damping mechanism. Generally the resonances in the mechanical elements are chosen to be outside of the LIGO's gravitational wave band: the suspensions are designed to have resonances below that band, while the internal resonant modes of the optical components have resonances above it. By modeling the mechanical modes of an element as harmonic oscillators driven by the force spectral density, one computes for the spectral density of the displacement noise in a mode

$$x^2(f) = \frac{4kT\alpha(f)}{m^2((\omega_0^2 - \omega^2)^2 + (\frac{\alpha(f)\omega}{m})^2)} \quad (\text{B.37})$$

$$x^2(f \gg f_0) \approx \frac{4kT\alpha(f)}{m^2\omega^4} \rightarrow \frac{4kT\omega_0}{mQ\omega^4} \quad \text{if } \alpha(f) = \alpha(f_0), \quad (\text{B.38})$$

$$x^2(f \ll f_0) \approx \frac{4kT\alpha(f)}{m^2\omega_0^4} \rightarrow \frac{4kT}{mQ\omega_0^3} \quad \text{if } \alpha(f) = \alpha(f_0), \quad (\text{B.39})$$

where $Q = m\omega_0/\alpha(f_0) =$ oscillator quality factor, $m =$ the mode's effective mass, $\omega_0 = 2\pi f_0 =$ the mode's resonance frequency.

In estimating the equivalent gravitational-strain noise due to the thermal noise from several elements, assumed uncorrelated, the noise power is summed

$$h^2(f) = \frac{\sum_{n=1}^m x^2(f)}{L^2} \quad (\text{B.40})$$

Several subtleties arise in estimating the thermal noise: (i) As indicated, the damping can be frequency dependent so that a simple measurement of the Q of an oscillator is not sufficient to predict the thermal noise off resonance. (ii) In an oscillator under the influence of several restoring mechanisms, such as in a pendulum where both gravity and the elasticity of the suspension fibers apply restoring forces, the Q of the entire mechanical system can be much larger than the intrinsic Q of the suspension fiber material. The Q of the pendulum is larger than the Q of the suspension material by the ratio of the energy stored in the gravitational field to that stored in the elastic deformation of the fiber. (iii) Estimates of the equivalent gravitational-wave strain due to thermal excitation of the normal modes of the test masses and mirrors depend on the overlap integral of the optical mode shape with the mechanical mode of the mass. The test masses and mirrors in the gravitational wave interferometer will usually be cylinders. The modal frequencies and shapes for cylinders with radii comparable to their height have been studied extensively [B-4]. The most perturbative modes are those that cause a net phase shift over a large part of the optical wavefront and are at the lowest frequencies. The lower order flexural modes tend to increase in frequency with cylinder height, while the longitudinal-mode frequencies decrease. Cylinders with ratio of height to radius between 1 to 2 give the best compromise. The modal frequencies are given by $f = \Lambda v_s/a$, where Λ is usually an eigenvalue between 1 and 5, v_s is the shear speed of sound in the material, and a is the radius.

e. Radiation-pressure noise and the standard quantum limit. The laser light, through the momentum it carries, imparts forces to the optical components of the interferometer. Fluctuations in the laser intensity introduce random forces on the cavity mirrors. The intensity fluctuations are symmetric between the two arms of the interferometer so that the resulting noise, which affects the gravitational-wave measurement, cancels except for the mechanical and optical unbalance of the two interferometer arms. The noise due to this source is not expected to be a major factor in the initial LIGO interferometer but will have to be considered in the advanced interferometers in which it may be necessary to amplitude stabilize the laser light by feedback techniques in the gravitational-wave band.

In addition to these symmetric radiation pressure fluctuations, there are pressure fluctuations antisymmetric between the two arms. These are produced by a superposition of the main beam's electromagnetic field and quantum electrodynamic vacuum fluctuations that enter the interferometer through the dark side of the beam splitter [B-5]. These pressure fluctuations are one source of the "standard quantum" limit for the interferometric gravitational-wave detector and are a macroscopic example of the "Heisenberg microscope." Because the fluctuating radiation pressure is proportional to the correlated product of the vacuum field and the laser field, it varies as the square root of the laser power and fluctuates on time scales of the cavity storage time, a characteristic time for the vacuum electric-field fluctuations to change phase by π relative to the laser field.

Following this model, the rms fluctuating differential force on the pair of mirrors in one cavity is

$$\Delta F = \sqrt{\langle N \rangle} \left[\frac{h\nu}{L} \right] \quad (\text{B.41})$$

where $\langle N \rangle$ is the average number of quanta stored in the cavity mode and L is the cavity length. The spectral density of the fluctuating force is determined from

$$(\Delta F)^2 = \int_0^{1/2\tau} F^2(f) df,$$

where

$$F^2(f) = 2\tau(\Delta F)^2 = 2\tau \langle N \rangle \left(\frac{h\nu}{L} \right)^2,$$

$$\tau \approx \frac{2L}{cT},$$

$$F^2(f) = \frac{4 \langle N \rangle (h\nu)^2}{cTL}, \quad (\text{B.42})$$

and we assume negligible losses in the cavity's central mirror, $A \ll T$. Assuming that the mirror masses, m , can be considered free, the force produces a differential motion $x(f) \approx F(f)/m\omega^2$. The average number of quanta in the mode and the laser power are related by

$$\langle N \rangle = \frac{2LP_{\text{in}}}{cTh\nu}, \quad (\text{B.43})$$

$$P_{\text{in}} = \frac{\epsilon_{\text{opt}} P_{\text{laser}}}{2}, \quad (\text{B.44})$$

where it is assumed that the beam splitter divides the input power evenly between the two cavities. Finally, the equivalent gravitational-strain noise induced in both cavities is

$$\begin{aligned} \tilde{h}(f)_{\text{pressure}} &= \frac{\sqrt{2}x(f)}{L} \\ &= \frac{4(\epsilon_{\text{opt}} P_{\text{laser}} h\nu)^{1/2}}{cTLm\omega^2} \end{aligned} \quad (\text{B.45})$$

The sensing noise (shot noise) in the detection of the interferometer fringe at low frequencies is

$$\tilde{h}(f)_{\text{sense}} = \frac{T}{8\pi L} \left(\frac{h\lambda c}{\eta\epsilon_{\text{opt}} P_{\text{laser}}} \right)^{1/2}. \quad (\text{B.46})$$

The total noise of the interferometer if only due to optical field fluctuations is the incoherent sum

$$h^2(f) = h_{\text{pressure}}^2(f) + h_{\text{sense}}^2(f). \quad (\text{B.47})$$

Since the radiation pressure noise power varies directly as the laser power, while the sensing noise varies inversely as the laser power, there is a minimum in the total noise at a specific, optimum laser power given by

$$\begin{aligned} P_{\text{opt}} &= \frac{T^2 \lambda m c \omega^2}{32 \pi \epsilon_{\text{opt}} \eta^{1/2}} \\ &= \frac{L^2 \lambda m \omega^4}{2 \pi \epsilon_{\text{opt}} c \eta^{1/2}}. \end{aligned} \quad (\text{B.48})$$

The lower equation reexpresses the optimum input power in terms of the optimum cavity input mirror transmission for a gravitational wave frequency at $\omega = 2\pi f$. This is given by $T_{\text{opt}} = 4L\omega/c$. One contribution to the standard quantum limit for an interferometric detector at a gravitational-wave frequency f is the net pressure and sensing noise at the optimized power with photodetector efficiency $\eta = 1$. The quantum limit is actually $\sqrt{2}$ larger than that net noise, because of a contribution from the uncertainty principle associated with the center-of-mass motion of the mirrors [B-5]:

$$\tilde{h}(f)_{\text{QL}} = \sqrt{4/\pi} \left(\frac{\hbar}{m} \right)^{1/2} \frac{1}{2\pi f L} \quad (\text{B.49})$$

This noise is shown in Section V, Figure V-3 for the initial LIGO interferometer and Figure V-4 for an advanced detector. The quantum noise is not a factor in the initial interferometers but it does set a fundamental limit to the technique and is one of the reasons along with all other sources of random forces that argues for a large arm length L .

There are methods, in principle, for circumventing the standard quantum limit in interferometers but it is not at all clear whether these methods can be realized in practice.

References

- B-1. See, e.g., J.-Y. Vinet, B. Meers, C. N. Man, and A. Brillet, *Physical Review D* **38**, 433 (1988), and references cited therein.
- B-2. See, e.g., L. D. Landau and E. M. Lifschitz, *The Classical Theory of Fields* (Pergamon Press, Oxford, 1962); or C. W. Misner, K. S. Thorne, and J. A. Wheeler, *Gravitation* (W.H. Freeman, San Francisco, 1973).
- B-3. F. Reif, *Fundamentals of Statistical and Thermal Physics* (McGraw-Hill, New York, 1965).
- B-4. J. Hutchinson, *Journal of Applied Mechanics* **47**, 901, (1980); G. McMahon, *Journal of the Acoustical Society of America* **36**, 85, (1964).
- B-5. C. M. Caves, *Physical Review D*, **23**, 1693 (1981).
- B-6. P. R. Saulson, *Physical Review D*, **30**, 643 (1984).

APPENDIX C

CONCEPTS FOR ADVANCED INTERFEROMETERS

1. Introduction

In Section V.B., "Evolution of LIGO Interferometers," we discussed a set of long-range scientific objectives for the LIGO that are based on our current view of the directions in which gravitational-wave physics and astrophysics may develop from LIGO's initial stages. In this appendix we present some of the technical concepts that have been proposed to attain these long-range objectives. The specific plan and emphasis of the research towards these objectives will be strongly influenced by the scientific results and technical experience gained with the initial LIGO interferometer and the prototypes; and also by new interferometer concepts, as they emerge.

2. Review of the Initial LIGO Interferometers

To help clarify the concepts underlying the developing sequence of interferometer designs, we first review the operation of the initial interferometers and then discuss some proposed developments. The initial interferometers will be broadband, Fabry-Perot interferometers [C-1] designed for operation with recycling of light. Initial testing will be done during installation, with the recycling mirror temporarily moved out of the optical train. We begin by reviewing operation in this non-recycling mode.

a. The basic interferometer: non-recycling mode of operation. A simplified diagram of the initial interferometer in the non-recycling mode is given in Figure C-1. The laser frequency is stabilized to a separate reference cavity (not shown) and is in resonance with the main 4-km cavities. Monochromatic light from the laser passes, via a 50% beam splitter, through two phase modulators, PM1 and PM2, which are driven in antiphase by a radio-frequency source, to the main cavities. The distant end mirrors of the two cavities have the highest possible reflectivity (about 99.995%). The input mirrors have lower reflectivity, to give a transmission that makes the storage time of light within each cavity comparable to the period of the gravitational waves to be studied. A typical transmission could be about 1%, with scattering and absorption losses much smaller (total loss on the order of 0.005%). When the cavity length is an integral multiple of a half-wavelength of the light there is a large resonant buildup of light intensity within each cavity.

If losses are negligible, the cavity light (labeled C1 and C2) passing back out through the input mirror of each arm has an equilibrium amplitude equal to twice the amplitude of the light coming to the cavity from the laser. It has opposite phase to that of the light (labeled F1 and F2) externally reflected by the front mirror, so interference between the C and F light types leaving each front mirror would give a resultant reflected beam equal in intensity to that of the incident beam.

However, the light within the cavity has traveled back and forth many times (about 100 times, if the transmission is 1%) so any change in cavity length gives a change in optical path, and thence in phase, for the light emerging from the front mirror that is increased (by about 100 times). A gravitational wave that causes the length of one cavity to increase and that of the other to decrease will give phase changes of opposite sign in the light emerging from the two cavities; this difference is detected by the photodiode, D1, after the beams have been brought into interference with one another by the beam splitter [C-2].

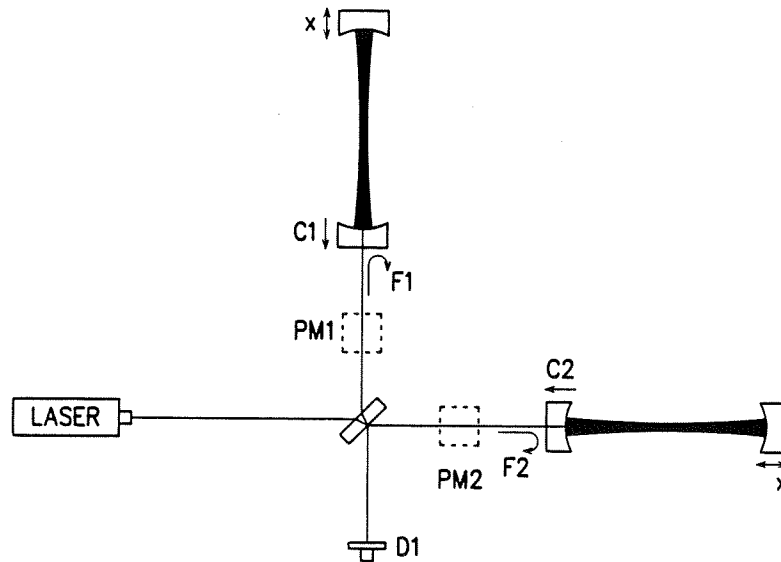


Figure C-1 Schematic diagram of a Fabry-Perot interferometer without recycling. PM1 and PM2 refer to modulation functions that are accomplished either by in-line Pockels cells or Pockels cells in side arms. F1 and F2 denote the wave components arising from direct reflection from the cavity input mirrors. C1 and C2 denote the wave components which arise from leakage of stored light from inside the cavities.

In operation, the distances between the input cavity mirrors and the beam splitter are controlled so that in the absence of a gravitational wave (or of any phase modulation), the light components from the two cavities will destructively interfere with the beam traveling to the photodiode. (The photodiode is at a "dark fringe" that is perhaps at 0.1 percent of the intensity of the input beam). A radio-frequency-modulation technique is used to enhance the sensitivity and linearity of the final phase-difference measurement. Two optical-phase modulators, labeled PM1 and PM2, are driven in antiphase at a frequency near 12 MHz. Any small additional phase deviation between the beams C1 and C2 modifies the symmetry of the intensity waveform at the photodiode, resulting in a signal that is proportional to the phase deviation and has the same frequency as the modulation. The signal is detected by coherent demodulation of the photodiode output. This technique enables the critical optical-phase measurement to be made at a frequency where

laser intensity noise is low and makes it possible to measure optical phase with a sensitivity close to the photon shot noise limit. Servo systems apply differential feedback forces to the test masses in each cavity to hold the interferometer precisely at an intensity minimum, and the feedback forces required to do this are recorded. This provides a measure of the gravitational-wave-induced forces on the test masses.

The phase modulators, PM1 and PM2, could be Pockels cells (electro-optic modulators) as used in some prototype experiments. In the LIGO interferometers, however, we will perform phase modulation at the location of PM1 and PM2 in the optical train by using a nearly transparent beam splitter to reflect a small fraction of the light into and out of an auxiliary side arm (not shown here), where the small modulation is applied by a low-power Pockels cell. This reduces losses in a critical region of the interferometer and avoids the need for Pockels cells that can accommodate the large diameter of the main beam at that point.

To give some idea of the sensitivity of this basic interferometer in non-recycling operation, we note that, for a burst search, the photon-shot-noise limit to strain sensitivity at a mean frequency f , over a bandwidth equal to f , and for optimal source direction and polarization and unity signal-to-noise ratio is given by (see Appendix B, Equation (B.33))

$$h_N = \tilde{h}(f)\sqrt{f} = \left[\frac{\pi\lambda\hbar f^3}{P\eta c} \right]^{\frac{1}{2}} \quad (\text{C.1})$$

Here, $\tilde{h}(f)$ is gravitational-wave strain sensitivity per root hertz at frequency f ; λ is the wavelength of light used; \hbar is Planck's constant/ 2π ; P is the input-light power; η is the quantum efficiency of the photodiode; and c is the velocity of light. If we take the values $f = 1$ kHz, $P = 10$ watts, $\lambda = 514$ nm, and $\eta = 1$, this gives a burst sensitivity of approximately $h_N \simeq 8 \times 10^{-21}$.

In the arrangement just outlined, the photodiode has to monitor only a very small fraction of the total light entering the system. Most of the input light emerges from the other side of the main beam splitter, where constructive interference occurs, and passes back toward the laser. Recycling [C-2] takes advantage of this otherwise wasted light.

b. The basic interferometer: recycling mode of operation. Broad-band recycling is achieved by introducing an additional mirror to return light to the interferometer, and servo controls to maintain correct phase of the recycled light. A schematic diagram of the arrangement is shown in Figure C-2.

In effect, the recycling mirror forms a large Fabry-Perot cavity with the two main cavities and the beam splitter and is arranged so that a resonant buildup of light occurs in this whole system. The technique used to maintain resonance is similar to that employed to lock the laser to a stabilizing resonant cavity [C-3] (as described in detail in Section III-B). The phase difference between light reflected back

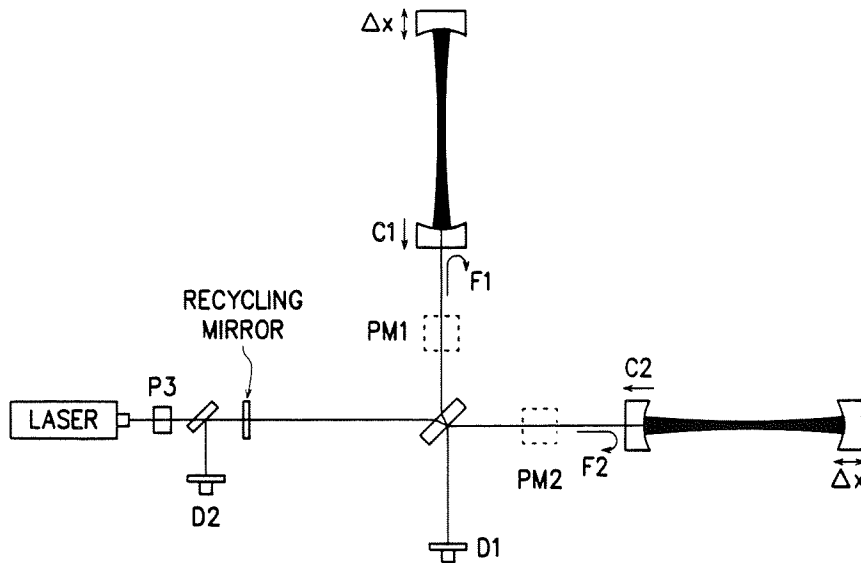


Figure C-2 Schematic diagram of a Fabry-Perot interferometer with broad-band recycling. This change is accomplished by addition of the recycling mirror and the standard modulation and detection optics used for reflection-locking the light to a cavity. Photodiode *D2* is used to monitor and correct the position of the recycling mirror.

toward the laser from the recycling mirror and light transmitted through the mirror from inside the interferometer is monitored by phase-modulating the laser light and detecting interference between the two components with a photodiode, *D2*. On resonance, the phase difference is exactly 180 degrees; this gives a minimum of intensity in the light reflected by the cavity and maximum acceptance of light by the interferometer. If the system is slightly off resonance, a signal at the modulation frequency (the frequency is in the range of 10 to 20 MHz) appears at the photodiode, and measurement of the amplitude of the photocurrent with a phase-sensitive detector gives a correction signal that moves the recycling mirror to the resonance position.

The optimum transmission of the recycling mirror is approximately equal to the total optical loss in the system. We propose to use a variable-reflectivity mirror formed from two closely spaced mirrors with adjustable separation to give partial destructive interference of the reflected light. This will aid the transition from a non-recycling mode of operation to a recycling one, as well as enable the light buildup to be measured.

The phase modulator, *P3*, used for controlling the recycling mirror can be a simple Pockels cell, because losses are less important here; lenses can be used to bring the laser beam to a convenient diameter.

The overall effect of light recycling in this interferometer is to increase the power in the interferometer and thereby improve the photon-shot noise without altering

the wide bandwidth of the system. An additional benefit is that the recycling cavity formed by the whole system will act as a narrow-band, 4-km filter and mode-cleaning cavity for the input laser light.

An estimate of the sensitivity of this type of recycling interferometer may be obtained by assuming the light storage time to be determined by the losses associated with the cavity's end mirrors (of reflectivity R). In this approximation, the burst sensitivity set by photon shot noise is given by Appendix B, Equation (B.34).

$$h_N = \tilde{h}(f)\sqrt{f} = \left[\frac{\hbar\lambda f^2(1-R)}{P\eta L} \right]^{\frac{1}{2}} \quad (\text{C.2})$$

with the same notation as used earlier. Here L is the arm length of the gravitational-wave detector. For a burst search at 1 kHz, an input power of 10 W, an output-mirror reflectivity of 0.99995, and an armlength of 4 km, the sensitivity over a 1-kHz bandwidth, at unity signal-to-noise ratio, becomes $h_N = 3 \times 10^{-22}$.

The number of recycles, and thus the potential sensitivity improvement, can be affected in practice by many factors. These include light losses in the mirrors and beam splitters, and any residual mismatch in the light wavefronts from the two cavities when the wavefronts are combined at the beam splitter. These effects have been taken into account in predicting sensitivities for this type of interferometer in Section V.

c. A resonant recycling interferometer. Another optical technique, "resonant recycling" [C-4], has been devised to obtain high shot-noise sensitivity over a narrow bandwidth. This technique has good prospects of bringing periodic signals from sources such as pulsars within range of the LIGO. It also gives optimum sensitivity in searches for a stochastic background of gravitational waves.

A simplified diagram of a version of the first proposed type of resonantly recycled interferometer is shown in Figure C-3.

The Fabry-Perot cavities are configured as in the broad-band interferometer of Figure C-1. In this system, however, the two cavities are coupled to one another by the mirror M2, which directly reflects light emerging from one cavity into the other cavity. Light from a stabilized laser passes through a 50 percent beam splitter M1 and is directed to the mirror M2 by the two paths shown. The transmission of mirror M2 is chosen to maximize buildup of light within the system formed by the two main cavities.

Mirror M2 couples the two main cavities to one another much more strongly than they are coupled to the input system. If there is a single axial-resonance mode of the same order in each cavity, then the coupling between the cavities has the effect of giving the combined system two modes of oscillation, a symmetrical one in which the light is in-phase in the two cavities, and an antisymmetrical one in which it is out of phase. The degree of coupling between the two cavities is determined by the transmission of their input mirrors, M3 and M3', and also by interference effects

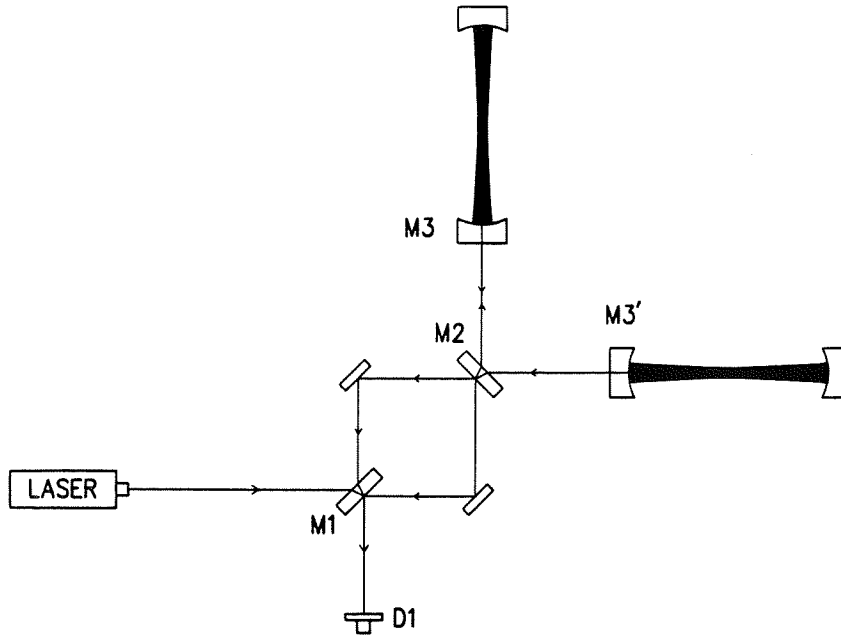


Figure C-3 A Fabry-Perot interferometer incorporating resonant recycling. The input light is divided into two beams at the beam splitter, M1, and directed into the two Fabry-Perot cavities. Light returned from the upper cavity, upon striking the recycling mirror, M2, is mostly deflected into the cavity on the right, and vice-versa. Eventually the stored light leaks out through M2, is recombined at the beam splitter and detected at photodiode D1. The modulation functions are not shown.

in the optical path between these two mirrors. In fact, the space between M3 and M3' acts as a third, shorter, optical cavity. To tune the interferometer to a known gravitational-wave frequency, the transmissions of M3 and M3', and the mirrors' spacing, are chosen so that the frequency splitting between the main symmetrical and antisymmetrical modes of the long cavities is equal to the frequency of the gravitational wave. The system is then adjusted so that the light from the laser is in resonance with the symmetrical mode of the long cavities, and a large buildup of intensity in that mode occurs.

A periodic gravitational wave incident on the system will move the cavity end mirrors and frequency modulate the cavities in such a way that some of the stored laser light is pumped into sidebands that are spaced from the laser frequency by the frequency of the gravitational wave. If one of these sideband frequencies matches an antisymmetrical resonance mode of the coupled-cavity system, there will be a buildup of this sideband component. There is thus both a resonant buildup of the laser light inside the system and also of the signal produced by the periodic gravitational wave.

In a perfectly balanced system, light at the laser frequency, traveling downward from the beam splitter, M1, should undergo complete destructive interference, so

only light from the cavities' antisymmetrical mode should emerge from that direction. That light is the interferometer's output; it is detected by photodiode D1.

This system of coupled cavities can be considered as a mechanical parametric amplifier of the laser light and as driven by the mirror motions induced by the gravitational wave. The total light-storage time in the system can approach one second, so that the buildup can extend over many cycles of the gravitational wave, and a large enhancement of sensitivity can be obtained. The photon-shot-noise-limited sensitivity is improved over that of a non-recycling interferometer by a factor approximately equal to the number of gravitational-wave periods in the light-storage time of the system. More specifically, the light-storage time in the system is determined by the maximum reflectivity, R , of the mirrors at the far ends of the cavities, the photon-shot-noise limit to sensitivity in the case of a search that extends over a measuring time $\hat{\tau}$ and is given for a periodic gravitational wave of known frequency by [C-4]

$$h_N = \left[\frac{\hbar \lambda c (1 - R)^2}{\pi P \eta L^2 \hat{\tau}} \right]^{\frac{1}{2}} \quad (\text{C.3})$$

Here h_N is the amplitude of the periodic wave for unity signal-to-noise ratio and optimal source direction and polarization; the other symbols are as defined earlier. If we take a measuring time of 10^7 seconds, a light power of 10 W, and a mirror reflectivity of 0.99995, this gives a limit to sensitivity at unity signal-to-noise ratio of $h_N \simeq 1 \times 10^{-28}$. This sensitivity is achieved over a bandwidth equal to the reciprocal of the light storage time $\Delta f \simeq (1 - R)C/2\pi L \simeq 0.6$ Hz.

This is an impressive limit to sensitivity; it should be emphasized, however, that there is an assumption that the gravitational-wave frequency is accurately known and that Doppler shift variations in this frequency that are the result of the rotation of the Earth and the motion of the Earth in its orbit are allowed for. The technique is also useful for searches for signals of unknown frequency, over a bandwidth determined by the overall interferometer storage time.

d. A dual recycling interferometer. The two resonances required for a resonant recycling interferometer could also be obtained by adding a second recycling mirror to the output of a broad-band recycling interferometer [C-5]. One possible configuration for such a "dual-recycling" system is shown in Figure C-4. A periodic gravitational wave acting on the system will generate antiphase sidebands in the two Fabry-Perot cavities, which will give an output coming downward from the beam splitter. The second recycling mirror, M4, is arranged to reflect much of this output light back in such a way that a gravitational-wave-induced sideband of the laser light resonates within the effective cavity formed by mirror M4 and the two Fabry-Perot cavities. This gives a buildup of light at both the laser frequency and a gravitational-wave sideband frequency, just as in the earlier resonant recycling system shown in Figure C-3.

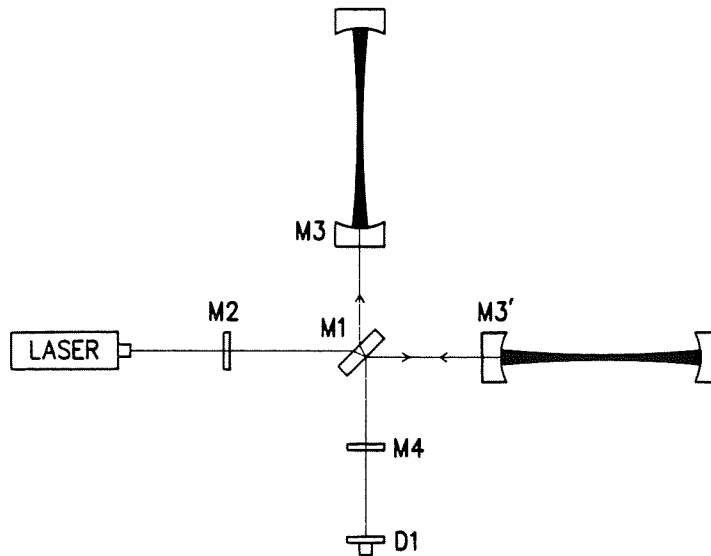


Figure C-4 A Fabry-Perot interferometer incorporating dual recycling. This configuration is identical to the broad-band recycling interferometer of Figure C-2, except for the addition of the output recycling mirror, M4.

In narrow-band operation, the maximum sensitivity of this dual-recycling system is similar to that of the standard resonant recycling configuration. The five mirrors, M1, M2, M3, M3', and M4, in Figure C-4, however, provide more flexibility in adjustment of overall response and a potentially wider bandwidth for a given sensitivity than the three corresponding mirrors, M2, M3, and M3', in Figure C-3; but the losses in the substrates may be higher.

Resonant recycling interferometers, and particularly the dual recycling configuration, are likely to have application more general than investigation of periodic signals. When adjusted for relatively broad-band response, these interferometers can be competitive with broad-band recycling systems for pulse searches, and for some pulse waveforms they can be more sensitive. Also, since reduced shot noise over a narrow bandwidth is obtainable in a resonant system, the system can give higher overall sensitivity in searches for a stochastic background of gravitational radiation (see Section V.B). Furthermore, these dual-recycling techniques are likely to be rather tolerant of optical distortions and figure errors because the exchange of light between the two interferometer arms in resonant recycling systems tends to average out some imperfections.

3. Concepts to Improve the High-frequency Sensitivity of Interferometers by Reducing Photon Shot Noise

a. Interferometer configurations for high-power operation. The mirror heating effects described in Section VIII are particularly important in advanced interferometers, which use high-power lasers and recycling to build up the power

within the main cavities to hundreds of kilowatts. The thermal distortions resulting from such high power levels may be reduced by developing low-absorption mirror coatings or by using substrate materials with higher thermal conductivity or with smaller temperature coefficients of expansion or of refractive index. It is also possible to design different optical systems that are less affected by a given heat input. We discuss such optical systems here.

i. Reduction of thermal effects in optical cavities. The relative importance of thermal expansion in the substrate and thermal lensing that results from a change of refractive index depends on the material and on the optical configuration. For a typical Fabry-Perot cavity with mirrors on fused quartz substrates and the input light passing through one of the mirrors, the lensing effect dominates over thermal expansion distortion by a factor of approximately 10. One way to avoid thermal lensing in the substrate is to arrange that no light passes through the substrate. The substrate material may then be chosen for high thermal conductivity and low expansion rather than for good optical properties, thereby further reducing thermal effects.

One way to build a cavity with nontransmitting mirrors is by use of a tilted transparent plate within the cavity as a coupling device (see Figure C-5). Light can be fed into or out of the cavity by reflection at one or both surfaces of the plate. The plate can be a thin wedge inclined to the stored beam in such a way that one surface is at Brewster's angle for (in principle) zero reflection while the other surface is at an angle chosen to give the required degree of coupling. In this arrangement, the coupling plate is free of coatings, and thermal effects in it arise only through its intrinsic absorption. The absorption may be reduced by making the plate as thin as is consistent with thermal noise arising from bending modes of vibration. Motion of the coupling plate can introduce phase noise in the output light from the cavity, although the noise amplitude is smaller than that from an equal motion of the main cavity mirrors by a factor close to the cavity finesse.

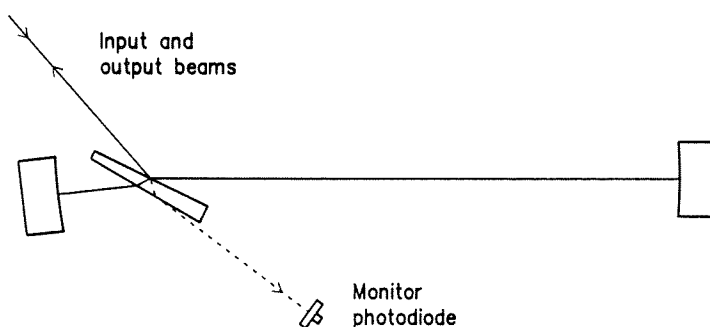


Figure C-5 Schematic of Fabry-Perot cavity with Brewster plate coupling, to avoid transmission of the input and output beams through the mirror substrates. When the cavity is resonant with the input light, a "dark fringe" appears at the photodiode and the output beam is reflected back along the input beam.

The optical action of this coupling system is slightly different from that of a partially transmitting input mirror. With the tilted plate coupler, the plate appears transparent to the input beam when the cavity is off resonance. When precisely on resonance, the plate reflects maximum light back toward the input and there is a minimum of transmitted light leaving the other side of the plate.

ii. Other heating effects in a Fabry-Perot interferometer. If cavity-heating effects are sufficiently reduced by use of tilted-plate couplers or by other means, then heating in the main beam splitter of the interferometer may become a factor limiting operating power. In a conventional symmetric beam splitter, heat absorption in the coating may give lensing and distortion effects similar to those in a cavity mirror.

One way to reduce the absorption is to make a symmetrical beam splitter by using two prisms coupled by the evanescent wave from a beam undergoing internal reflection. The distance between the coupling surfaces is of order one-tenth of the wavelength of the light and can be adjusted by piezoelectric transducers thereby varying the transmission. Beam splitters of this type have been tested by members of the LIGO team and used in interferometers by others [C-6]. By choosing the angles of the prisms so that all the light beams enter and leave the system at Brewster's angle it is possible to avoid requiring any optical coating. Heating then results only from intrinsic losses in the material. In this case, it is difficult to make the light-path length in the material as short as that in a cavity pick-off plate. However, this may not be important since the power at the beam splitter is less than that in the main cavities.

A Fabry-Perot interferometer using these techniques could operate at significantly higher power than is planned for initial LIGO interferometers and may be adequate to handle the power levels anticipated for advanced interferometers. However, if further power-handling capacity is required, enhancements are possible. For example, the cavity in each arm can be folded back and forth between large mirrors, using a configuration like that of a Herriott delay line [C-7, C-8], or of a White multireflection cell [C-9, C-10], so that the mirror heating is distributed over several reflection spots on the mirrors. This system would consume more space in the vacuum tubes than an unfolded system, but it is possible that hybrid interferometers like this may be desirable at the highest powers.

iii. Delay line interferometers. A delay-line interferometer in its simplest form can be relatively tolerant of high light power because the main cavity mirrors can be nontransmitting, and, in addition, the heat is distributed over a number of reflection spots on each mirror. Heating of the beam splitter may be the limiting factor. This system requires larger mirrors and more space in the beam tubes than a Fabry-Perot system, and it may be difficult to accommodate the optimal number of reflection spots. Use of dual recycling may make the system more compact, although this will increase the light power in the beam splitter to a level higher than that in an equivalent single-recycling delay-line or Fabry-Perot interferometer. Like the folded Fabry-Perot, this dual-recycling, delay-line system is a hybrid, incorporating

elements of both Fabry-Perot and delay-line interferometers. Both of these hybrid systems are compromises between power-handling capacity and usage of beam-tube space. If the power levels are so high that they cannot be accommodated by an unfolded Fabry-Perot, then it is likely that each of these hybrid systems could handle approximately equal light power for the same space usage, with a possible slight advantage to the Fabry-Perot that results from the less stringent demands on the beam splitter.

b. Concepts and techniques to increase the laser power

i. Coherent addition of argon-ion lasers. Coherent addition of several lasers can be used both to increase the power injected into an interferometer and to increase system reliability. In coherent addition, the primary laser is locked to a frequency-reference cavity. Any number of secondary lasers may be combined with the primary beam by adjusting their phases to match at combining beam splitters. This is accomplished by using the signal generated by the interference between the primary and secondary beams at a photodetector to control the frequency and phase of the secondary laser. The phase of the secondary laser is adjusted for destructive interference at one port while the beam emerging from the other port of the combining beam splitter constructively interferes. This combined beam has the frequency stability of the primary laser but a power equal to the sum of the two lasers. The scheme has been tested by members of the LIGO team and more extensively developed at University of Glasgow [C-11].

ii. Use of frequency-doubled Nd:YAG lasers. Frequency-doubled Nd:YAG and other solid-state lasers appear promising as future light sources for operation of LIGO interferometers. They have the potential advantage over argon-ion lasers of higher power efficiency, higher output power, and more stable operation (see Section V-B).

c. The application of “squeezed states” of light. Analyses of quantum limits in optical measurements [C-12] have shown that the statistical properties of light can be modified so as to reduce photon shot noise in an interferometer below its usual $\Delta N = \sqrt{N}$ level. The statistical fluctuations in the output of a Michelson interferometer can be regarded as arising from vacuum fluctuations that can enter the system through the normally unused path to the beam splitter. These fluctuations can be modified by injecting squeezed-vacuum light from the unused direction, in place of ordinary vacuum. (The squeezed vacuum is produced by parametrically modulating the ordinary vacuum with a nonlinear medium that is pumped by light phase-coherent with the interferometer’s laser light.) In the interferometer the squeezed vacuum superposes on the laser light in such a way as to decrease the photon shot noise in the interferometer’s output, while increasing the difference in light-pressure fluctuations in the two arms. Thus, this squeezed vacuum technique has the same effect on noise as increasing the power of the input laser.

Squeezed-light techniques show promise, but also have some limitations. Any

optical losses in the interferometer arms and in other key areas can introduce statistical fluctuations that are not reduced by the squeezing procedure and which may, in some situations, outweigh the potential gains. In particular, when narrow-band resonant and dual-recycling techniques are pushed to the limit where mirror losses prior to detection are dominant, squeezing techniques are unlikely to give any advantage. However, squeezing techniques are complimentary to broad-band recycling: in principle, the two operating together can reduce an interferometer's noise over broad bands to that of the resonant recycling envelope in Figure A-4b.

We do not plan near-term development of squeezed-light techniques in the LIGO program because the major advantages seem likely to be further in the future than do those from some of the other interferometer developments outlined above. However, expertise in squeezed-light experimental techniques exists at Caltech and MIT (H. J. Kimble and H. Haus groups); so when it becomes appropriate to develop squeezed-light interferometers for the LIGO, the team will be well positioned to do so.

4. Concepts to Improve the Low-frequency Performance

The initial LIGO interferometer will use relatively simple, passive-isolation systems effective above a few tens of Hz. Current astrophysical estimates suggest that the gravitational-wave signals that are strongest in terms of LIGO signal-to-noise ratios, are likely to occur toward the lower frequencies (see Figure A-4). The extension of operation downward in frequency is thus a major goal for the evolution of the LIGO and has had a substantial influence in the conceptual design of the facilities. We discuss here two concepts that will improve the sensitivity at lower frequencies.

a. The seismic-monitor interferometer and its developments. We plan to enhance performance at lower frequencies by adding an auxiliary interferometer [C-2] to monitor relative motions of the pendulum suspension points and, by feedback, to cause one of the points to track the longitudinal motion of the other. This arrangement is shown schematically in Figure C-6. Two unequal-arm Michelson interferometers sense relative motions of the suspension points of the test masses at the two ends of each 4-km arm. At frequencies above the 1-Hz pendulum resonance, the suspension point moves more than the suspended test mass. Therefore, even a single-bounce interferometer with relatively low-sensitivity can provide useful suspension-point signals. The signals from this interferometer will be monitored and will provide feedback to magnetic transducers driving the suspension points for the test masses that are remote from the corner station. This will reduce vibration-induced motions of the suspension points by a factor of 100 or more in the LIGO frequency range. Because of the isolating effect of the wire suspensions, reduction of this seismic noise does not affect the gravitational-wave signal as measured by the test masses.

Although the seismic interferometers shown are single-pass Michelson inter-

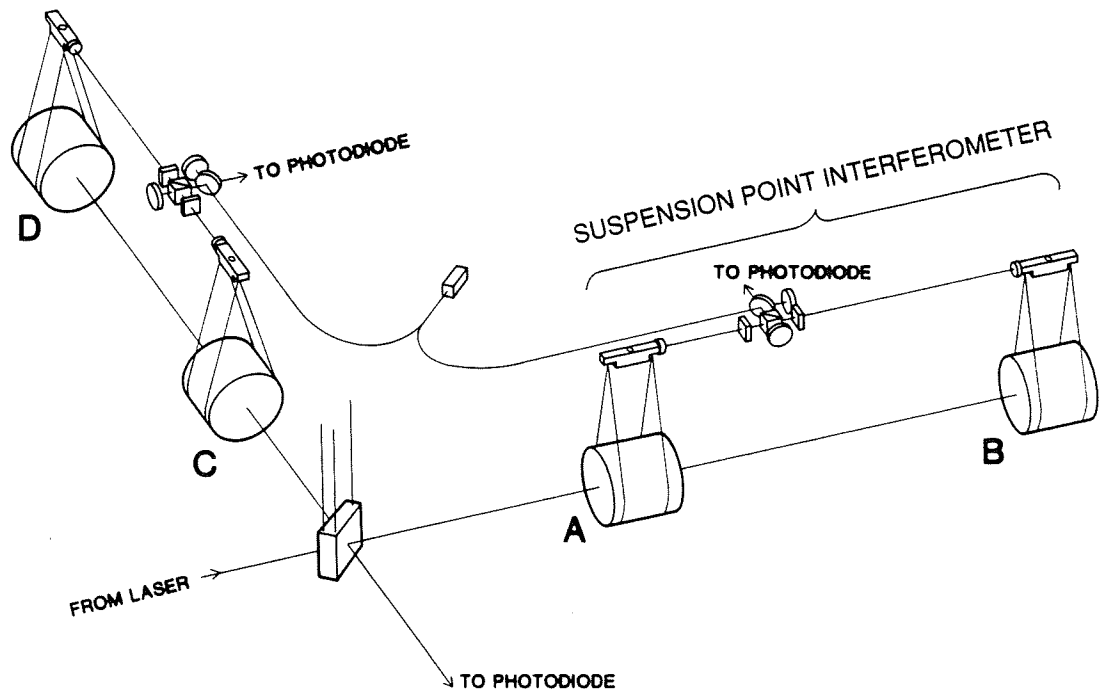


Figure C-6 Schematic representation of a suspension-point interferometer. A stabilized low-power laser excites two unequal-arm Michelson interferometers—one for each Fabry-Perot cavity. Each interferometer senses changes in the separation of the suspension points for the test masses in the associated cavity. The suspended test masses and beam splitter of the main interferometer are shown for context.

ferometers, the optical performance of the system can be improved by forming Fabry-Perot cavities between the suspension points. In either configuration, a lens, omitted from the diagram for simplicity, is used to form a cats-eye retroreflector with each small suspension-point mirror, making the system insensitive to small misalignment of the mirrors.

b. An active seismic-isolation system. A significant improvement in seismic isolation can be achieved by adding active control to a good passive-isolation system. Several concepts that use a well-isolated mass as an inertial reference in a feedback system to control the motion of a point of support have been proposed by gravitational-wave research groups [C-2, C-13, C-14, C-15]. A specific concept is shown schematically in Figure C-7.

Two basic ideas are used in this concept to achieve a good approximation to an inertial mass. The first is that the well isolated suspended test masses are the primary inertial reference for the feedback system. The second is that the feedback is arranged to null the motion of the point of support relative to the test mass by application of forces to the *point of support*. By this process the motion of the test mass relative to inertial space is reduced since the feedback forces on the point of support will tend to cancel the external disturbing forces. This “bootstrapping”

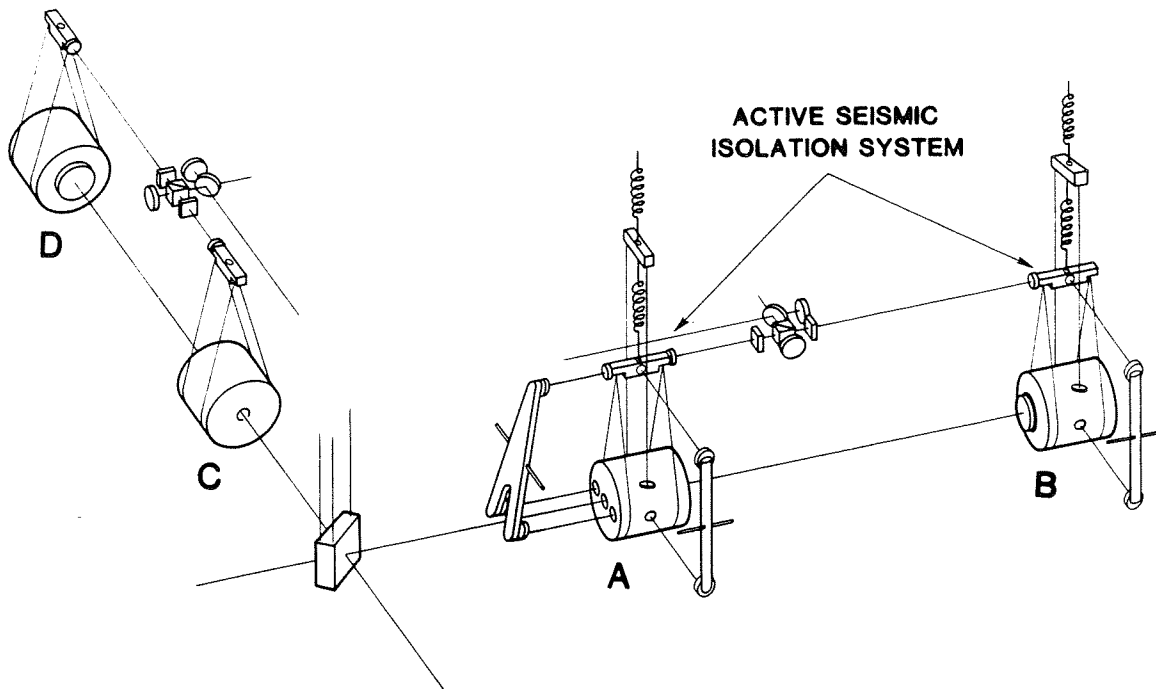


Figure C-7 Sketch of test mass suspension concept for extending interferometer operation to low frequency. An active anti-vibration guard system is shown for test masses A and B. The suspension block of the master test mass A is driven to track the longitudinal and sideways motions of the mass, using monitoring signals from auxiliary interferometers. The upper support piece, from which the main suspension block hangs by a spring, is driven to track the vertical motions of the test mass [C-16], using vertical-monitoring laser beams. Control of sideways and vertical motions of the effective suspension points of slave mass B is similar, but the longitudinal position of mass B is driven to track that of master mass A by the suspension point interferometer. The guard systems for test masses C and D are similar to those for A and B, respectively, but are not shown in the figure.

procedure is referred to as an active guard system. It realizes an inertial mass to a good, but finite, precision.

A third concept is now introduced, to further improve precision. The suspension points for the four test masses in the interferometer are tied together optically, so that if any residual disturbance does leak through the guard system, it will affect all the masses in the same way and cancel out motions in the directions of the optic axes. This is done by treating the test mass motions along and transverse to the optic axis by different techniques. The motions of the point of support relative to the test mass in the *transverse* directions are measured by two auxiliary interferometers which refer the motion of the point of support and the test mass to a well isolated reference arm. The reference arm is mounted on a long period torsional support so that it is isolated from rotational disturbances. The difference in the separations measured by the two interferometers thereby becomes proportional to the relative motion of the test mass and its point of support. The feedback to the

point of support is derived from this signal and applied locally to each test mass suspension.

Motions along the optic axis are dealt with globally. Test mass A is regarded as the “master” which defines an inertial frame for motions of all masses along the optic axis. The suspension points of the other masses are slaved to the “master” using signals provided by the main and seismic interferometers. Relevant degrees of freedom of each test-mass suspension are controlled as follows:

i. Mass A: the master mass. Translational motion in longitudinal, horizontal, and vertical directions is free, aided by the active guard system shown in Figure C-7. (Rotational degrees of freedom for this and the other masses are separately controlled by an automatic alignment system.)

ii. Mass B: a slave mass. Mass B has longitudinal motion of the suspension block forced to track the motion of the suspension block of mass A using the seismic-monitor interferometer. Transverse motions of the mass in horizontal and vertical directions are made free by the active guard system.

iii. Mass C: the “secondary master” mass. Mass C acts similarly to mass A, but very-low-frequency components (0 to 1 Hz, approximately) of horizontal and vertical transverse mass position are forced to track the position of the main interferometer beam by using signals from additional monitors.

iv. Mass D: a slave mass. This mass features suspension-block control similar to that of slave mass B, with longitudinal position slaved to mass C by the seismic-monitor interferometer. Additional high-precision control of the longitudinal position of the mass makes the main interferometer arms very closely equal (plus or minus an integral number of half-wavelengths).

The overall effect is to simulate a rigid, inertial, optical table, 4 km on a side, from which the masses are suspended.

Reliable prediction of the performance of an isolation system of this type is difficult since, at the large attenuation factors involved, leakage of seismic noise is likely to be determined by complex nonlinear coupling mechanisms and by limitations of servo-loop gain set by mechanical resonances. Active-isolation systems are expected to be an essential concept in bringing the performance of advanced LIGO interferometers within reach of the fundamental limits imposed by natural gravity-gradient fluctuations present near the surface of the Earth and by the quantum limit for the test masses.

References

- C-1. R.W.P. Drever, G. M. Ford, J. Hough, I. M. Kerr, A.J. Munley, J. R. Pugh, N. A. Robertson, and H. Ward, “A Gravity-Wave Detector Using Optical Sensing,” *Proceedings of the Ninth International Conference on General Relativity and Gravitation* (Jena 1980), ed. E. Schmutzer (VEB Deutscher Verlag der Wissenschaften, Berlin, 1983), 265.

- C-2. R.W.P. Drever, J. Hough, A. J. Munley, S.-A. Lee, R. Spero, S. E. Whitcomb, J. Pugh, G. Newton, B. Meers, E. Brooks III, Y. Gürsel, "Gravitational-Wave Detectors Using Laser-Interferometers and Optical Cavities," *Quantum Optics, Experimental Gravity, and Measurement Theory* ed. P Meystere and M.O. Scully, (Plenum Publishing, 1983), 503.
- C-3. R.W.P. Drever, J. L. Hall, F. V. Kowalski, J. Hough, G. M. Ford, A. J. Munley, and H. Ward, *Appl. Phys.* **B31**, 97, (1983).
- C-4. R.W.P. Drever, "Interferometric Detectors for Gravitational Radiation," *Gravitational Radiation*, NATO Advanced Physics Institute, Les Houches, ed. N. Deruelle and T. Piran, (North Holland Publishing, 1983), 321.
- C-5. B. J. Meers, *Phys. Rev.* **D38**, 2317 (1988).
- C-6. M. Daehler and P. A. Ade, *Journal of the Optical Society of America*, **65**, 124 (1975).
- C-7. D. R. Herriott and H. J. Schulte, *Appl. Optics* **4**, 883 (1972).
- C-8. R. Weiss, *Quarterly Progress Report of the Research Laboratory of Electronics*, MIT, **105**, 54 (1972).
- C-9. J. U. White, *J. Opt. Soc. Am.* **32**, 285 (1942).
- C-10. N. A. Robertson, "Experiments Relating to the Detection of Gravitational Radiation and to the Suppression of Seismic Noise in Sensitive Measurements," Ph.D. Thesis, University of Glasgow, 1981.
- C-11. G. A. Kerr and J. Hough, *Appl. Phys.* **B** (in press 1989).
- C-12. C. M. Caves, *Phys. Rev.* **D23**, 1693, (1981).
- C-13. N. A. Robertson, R.W.P. Drever, I. Kerr, and J. Hough, *J. Phys. E. Sci. Instr.* **15**, 1101, (1982).
- C-14. A. Giazotto, D. Passuello, and A. Stefanini, *Rev. Sci. Instr.* **57**, 1145 (1986).
- C-15. P. R. Saulson, *Review of Scientific Instruments*, **55**, 1315 (1984).
- C-16. J. E. Faller, R. L. Rinker, *NBS Dimensions*, **63**, 25 (1979).

APPENDIX D

CALCULATION OF VIBRATION ISOLATION

The test masses in a gravitational-wave interferometer must be held in place against the earth's gravitational field without disturbance by the substantial seismic motion of the earth's surface. At the same time, they must be free to respond to gravitational waves. The vibration-isolation and test-mass suspension systems of the LIGO are designed to meet these requirements.

The forces applied to balance gravity connect the test masses to the noisy outside world. If the connection is made through a compliant element such as a spring or a pendulum, then at frequencies large compared to the element's resonant frequency the mass is almost free in inertial space. This follows from the one-dimensional equation of motion for a mass on a spring: $m\ddot{x} = -k(x - x_g)$, where m is the mass and k is the spring constant of the support for the mass, x is the coordinate of the mass in inertial space and x_g is the coordinate describing the ground motion relative to inertial space. A frequency-domain solution to this equation, representing the response of the mass to a steady excitation of the form $x_g = X_g e^{i\omega t}$, yields the transfer function $T(\omega) = X/X_g$, which represents the response of the system. Assuming a sinusoidal response of the form $x = X e^{i\omega t}$,

$$T(\omega) = \frac{X}{X_g} = \frac{\omega_0^2}{\omega_0^2 - \omega^2}. \quad (\text{D.1})$$

(Here $\omega_0 = \sqrt{k/m}$, and $\omega = 2\pi f$.) This transfer function shows that at high frequencies, the influence of ground motion x_g on the motion of the mass x is small.

In gravitational wave detectors the amount of isolation given by a single spring is insufficient. The design adopted for the LIGO test mass isolation system includes the cascade of several vibration isolators, each consisting of a mass and a spring in series. Five sets of alternating layers of springs and masses make up the vibration-isolating stack. The test mass is suspended by a pendulum from the final layer of the stack. To a good approximation, the *high* frequency performance of such a multi-stage vibration isolator is given by the product of the transfer functions of the individual stages.

In practice, several complications arise. (1) Damping alters the transfer function; (2) the *low* frequency transfer function depends on the coupling between stages, the system must be considered in three dimensions to account for cross-coupling between different degrees of freedom; and (3) there is degradation of high frequency isolation due to the non-negligible mass of the springs and compliance in the masses. This third factor causes a sharp departure from the $1/\omega^2$ isolation at frequencies where the resonances of the internal modes of the individual suspension elements are excited. In the suspension systems proposed for the LIGO, these resonances are not expected to be a factor in the overall noise budget of the initial interferometer.

In the remainder of this appendix, we illustrate the method by which we have predicted the seismic noise that penetrates the isolation system planned for the LIGO.

A schematic diagram of a vibration isolation stack is shown in Figure D-1. It shows a model of a stack consisting of three layers of equal mass m and moment of inertia I , separated by springs. (A simpler system than the full LIGO suspension is described here merely to make the algebra less lengthy—the method of analysis is the same.)

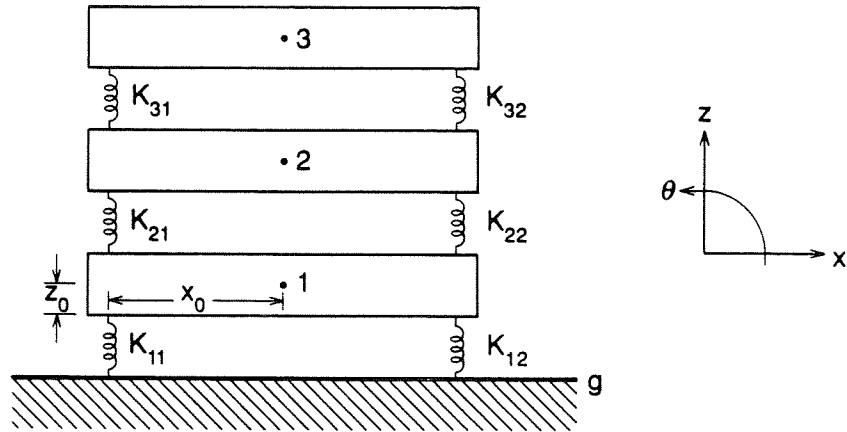


Figure D-1 Schematic diagram of a three-stage spring/mass isolation stack. Seismic noise enters at level g , and is attenuated by successive stages. The three masses (1, 2, 3) are separated by pairs of springs (k_{ij}). The vector from the attachment point of the springs to the center of mass for each layer has coordinates $(\pm x_0, 0, \pm y_0)$. The pitch angle of layer i is θ_i .

We treat each of the masses as a rigid body, and each of the springs as massless. The springs are not necessarily isotropic—they may have different spring constants for displacements in different directions. In general, we would need to keep track of six degrees of freedom for each mass, but if we align the principal axes of the springs with the symmetry axes of the system, then we need only follow three coordinates of a rigid body confined to a plane: the horizontal direction x parallel to the optic axis, the vertical z , and the angle θ about the third coordinate axis (the pitch angle).

Assuming that all of the springs and all of the masses are identical, the Lagrangian is

$$\begin{aligned}
 L = T - V = & \frac{1}{2}m(\dot{x}_1^2 + \dot{z}_1^2 + \dot{x}_2^2 + \dot{z}_2^2 + \dot{x}_3^2 + \dot{z}_3^2) + \frac{1}{2}I(\dot{\theta}_1^2 + \dot{\theta}_2^2 + \dot{\theta}_3^2) \\
 & - \frac{1}{2}k_x(\Delta x_{11}^2 + \Delta x_{12}^2 + \Delta x_{21}^2 + \Delta x_{22}^2 + \Delta x_{31}^2 + \Delta x_{32}^2) \\
 & - \frac{1}{2}k_z(\Delta z_{11}^2 + \Delta z_{12}^2 + \Delta z_{21}^2 + \Delta z_{22}^2 + \Delta z_{31}^2 + \Delta z_{32}^2) \\
 & - mg(z_1 + z_2 + z_3).
 \end{aligned} \tag{D.2}$$

Here the coordinates with single subscripts refer to the motions of the masses, while those with double subscripts represent the length changes of the springs, which can be expressed in terms of the x_i, z_i, θ_i , and the ground motion x_g, z_g, θ_g .

In the limit of small displacements, the resulting equations of motion are

$$\begin{aligned}
m\ddot{x}_1 &= 4k_x x_1 - 4k_x z_0 \theta_1 + 2k_x x_2 + 2k_x z_0 \theta_2 + 2k_x x_g, \\
I\ddot{\theta}_1 &= 4k_x z_0 x_1 - 4(k_x z_0^2 + k_z x_0^2) \theta_1 + 2k_x z_0 x_2 + 2(k_x z_0^2 + k_z x_0^2) \theta_2 \\
&\quad + 2k_x z_0 x_g + 2(k_x z_0^2 + k_z x_0^2) \theta_g, \\
m\ddot{z}_1 &= -4k_z z_1 + 2k_z z_2 - 2k_z z_0 - mg + 2k_z z_g, \\
m\ddot{x}_2 &= 2k_x x_1 + 2k_x z_0 \theta_1 - 4k_x x_2 - 4k_x z_0 \theta_2 + 2k_x z_0 \theta_3, \\
I\ddot{\theta}_2 &= 2k_x z_0 x_1 + 2(k_x z_0^2 + k_z x_0^2) \theta_1 - 4k_x z_0 x_2 - 4(k_x z_0^2 + k_z x_0^2) \theta_2, \\
&\quad + 2k_x z_0 x_3 + 2(k_x z_0^2 + k_z x_0^2) \theta_3, \\
m\ddot{z}_2 &= 2k_z z_1 - 4k_z z_2 + 2k_z z_3 + 2k_z l + 4k_z z_0 - mg, \\
m\ddot{x}_3 &= 2k_x x_2 + 2k_x z_0 \theta_2 - 2k_x x_3 - 2k_x z_0 \theta_3, \\
I\ddot{\theta}_3 &= 2k_x z_0 x_2 + 2(k_x z_0^2 + k_z x_0^2) \theta_2 - 2k_x z_0 x_3 - 2(k_x z_0^2 + k_z x_0^2) \theta_3, \\
m\ddot{z}_3 &= 2k_z z_2 - 2k_z z_3 + 2k_z l + 4k_z z_0 - mg.
\end{aligned} \tag{D.3}$$

The position of the attachment points of the springs with respect to the centers of mass of the masses are given by the parameters x_0 and z_0 . The springs have equilibrium length l .

These equations of motion do not include damping. For velocity damping, a term proportional to the time derivative of length is added to each spring term. Another method of modeling damping, called structural damping [D-1], is to multiply each spring constant by $1 + i\gamma$, where $\gamma \ll 1$. We have chosen to model the LIGO isolation system with structural damping of $\gamma = 0.03$, in accord with our laboratory measurements of the behavior of rubber springs.

The transfer function from the input noise spectrum, $x_g(f)$, to the motion of the top mass, here $x_3(f)$, is obtained using matrix methods [D-2].

Stacks such as those in the 40-meter prototype interferometer incorporate rubber springs that have good damping properties but are anisotropic: they are typically stiffer in the vertical direction than in the horizontal direction. Further, the rubber springs are in the form of blocks placed between thick masses, giving a non-zero value of the parameter z_0 , the difference in height between a spring end and the center of mass of a mass layer to which it is attached. Under these circumstances, horizontal displacements cause torques on the masses, so the horizontal isolation depends in part on response of the springs to the vertical displacements of the rotating ends of the masses.

Interferometer sensitivity as limited by seismic noise is calculated from the isolation transfer function (including the isolation provided by any extra-vacuum

isolation, the stacks, and the final suspension) as

$$\tilde{h}_{\text{seismic}}(\omega) = \frac{2T(\omega)X_g(\omega)}{L} \quad (\text{D.4})$$

where L is the interferometer arm length and $X_g(\omega)$ is the input seismic noise, as approximated in Section V.A. If vertical noise dominates because of cross-coupling and poorer vertical isolation, then the transfer function for vertical noise, multiplied by the vertical-to-horizontal coupling coefficient—is used.

The seismic noise estimate for initial interferometers (“SEISMIC” line in Figure V-3) is based on the isolation system described in Volume 2, Section IV.B, including a 1-Hz final suspension, and the conservative factor of 10^{-2} for the coupling of vertical to horizontal motion. In the limit of ideal seismic isolation, sensitivity at low frequencies ($< 10\text{Hz}$) may be limited by fluctuating gravitational gradients resulting from seismic waves [D-3].

Mechanical cross-coupling is reduced by careful design. Optical cross-coupling resulting from a slope of the interferometer arms (or at flat sites from the curvature of the earth) may set the ultimate limit to seismic noise. The effective noise is then the sum of the horizontal noise and the vertical noise weighted by the sine of the angle between the optic axis and the horizontal. To generate the seismic noise curve shown in Figure D-2 we assumed that the coupling can be reduced to the level that causes horizontal motion to dominate. The horizontal resonances in the isolation stacks are taken to be 2 Hz and an additional stage of extra-vacuum isolation, provided by commercial air springs, has been included.

References

- D-1. Meirovitch, L., *Elements of Vibration Analysis*, McGraw-Hill, New York, (1986).
- D-2. Friedland, B., *Control System Design: An Introduction to State-Space Methods*, McGraw-Hill, New York, (1985).
- D-3. Saulson, P. R., *Physical Review* **D30**, 643, (1984).

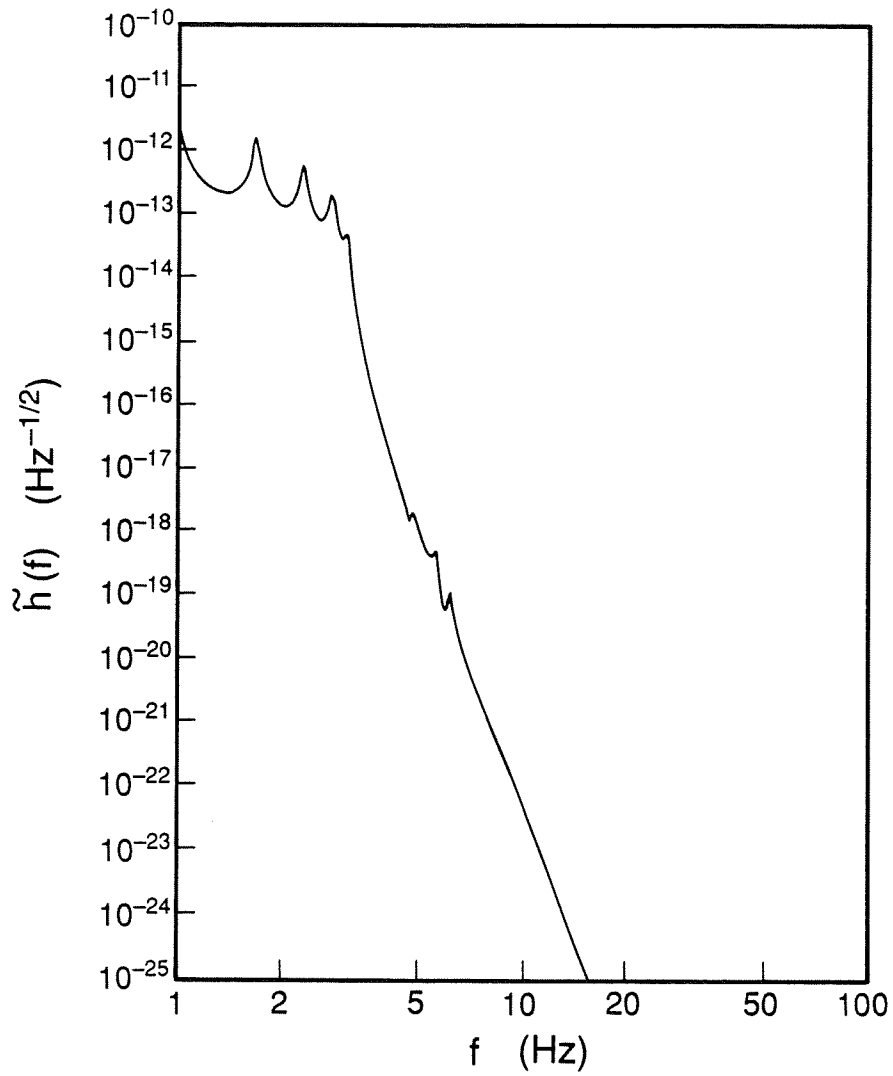


Figure D-2 The seismic noise in a LIGO interferometer of the “more advanced” design. The peaks in the spectrum are due to the pendulum suspension resonance ($f = 1$ Hz), and resonances in the isolation stack, ($f > 2$ Hz). The seismic excitation used in the model is the “standard” spectrum given in Table V-2.

APPENDIX E

POWER SPECTRAL DENSITY AND DETECTOR SENSITIVITY

The sensitivity of gravitational-wave detectors is defined as the minimum detectable signal in the presence of background noise generated within the instrument or by the terrestrial environment. The noise is random in nature, and can be reduced relative to signals by averaging over time T = (duration of the signal or the measurement interval, whichever is shorter). The average value of random fluctuations diminishes as $1/\sqrt{T}$. Noise is most conveniently measured and estimated in the frequency domain. There, the measurement bandwidth is $\Delta f = 1/T$, and a long-duration (for high-sensitivity) measurement corresponds to narrow bandwidth. To characterize the sensitivity of a detector independently of the bandwidth, the noise is conventionally normalized to a bandwidth of 1 Hz and expressed in units of (noise/ $\sqrt{\text{Hz}}$).

The noise spectrum, or noise level as a function of frequency, for a device that measures a quantity h is characterized by its power spectral density $S_h(f)$. This S_h is defined in terms of the noise level observed in the time domain, $h_N(t)$:

$$S_h(f) = \lim_{T \rightarrow \infty} \frac{2}{T} \left| \int_{-T/2}^{T/2} h_N(t) e^{-2\pi i f t} dt \right|^2. \quad (\text{E.1})$$

$S_h(f)$ is the noise power per unit frequency measured at frequency f . For gravitational-wave detectors, $h_N(t)$ is the noise of the detector expressed in equivalent dimensionless gravitational-wave strain amplitude, and $S_h(f)$ has the units of $[\text{strain}]^2/\text{Hz}$, or simply Hz^{-1} . The *amplitude* spectral density is defined by $\tilde{h}(f) = \sqrt{S_h(f)}$, and has units $\text{Hz}^{-1/2}$.

To compare the instrument noise to its signal, define the Fourier transform

$$H(f) = \int_{-\infty}^{\infty} h(t) e^{-2\pi i f t} dt \quad (\text{E.2})$$

where $h(t)$ (Section II, Equation (II.1)) is the signal output of the apparatus in the absence of noise. The exact value of the signal-to-noise-ratio (SNR) depends on the details of how the signal is filtered; the maximum SNR is achieved with optimal filtering¹ of the detector output:

$$\text{SNR} = \left[\int_0^{\infty} \frac{2 |H(f)|^2}{S_h(f)} df \right]^{1/2}. \quad (\text{E.3})$$

¹ The optimal linear filter, as defined by the Wiener-Hopf relations, minimizes the least square error between the output signal corrupted by noise and the noise-free input signal, once the signal waveform and the power spectral density of the noise are known. See Wiener, N., *The Extrapolation, Interpolation and Smoothing of Stationary Time Series with Engineering Applications*, John Wiley (1949).

(If there is no prior information available on the expected waveform—as in a general search for burst events—the filtering will not in general be optimal and the SNR will be reduced, though only slightly.)

Typically the signal has a maximum value $H_m(f_c)$ at characteristic frequency f_c , and S_h is approximately constant near f_c ; then:

$$\text{SNR} \approx \left[\frac{\int_0^\infty 2 |H(f)|^2 df}{S_h(f_c)} \right]^{1/2} \approx \sqrt{\frac{2H_m^2 \Delta f}{S_h(f_c)}}, \quad (\text{E.4})$$

where the signal bandwidth Δf is

$$\Delta f \equiv \frac{\int_0^\infty |H(f)|^2 df}{|H_m|^2}. \quad (\text{E.5})$$

The two components in the signal-to-noise ratio expressed in comparable units of equivalent gravitational wave strain are

$$\begin{aligned} h_{\text{sig}} &\equiv \sqrt{2} H_m \Delta f && \text{(signal)} \\ h_{\text{rms}} &\equiv \sqrt{S_h(f_c) \Delta f} = \tilde{h}(f_c) \sqrt{\Delta f} && \text{(noise),} \end{aligned} \quad (\text{E.6})$$

so $\text{SNR} = h_{\text{sig}}/h_{\text{rms}}$. Astrophysical models are used to predict expected values for H_m . $\tilde{h}(f)$ is the quadrature sum of uncorrelated noise sources, such as residual gas effects and photon shot noise.

As one application of these results, consider a search for periodic waves. In this case the bandwidth is $\Delta f = 1/\hat{\tau}$, where $\hat{\tau}$ is the observation time (10^7 s for a long-duration search), and h_{sig} as defined above is $1/\sqrt{2}$ times the amplitude of oscillation of $h(t)$. The unity signal-to-noise strength for a periodic source with optimal direction and polarization is then $h_{\text{sig}} = h_{\text{rms}} = \tilde{h}(f_c) \sqrt{1/\hat{\tau}}$. In Appendix A, periodic sources are described by a characteristic amplitude that is equal to h_{sig} : $h_c = h_{\text{sig}}$; and detectors are described by a noise amplitude that is equal to this h_{rms} : $h_N = h_{\text{rms}}$. As a second application, a gravitational wave burst that lasts for n cycles of oscillation, has bandwidth $\Delta f \approx f_c/n$. Correspondingly, the signal h_{sig} is approximately the amplitude of oscillation of $h(t)$ during the waves n cycles, and the rms noise level, assuming optimum direction and polarization, is thus $h_{\text{rms}} \approx \tilde{h}(f_c) \sqrt{f_c/n}$. The signal-to-noise ratio is then $h_{\text{sig}}/h_{\text{rms}} \simeq h_{\text{sig}} \sqrt{n}/\tilde{h}(f_c) \sqrt{f_c}$. In Appendix A and Section II the wave is described by a characteristic amplitude $h_c = h_{\text{sig}} \sqrt{n}$ and the detector by a sensitivity $h_N = \tilde{h}(f_c) \sqrt{f_c}$; i.e., the factor \sqrt{n} is absorbed in the source's amplitude rather than in the detector's noise.

This brief discussion ignores the reduction in the signal-to-noise ratio that results from the non-optimal direction and polarization of realistic sources of gravitational waves, and also ignores the issue of how large the SNR must be for, say, 90% confidence that an observed signal is real. These issues are discussed quantitatively in Appendix A.

APPENDIX F

SCATTERING AND OPTICAL PROPERTIES OF THE BEAM TUBES

A substantial effort was made during the conceptual design to understand the influence of scattered light on the noise in the interferometer and to develop a scheme to reduce the noise due to scattering [F-1]. The scattered light originates in both the optical components and the residual gas and arrives at the photodetector by various mechanisms involving both single and multiple scatterings.

The basic mechanism by which scattered light can disturb the gravitational-wave measurement is by adding optical fields of random phase and amplitude to the small main field in the "dark fringe" at the antisymmetric port of the interferometer. The fluctuations in the phase of the total field (scattered light added to the main field) are the critical parameter; the additional photon shot noise from the scattered light is far less important. The analysis of the scattering effects takes into account that: (1) that the main and scattered fields will usually have different spatial distributions at the photodetector, (2) the main field and the scattered fields may have taken different times to traverse the interferometer, and (3) the scatterers may be moving and the scattered light may reflect or diffract from moving elements, such as the inside wall of the vacuum tube.

1. Spatial Distribution

The main field defines a mode of the radiation field; the disturbing phase fluctuations are proportional to the fraction of the scattered field that projects onto this mode. The main field can be thought of as a spatial filter for the scattered field. This leads to both a substantial reduction in the effects of scattered light and a simplification in the analysis due to the orthogonality of the modes defined by the main beam geometry. The orthogonality, however, is not maintained if the spatial response of the photodetector is nonuniform. The photodetector and the main beam then define a new set of orthogonal modes different from those of the cavities. We have considered this in the analysis and have estimated the noise both for a bare photodetector and the case when a mode filter is placed before the photodetector. The design goal is that the estimated scattering noise in an interferometer be less than 1/10 of the noise due to the standard quantum limit for a one-ton test mass. We have adopted this conservative goal to allow for a reasonable safety margin, given the difficulty of the calculations.

2. Noise Due to Different Travel Times

We will attempt to make the travel times of the main light beams close to equal in the two interferometer arms, so as to reduce the sensitivity to laser frequency and amplitude fluctuations at the antisymmetric output. Scattered light will traverse a different path through the system and thereby degrade this symmetry. The noise is proportional to the amplitude of the scattered light, the difference in travel time

between the main beam and the scattered light and the spectrum of the laser amplitude and frequency fluctuations. With proper design of the interferometer and laser stabilization systems, we do not believe that this noise will be significant.

3. Noise From Moving Objects in the Scattered Light Paths

The dominant contributions to the scattering noise arise from the motion of the scatterers and other objects that reflect or diffract the scattered light. A successful strategy to suppress scattering noise seeks to eliminate the sources of single scatterings and to arrange that the individual amplitudes in multiple scatterings and diffraction processes are small. One important single-scattering process is the fluctuation in the forward scattering of the moving residual gas molecules. This is controlled by evacuating the optical path. Another important mechanism, in the absence of baffles, proceeds through the following steps: light from the main beam scatters from one of the main cavity mirrors, then reflects from the *moving* tube wall one or more times and then recombines with the main beam mode (either by scattering or diffraction at another optical component or through the nonuniformity of the photodetector). This process and considerations related to the angular fluctuations of the main mode (beam wiggle) have imposed the requirement for baffles in the LIGO beam tubes, and for baffles, blackening and possibly mode filtering in the paths following the antisymmetric port of the interferometer.

4. Concept for Specifying Baffles and the Optical Properties of the Tubes

The classical strategy for baffling in optical instruments is to arrange that no scattering path from an optical component in the main beam will arrive at the exit pupil due to specular or diffuse reflection from enclosures or other surfaces. We adopt the same strategy in the LIGO beam tubes (described in Volume 2, Section IV.C). This sets a relation between the baffle spacing, the baffle height and the clear aperture.

Scattered light that reflects from the tube walls at large grazing angles is strongly attenuated because: (1) the ratio of R/L (where R is the clear aperture radius and L is the beam-tube length) is extremely small, causing a large number of reflections, and (2) the tube walls are poor reflectors, except at grazing incidence. For example, the attenuation of scattered rays is greater than 80 dB at grazing angles of 0.1 radians for smooth stainless steel, .05 radians for the finishes being specified for the straight wall beam tubes, and .003 radians for standard corrugated tubing [F-2]. Because of this large attenuation the baffle design is particularly simple and exploits the principle of converting shallow grazing rays into paths with larger grazing angles that are strongly attenuated.¹

¹ The small grazing angle rays must be stopped by the baffles both because they suffer little attenuation in the tubes and because the differential scattering and recombining function of the mirrors grows as $1/\theta^n$ where θ is the grazing angle and n lies between 1.5 and 2, depending on the spatial spectrum of long-wavelength mirror distortions [F-3].

With the proposed baffle design a mechanism remains in which a scattered ray from a mirror is diffracted toward the wall by a baffle and continues to propagate down the tube by multiple reflections at small grazing angles until it is diffracted a second time toward the other mirror or the photodetector and recombines with the main field. Analysis of this mechanism predicts that, without an output mode filter, the scattering noise due to seismically induced motion of the tube walls becomes larger than 1/10 the standard quantum limit at frequencies above 30 Hz. With an output mode filter the design goal is met with a safety margin of several hundred.

Another mechanism considered in the analysis is backscatter from the seismically driven baffles. This results in specifications on the closest distance of baffles to the cavity mirrors and on the surface finish of these close baffles.

An extremely useful and non-obvious result of the analysis is that noise due to the coherent superposition of the scattered light is easily eliminated by simple measures that randomize the phases from multiple scattering, reflection and diffraction. The typical misalignment of the tubes during assembly as well as the standard manufacturing tolerances on tube roundness are sufficient to destroy the coherence. As an additional precaution we have designed the baffles with serrated edges, as has been done in coronagraphs, to average over several Fresnel zones [F-4].

The scattering analysis suggests that the LIGO will be able to meet the design goal providing that the tube walls and baffles move no more than the naturally occurring seismic ground motion. The tube enclosure should reduce acoustic and wind driven motions of the tubes sufficiently to maintain the scattering at acceptable limits.

A recommendation of the initial analytic study of the scattering [F-1] is to carry out computer modeling with available scattering codes, both to test the analytic model and to be sure that all important scattering mechanisms have been accounted for. A directed Monte Carlo technique such as the APART [F-5] code is appropriate for the calculation and this will be done during the engineering design.

References

- F-1. Thorne, K. S., "Light Scattering and Proposed Baffle Configuration for the LIGO," Preprint GRP-200, California Institute of Technology, Pasadena, CA 91125.
- F-2. Beckmann, P., A. Spizzichino, "The Scattering of Electromagnetic Waves from Rough Surfaces," Pergamon Press, 1967.
- F-3. Elson, J. M., H. E. Bennett, J. M. Bennett, "Scattering from Optical Surfaces," *Applied Optics and Optical Engineering*, Vol. III, Academic Press Inc., 1979.
- F-4. Newkirk, G. Jr., and D. Bohlin, "Reduction of Scattered Light in the Coronagraph," *Applied Optics*, Vol. 2, p. 131, 1963.
- F-5. APART, Breault Research Organization, Inc., Tucson Arizona.

APPENDIX G

LIGO PROJECT GRAVITATIONAL-WAVE SEARCHES

Several data runs and subsequent analyses have been performed using the LIGO Project prototype interferometers. Although such searches with the prototypes lack sufficient sensitivity to discover gravitational waves, they provide useful experience with data collection and analysis procedures. A brief description of previous gravitational-wave searches is given below.

1. Periodic Source of Known Period and Known Position

(M. Hereld, Ph.D. thesis, Caltech 1983).

A search was done for sinusoidal strain signals at 642 and 1284 Hz from PSR 1937+214 using the observed radio period to simplify the data recording and enhance the sensitivity. The data were analyzed for both gravitational-wave polarizations h_+ and h_\times by correcting for the Doppler shift due to the Earth's motion in the barycentric coordinate system. The noise exhibited the anticipated Rayleigh distribution associated with the noise of the instrument.

2. Burst Search Using Generic Templates

(D. Dewey, Ph.D. thesis, MIT 1986)

A search was done for gravitational wave bursts in the 800 to 5500 Hz band using a set of 22 generic, digital, three-state (-1,0,1) filter templates modeled on theoretical wave forms. The noise distribution of the filtered data exhibited Gaussian statistics appropriate to the instrument noise after correction for large amplitude but low-rate, non-Gaussian events; which were identified as instrument related.

3. Periodic Search for Sources of Unknown Period at Both Known and Unknown Positions

(J. Livas, Ph.D. thesis, MIT 1987)

A search was done for periodic sources in the 2 to 5 kHz band using a sinusoidal source model and two different methods. The first method involved an all-sky survey using a large Fourier transform ($2 \cdot 10^7$ points); a Cray 2 computer was utilized to search for peaks in the spectrum that exhibit characteristic FM and AM modulations due to the motion of the Earth. With the second method, a search for periodic sources in the galactic-center region was performed by applying Doppler corrections to the data in the time domain, so as to concentrate the Doppler FM sidebands into a single resolution bin of the Fourier transformation. The distribution of spectral peaks obeyed a Rayleigh distribution as expected, except for some large peaks associated with instrument resonances.

4. Search for Coalescing Binary Chirps

(S. Smith, Ph.D. thesis, Caltech 1988)

A search was done for the characteristic chirp of the radiative decay of a coalescing black-hole or neutron star binary (Appendix A, Equations (A.8) and (A.9); Figure A-3). The waveform for such a chirp is characterized (aside from overall amplitude and start time) by a single parameter $\mu^{2/5} M^{3/5}$, where μ is the binary's reduced mass and M is the total mass. This parameter was varied to make an optimized search for all possible masses. The algorithm that was developed distorts the time series so as to concentrate all the energy into one frequency before Fourier transformation of the data.

5. Search for Periodic Signals Following SN 1987A

(M. Zucker, Ph.D. thesis, Caltech 1989)

A search was done for periodic gravitational waves from Supernova 1987A in the band between 300 Hz and 5 kHz. The search was started ten days after the supernova explosion which occurred in the Large Magellanic Cloud in February 1987. Five samples, each lasting 105 seconds ($2 \cdot 10^6$ points), were Fourier analyzed after apodization. No signals other than apparatus resonances were detected.

APPENDIX H
REPORT ON RECENT PROGRESS¹

CONTINUATION PROPOSAL
NSF GRANT NO. PHY-8803557

CONTINUED PROTOTYPE RESEARCH & DEVELOPMENT
AND PLANNING FOR THE
CALTECH/MIT
LASER GRAVITATIONAL WAVE DETECTOR
(PHYSICS)

Rochus E. Vogt, Principal Investigator
and Project Director
Ronald W. Drever, Co-Investigator
Kip S. Thorne, Co-Investigator
Rainer Weiss, Co-Investigator

October 1989

This section covers progress since the last continuation proposal (October 1988) on prototype research and development and on planning for a Laser Interferometer Gravitational Wave Observatory (LIGO) by the Caltech and MIT science groups and the LIGO engineering team located at Caltech.

Areas of highest priority included: (1) conceptual design of LIGO, (2) interferometer prototypes, (3) preparation of the LIGO construction proposal.

¹ This summary of progress from October 1988 to October 1989 is excerpted from our Continuation Proposal to the National Science Foundation, October 1989. It is printed here in the same format as submitted.

A. LIGO Development

Work continued on the planning and conceptual design for the Caltech/MIT Laser Interferometer Gravitational Wave Observatory (LIGO).

1. Sites

Louisiana State University (LSU) delivered a report on a preliminary seismic survey of a potential LIGO site in Louisiana. This work was carried out under the direction of Drs. Warren Johnson of the Department of Physics and Astronomy and Don Stevenson of the Louisiana Geological Survey. The report revealed that an oil pipeline crossing the property is a source of low-frequency (< 10 Hz) seismic noise; this may restrict alignments of the LIGO at this site. A site plan with two possible alignments has been prepared.

A preliminary soil and geotechnical exploration of the LIGO site at Edwards Air Force Base, California, was carried out in October 1988, and the report of these studies was completed. A review of this preliminary survey yielded the conclusion that, because of the instability of the lake bed soils in the area, it would be necessary to support the LIGO installation on piles driven to a depth varying between 60 and 120 feet. The cost impact of these piles partially offsets the very low earthwork costs at this site, but Edwards remains a relatively low-cost potential site for the LIGO.

A hydrology study and a biological survey of the Edwards site were completed in January 1989. The biological survey of one of the potential LIGO sites there was submitted to, and accepted by the Air Force. A preliminary archeological/paleontological survey (Phase 1) was submitted to and accepted by the California State Historical Preservation Office. This survey brings together existing records and surveys, and recommends additional survey work in several regions of "cultural significance," as defined by the National Historic Preservation Act of 1966.

At the request of the NSF, the LIGO Project explored the feasibility of building a 4-km LIGO installation at the National Radio Astronomy Observatory (NRAO) site near Green Bank, West Virginia. We visited the site, collected and evaluated available data, and identified two possible LIGO alignments. We concluded that it is technically feasible to build a LIGO at Green Bank, although the site is topographically more complex than other sites we have studied. A series of reports containing details and conclusions were submitted to the NSF.

We have initiated a preliminary inquiry into the feasibility of a 4-km LIGO at the site of the Owens Valley Radio Observatory (OVRO). The 1983 Stone & Webster survey concluded that there was insufficient space for a 5-km LIGO, but more recent analysis shows that a 4-km installation will fit. The site possesses many attributes of a good LIGO site: a well-developed infrastructure, very flat topography, stable soil conditions, and a single landowner with whom Caltech has historically excellent relations.

2. Materials Testing

We have constructed a Vacuum Test Facility (VTF) and used the facility to evaluate outgassing properties of steel samples that are candidate materials for construction of the

LIGO vacuum system. Data from the VTF have been used in conjunction with theoretical modelling to design the vacuum pumping strategy for LIGO. The VTF measurements were required because there was no adequate data base on the outgassing properties of steel subject to very-long-term vacuum exposure. VTF results indicate that at least one supplier can deliver 304L stainless steel with sufficiently low hydrogen content to achieve the requisite hydrogen outgassing rate without high-temperature bakeout. We have also identified adequate cleaning and other procedures (including low-temperature bakeout techniques for water vapor) to reduce all other contaminants to sufficiently low outgassing rates.

3. Conceptual Design

During the past year we have conducted an extensive conceptual design process for the LIGO facilities. The purpose of this effort was to translate the scientific requirements for the facilities into technical solutions and provide the basis for costing the construction of the facilities. In this process we studied the interactions between solutions to various technical problems and clarified certain design criteria which were previously ill-defined.

a. Identification of scientific functional requirements:

A major effort was conducted during the past year to specify and document the scientific functional requirements for the LIGO. This process required unification and rationalization of previous work done by the Caltech and MIT teams as well as formulation of requirements for many specifications which were not yet well defined. Over one hundred internal working papers and reviews were written covering the following broad topics:

- Site requirements.
- Vacuum studies.
- Noise source analysis.
- Interferometer design requirements.
- Environmental requirements.
- Auxiliary physical measurements.
- Data and control system requirements.
- Scientific requirements for operations.

b. Formulation of operations scenario:

In addition to scientific specifications, the scenario for how the LIGO will operate plays an important role in defining the facilities to be built. We have defined such a strategy and analyzed its implications for the design of the LIGO. We have decided to pursue a phased construction approach to deliver at the earliest date a system capable of discovering gravity waves and exploiting the initial discovery. The later phases of construction will enhance the scientific capabilities of LIGO and allow broader participation by others in the new field of gravity wave astronomy. We have identified the need for a simultaneous search and development capability, with minimum interference between these missions, as the optimum strategy to ensure successful LIGO operation. This has defined the need for three distinct detector units (observation, development, and special investigation detectors), and a flexible modular vacuum system capable of supporting simultaneous operation of multiple interferometers. Finally we have developed a plan for early use and later evolution of the LIGO facilities.

c. *Development of vacuum system concept:*

i. *Beam tubes:*

A concept for the LIGO beam tubes which specifies physical characteristics, environmental requirements, and construction implementation was developed. Two possible construction implementations for the tube have been evaluated: smooth wall tubing with periodic reinforcement, and corrugated tubing. Construction and maintenance scenarios have been formulated.

ii. *Vacuum chambers:*

The LIGO concept requires a flexible vacuum system. We have conceptually defined four vacuum chamber types: test mass chambers types 1 and 2, diagonal chambers (which house the beamsplitter optics), and horizontal axis modules (for conditioning optics).

a) *Test mass chambers:*

The LIGO concept places strong demands on the test mass chambers (TMCs). These chambers house the critical test mass assemblies and Fabry-Perot cavity mirrors. These elements must receive the highest level of vibration isolation. The chambers need to accommodate different sizes of test masses and possible different configurations of test masses while allowing optical beams from other simultaneously operating interferometers to pass through the chambers unperturbed. Most importantly, some of the chambers (TMC, Type 1) must accommodate removal and installation of entire test mass assemblies for a given interferometer with minimal disturbance to the vacuum system and other interferometers. We have developed a solution which employs an airlock chamber design.

For those chambers located at the ends which may be opened without disturbing the remaining vacuum system and operating interferometers, a simpler and less expensive configuration, TMC Type 2, has been designed.

b) *Diagonal chambers:*

The diagonal chambers house the beamsplitter optics for the interferometers. While the diagonal chambers must accommodate vibration isolation systems similar to those employed in test mass chambers, a given diagonal chamber interfaces to only one detector. These chambers, therefore, do not require the complication of an airlock design.

c) *Horizontal axis modules:*

The conditioning optics chains at each interferometer input and output do not require the same degree of vibration isolation as test masses and beamsplitter optics. However, these optical chains have a high degree of complexity and will change more than other interferometer parts over the course of LIGO evolution. The corresponding vacuum chambers require the greatest degree of modularity, flexibility, and ease of access. We have developed a simple concept for these chambers in terms of modules which can be

connected or stacked together in open-ended fashion. Removable endcaps on both sides of each chamber will allow convenient access to all internal components.

iii. Pumping and leak testing strategies:

We have developed strategies for pumping and leak testing the LIGO vacuum system. The pumping strategy involves specifying type, placement, and capacity of pumping stations, based on estimates of interferometer gas loads and vacuum system outgassing properties. The leak testing strategy for the beam tubes is based on pulsed exposure to He gas with recovery and compression in the pumping stations.

d. Interferometer conceptual design:

We have worked to develop a conceptual design for LIGO interferometers in general, to establish boundaries on the facilities which would be compatible with future evolution, and in particular have developed a more specific conceptual design for the initial LIGO interferometers. We have developed a vibration-isolation strategy which is based on stacks of metal spaced by encapsulated rubber springs, and which takes account of the level of isolation required for different classes of interferometer components. The design has an open-ended feature in that the primary isolation stacks rest on platforms which can be further isolated, if required, due to care taken in the design of the various vacuum chambers.

During the conceptual design of the input and output conditioning optics chains for the interferometers, we discovered that the level of complexity of this part of the facilities had been seriously underestimated in all previous planning for interferometric gravity wave detectors. In fact the requirements for conditioning optics drive key aspects of the facilities design and have significant impact on how the remote and campus facilities will be used in LIGO. The outcome of this work led to the requirement of a flexible modular envelope for the conditioning optics chains, using the horizontal axis modules described above.

e. Supporting equipment and facilities:

i. Laser power, cooling and electrical capacity:

We have developed a plan for allotting electrical power for the lasers, pumps, electronics and building functions. We have chosen to allot sufficient electrical capacity to operate one large-frame argon ion laser per interferometer in the facility. This power level will be sufficient to allow initial interferometers to be shot-noise limited at sensitivity levels adequate to conduct viable gravity wave searches. For advanced interferometers we anticipate the use of more powerful and efficient systems such as Nd:YAG lasers which are currently under development. Because such lasers should be more efficient by orders of magnitude than current ion lasers, the initial laser power capacity will be sufficient for operation of advanced interferometers. Power for lasers represents approximately half of the

planned electrical capacity. The rest will be used for lighting, pumps, electronics and other building functions.

ii. Environmental specifications and auxiliary parameter monitors:

We have developed specifications for the laboratory environment required for LIGO and plans for implementation. This includes items such as power conditioning, temperature and air flow constraints, allowable mechanical noise, and drift and creep in structures. A significant problem which was identified is the cleanliness level of the lab environment. Measures were planned to ameliorate contamination of the optics and vacuum chambers. We have also formulated a plan for monitoring auxiliary physical parameters for the interferometers such as magnetic fields and line voltage, which will help to rule out spurious candidate gravity wave events.

iii. Interferometer/facility interfaces:

We have enumerated the mechanical, optical, and electrical interfaces between the interferometers and the facilities, and between separate site buildings. This work includes, for example, specifying the number and type of analog and digital signal lines which penetrate vacuum chambers, number and type of feedthroughs required, and possible levels of multiplexing.

iv. Data and control systems:

We have outlined the requirements for automated acquisition and logging of housekeeping data for the facilities, computer-assisted operation of control loops, and acquisition and logging of actual interferometer data. This includes enumeration of functions to be provided and estimation of signal bandwidths required.

v. Auxiliary and campus facilities:

We have identified auxiliary facilities to be provided at the LIGO sites and the campus facilities required to support LIGO operations. This has been done by developing scenarios for accomplishing various tasks associated with LIGO operations. For example, we have established procedures by which equipment is delivered to the sites, undergoes final assembly and testing, and is installed into the facility. From such scenarios we have identified what shop and storage facilities are required on site, and how quality and cleanliness controls are instituted. Similarly we have developed a concept of what type of tests, construction, etc., will be conducted at the LIGO sites, and which functions will be carried out on the campuses.

f. LIGO buildings and enclosures:

We have developed a conceptual design for buildings which will house the LIGO facilities and for an enclosure for the beam tubes. The building design seeks to provide an appropriate environment for LIGO activities while providing sufficient floor space and generality to accommodate future LIGO evolution. This need is especially

important in the corner buildings at each site. The tube enclosure is required to reduce wind-induced motion of the beam tubes, thus making noise induced by scattered light inside the tubes a tractable problem. Simultaneously it provides a more temperature-stable environment and affords some protection from vandalism.

B. Prototype Activities

The best displacement sensitivity in the 40-meter prototype so far has been measured at 3×10^{-18} m/ $\sqrt{\text{Hz}}$. Assuming this sensitivity is primarily limited by displacement noise (random motion of test masses) and that LIGO interferometers would be dominated by the same noise source, a 4km baseline LIGO would exhibit a strain sensitivity of 8×10^{-22} / $\sqrt{\text{Hz}}$, and would have a reasonable chance to discover gravity waves. However, this configuration of the 40-meter prototype could not be directly scaled up to an operating LIGO system. For instance, the frequency stabilization scheme was well suited for operation at low optical power levels but not at levels needed for the LIGO interferometers. Furthermore, the LIGO will require significant changes in the orientation and position control systems. During the current grant period we have emphasized the development of techniques which should not only lead to improved sensitivity in prototypes, but which can be directly scaled up to operating LIGO interferometers.

1. Development of a laser stabilization scheme consistent with LIGO power levels:

The Innova 100-20 large frame argon ion lasers at the 40-meter prototype have been tested at 7 watt single-mode output at 514 nm. The original stabilization scheme used an intracavity Pockels cell which required operation of the laser below 2 watt output power. In addition, an optical fiber used to inject light into the interferometer cavities, while providing reduction of fluctuations in laser beam geometry, severely limited the optical power that could be coupled into the interferometer.

We have constructed a new configuration for injecting light into the 40-meter interferometer. We have implemented a new two-stage frequency stabilization scheme. In the first stage, the laser is locked to a fixed length mode cleaning cavity. In the second stage, the phase of the light transmitted by this cavity is matched to one of the 40-meter cavities using a Pockels cell. We have extended the prototype's vacuum envelope to contain more of the conditioning optics, starting with the input mirror of the mode cleaner. This eliminates the optical fiber and any beam geometry perturbations caused by motion of the air path after the mode cleaner.

2. Development of the 5-meter facility:

Work began on the design of a 5-meter facility in 1986 and construction was completed near the beginning of the present grant period. The facility has 4 vacuum tanks. Three of the tanks are designed to house the 5-meter prototype. The fourth tank is configured to test suspensions. This tank is instrumented with an electromagnetic shaker to test vibration isolation of sample suspensions under vacuum.

At present, the central tank is dedicated to research on optical concepts in a stationary interferometer and the suspension tank is being used to carry out tests of a prototype

suspension. The facility is adequate in scale to develop and test selected LIGO optical and suspension subsystems during the next 4 years.

3. Development of recombination techniques in a stationary interferometer:

Work was begun on a stationary (not suspended) interferometer to test an interferometer configuration in which the beams reflected by the Fabry-Perot cavities are recombined. Beam recombination is required in any LIGO interferometer using high optical power or recycling. Because the components of the stationary interferometer are held in standard mounts on an optical table, seismic, acoustic and thermal noise are not attenuated; consequently the interferometer can approach theoretical shot-noise limits only at frequencies $\gtrsim 10$ kHz. This frequency range is useful for testing optical concepts and for developing the servo systems and electronics. The interferometer is assembled on an optical table inside the central tank of the 5-meter facility.

The system is being used to study different servo-control concepts of holding the interferometer in lock and to test two different techniques of applying RF modulation to the light. The stationary interferometer will also be used to develop a recombination system in which the phase modulators are placed in sidearms to reduce the optical power in the Pockels cells, much as is planned for the initial LIGO interferometer. Finally, the system will be used to test broad-band recycling by adding a recycling mirror and associated phase control servos.

4. Development of orientation and position control systems suitable for very long baseline interferometers:

The position and orientation of many optical components must be controlled precisely for interferometer operation. The elements requiring the most critical control and adjustment are the test masses that bear the main interferometer mirrors. During the current grant period we have designed, constructed, and tested new control subsystems which are suitable for LIGO scale applications:

a. Prototype work on a more sensitive orientation and position control system:

We have designed and tested a new position and orientation control system, suitable for controlling test masses and other suspended components. This compact self-contained system uses shadow sensing and electromagnetic feedback local to the suspended component being controlled. The design allows for simultaneous control of up to six degrees of freedom per component.

b. Development of a new diagnostic tool for detecting errors in coupling light into cavities:

A new device, called a phase camera, has been developed to diagnose errors in mode matching an input laser beam to a Fabry-Perot cavity. The device produces three-dimensional images of the phase difference between the input beam and the cavity. It can be installed in front of any of the cavities in the system.

5. Optics research and development:

a. Investigation of heating effects in mirrors:

Advanced LIGO interferometers will have very high light levels in the Fabry-Perot cavities. During the current grant period we have investigated the power handling capability of fused silica supermirrors coated by Litton Guidance and Control Division. We have measured the throughput of high-finesse-transmission Fabry-Perot cavities of different length, mirror spot size, and ratio of length to mirror radius. In these preliminary studies we found that most of the cavities exhibited a saturation phenomenon when the power stored in the cavity exceeded approximately 1 kW. In the saturation regime, the throughput efficiency decreased and the output mode distorted. We have developed a model which attributes these effects to thermal lensing in the input mirror substrate. This model predicts that these thermal distortion effects will persist even in very long baseline cavities as are planned for LIGO.

We plan to institute a systematic research program to characterize the thermal distortion effects in cavities and to develop better mirrors in a cooperative effort with industry.

b. Developments toward improving optics test and characterization capabilities:

We are currently planning to expand our capabilities to test and analyze optical components. Recent activities include:

i. Investigation of radiometric mapping to determine temperature profiles of mirrors:

An infrared camera was used to make a radiometric image (using 10μ radiation) of the heating of a mirror coating by the absorption of laser light. The test showed that surface temperature increments as small as 0.1°K could be measured by this technique. This method promises to be useful for experimental studies of thermal distortion in optical components.

ii. Preliminary tests of homogeneity and birefringence on large, fused-silica substrates:

The LIGO mirrors will require a high degree of optical homogeneity and low birefringence in blanks which are much larger than those currently in prototype use. We have obtained slow-annealed fused silica blanks comparable in size to LIGO mirrors. These were ground flat to $\lambda/50$ and tested under our supervision at Zygo Corp. We collaborated on a modification to Zygo's phase mapping interferometer which allowed us to measure both homogeneity and birefringence of these thick substrates over a large aperture. The Zygo measurements are now being analyzed in part to determine the expected performance of thick substrates in a recycled interferometer.

iii. Development of improved experimental and analytical tools for scattering characterization:

The scattering angular distribution function for small angles is a key variable in estimating the noise due to scattered light in the LIGO. We have developed an apparatus which uses an optical fiber to map the scattered field in the region around the focal point of the mirror.

A substantial amount of analytic work was done to evaluate the effect of scattering in the LIGO beam tubes. The results of this analysis now form the basis for the design and placement of baffles.

6. Studies of vibration isolation and thermal noise:

a. Vibration isolation studies:

Research has continued on the development of a double suspension system in which the mirror is suspended from another object, the guard mass, which in turn is also suspended. This system should provide improved seismic isolation at frequencies below a few hundred Hz.

b. Thermal noise characterization:

Thermal noise in suspensions could limit the performance of high sensitivity interferometric gravitational wave detectors in the region of about 100 Hz. A new effort was begun to measure the internal dissipation of candidate suspension fiber materials in flexure at frequencies between a few hertz to several hundred hertz. The experiment in progress measures the Q , in vacuum, of the flexural resonances of suspension fibers clamped at one end. Once a short catalog of material Q has been established, the experiment will be used to measure the scaling of the loss with fiber dimensions.

C. Construction Proposal

Most of the work described in the preceding pages for this grant period was done in preparation for the LIGO construction proposal. This work has led to a design concept that serves as basis for an engineering design and cost estimate. A major effort on preparation of the construction proposal was started in May 1989.

Although a significant reduction in scope of the LIGO configuration occurred in July as a result of discussions with the NSF, most of the proposal has now (September 1989) been written and reflects the new configuration. Staged construction of the LIGO will be proposed. The construction proposal, to be submitted in the fourth quarter of 1989, will request funds for the first of these stages.

D. Other Progress

In November we began a series of monthly Project Status Review meetings. The purpose of these meetings was to convene members of the LIGO Project Office, the engineering group, and both science groups to review the current status and plans for developing the contents of the construction proposal.

A Sun 4/260 and 4/110 distributed computer system was installed and brought on line at MIT. The system is the same as that previously installed at Caltech and enhances as well as unifies the computing environment across the LIGO project. The system now has common software for engineering and scientific analysis at both locations.

Computer analysis of simulated gravity-wave signals continued, concentrating on extracting source location and polarization information from coincident detection of bursts in three or more detectors. Results obtained with the San Diego supercomputer facility indicate that the information from three detectors, each recording bursts with signal-to-noise ratios on the order of 5, spans approximately 80% of the sky.

An NSF/LIGO meeting was held at Caltech on April 10 and 11, 1989. LIGO design concepts, preliminary cost estimates, and management aspects were discussed.

E. International Cooperation

R. Vogt participated in a February 14, 1989 meeting in Paris, France, which had been convened upon initiative of and chaired by the NSF. Representatives of all major European gravity-interferometer research groups and their funding agencies attended. A principal focus of the discussion was the exploration of possibilities for international collaboration in the development of gravity wave interferometry, and several technical and scientific working groups were established.

As agreed at the Paris workshop, LIGO personnel have taken on the coordination of two international working groups: vacuum systems and control systems. The LIGO team also has assigned members to all other working groups coordinated by European scientists.

Full engineering and science briefings on the LIGO project were given, over the period of several days, to Drs. Hough and Leuchs, the respective leaders of the British and German gravity wave research groups. Similar courtesies were extended to Dr. Blair, who is organizing a new laser interferometer program in Australia.

Information on engineering advances also is being provided to Britain's Rutherford Laboratory on a continuing basis.

RECENT PUBLICATIONS AND CONFERENCE PAPERS

1. "Measuring High Mechanical Quality Factors of Bodies Made of Bare Insulating Materials," A. Čadež and A. Abramovici, *J. Phys. E: Scientific Instruments*, **21**, 453, 1988.
2. "Development of a Multi-dimensional Optimization Servo for Gravity Wave Detector Mirror Alignment," B. Lemoff, *Senior Thesis*, Caltech, May 1989.
3. "A Near Optimal Solution to the Inverse Problem for Gravitational Wave Bursts," Y. Gürsel and M. Tinto, LIGO Preprint 89-1, *submitted to Physical Review D*, June 1989.
4. "Frequency Fluctuations of a Diode-pumped Nd:YAG Ring Laser," P. Fritschel, A. Jeffries, T. Kane, *Optics Letters*, accepted for publication, 1989.

5. Conference Papers, 12th International Conference on General Relativity and Gravitation, Boulder, Colorado, 1989.
 - i. "Tests of Recombination Schemes in a Fixed Arm Fabry-Perot Laser Interferometer," N. Christensen, P. Fritschel, J. Giaime.
 - ii. "Developments in Interferometric Gravity Wave Detectors for Large Scale Operation," R.W.P. Drever.
 - iii. "The Performance of a Double Pendulum Vibration Isolation System," J. Kovalik, P. Saulson, M. Stephens.
 - iv. "Observation and Analysis of a Mirror Heating Threshold in Fabry-Perot Cavities," F. J. Raab.
 - v. "Thermal Noise in Suspensions for Interferometric Gravitational Wave Antennas," P. Saulson.
 - vi. "Status Report on the Caltech 40-meter Fabry-Perot Prototype Gravitational Wave Detector," R. Spero.
 - vii. "The LIGO Project—A Progress Report," R. Vogt.
 - viii. "Laser Interferometer Detectors," R. Weiss.

APPENDIX J

HISTORY OF THE PROJECT

The LIGO project is based upon a large body of research and technical development over a period of almost 30 years.

After Joseph Weber's pioneering work on bar detectors for gravitational waves in the 1960s [J-1], other groups began to develop gravitational-wave detectors. In the late 60s, the idea of interferometric detectors was conceived independently by Weber, Weiss, and others. The basic design for a delay-line variant of an interferometric detector was described and the dominant noise sources quantified in 1972 by Weiss [J-2]. The first operation of an interferometric detector was conducted by Moss, Miller, and Forward in 1971-72 [J-3].

In the early 1970s, many groups, including Drever at Glasgow and others at Stanford, LSU, IBM, Bell Labs, Rochester, Munich, Rome, and Moscow began research with bar detectors. Several of these groups have continued a strong program of research with successive detectors. A switch from bar detectors to interferometers was made by the Munich group under Billing in 1975 and the Glasgow group under Drever in 1977. A year later, Drever at Glasgow introduced the concept of the Fabry-Perot variant of an interferometric detector [J-4].

In 1979 Drever started experimental gravitational-wave research at Caltech. In the same year, the National Science Foundation convened the Deslattes Committee which recommended strong funding of the gravitational-wave field, including new interferometer projects at Caltech (Drever) and MIT (Weiss). Weiss pursued a delay-line interferometer, while Drever continued development of Fabry-Perot interferometers.

In 1981, Weiss at MIT, with the firms of Stone & Webster and A. D. Little, began a detailed study of the design and costs of a large-scale Laser Interferometer Gravitational-Wave Observatory, or LIGO [J-5]. A presentation by Drever, Thorne, and Weiss in 1983 to the NSF Advisory Committee for Physics led to its strong endorsement of the LIGO concept. In 1984, Caltech and MIT formally joined in a project for the design, construction, and operation of the LIGO facility, with Drever, Thorne, and Weiss as a steering committee. In the same year the National Science Board approved project planning and feasibility studies. Further studies of design and cost were undertaken with the Caltech's Jet Propulsion Laboratory in this period.

In 1986, the NAS Physics Survey strongly endorsed the LIGO for ground-based research in gravity [J-6]. Concurrently, the International Society of General Relativity and Gravitation strongly endorsed the LIGO.

In November 1986 an NSF-sponsored Workshop was convened at Cambridge, Massachusetts to review the state of developments in the field with particular attention to plans for the LIGO Project. The Workshop was attended by 55 interna-

tional participants, and a report of the meeting was prepared by an eight-member panel from disciplines other than experimental gravity. The report was supportive of the program and endorsed a vigorous pursuit of its goals. The Summary of this January 1987 report to the NSF by the Panel on Interferometric Observatories for Gravitational Waves is included at the end of this Appendix. Two recommendations of the Panel have been implemented: management of the project was transferred in Fall 1987 from the steering committee to a Project Director, and a choice has been made of the type of interferometer (Fabry-Perot) to be used in the initial operations with the LIGO.

More recent reviews of the LIGO Project occurred in February 1988 (NSF Site Visit Committee, consisting of Drs. R. Byer, J. Faller, H. Grunder, A. Sessler, S. Teukolsky, D. Wilkinson, and R. Wilson) and in September 1988 (presentation by R. Vogt to the NSF Advisory Committee on Physics).

References

- J-1. J. Weber, *Physical Review* **D22** (1969), 1302.
- J-2. R. Weiss, *Quart. Progr. Rep. Res. Lab. Elect. MIT* **105** (1972), 54.
- J-3. G. E. Moss, L. R. Miller, and R. L. Forward, *Applied Optics* **10** (1971), 2495.
- J-4. R. W. P. Drever, G. M. Ford, J. Hough, I. M. Kerr, A. J. Munley, J. R. Pugh, N. A. Robertson, and H. Ward, "A Gravity-Wave Detector Using Optical Sensing," *Proceedings of the Ninth International Conference on General Relativity and Gravitation* (Jena 1980), ed. E. Schmutzer (VEB Deutscher Verlag der Wissenschaften, Berlin, 1983), 265.
- J-5. P. Linsay, P. Saulson, R. Weiss, "A Study of a Long Baseline Gravitational Wave Antenna System", Report to the National Science Foundation (1983).
- J-6. "Physics Through the 1990's—Gravitation, Cosmology, and Cosmic Ray Physics", National Research Council, National Academy Press, Washington, D. C., 1986.

SUMMARY OF NOVEMBER 1986 NSF REVIEW

The following is a copy of the title page and Summary from "Report to the National Science Foundation by the Panel on Interferometric Observatories for Gravitational Waves," which was submitted to NSF in January 1987 after a one-week (November 1986) review of the LIGO Project.

Report to the National Science Foundation

by the

Panel on Interferometric Observatories for Gravitational Waves

January 1987

5. SUMMARY

A) A strong case has been made for the scientific value of the goals of the project.

B) Though there are large uncertainties associated with the strengths of the many different kinds of astrophysical sources and the ultimate capability of interferometric detectors, there is a high probability that this facility will ultimately provide for a giant leap in our understanding of the gravitational force, one of the most fundamental forces of nature, as well as our knowledge of astrophysical phenomena.

C) It is anticipated that this facility would uniquely provide the most sensitive and certain prospect for detecting astrophysical events and identifying their nature. Essential to this capability is the twin nature of the two interferometers. Though companion efforts in other countries are highly desirable, a common management of the two LIGO detectors is important both for the coordination of the observational program and for the analysis and identification of observed events. This facility would provide for a continued and thriving development of the field.

D) It is important to proceed directly to the construction of a long baseline interferometer in a timely manner since many aspects of the detector development program cannot otherwise be tested.

E) The rate of detectable extragalactic events increases as the cube of the interferometer sensitivity, thus putting a high premium on the long baseline. Though a multistage, or phased authorization to the final configuration was carefully considered, the panel does *not* recommend this approach. We recommend full authorization with phased construction and appropriate milestones.

F) The plans as described in the presentations and in the various documents provided appear to be well conceived. The procedure which has been employed in drawing up the existing designs and in making the cost estimates appears reasonable and adequate for proceeding to the final design for submission. Effort should continue to examine design alternatives which may decrease costs, particularly in the area of the vacuum system and enclosure. We do not recommend that the project be delayed by this process of re-examination. It is important to make the choice between Fabry-Perot and Michelson interferometer type detectors before submission of the final design. However, it remains important to develop advanced detectors and therefore research should continue to this end.

G) Because of the magnitude and dual nature of the facility, with laboratory sites widely separated, it is especially important that the construction and operation be well managed. The panel feels that the project requires a single scientific project leader of high stature to direct the activities. Efforts should immediately be directed to providing such leadership.

H) In looking forward to the utilization of the facilities it should be recognized that in addition to a budget for its operation, adequate funds will be required to support both the needs of experimental groups and further detector development.

I) In conclusion, the panel enthusiastically supports this development effort and urges that the plans for the project be refined along the lines indicated and that the design be completed. We recommend, then, that the construction project be brought to the National Science Foundation Board for consideration and (hopefully) for funding.

Panel Members:

Daniel B. DeBra
Val L. Fitch
Richard L. Garwin
John L. Hall

Boyce D. McDaniel
Andrew M. Sessler
Saul A. Teukolsky
Alvin A. Tollestrup

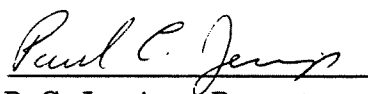
APPENDIX K
MEMORANDA OF UNDERSTANDING

Included here are copies of three signed memoranda of understanding (MOU).

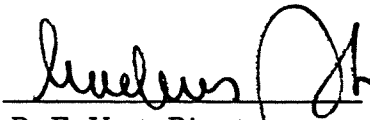
- (1) MOU between Caltech and MIT on the LIGO Project.
- (2) MOU between the LIGO Project and the Byer research group at Stanford University.
- (3) MOU between the LIGO Project and the Low Frequency Isolation Project at the University of Colorado.

MEMORANDUM OF UNDERSTANDING
BETWEEN THE
CALIFORNIA INSTITUTE OF TECHNOLOGY (CALTECH)
AND THE
MASSACHUSETTS INSTITUTE OF TECHNOLOGY (MIT)
ON THE
LIGO PROJECT

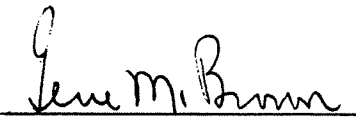
- 1) The LIGO project is an integrated and collaborative effort by Caltech and MIT scientists to design, build and operate an observatory to measure gravitational waves from astrophysical sources by laser interferometry.
- 2) Caltech serves as the prime contractor for the LIGO project with the National Science Foundation, and the activities of the MIT science team are supported under a subcontract from Caltech.
- 3) The project director is the Principal Investigator for the LIGO and has overall responsibility for the design, construction and operation of the LIGO.
 - a) The director reports to the Caltech provost and is appointed by Caltech in consultation with MIT.
 - b) The director's administrative contacts at MIT are the chairman of the department of physics and the director of the Center for Space Research.
- 4) Caltech and MIT Co-investigators have equal rights within the project, have access to the technical resources of the project and share in the responsibilities to make the project a success.
- 5) The functions carried out by Caltech and MIT scientists include the following:
 - a) Support the design, construction, and operation of the LIGO.
 - b) Carry out research and development of the initial and advanced interferometers.
 - c) Take responsibility for the development and testing of LIGO interferometer subsystems as appropriate.
 - d) Develop data analysis and diagnostic procedures for the LIGO.



P. C. Jennings, Provost
Caltech



R. E. Vogt, Director
LIGO Project



G. M. Brown, Dean of the
School of Science, MIT

11-13-89

10 November 1989

Memorandum of Understanding
between
The LIGO PROJECT (Caltech/MIT)
and
The Byer research group at Stanford University

This memorandum of understanding describes technical and scientific exchanges that have occurred during the proposal preparation period, the proposal review period and those that are planned for the period during which the laser source will be under investigation by the Byer group at Stanford University for eventual application to the Laser Interferometer that is the key technical element of the Laser Interferometer Gravity Wave Observatory (LIGO).

Proposal Preparation Period

The Stanford group was in communication with the LIGO group during the preparation of the Stanford NSF proposal to study solid state lasers that will meet the requirements for the LIGO project. LIGO researchers provided invaluable information to the Stanford Group on the laser source requirements. In addition, during the preparation of the Stanford proposal, Professor Byer visited Cal Tech and MIT to learn first hand about the laser interferometer experiments and about the laser requirements. Both Professor R. Vogt and Professor R. Weiss visited the Stanford campus during the proposal preparation period to learn first hand of the solid state laser technology that was being proposed to meet the LIGO laser requirements.

Technical Discussions following the submission of the Proposal to the NSF

Since the submission of the Stanford Proposal to the National Science Foundation in June 1988, the contacts between the Stanford and the LIGO group have increased both in frequency and in the depth of the technical discussion. Stanford researchers have visited Caltech twice and LIGO researchers have visited Stanford once. During the first Stanford group visit, M. Zucker and A. Abramovici gave useful advice to T. Day and to E. Gustafson on control circuits for Pound-Drever locking and gave technical information on frequency stability measurements. In addition, Y. Gursel provided useful information on vibration isolation. The LIGO group offered assistance in the construction of a high finesse Fabry Perot interferometer. On a second visit to Caltech, Y. Gursel assisted T. Day in the construction of a 25 cm long, 600MHz free spectral range, high finesse interferometer to act as a reference cavity for laser stability measurements.

On August 16 and 17, A. Abramovici visited Stanford, presented a talk to the Byer Group on the laser requirements for the LIGO system and engaged in detailed technical discussions about the solid state laser sources being researched for the LIGO project.

Future Scientific and Technical Exchanges

Biannual technical reviews of the Byer group diode pumped solid state laser research program are planned to insure that the work on the laser sources is consistent with the requirements of the LIGO project. These reviews will take place alternatively at the Caltech and at the Stanford locations. The Byer group will work to transfer the knowledge gained in the laser sources in a timely manner to the LIGO project. Work on laser amplitude and phase noise, spatial mode characteristics, temporal and spatial mode clean up, and on high power optics will be areas of continued discussion. To insure that the technical and scientific discussions occur in a timely manner, the Byer Group assigns liaison responsibilities to Dr. E. Gustafson. The technical liaison responsibilities for the LIGO project are assigned to Dr. F. J. Raab.

For the Byer Group

Robert L. Byer

Robert L. Byer, Date 9/14/89

For the LIGO Project

Rochus E. Vogt

Rochus E. Vogt, Date 9/18/89

MEMORANDUM OF UNDERSTANDING

on

LOW FREQUENCY ISOLATION RESEARCH

between the

Laser Interferometer Gravitational Wave Observatory Project

(California Institute of Technology and Massachusetts Institute of Technology)

and the

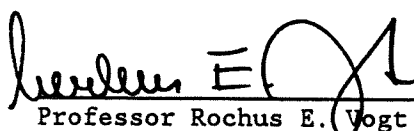
Low Frequency Isolation Project


(University of Colorado)

The University of Colorado is proposing to develop a prototype two-stage vibration isolation system capable of achieving a factor 10^4 isolation in all 6 degrees of freedom over the frequency band from 1 to 10 Hz. The goal for the internal noise level of the prototype system is $10^{-11} \times (1 \text{ Hz/f})^2 \text{cm/sec}^2/\text{Hz}^{0.5}$ or less for horizontal displacements. The time scale for carrying out this work is about four years.

After the prototype system is successful, the objective of the University of Colorado group is to join with the Laser Interferometer Gravitational Wave Observatory (LIGO) Project to design and build a 4 km low-frequency gravitational wave detector, probably covering the frequency range 1 to 30 Hz, to operate in the LIGO vacuum systems. It is recognized that the LIGO Project cannot commit itself at this time to participating in such a future program. However, collaboration between the Low Frequency Isolation (LFI) Project and the LIGO Project on the prototype isolation system and on tests of thermal noise using the prototype system is necessary in order to make the results as useful as possible to the LIGO Project and to achieve as rapid progress as possible by the LFI Project. To achieve these objectives, the LIGO Project and the LFI Project approve the following agreement.

1. The LFI Project will provide preliminary design information on the first stage of the isolation system to the LIGO Project, and utilize suggestions from the LIGO Project in the final design. It will keep the LIGO Project informed of progress on building and testing the first stage, and present the results to the LIGO Project for discussion before proceeding with construction of the second stage. Finally, the LIGO Project will be kept informed of all significant results from testing of the second stage and from tests of thermal noise in pendulums hung from the second stage.
2. The LIGO Project will provide information and advice to the LFI Project, in particular on desirable characteristics for the prototype low-frequency isolation system, and will make suggestions concerning the design and testing of the system. Finally, after measurements on the prototype low-frequency isolation system have been made, the LIGO Project will take part in discussions of whether to proceed further toward the design of a low-frequency gravitational detector, either as a supplement to the main LIGO program or as part of a future LIGO users program.
3. Annual joint meetings of the LFI Project and the LIGO Project will be held in order to achieve a necessary level of interaction between the two Projects.

 10/17/89
Professor Rochus E. Vogt
Director, LIGO Project

 10/16/89
Professor James E. Faller
Principal Investigator, LFI Project

